BALANCING PLANAR LINKAGE MECHANISMS

by

M. J. WALKER

A thesis submitted to the University of Newcastle upon Tyne for the degree of Doctor of Philosophy.

FEBRUARY, 1979

DEDICATED TO MY WIFE ANN.

'And he who is versed in the science of numbers
can tell of the regions of weight and measure,
but he cannot conduct you thither'.

Kahlil Gibran 'The Prophet', 1923, P.67.

ACKNOWLEDGEMENTS

The author wishes to express his thanks to the Science Research Council who supported the work presented in this thesis with grants B/RG 1285, 9466 and GRA 28374. Also the author is indebted to Professor Maunder for his advice and encouragement, and for making available the facilities of the Stephenson Laboratories. In addition, he would like to express his thanks to colleagues in the Department of Mechanical Engineering, and, in particular, to Dr. K. Oldham and Mr. R.S. Haines for their stimulating discussions on certain aspects of this work. The author would also like to thank the University Computing Centre for the use of their I.B.M. 360/370 computer. The manufacture of the test rig described in this thesis would not have been possible without the willing assistance of the technical staff of the Mechanical Engineering Department. Thanks are also due to Mr. B. Young and Mr. T. Clarke of the electronics workshop; Mr. M. McGilligan of the photographic department and Mrs. S.M. Stone for her patience and accuracy in typing this thesis.

The work described in this thesis has not been submitted to any other University, and, apart from two exceptions noted hereunder, consists of original work by the author. First Dr. K. Oldham suggested that the loops considered in Chapter Two of this thesis were the 'independent loops' previously identified by other research workers concerned with linkage topology, although the arguments confirming this to be so are those of the author. Second Mr. R.S. Haines identified the condition under which a counterweight can be omitted from one of the two links connected by a prismatic joint: the author subsequently used this condition to develop the relevant equations of this thesis.

ABSTRACT

This thesis concerns the synthesis of counterweights for balancing the forces, moments and driving torque generated by planar linkage mechanisms. Part I reports the development of theory and an associated procedure by which multi-link, multi-degree-of-freedom planar linkage mechanisms may be fully force-balanced without reference to the kinematic equations of motion. The procedure includes rules to determine whether a particular linkage may be fully force-balanced, and if so how many counterweights are needed, together with a means of selecting an appropriate counterweight set.

Part II reports the development and use of a general computer-based approach to synthesizing counterweights by means of numerical minimization. The illustrative computer program described can be used to improve the unbalanced forces, moment and/or driving torque of two types of planar linkages, a four-bar linkage and a particular Watt's six-bar chain. Quantitative criteria for evaluating the improvements are considered in some detail. The worth of the two approaches is examined theoretically and experimentally in the case of a particular Watt's six-bar chain.

Part III contains the overall discussions on and conclusions to the work of this thesis, along with suggestions for further work.

CONTENTS

Page No.

CHAPTER ONE

INTRODUCTION

At present the dynamics of linkages is usually considered from the point of view of inertia load analysis, rather than synthesis, since linkage kinematics and engineering experience have, up to now, tended to pre-determine the masses and moments of inertia of the links. There has been a considerable amount of research concerned with the development of general purpose computer-based dynamic analysis, e.g. Chace and Smith [1] and Uicker [2]. However it appears that designers are increasingly concerned with modifying the dynamic characteristics of their linkages, and consequently require appropriate design techniques which take into account all their main dynamic criteria. These criteria are likely to include (i) reduction of the frame shaking force, (ii) reduction of the frame shaking moment, (iii) reduction of each joint load to below its safe limit, (iv) reduction of the fluctuations in the driving torque, (v) reduction of the effective inertia at the input and (vi) maintenance of contact in all the bearings.

It seems appropriate to deal first with methods which satisfy or partially satisfy single dynamic criterion followed by those concerned with two and then more than two criteria.

In 1968 Lowen and Berkof [3] surveyed 119 references on balancing linkages and related subjects. One reference is the work by Kamenskii [4] on balancing the shaking moment of linkages using a cam operated oscillating counterweight.

Grant and Fawcett [5] suggest that impacts due to loss of bearing contact can be controlled by the use of spring loaded bearings. The spring merely translates the bearing force locus away from the origin thus helping the bearing pin and journal to maintain contact. Assuming that the spring is light, the importance of this method is that it only affects the bearing in question.

It seems that a frequently desired property of a dynamical system is that it should be fully force-balanced, i.e. its mass centre remains stationary. To obtain this force-balance two distinct approaches exist. First a balance can be achieved externally by the addition of supplementary mechanisms to the frame, typical of which are the cam operated eccentric masses proposed by Kamenskii [4] or a mirror image mechanism reviewed by Davies [6]. This type of approach is concerned with balancing the original mechanism by supplying either an opposing force or a set of forces.

A second approach to balancing is concerned with moving the mass centre position of the mechanism, by the addition of counterweights, such that it lies at a stationary point. In the special case of linkage mechanisms Berkof and Lowen [7] analysed the trajectories of the mass centres of a number of single degree of freedom linkages and obtained a set of balance conditions for each linkage. Later Tepper and Lowen [8] generalized this method.

The first part of this thesis is concerned with developing a general approach to force-balancing multi-degree of freedom multi-bar linkages using counterweights. It is titled 'Full Force-Balance'. Five equations are derived (in Chapter Two) from which may be obtained those conditions counterweights must satisfy to force-balance a given linkage. Chapter Three is concerned with developing a check to see if a linkage may be force-balanced; a formula which defines how many counterweights are required and a method indicating suitable links to leave uncounterweighted. An explicit procedure by which to force-balance linkages is then given in Chapter Four and is used on an industrial two-degree-of-freedom nine-bar linkage. The design of an experimental rig is reported in Chapter Five and the search for the 'best' force-balance for a linkage

constructed for the experimental work is detailed in Chapter Six. The succeeding chapter is concerned with both experimental tests on this linkage and an experimental examination of the worth of the force-balances of Chapter Six.

As will be highlighted by the first part of this thesis, the drawback with the above force-balance method is that the frame shaking moments, input torque fluctuations and bearing loads are usually increased, typically by a factor of about two.

Other methods have been developed for satisfying or partially satisfying two criteria. The survey of Lowen and Berkof [3] included such approaches typical of which is the method of Shchepetil'nikov [9]. Shchepetil'nikov deduced that the original mass centre of a linkage can be moved to a point on a rotating part of a 'proportional auxiliary mechanism'. This allows the introduction of a counterweight which causes the final mass centre to be brought to a stationary point. The rotating counterweight generates a moment relative to this linkage, and, by careful positioning, the first harmonic of the shaking moment may be eliminated.

Berkof and Lowen [10] showed that for a fully force-balanced linkage there are optimum conditions of partial moment balance, which are given by certain link length ratios only. Unfortunately, this particular approach uses design curves which are restricted to specific link shapes.

Berkof [11] obtained a complete dynamic balance of a four-bar linkage by using geared oscillating counterweights on the crank and rocker. Unfortunately this has been found to cause large increases in both input torque fluctuations and bearing forces, as well as the effective inertia at the crank.

A novel approach taken by Tomas [12] is to determine the kinematic bounds within which a given linkage performs its kinematic function satisfactorily. Next linkages are randomly generated within these bounds until one having suitable dynamic characteristics is found.

Porter and Sanger [13] use a Rosenbrock numerical minimization procedure to seek reductions in the shaking force, the shaking moment and three bearing loads of a four-bar linkage operating in a kineto-static mode. In this study the parameters of the crank counterweight and the angular offset of that on the rocker are fixed according to the force-balance conditions previously formulated by Smith and Maunder [14a]for this linkage. An equation is then formed from a points approximation of the mean square of each of the above criteria along with associated weighting factors. The number of points of evaluation obviously defines the accuracy, and, by use of a plotted graph, it is shown that increasing the number of evaluation points beyond 36 yields changes of less than 1% in the magnitude of the equation. Accordingly 36 points are used. The Rosenbrock procedure is used to find a series of values of both the radius of the disc-shaped counterweight attached to the rocker and the radial offset of its mass centre from the rocker frame pivot which yield constant magnitudes of this equation. The cases studied are the separate establishment of contours for the shaking force, the shaking moment and three bearing loads. Additionally four cases of attempting to satisfy two criteria simultaneously are studied.

Sadler and Mayne [14b]also examined the ability of numerical minimization techniques to find counterweights which satisfy more than one criterion. They also used a four-bar linkage operating in a kineto-static mode as their model, but non-dimensionalized the predicted forces and moments by dividing them by the product of the linkage mass, crank

length and (crank angular velocity)^2. In the case of the moment, which is measured about the mid-point between the two frame pivots, the crank length is squared. A Davidon-Fletcher-Powell search is used which is switched to a Powell conjugate gradient method if the gradient discontinuities appear to hinder the more efficient variable metric method. A number of optimizations are carried out for each of two cases: first when the mass of the two counterweights used are each defined to be half the mass of the linkage and second when only the combined mass of both counterweights is required to equal the mass of the linkage. Typical optimizations tried with this approach are the minimization of the shaking force subject to the constraint that the maximum moment does not exceed defined values; the minimization of the maximum moment subject to the constraint that the linkage must remain force-balanced and the minimization of the maximum shaking force subject to the constraint that the maximum bearing loads and moments do not exceed defined values.

As seen from this brief survey, there are techniques available for obtaining specific results by the use of given devices. However, to the author's knowledge, no technique has yet been produced which enables industrial designers to define criteria they wish to change; to what degree they wish to change each criterion and by what means they wish to attempt to achieve these changes. However the computer-based minimization approach used in the last two papers is felt to hold promise. As indicated by these authors, there is no reason why such techniques cannot be used to attempt to improve any of the criteria with any conceivable device provided that both can be mathematically modelled. Accordingly such techniques are studied in the second part of this thesis under the title "Computer-Based Synthesis of Devices".

The preliminary investigation of such techniques reported in Chapter Eight is for the purpose of establishing a usable technique and familiarizing the researcher with the problems of such an approach. This investigation takes the form of a computer program which synthesizes mass devices for crank-driven all revolute-jointed four-bar linkages. The program is found to work and results are presented.

Based on the above work, a more sophisticated program is developed (Chapter Nine) which avoids some of the problems of the earlier one. This program caters for both the same type of four-bar linkage as the previous one and a particular Watt's six-bar chain. The program is used to improve the performance of a linkage constructed for experimental purposes (Chapter Ten).

In Part III, which is entitled 'Concluding Remarks', a discussion on the work reported in this thesis and suggestions for further work are presented along with the overall conclusions.

PART I

FULL FORCE-BALANCE

CHAPTER TWO

A GENERAL APPROACH TO FORCE-BALANCING PLANAR LINKAGES

2.1. Introduction

This chapter is concerned with the approach of Berkof and Lowen [7]. In examining their work it was observed that the form of the terms associated with those links to be left uncounterweighted are similar. Additionally, the counterweighted links seemed to form themselves into chains of such links. Consequently, the determination of the force-balance conditions of a chain of counterweighted links should be obtainable from a standardized equation. These observations seemed to suggest that an approach based on a set of standardized equations could be formulated for determining the force-balance conditions of a linkage. The aim of this chapter is to examine this hypothesis.

For brevity, two terms will be used to describe certain quantities used in this thesis. First a moment vector: the moment vector of a body is the product of its mass and the position of its mass centre with respect to a given reference system. Second a loop: a loop is defined as a closed chain of revolute-joint-connected links which may, when stated, contain prismatic joints.

2.2 Balancing Revolute Jointed Chains of Links

A force-balance of a chain of links pivoted about the frame is achieved when its mass centre is made to lie at a stationary point, i.e. the frame pivot for all configurations of the chain of Figure 2.1. A chain is numbered sequentially starting from the free end which is considered to be the top of the chain. The line between two joints of a link is termed an arc. It is shown in Appendix I that if simple counterweights are used s balance conditions have to be satisfied to force-balance an s-linked chain of links. A simple counterweight has a constant mass with its mass centre fixed with respect to the link to which it is attached. In Appendix I it is further shown that the

condition to be satisfied on the k^{th} link of Figure 2.2 within a chain and with respect to the $\ell_k{}^{th}$ arc and point K is:

$$\mu_k.\lambda_k.e^{i\beta_k} + m_k.r_k.e^{i\gamma_k} + \ell_k.H(k-1)\sum_{n=1}^{k-1}(m_n+\mu_n) = 0 \qquad (2.1)$$

where k = subscript which identifies each link and its counterweights from the others in the chain (i.e. starting from the top link k=1, 2, ...s),

μ,m = mass of counterweight and link respectively,

r,γ = radial and angular polar co-ordinates respectively of the mass centre of a link with respect to the axis of its lower joint in the chain and the arc connecting this joint to the joint above it,

ℓ = length of an arc,

λ,β = radial and angular co-ordinates respectively of the mass centre of a counterweight referred to the axis of the lower joint of the link to which it is attached and the arc connecting this joint to the one above it in the chain,

H(i) = Heavyside unit operator (i.e. H(i)=1 for i>0 and H(i)=0 for i$\leqslant$0).

The above parameters are illustrated in Figures 2.1 and 2.2. Equation (2.1) defines a moment vector.

One important point to emerge from the analysis in Appendix I is a progressive increase in counterweight mass is incurred at each counterbalancing stage, owing to the need for counterbalancing the counterweights used higher up in the chain. Thus counterbalancing over chains with large numbers of links should be avoided.

2.3 The Dependence within a Loop

Berkof and Lowen [7] showed by example that not all the links of a linkage need be counterweighted. Later Tepper and Lowen [8] observed what they described as an 'apparent minimum' number of counterweights, namely n/2 where n is the number of links of the linkage. However, their work was restricted to single degree of freedom linkages, and the minimum defined by n/2 was not proved. But, from an examination of this work, it became clear that a loop has an important property, and this section of the thesis is concerned with evaluating it.

Consider a general loop, say loop QRSTQ of Figure 2.3. Link P of the loop is a general polygonal link and has a point mass M fixed at an arbitrary point A. Consequently the moment vector of a mass M with reference to point O and the arc QT is $M.\rho_p.e^{i\phi_p}$, see Figure 2.3. Mehmke's theorem [15] implies that the locus of a point on a rigid body can be expressed as a linear function of the loci of two other body points. From this, it follows that the locus of any mass centre, fixed in P, can be expressed as a function of the loci of two of the joints of P. Hence it can be deduced that the locus of the mass centres fixed in P can be related to the kinematics of two attached chains of links, if link P is connected to the frame link by two revolute-jointed chains of links. For example, the locus of a general fixed point, A in Figure 2.3, is equivalent to the summation of the two vectors, $\underset{\sim}{B}$ and $\underset{\sim}{C}$, each of which is a constant function of one of the attached chains of links (see Appendix II). The association of $\underset{\sim}{B}$ is with the RQ chain, where $\underset{\sim}{B}$ is a factored length ℓ'_a/ℓ_p of RQ and offset from it by a phase angle $\varepsilon'_a + \pi$. Similarly, the vector $\underset{\sim}{C}$ is associated with the STQ chain, where $\underset{\sim}{C}$ is a factored length ℓ_a/ℓ_p of STQ and offset from it by an angle ε_a. Consequently, the moment vector with reference to point Q and the arc ℓ_s of the mass M at A (i.e. $M.\rho_p.e^{i\phi_p}$) is equivalent to $M.\underset{\sim}{B} + M.\underset{\sim}{C}$. The conditions to eliminate the two vector components $M.\underset{\sim}{B}$ and $M.\underset{\sim}{C}$, by attaching counterweights to the links of the chains RQ and STQ respectively, are derived in Appendix III. To eliminate the vector component $M.\underset{\sim}{B}$, the mass term, M'_a, to be counterbalanced over each link within the RQ chain is:

$$M'_a = M.\frac{\ell'_a}{\ell_p}.e^{i(\varepsilon'_a+\pi)} \qquad (2.2)$$

Whilst to eliminate the time-variant part of the vector component $M.\underset{\sim}{C}$, the mass term, M_a, to be counterbalanced over the links in the ST chain is:

$$M_a = M.\frac{\ell_a}{\ell_p}.e^{i\varepsilon_a} \qquad (2.3)$$

The link TQ is the frame and so need not be considered. The mass terms defined by equation (2.2) and (2.3) are said to be 'assigned to' the force-balancing chains as their mass centre positions are referred to, rather than fixed in, the links of the chain.

Thus there is a linear dependency within a loop in that the locus of a point fixed in one of the links can be expressed as a linear function of the kinematics of the other links in the loop. Accordingly, the moment vectors of any masses fixed in one of the links within a loop can be made time-invariant without counterweighting the link. The link left uncounter-weighted will be called a 'dependent' link, since its balance is achieved using the dependency that exists within a loop.

If a dependent link is pivoted about a frame pivot then one of its counterweighted chains, namely that from the dependent link to the frame/pivot, is both stationary and of zero length. As a result, the mass assigned from the dependent link to this chain is assigned directly to a stationary point. Consequently, this chain needs no counterweights.

2.4 Prismatic Joints

Consider a loop QRSTOQ which contains s links all connected by revolute joints except links RS and ST which are joined by a prismatic joint, see Figure 2.4. In Appendix IV, it is shown that to balance these two links a counterweight does not have to be added to both of them. If the counter-weight is to be added to the first link met in going clockwise round the loop, i.e. link RS, then a moment vector, $\underset{\sim}{M}'_a$, is referred for elimination from link ST to RS and with respect to joint R and the arc ℓ_{k-1}. The moment vector $\underset{\sim}{M}'_a$ is shown, in Appendix IV, to be:

$$\underset{\sim}{M}'_a = M.\ell'_a.e^{i(\varepsilon'_a + \eta - \pi)} \qquad (2.4)$$

where M = the mass referred to or fixed in link RS,

ℓ_a' = radial offset of the mass centre of the mass M from the joint T,

ε_a' = angular offset between the arc ℓ_a' and the arc ℓ_k,

η = the angular separation of the arc ℓ_{k-1} from the arc ℓ_k in an anticlockwise direction.

Thereafter, the mass M, which now appears at joint T, is balanced down the chain of links TO.

Alternatively, if the counterweight is to be added to the second link, i.e. link ST, then a moment vector, $\underset{\sim}{M}_a$, is referred for elimination from link RS to ST, and specifically to the joint T and the arc ℓ_k. The moment vector $\underset{\sim}{M}_a$ is shown, in Appendix IV, to be:

$$\underset{\sim}{M}_a = M.\ell_a.e^{i(\varepsilon_a-\eta)} \qquad (2.5)$$

Thereafter, the mass M, which now appears at joint R, is balanced down the chain of links RQ.

Tepper and Lowen [8] showed that 'whenever a mechanism without axisymmetric link groupings does not contain a contour from each link to the ground by way of revolute joints only, it cannot be completely force-balanced'. Therefore, it can be deduced from this statement that a loop which contains at least two prismatic joints cannot be fully force-balanced. This is because those links lying between two prismatic joints of which none is a frame link have no such contour. Thus, to obtain a force-balance, each prismatic joint of a linkage must be contained in a loop containing no other such joint. The work of this thesis also shows that the link to be left uncounterweighted in a loop containing a prismatic joint must be one of the two links it connects.

2.5 Linkages formed from more than one Loop

Within a linkage, except in the limited case of those consisting of a single loop, (i.e. a four-bar linkage), parts of different loops will be formed

from the same link or links. In degenerate cases, the common links reduce to the pins of revolute joints, e.g. a ternary link becomes a binary link with a double joint. The existence of links in more than one loop causes the counterweighted chains of some loops to be incident on the counterweighted chains or dependent links of other loops. In the latter case, the chain will terminate at the dependent link and the force-balance of this chain is completed by the two counterweighted chains associated with this dependent link.

First consider the case of incidence between counterweighted chains. The incidence will occur at a common joint or link, and only involves the addition of the different moment vectors. From this, it is seen that counterweighted chains incident on one another merge to form one such chain.

Second consider the case where a counterweighted chain is incident on another dependent link. For example, observe the counterweighted chain, i.e. point W, of the dependent link G which terminates on the dependent link P in Figure 2.5. Previously it was shown that the mass m_g, of link G can be assigned as two mass terms to two points on link G, in this case points W and X. The mass assigned to W from equation (2.2) is:

$$m_g \cdot \frac{r'_g}{\ell_g} \cdot e^{i(\gamma'_g + \pi)}$$

For force-balance purposes this can be considered as fixed in W. Consequently it can be re-assigned to points R and S in the dependent link P using equation (2.2) and (2.3) respectively. The mass assigned to R is:

$$m_g \cdot \frac{r'_g}{\ell_g} \cdot e^{i(\gamma'_g+\pi)} \cdot \frac{\ell'_b}{\ell_p} \cdot e^{i(\varepsilon'_b+\pi)}$$

and to S is:

$$m_g \cdot \frac{r'_g}{\ell_g} \cdot e^{i(\gamma'_g+\pi)} \cdot \frac{\ell_b}{\ell_p} \cdot e^{i\varepsilon_b}$$

From this, it is seen that in transferring counterweighted chains over dependent links the link length factors are multiplicative whereas the offset angles are additive. It must be remembered that for this example there is still a term:

$$m_g . \frac{r_g}{\ell_g} . e^{i\gamma_g}$$

to be assigned to point X. Hence the moment vector of a mass fixed in link G can be represented by three mass terms assigned to R, S and X. To balance the masses fixed in G, the mass terms assigned to R, S and X will have to be balanced over the chains RQ, ST and XY respectively. Thus counterweighted chains, as defined by equation (2.1), cannot be considered in isolation. Provision must be made for masses which are either fixed in or assigned to the links of these counterweighted chains as a result of the incidence of other such chains.

Consider a general link, i.e. the k^{th} link, which forms part of a counterweighted chain, see Figure 2.6. Let there be x masses, M_t, assigned to the top joint, i.e. k/k-1, of the two joints that contain this link within the counterweighted chain in question. Assume also that this link has u other revolute joints; one is denoted by q, and y_q masses, M_d are assumed to be fixed in or assigned to it. Lastly assume that this link has v prismatic joints of which one is denoted by p. To this link, from the link connected by the p^{th} joint, are assigned z moment vectors, $\underset{\sim}{M}_b$, for elimination. On taking into account all the different assigned masses and moment vectors, the general force-balance condition to be satisfied on the k^{th} link can be formulated, and this is done with respect to the axis of the joint k/k-1 and the ℓ_k^{th} arc. This condition is:

$$\mu_k.\lambda_k.e^{i\beta_k} + m_k.r_k.e^{i\gamma_k} + \ell_k.H(k-1).\sum_{n=1}^{k-1}(m_n+\mu_n) +$$

$$\ell_k.H(x).\sum_{t=1}^{x} M_t + H(u).\sum_{q=1}^{u} \ell_q.e^{i\delta q} .H(y_q).\sum_{d=1}^{y_q} M_d + H(v).\sum_{p=1}^{v} .H(z_p).\sum_{b=1}^{z_p} \underset{\sim}{M}_b = 0 \qquad (2.6)$$

where k=1, 2, ...s for a counterweighted chain formed from s links.

The work in this and preceding sections has covered all the possible elementary cases of incidence between counterweighted chains and dependent links with or without prismatic joints. Consequently, equation (2.6) along with equations (2.2), (2.3), (2.4) and (2.5) form a necessary and sufficient set for establishing the force-balance conditions for any linkage capable of being balanced.

2.6 The Properties of a Loop

From the foregoing work, certain properties of a loop can be deduced. First, if a linkage which contains some prismatic joints can be fully force-balanced then each of its prismatic joints lies within a loop containing no other such joint. Second, a link can still be left uncounterweighted within a loop containing a prismatic joint, but it must be one of the links connected by this joint. Third, loops which do not contain prismatic joints have an arbitrary choice as to which of its links is left uncounterweighted. Fourth, based on a loop and emanating from the associated dependent link will be two counterweighted chains. Fifth, only one of the counterweighted chains of a loop may be connected to the associated dependent link by a prismatic joint. Sixth, each counterweight chain of a loop will proceed, via some of the links of the loop, towards frame pivots. Seventh, the loops do not all have to contain a frame link, since the balance of its links can be achieved via other loops. In other words, a loop can be attached to the frame link by any number of intermediate loops without destroying the theoretical capability of force-balancing the loop. This assumes that these intermediate loops do

not contain more than one prismatic joint. Some of these seven properties will be used in the next chapter to formulate a means of checking whether a linkage containing more than one prismatic joint can be fully force-balanced.

2.7. Example

The linkage mechanism of Figure 2.7 is used for feeding paper in a duplicating machine. Link AD rotates at constant speed and the paper is fed by link FG.

The balance conditions for the mechanism will now be determined. There are two loops which can contain a separate dependent link. For convenience, these are taken as the internal loop. One loop, loop AGFECDA, includes a prismatic joint, and so the link to be left uncounterweighted must be one of the two links this joint connects. Link AG of these two links is the frame, and therefore the link to be left uncounterweighted must be link FG. The other internal loop is ABCDA, and, from this loop, the link selected to be left uncounterweighted is link BCE.

2.7.1 To Balance Loop AGFECDA

Two counterweighted chains emanate from link FG. One is both of zero length and stationary, namely G which is on the frame. Consequently, the moment vector normally referred from link FG to joint A on link AG is already time-invariant, and so does not need to be eliminated. Link FE forms the initial part of the other attached counterweighted chain. This link is incident on link BCE which is a dependent link. Accordingly, at this joint, the mass terms associated with this counterweighted chain are transposed, using the relationships defined by equations (2.2) and (2.3), to the counterweighted chains of link BCE namely to joints C and B. For link FE, the force-balance condition to be satisfied with respect to point E and the arc FE is:

$$\mu_4.\lambda_4.\, e^{i\beta_4} + m_4.r_4.e^{i\gamma_4} + m_5.\ell_4 = 0 \qquad (2.7)$$

The mass now fixed at point E is $(m_5 + m_4 + \mu_4)$. This is now transposed to the counterweighted chains of link BCE, i.e. joints C and B, using the relationships (2.2) and (2.3). From equation (2.2), the mass term, M_5', referred to B is:

$$M_5' = (m_5 + m_4 + \mu_4).\frac{\ell_{3b}}{\ell_{3c}} .e^{i(\varepsilon_3'+\pi)} \qquad (2.8)$$

and the mass term, M_5, referred to joint C, from equation (2.3), is:

$$M_5 = (m_5 + m_4 + \mu_4) .\frac{\ell_{3a}}{\ell_{3c}} . e^{i\varepsilon_3} \qquad (2.9)$$

This completes the evaluation of the conditions for the counterweights used in this chain. Those appertaining to links AD and DC will be determined whilst considering the other loop, as they also include the effect of the dependent link of this loop.

2.7.2 To Balance Loop ABCDA

Link BCE is frame-pivoted, and so one of its associated counter-weighted chains is both of zero length and stationary, i.e. point B. From equation (2.2), the actual mass term, M_3', of link BCE assigned to the stationary point C, in addition to M_5', is:

$$M_3' = m_3.\frac{r_3'}{\ell_{3c}} . e^{i(\gamma_3' +\pi)} \qquad (2.10)$$

The other counterweighted chain associated with this loop is formed from links CD and DA. From equation (2.3), the mass term, M_3, assigned to joint C on this chain is:

$$M_3 = m_3.\frac{r_3}{\ell_{3c}} . e^{i\gamma_3} \qquad (2.11)$$

Since all the mass terms assigned to and fixed in link CD are known from equations (2.9) and (2.11), the counterweight condition for this link

may be determined from equation (2.6), and with respect to point D and the arc DC is:

$$\mu_2.\lambda_2.e^{i\beta_2} + m_2.r_2.e^{i\gamma_2} + \ell_2.\{m_3.\frac{r_3}{\ell_{3c}}.e^{i\gamma_3} + (m_5+m_4+\mu_4).\frac{\ell_{3a}}{\ell_{3c}}.e^{i\varepsilon_3}\} = 0 \qquad (2.12)$$

Having determined this condition, that to be satisfied on link DA may be established, and with reference to point A and the arc AD is:

$$\mu_1.\lambda_1.e^{i\beta_1} + m_1.r_1.e^{i\gamma_1} + \ell_1.\{m_3.\frac{r_3}{\ell_{3c}}.e^{i\gamma_3} + (m_5+m_4+\mu_4).\frac{\ell_{3a}}{\ell_{3c}}.e^{i\varepsilon_3} + m_2 + \mu_2\} = 0 \qquad (2.13)$$

On satisfying equations (2.7),(2.12) and (2.13) this linkage will be fully force-balanced.

2.8 Discussion

It is felt that the theory in this chapter can be extended into a spatial form, and so give the capability of establishing the balance conditions of spatial linkages. However, to do so, the restrictions on prismatic joints must be extended to any joint with a sliding pair axis, e.g. a cylindric joint. Additionally, equations (2.2), (2.3), (2.4), (2.5) and (2.6) must be re-derived in terms of spatial geometry. In regard to dependent links, it is felt that such links must lie within two loops which lie in separate planes. This will then enable its vector position in space to be defined in terms of the two associated chains of each of these loops. Note, however, that it is probable that one of these chains can be identical to each loop.

It was deduced by Tepper and Lowen [8] that for a linkage to be fully force-balanced in the absence of special geometries, a contour from each of its prismatic joints must exist to ground via only revolute joint connected links. In other words, a loop can only contain one prismatic joint.

However there are felt to be three special cases which can allow more than one prismatic joint per loop to exist. First, when two links have identical motions, the balance of one link can be obtained by counterweighting the other link, and so the counterweighted chain of one link is redundant. Secondly, when two links have equal and opposite motions, the inertia forces automatically cancel each other out so that no counterweights are required. This principle is used when balancing with mirror-image linkages [6]. Thirdly, when one link is undergoing pure rotation, an additional effective frame-pivot is provided, i.e. the axis of rotation of the link. This additional stationary point might provide other counterweighted chains which do not pass through any prismatic joints, and, because of the links from which they are formed, enable the balance of the linkage to be completed.

A means of determining the force-balance conditions of linkages has been devised without a need to examine either their generated inertia forces or mass centre trajectories. This is amply displayed by this example. However, as more complex linkages are encountered, it may sometimes be difficult to decide how many links may be left uncounter-weighted; which ones are the most advantageous to do so and with what loop is each of these uncounterweighted links associated, if any. Thus, in the succeeding chapter, the following questions will be examined,

i) How can a particular linkage be examined to see if it can be fully force-balanced?

ii) How many counterweights are required to balance a given linkage?

iii) Which links of a given linkage are the most advantageous to leave uncounterweighted?

2.9 Conclusion

Equations (2.2), (2.3), (2.4), (2.5) and (2.6) form a necessary and sufficient set by which the counterweight conditions for fully force-

balancing a planar linkage can be determined.

A major advantage of these equations is that the conditions for a force-balance can be written down directly instead of extracting them from the kinematic equations of the linkage.

Linkages possessing prismatic joints which appear only in loops containing other such joints cannot, in general, be fully force-balanced.

Pages Missing not Available

CHAPTER THREE

FURTHER THEORY RELATED TO THE FULL FORCE-BALANCE OF LINKAGE MECHANISMS

3.1 Introduction

This chapter is concerned with answering the three questions posed in the discussion section of the preceding chapter. First a method is sought for checking whether a linkage can be fully force-balanced with simple counterweights. Second the occurrence of a minimum in the required number of such counterweights to force-balance in the general case multi-degree-of-freedom linkages containing both prismatic and revolute joints is examined. The results confirm the 'apparent minimum' discussed by Tepper and Lowen [8]. Third, since for a given linkage there can be many alternative sets of simple counterweights which will fully force-balance it, a means is sought for guiding the choice towards the set most likely to give the greatest advantage.

3.2 Full Force-Balance Check

3.2.1 Prismatic Joints and Prohibited Links

This section is concerned with developing a technique for establishing whether a linkage can be fully force-balanced. Two factors which can destroy the ability to fully force-balance a linkage will be considered. The first was demonstrated by Tepper and Lowen [8]. They showed that to be able to completely force-balance a linkage a contour of revolute-joint-connected links must be traceable from each prismatic joint to the frame. In the light of Chapter Two, this contour rule is seen to check that a route exists from each link via revolute joints only, as only such connections provide the mutually stationary point needed between two links to achieve a force-balance. Specifically this point enables a mass centre lying in one link to be transferred to the other. Consequently a prismatic joint cannot lie within these contours, since it does not possess such a point.

The second factor arises when, because of space limitations, it is physically impossible to place counterweights on one or more links of a linkage. These uncounterweightable links will be termed 'prohibited links'. Chapter Two showed that within a loop of revolute-joint-connected links one link may be left uncounterweighted. This link is termed a dependent link. Accordingly, a prohibited link must be capable of being defined as a dependent link to enable its linkage to be fully force-balanced.

A prismatic joint which lies within a loop satisfies the contour theorem of Tepper and Lowen, because it is self evident that paths can be traced to the frame from each of these links without passing over this joint. Chapter Two showed that the dependent link of a loop containing a prismatic joint must be one of the two links this joint connects. Thus a prohibited link possessing one prismatic joint should be classed as the dependent link of that loop associated with this joint.

3.2.2 Loops

From above, it can be seen that loops provide a useful concept to use in full force-balance techniques for, by dividing the linkage into loops, the links that may be left uncounterweighted are more readily identified. Care must be taken in the division of a linkage into loops to ensure that each loop selected for a prismatic joint does not contain either a prohibited link not connected by this joint and which lies only in this loop or another prismatic joint. A similar argument applies to a loop selected for a prohibited link. This is necessary because one or both of the two counterweighted chains associated with each dependent link would be invalid, because they would contain either a prohibited link which lies in only one loop or a prismatic joint.

The loops must each contain an arc of a link not contained in any other loop: an arc is considered here as a line which is drawn between two joints of a link. This is because Appendix II shows that each dependent link requires its own unique loop of arcs to enable it to

remain uncounterweighted. Paul [16] showed that a linkage contains a specific number of such loops; he called them 'independent loops'. Deo [17] further showed that for any planar linkage the number of independent loops, L, is given by:

$$L = j - n + 1 \qquad (3.1)$$

where j = effective number of simple joints,
n = effective number of links.

A simple joint connects two links and has one degree-of-freedom. Consequently a multiple joint connecting i links counts as i - 1 simple joints. Similarly a joint with two degrees-of-freedom is equivalent to two simple joints connected by a link of zero length. For example, the pin in the slot of the scotch yoke mechanism in Figure 3.1 both rotates and slides relative to the sliding link. It is therefore equivalent to a revolute joint and a prismatic joint connected by a link of zero length. Accordingly, this linkage is considered to have two revolute joints, two prismatic joints and four links. It therefore contains one independent loop. Similarly the seven bar linkage in Figure 3.2 contains two independent loops.

It follows from this work that the total number of prismatic joints, p, and prohibited links, q, not associated with prismatic joints must not exceed the number of independent loops, L, i.e.

$$L \geqslant p + q \qquad (3.2)$$

This unequality does not ensure that the prismatic joints and the prohibited links are associated with appropriate independent loops.

3.2.3 Disconnections of Joints

A check that not more than one prismatic joint lies within each independent

loop is achieved by disconnecting these joints. Equation (3.1) shows that each disconnection eliminates an independent loop, and it is evident that they are those that contain these joints. If more than one prismatic joint lies within an independent loop, on disconnecting them the part not containing a contour to the frame will become completely detached from it. The work of Tepper and Lowen [8] can be used to show that it is these links which cannot be force-balanced, and thus cause the inability to fully force-balance the associated linkage.

Associated with each prismatic joint is a dependent link. Accordingly each prohibited link defined to be that dependent link of a prismatic joint need not be checked further.

A check can be formulated for the remaining unassociated prohibited links, which is also based on disconnecting joints. Each disconnection is used to retain an independent loop containing a prohibited link for the purpose of allowing this link to remain uncounterweighted. The disconnection eliminates the loop so that no attempt is made to use it for another such link. In practice, the disconnections are achieved by individually disconnecting a joint on each unassociated prohibited link, but it must be one which contains it within a still formed loop.

Prohibited links which possess only two joints lie only within one independent loop. Thus care must be taken to ensure a linkage is not wrongly classified as incapable of being fully force-balanced by unnecessarily eliminating this loop. For example, assume links BCG and AB of the seven-bar linkage of Figure 3.2 are prohibited. If joint B is disconnected to check the prohibited link BCG, the prohibited link AB is seen not now to lie within a loop. However, had it been joint C that was disconnected, this same link would still lie within a loop.

Such occurrences as these above can be avoided by progressively making that disconnection on that, as yet, undisconnected prohibited link which is connected to the frame by the least number of links. The joint disconnected is that one which connects this prohibited link to the chain of links formed from the least number of links. Because the prohibited link to be disconnected must be the less remote one, this rule first stops that loop containing a prohibited link with only two connected joints from being eliminated for a more remote prohibited link which lies both within this and other loops. A more remote link is connected to the frame by a greater number of links. Second, in the converse situation where the more remote link is the prohibited link with two connected joints, this rule ensures that this loop is retained for this link. This is because the chains of links detached from the less remote prohibited link will not contain it.

3.2.4 Ordering of Links

To enable these appropriate disconnections to be more easily identified, the links of a linkage are ordered. The frame is of order zero. Those attached to links of order one are order two. This is continued until all the links are ordered. This ordering starts at the frame and continues simultaneously along each of the chains until either a prismatic joint is met or two chains meet at a joint or on a link.

3.2.5 Ordered Disconnections of Revolute Joints

To check the prohibited links the joint disconnected first is that one which connects the, as yet, undisconnected lowest order prohibited link to the lowest order link. This is repeated until each prohibited link has been disconnected. If two prohibited links are of the same order there is an arbitrary choice as to which is disconnected first, because they must

both possess different but suitable chains of links. Another arbitrary choice is which of two links to detach from a prohibited link when both have the same order.

3.2.6 Example

Consider applying this check to the scotch yoke mechanism of Figure 3.1. On disconnecting the prismatic joints the sliding link becomes completely detached from the frame. Consequently this linkage cannot be fully force-balanced.

Now consider the seven-bar linkage of Figure 3.2 It has two independent loops and so two links may be left uncounterweighted. Two cases are considered. First assume that links BCG and HDE cannot be counterweighted and so are prohibited links. The links are ordered as shown by the numbers enclosed by squares in Figure 3.2. Links BCG and HDE have the same order. Arbitrarily the joint connecting link BCG to the lowest order link is detached first, i.e. joint B. The lowest order link connected to link HDE is joint E, but on disconnecting it links BCG, CD, GH and HDE become completely detached from the frame. Thus this linkage cannot be fully force-balanced with these restrictions.

Consider the second case where links BCG and GH are assumed to be prohibited. Joint B is disconnected first, since it connects the lowest order prohibited link, BCG, to the lowest order link, AB. Joints H and G both connect link GH to links having the same lowest order of those both connected to GH and lying within a still formed loop. Arbitrarily joint G is selected to be disconnected. No links have become completely detached from the frame in doing this, and so this linkage with these restrictions can be fully force-balanced.

3.3 The Minimum Number of Counterweights Required

It is seen that the number of independent loops within a linkage defines the number of its links which may be left uncounterweighted. Thus the number of counterweights, c, required to fully force-balance a given linkage possessing n links equals the number of moving links (i.e. n-1) minus the number of independent loops. Hence:

$$c = n-1-L \tag{3.3}$$

which, using equation (3.1), can be rearranged to give:

$$c = 2(n-1) - j \tag{3.4}$$

Consider the restricted case of linkages having only a single-degree-of-freedom. From Grubler's criterion [18], the number of degrees-of-freedom of a planar linkage, f, is:

$$f = 3(n-1)-2j \tag{3.5}$$

Hence, for single-degree-of-freedom linkages, this gives:

$$j = \frac{3}{2} n-2 \tag{3.6}$$

Eliminating j from equation (3.4) by the use of equation (3.6) the number of counterweights needed to fully force-balance single degree-of-freedom linkages, c_s, can be shown to be:

$$c_s = \frac{n}{2} \tag{3.7}$$

3.4 Selecting the Most Advantageous Set of Counterweights

For a given linkage, there can be many combinations of its links which may be counterweighted to give a full force-balance. Consider the inversion of the Stephenson chain shown in Figure 3.3. It contains six links and seven joints and so three counterweights are necessary for a force-balance.

Now there are five moving links and so there are 5!/(3!2!)=10 possible balance combinations. However, in two cases where the pair of binary links and the two ternary links respectively are left uncounterweighted, it is not possible to assign the dependent links to different independent loops. Hence there are only eight valid combinations and these are shown in Figure 3.3

The number of valid combinations may be different for different inversions of the same kinematic chain. For example, when one of the ternary links of the Stephenson chain is the frame, nine different combinations are valid. Some work was done to attempt to establish a formula for determining the number of ways of balancing a linkage. This will be considered in the discussion section. However of practical importance is the ability to select from amongst those sets of counter-weights that set which gives the best advantage.

In reference[19] it was realised that the addition of counterweights to a particular linkage caused increases as high as 100% or more in the observed r.m.s. and peak values of the bearing forces, driving torque and shaking moment. It has been observed whilst fully force-balancing a wide variety of linkages that these increases can usually be lessened by reducing the added counterweight inertia. The greatest reductions were achieved in practice by decreasing both the number of counterweights needing balancing and the number of times each is required to be balanced.

A typical linkage studied is the Watt's six-bar linkage of Figure 3.4. In the first case counterweights are attached to links FG, BCE and CDG. The incurred rises are shown in the first row of Table 3.1 The loads at the bearings of links EF and FG are not included, since in the two cases to be studied the counterweight is placed on link FG, and so the loads are identical for each case. In the second case, counterweights

are placed on links FG, AB and CDG, because this reduced both the number of times a counterweight is balanced and the total number of counterweights balanced. Specifically, instead of the counterweight on link FG needing balancing by that on BCE and then both of these by that on CDG, only the counterweight on FG needs balancing for this second set. The second row of Table 3.1 shows that a substantial reduction in the loads has been obtained with reference to those of the first set, i.e. row one.

Reductions such as those above have so far always been obtained by this approach, and never less than 20%. Accordingly this criterion is offered as a means of keeping the incurred rises in loads low when it is difficult to undertake the required analysis for every valid counterweight set. Thus the link to be left uncounterweighted in an independent loop having no previously assigned prohibited link or prismatic joint is one whose minimum number of links connecting it to the frame is the largest. A loop formed from an even number of links has one such link, but an odd-linked loop has two. In the latter case there is an arbitrary choice of which of the two links is left uncounterweighted. The above approach suggests that two counterweight sets for the Stephenson chain of Figure 3.3 are equally suitable, namely (a) and (b).

3.5 Discussion

This chapter confirms that to force-balance single-degree-of-freedom linkages the 'apparent' minimum number of counterweights is as stated by Tepper and Lowen [8], namely half the number of links in a linkage. They applied the term 'apparent' because they found certain mechanisms which could be balanced apparently with less than the minimum number, but they found in their studies that they always needed negative mass counter-weights.

The author knows such balances do exist, and for counterweights having positive mass. Consider a four-bar linkage constructed from uniform bars with no overhang. It normally requires two counterweights to balance it. Assume it to have been fully force-balanced by two appropriate counterweights. Next assume an increase in the mass of these counterweights. The resultant linkage can be re-balanced by the addition of a single counterweight to the coupler. A similar argument can be applied to a balance combination of the crank and coupler opposing the rocker or the coupler and rocker opposing the crank. Equally, these arguments can be applied to the six-bar linkage examined by Tepper and Lowen in Appendix 2 of their paper. Thus, while the minimum number of counterweights defined by equation (3.4) applies in the general case, a smaller number may be sufficient in particular cases.

Further criteria exist to establish advantages between different counterweight sets, e.g. incurred rises in the bearing loads, driving torque fluctuations and out of balance couples. However, to use these criteria a significant and perhaps unjustifiable increase in required analysis time is needed. Even with the aid of computer-based dynamic analysis programs this could still prove prohibitive. Consequently for the purpose of this chapter these criteria have been omitted.

In section 3.4 it is stated that some work had been done in attempting to establish a formula which would define how many ways there are to balance a given linkage. Some initial work showed that this relationship is complex in nature. For instance, the particular inversion of the Watt's chain of Figure 3.5 has only six valid ways of being balanced whilst the Stephenson chain of Figure 3.3 has eight. However both these linkages have identical numbers of stationary and moving joints; ternary and binary links and independent loops. Consequently other factors are involved. The major distinction between these two linkages is that the Stephenson

chain has four moving joints attached to frame pivoted links whilst the Watt's linkage has only three. It is felt that this tends to define how many counterweighted chains converge onto these links and so specify the number of routes over which a balance can be achieved. Thus, this is seen as a possible factor to be used in attempting to establish a formula for the number of valid counterweight sets. However, because of both the increasing complexity of the problem and the fact that no decisive advantage can be gained from its solution, it was abandoned at this stage.

Epstein and Steinvolf [20] have stated that, for minimum additional moment of inertia, a counterweight should be cylindrical with its circumference intersecting the combined centre of mass of the counterweight and masses it is balancing, see Figure 3.6. The counterweight should also be as long as possible. However, a further reduction in the moment of inertia can be achieved by attaching the counterweight to its particular link via a bearing, see Figure 3.7. Assuming the bearing friction is negligible, this eliminates the effect of the moment of inertia of the counterweight about its centre of gravity. To examine the practicality of this idea a set of counterweights is tested experimentally. An account of the test is contained in Chapter Seven.

The type of counterweight discussed by Epstein and Steinvolf is ideal where the combined centre of mass is at a frame pivot. However it is more difficult to determine the best shape and position for a counterweight that is itself balanced by other counterweights, since its mass will affect the mass of these others. For example, decreasing the mass of a counterweight and placing it at a correspondingly larger offset will further increase the combined moment of inertia of the link and counterweight. On the other hand, the complete chain of counterweights might,

as a result, have a lower total moment of inertia and mass. Probably the most practical approach to establish the optimum ratio of mass and radial offset for such a counterweight would be a computer-based numerical minimization technique.

3.6 Conclusion

Answers to the three questions posed in the introduction have been obtained as follows: (i) a set of three rules for checking whether a linkage can be balanced was developed, (ii) a formula for determining how many counterweights are required to balance a linkage was derived and (iii) in the absence of being able to analyse the effects of each possible counterweight set, a means is presented for identifying which links are most likely to yield the greatest advantage if left uncounterweighted.

CHAPTER FOUR

DEVELOPMENT OF A PROCEDURE FOR FORCE-BALANCING LINKAGES

4.1 Introduction

The purpose of this chapter is to develop a procedure for fully force-balancing planar linkages using simple counterweights. This procedure is intended to supersede a previous one developed with Dr. K. Oldham [21], as a number of limitations are identified in this first one. First it is realised that the check as to whether a linkage can be force-balanced may eliminate some linkages unnecessarily. This is clearly identified with the example of the seven-bar linkage in section 3.2.3 of Chapter Three. Second, it is now felt that a more meaningful and ordered means of identifying the masses each counterweight must balance has been developed. Third, the complex equation used to define the counterweight condition to be satisfied on a general link can be simplified. In particular, most of the terms involved in this equation can now be eliminated by inspection.

The work of this chapter consists of four parts. First a method is developed for identifying the masses a counterweight must force-balance. Second, the equation defining the general counterweight condition is re-arranged to enable terms to be eliminated by inspection. Third, the newly developed procedure is presented. As such, it again presents some of the equations and methods developed in earlier chapters. Fourth, the ease of use of this procedure is demonstrated by using it to obtain a force-balance of a two-degree-of-freedom nine-bar linkage which possesses three links which are impractical to counterweight.

4.2 Determining the Masses a Counterweight Must Force-Balance

By finding the counterweighted chains, the routes over which the positions of the mass centres of the linkage are transferred to the frame are known; and thus, in turn, the masses each counterweight must force-

balance are identified.

To identify the counterweighted chains, the independent loops can be used in conjunction with the order numbers used for the force-balance check of Chapter Three. Deo [17] showed that these loops can be identified by temporarily re-connecting the joints previously disconnected, but such that only one remains connected at any one time. This causes the independent loop associated with the reconnected joint to be formed.

Now, from the previous chapters, it is known that two counterweighted chains emanate from the dependent link of an independent loop and proceed towards the frame via links having an equal or descending order number. These counterweighted chains will then terminate at the frame unless, as described in Chapter Two, they are incident on either another such chain or a dependent link of another loop. An order of making reconnections will be used to ensure that the counterweighted chains are not too long. This has been found, in practice, to aid the formulation of the counterweight conditions. Accordingly the joints are reconnected starting with that connected to the lowest order link and continuing up to that connected to the highest order link.

A means of recording each of the identified counterweighted chains is needed. One way would be to label each of the joints of the linkage in question. Then, as each counterweighted chain is identified, the letters that lie on its route can be noted. In doing this, if a dependent link of another loop is met the counterweighted chain will be said to stop here, because the force-balance is transferred to the two counterweighted chains of this link. Also a counterweighted chain which is incident on another whose route has already been identified will be considered to have terminated at this chain, and its force-balance transferred to this previously identified chain.

4.3 A Simplification to the Counterweight Condition to be Satisfied on a General Link

Equation (2.6) of Chapter Two can be separated into three parts. Consider a chain of s links starting at link 1 and continuing via the k^{th} link onto the s^{th} link. The counterweight on a general link, i.e. the k^{th} link, must eliminate the moment vector, $\underset{\sim}{M}_v$, which is a result of the mass of the k^{th} link and those of the k-1 links and counterweights higher in the chain. Chapter Two shows that this moment vector with reference to the $k/k+1^{th}$ joint and the ℓ_k^{th} arc is:

$$\underset{\sim}{M}_v = m_k.r_k.e^{i\gamma_k} + \ell_k.\sum_{n=1}^{k-1}(m_n+\mu_n) \qquad (4.1)$$

The Heavyside unit operators used in the equations of Chapter Two are omitted to simplify the equations for use in the procedure. Instead a sentence will be appropriately placed at the beginning of the procedure which says 'if the upper limit of any summation in this procedure is less than the lower limit, the summation is equal to zero'.

There is another moment vector, $\underset{\sim}{M}_d$, which must also be considered, and it is the result of counterweighted chains being incident on the dependent link and the links higher than the k^{th} link in this chain. Two cases need to be considered. First when the joint connecting the k^{th} link to the one above it in the chain is revolute, and second when

1. A term of the form k/k+1 is used to define a joint, and in this case it is the one which connects the k^{th} link to the $k+1^{th}$ link.
2. The ℓ_k^{th} arc is the line drawn between the $k/k+1^{th}$ and $k/k-1^{th}$ joints.

this joint is prismatic. If the joint is revolute, y mass terms each defined by M_w are assumed to have been assigned to the associated dependent link and the k-1 links between this link and the k^{th} link. The positions of the mass centres of all these masses will now appear at the $k/k\text{-}1^{th}$ joint, as a result of the counterweights added to the k-1 links. Thus the moment vector, $\underset{\sim}{M}_d$, to be eliminated by the k^{th} counterweight is:

$$\underset{\sim}{M}_d = \ell_k . \sum_{w=1}^{y} M_w \qquad (4.2)$$

For the second case, when the $k/k\text{-}1^{th}$ joint is prismatic, the work of Chapter Two shows that the $k\text{-}1^{th}$ link must be the dependent link. Also, it is known that any masses which lie on this dependent link are each referred as a moment vector, say $\underset{\sim}{M}_p$, to the k^{th} link by the use of either equation (2.4) or (2.5) in Chapter Two. Accordingly, if z masses are assumed to lie in this link, the moment vector, $\underset{\sim}{M}_d$, to be eliminated on the k^{th} link is:

$$\underset{\sim}{M}_d = \sum_{p=1}^{z} \underset{\sim}{M}_p \qquad (4.3)$$

By the use of a factor q which is zero when the $k/k\text{-}1^{th}$ joint is prismatic and unity when it is revolute, the two expressions for $\underset{\sim}{M}_d$ can be combined to form one equation, namely:

$$\underset{\sim}{M}_d = (1-q). \sum_{p=1}^{z} \underset{\sim}{M}_p + q.\ell_k . \sum_{w=1}^{y} M_w \qquad (4.4)$$

If the k^{th} link possesses more than two joints, counterweighted chains can be incident at joints other than the $k/k\text{-}1^{th}$ joint. This gives rise to a moment vector, $\underset{\sim}{M}_c$, which must be eliminated. For a link with u joints there are u-2 joints to consider, i.e. those other than the

k/k+1th or k/k-1th joints. Consider the jth joint of the u-2 other joints. If it is revolute assume x mass terms each defined by M_t are assigned to the jth joint. Alternatively, if the jth joint is prismatic, assume g masses lie in the link this prismatic joint connects to the kth link. This link will be the dependent link of another independent loop. Consequently g moment vectors, $\underset{\sim}{M}_f$ are assigned to the jth arc of these u-2 other arcs at the k/k+1th joint. Now the moment vector, $\underset{\sim}{M}_c$, with reference to the $\ell_k{}^{th}$ arc and the k/k+1th joint can be expressed by one equation for both cases by again using the factor q for each of the u-2 joints. Accordingly the moment vector $\underset{\sim}{M}_c$ with reference to the $\ell_k{}^{th}$ arc and the k/k+1th joint can be expressed as:

$$\underset{\sim}{M}_c = \sum_{j=1}^{u-2} \left[(1-q_j).e^{i\varepsilon_j}. \sum_{f=1}^{g} \underset{\sim}{M}_f + q_j.\ell_j.e^{i\varepsilon_j}. \sum_{t=1}^{x} M_t \right] \qquad (4.5)$$

where ℓ,ε = the radial and angular co-ordinates of the jth joint with reference to the $\ell_k{}^{th}$ arc at the k/k+1th joint.

From equation (2.6) of Chapter Two, it can be seen that combining the terms $\underset{\sim}{M}_v$, $\underset{\sim}{M}_d$ and $\underset{\sim}{M}_c$ forms the counterweight condition to be satisfied on a general link. That is:

$$\mu_k.\lambda_k.e^{i\beta_k} + \underset{\sim}{M}_v + \underset{\sim}{M}_d + \underset{\sim}{M}_c = 0 \qquad (4.6)$$

The advantage of this equation over the corresponding one in either Chapter Two or reference [21] is that terms can be eliminated more easily by inspection. First $\underset{\sim}{M}_v$ reduces to $m_k.r_k.e^{i\gamma_k}$ if the kth link is the first in the counterweighted chain. Second, noting whether a revolute or prismatic joint connects the kth link to the link from which masses or moment vectors are assigned enables the appropriate term, i.e. $\underset{\sim}{M}_d$ or $\underset{\sim}{M}_c$, to be simplified. Third, if the kth link has only two joints the term $\underset{\sim}{M}_c$ is eliminated.

This section completes the development of the methods and equation needed for the full force-balance procedure. The next section contains this procedure, and it is intended to be entirely independent of this thesis except for section 4.5 and Figures 3.6 and 4.1 to 4.3.

4.4 A Procedure for Fully Force-Balancing Planar Linkage Mechanism using Simple Counterweights

A simple counterweight has a constant mass with its mass centre fixed with respect to the link to which it is attached.

4.4.1 To Check whether a Linkage Mechanism can be Fully Force-Balanced

Not all linkage mechanisms can be fully force-balanced, and so each must be checked to see that it can. The check has two stages. First, all the prismatic joints (sliding joints) are disconnected. If any links become completely detached from the frame in doing this, the linkage mechanism cannot be fully force-balanced.

Second, those links which cannot be counterweighted because of practical constraints, e.g. space limitations, must be checked. If such a link is connected by a prismatic joint it is eliminated from this check, but only one such link is eliminated for one such joint. The remaining uncounterweightable links are checked by disconnecting joints. To identify the joints which are to be disconnected the links are ordered. The frame is of order zero; the links connected to the frame are of order one and the unordered links connected to links of order one are order two etc. This is continued simultaneously along each of the chains of links emanating from the frame until either a disconnected prismatic joint is met or two chains meet either at a revolute joint or on a link. Typically a linkage is ordered as shown in Figure 4.2. The disconnections are made sequentially by disconnecting the joint on the lowest, as yet still disconnected uncounterweightable link which both contains this link within a closed loop of links and connects it to the lowest order link.

If there is more than one such link or joint, an arbitrary choice exists for both cases, i.e. which link to check first and which joint is disconnected to check a link. This is continued until all the uncounterweightable links have had an appropriate joint disconnected, and, if this is possible, the linkage mechanism may be fully force-balanced.

4.4.2 A Method to Indicate Suitable Links to Leave Uncounterweighted

After completing the full force-balance check it may be found that there are still some formed loops of links. These loops will allow other links to be left uncounterweighted. The actual links which may be left uncounterweighted are those that lie within still formed loops of links. On selecting a link to be left uncounterweighted a joint which both contains this link within a still formed loop and connects it to the lowest order link attached to it is disconnected. This is repeated with other links in other still formed loops until no loops remain. Obviously, different selections of these links will yield different counterweight sets.

Each counterweight set generally causes each of the loads, e.g. bearing forces, driving torque and out of balance couple, to rise by different amounts. Consequently it is advantageous to select those links to be left uncounterweighted which cause the lowest set of rises in the more critical loads, whatever these loads may be. If the time taken to find the optimum set is too great, a means presented in this procedure for selecting suitable links can be used. The links selected are those which are more likely to yield the lower rises in all the above mentioned loads. The link selected is that one which has both the highest order and lies within a still formed loop of links. The selection is again finalized by disconnecting one of the joints of this link which both connects it to the lowest order link attached to it and contains it within the closed loop. This process is repeated until no loops remain.

4.4.3 Identification of the Routes over which the Positions of the Mass Centres are Transferred to the Frame

The routes over which the positions of the mass centres are transferred to the frame are found by reconnecting a disconnected joint, but in such a way that only one is reconnected at any one time. The joints are connected in an order. First on the lowest order link to be left uncounterweighted and continuing for increasing order numbers, to end at that link to be left uncounterweighted which has the highest order. Each reconnection causes a loop to form. Two chains emanate from the link to be left uncounterweighted whose joint was just reconnected, and proceed down the links of the formed loop towards the frame. It is down these chains that the positions of both the mass centre of the link left uncounterweighted and those of the links forming these chains are transferred to the frame by the use of appropriate counterweights. Hence these chains must be recorded. This is done by labelling each joint, and then recording the sequence of letters met in traversing each chain.

A chain is said to terminate if, when identifying it, one of the links forming it is found to be one to be left uncounterweighted. The chain is considered to have terminated at this latter link. In such a case the force-balance is transferred to the two chains which will emanate from this link.

A chain is also considered to have terminated if it intersects with another already identified chain, in which event the force-balance is transferred to this other chain. Again this event must be recorded.
If a chain does not terminate either on another chain or a link to be left uncounterweighted, it will terminate at the frame. Once the identification of these routes is complete the counterweight conditions can be formulated.

4.4.4 The Terms Referred from Links to be Left Uncounterweighted

To find the terms referred from links to be left uncounterweighted

and eventually the conditions for force-balance counterweights must satisfy, a consistent way of specifying the parameters of a link is needed. The terms used for link P are illustrated in Figure 4.1. Note that the parameters on that side of the link met first in going clockwise around the smallest loop containing it and the frame link are undashed whilst those on the other side are dashed. An additional subscript is added to each parameter to identify the link to which it refers.

A number of formulae are used to find the terms referred from a link to be left uncounterweighted. Assume link P in Figure 4.1 is left uncounterweighted and that both its joints, C and D, are revolute. Then, for a mass M whose mass centre lies in link P at point G, two mass terms, M_a' and M_a, are referred to the two attached chains of links, namely to points C and D respectively. These two mass terms are:

$$M_a' = M.\frac{\ell_a'}{\ell_p} . e^{i(\varepsilon_a'+\pi)} \qquad (4.7)$$

and:

$$M_a = M.\frac{\ell_a}{\ell_p} .e^{i\varepsilon_a} \qquad (4.8)$$

The terms M_a' and M_a identify masses which do not lie on the chains to which they are referred. In fact they lie on a scaled and offset version, where the scaling is the link length ratio and the offset the angle contained in the expression defining them. Consequently these angles and link ratios associated with the mass M appear at the point of balance after each counterweighting stage. Accordingly the complete term, e.g. M_a, is treated as a mass for force-balance purposes. This includes the situation when one is referred to another link to be left uncounterweighted. In such a case the mass term is referred as two new terms from this latter link using equations (4.7) and (4.8), in which event the associated length ratios are seen to be multiplicative and the angles additive.

Next assume joint C of link P is prismatic. For this case and for the same mass M lying at G in link P, a mass M is referred to point D and a 'moment vector', $\underset{\sim}{M}_s$, referred for elimination to point B and the 'arc' BC. The 'moment vector' is given by:

$$\underset{\sim}{M}_s = M.\ell_a.e^{i(\varepsilon_a - \eta)} \qquad (4.9)$$

The above parameters are illustrated in Figure 4.1. A 'moment vector' is the term used to describe the product of a mass and the position of its mass centre with reference to a co-ordinate system, whilst an 'arc' refers to a line drawn between two points, e.g. the line between points B and C.

Now make the alternative assumption that joint D is prismatic whilst C is revolute. For this case and a mass M lying at point G in link P, a mass M is referred to point C and a moment vector, $\underset{\sim}{M}_s'$, referred to point E and the arc ED. The moment vector, $\underset{\sim}{M}_s'$, is defined by:

$$\underset{\sim}{M}_s' = M.\ell_a'.e^{i(\varepsilon_a' - \eta')} \qquad (4.10)$$

The above parameters are illustrated in Figure 4.1.

4.4.5 Formulating the Counterweight Condition

Consider a general link, say the k^{th} link, which lies within a chain of s links. The chain starts at a link connected to a link to be left uncounterweighted and ends at the s^{th} link. The condition the counterweight on the k^{th} link must satisfy is:

$$\mu_k.\lambda_k.e^{i\beta_k} + \underset{\sim}{M}_v + \underset{\sim}{M}_d + \underset{\sim}{M}_c = 0 \qquad (4.11)$$

This condition is defined with reference to the line drawn between the two joints containing the k^{th} link within this chain, i.e. the $\ell_k{}^{th}$ arc, and the axis of that joint connecting the k^{th} link to the one below it, namely the $k/k+1^{th}$ joint. The terms in the above equation are:

μ = mass of the counterweight,
λ, β = the position of the mass centre of the counterweight with reference to the ℓ_k^{th} arc and the k/k+1th joint.

The term $\underset{\sim}{M}_v$ is a result of the mass of the k^{th} link and each of the masses, m_n and μ_n, of the k-1 links and attached counterweights higher than the k^{th} link in the chain. It is given by:

$$\underset{\sim}{M}_v = m_k.r_k.e^{i\gamma_k} + \ell_k.\sum_{n=1}^{k-1}(m_n+\mu_n) \qquad (4.12)$$

If the upper limit of any summation in this procedure becomes less than the lower limit the summation is equal to zero, e.g. if k-1<1 in the above equation then $\sum_{n=1}^{k-1}(m_n+\mu_n)=0$.

The term $\underset{\sim}{M}_d$ is a result of either masses or moment vectors being assigned to both the link to be left uncounterweighted and the k-1 links of this chain above the k^{th} link. Two cases need to be considered. First when the k^{th} link is both the first link in the chain and is connected to the link to be left uncounterweighted by a prismatic joint. For this case, assume y masses lie in the link to be left uncounterweighted. Thus y moment vectors must be eliminated, where each is referred to the ℓ_k^{th} arc and the k/k+1th joint. Each of these moment vectors is defined by either equation (4.9) or (4.10). Now consider the second case when the k^{th} link is connected to the one above it by a revolute joint. In this case this latter link may be either the one left uncounterweighted or one of the k-1 links. Assume in all that y masses lie in the link to be left uncounterweighted and the k-1 links. The mass centres of these y masses will have been caused to lie at the k/k-1th joint, as a result of the previously attached k-1 counterweights. Hence each of the y masses, M_w, must be counterbalanced over the arc ℓ_k. Both this and the previous case are catered for by the same equation, namely:

$$\underset{\sim}{M}_d = (1-q).\sum_{p=1}^{y}\underset{\sim}{M}_p + q.\ell_k.\sum_{w=1}^{y}M_w \qquad (4.13)$$

where q=0 when the joint connecting the k^{th} link to the link to be left uncounterweighted is prismatic,
q=1 when the joint connecting the k^{th} link to the one above it in the chain is revolute.

If the k^{th} link possesses more than two joints, chains can be incident on this link at these additional joints. This gives rise to the term $\underset{\sim}{M}_c$. For each additional joint, two cases similar to those for the term $\underset{\sim}{M}_d$ occur. Assume the k^{th} link has u joints, and consider the j^{th} joint of these u-2 additional joints. If it is prismatic assume g masses lie in the link it connects to the k^{th} link (this other link will be one which is to be left uncounterweighted). For this case g moment vectors are assigned to the $\ell_j{}^{th}$ arc and the $k/k+1^{th}$ joint. Each moment vector is defined by either equation (4.9) or (4.10). Note that the angular offset between the $\ell_j{}^{th}$ and $\ell_k{}^{th}$ arcs must be accounted for, since the moment vector $\underset{\sim}{M}_c$ is defined with reference to the $\ell_k{}^{th}$ arc. The other case is when the j^{th} joint is revolute. In this situation assume x masses are assigned to the j^{th} joint, where each such mass is identified by the term M_t. Both cases are catered for by the same equation, namely:

$$\underset{\sim}{M}_c = \sum_{j=1}^{u-2} \left[(1-q_j).e^{i\varepsilon_j}. \sum_{f=1}^{g} \underset{\sim}{M}_f + q_j.\ell_j.e^{i\varepsilon_j}. \sum_{t=1}^{x} M_t \right] \qquad (4.14)$$

where: q_j = 0 when the j^{th} joint is prismatic,
q_j = 1 when the j^{th} joint is revolute,
ℓ_j, ε_j = radial and angular offset of the j^{th} joint from the $\ell_k{}^{th}$ arc and the $k/k+1^{th}$ joint.

Before calculating the counterweight parameters the component angles in the above equations should be added. Thus $e^{i\gamma_1}.e^{i(\varepsilon_2+\pi)} + e^{i(\gamma_2+\pi)}.e^{i(\gamma_5+\pi)}$ becomes $e^{i(\gamma_1+\varepsilon_2+\pi)} + e^{i(\gamma_2+\gamma_5)}$.

4.5 Example

4.5.1 Description of the Linkage to be Fully Force-Balanced

Figure 4.3 is a photograph of a two-degree-of-freedom nine-bar linkage. The linkage is the needle mechanism for a textile machine which produces a double-faced pile fabric. A schematic layout of the linkage is

presented in Figure 4.2, and a table of its inertial and kinematic parameters is given in Table 4.1.

A two component motion of this linkage mechanism is accomplished by having the two degrees of freedom of the linkage specified by two separate conjugate cam systems. The inputs are to links AB and JA, see Figure 4.3. In its industrial environment, this linkage is found to perform its kinematic function well, but, in doing so, large inertia forces are generated which cause the machine to shake. The extent of the shaking is such that it is necessary to balance the linkage. As the major problem appears to be a translational imbalance, it is felt that a force-balance might be appropriate. Hence the procedure of section 4.4 will be used to find a full force-balance providing it shows that such a balance is possible.

4.5.2 Full Force-Balance Check

The photograph of Figure 4.3 shows that there are three links which would be difficult to counterweight because of space limitations, namely links HJ, EF and DE. There are no prismatic joints to disconnect. The linkage is ordered as shown by the numbers enclosed in squares in Figure 4.2. All the uncounterweightable links are of order two. Thus the choice as to which to consider first is arbitrary. Joint J of link HJ is disconnected first. Next joint E of link DE is disconnected. In this case joint E is a double joint in that it connects three links together. Only link DE is disconnected from links EF and EK: the latter two links remain connected. Finally joint F for link EF is disconnected. Since suitable disconnections could be made for each uncounterweightable link, this linkage mechanism may be fully force-balanced.

4.5.3 Selecting the Links to be Left Uncounterweighted

No closed loops of links remain after the disconnections of the full force-balance check. Consequently there are no more links which may be left uncounterweighted.

4.5.4 Identifying the Routes over which the Positions of the Mass Centres are Transferred to the Frame

All the disconnected joints lie on similar low order uncounterweightable links. Consequently the order in which these joints are reconnected is arbitrary. Joint J of link HJ is reconnected and forms the loop AJHGA. Joint J is disconnected again. Next joint F of link EF is reconnected and forms the loop GFEKG. It is also disconnected again. Finally joint E of link DE is reconnected and forms the loop ABDEKA.

The first link reconnected was HJ and its loop is AJHGA. From this, it is seen that the two chains which must emanate from HJ are based first on link JA and second on link FGH. Link EF was the next link reconnected and its loop is GFEKG. The two chains can be seen to be link FGH and link EK. However link FGH is already defined to be one of the chains associated with link HJ. Thus the chain, link FGH, of link EF is now said to be the point F which is incident on the chain, link FGH, of loop AJHGA. The last link to consider is DE and its loop is ABDEKA. Consequently its two chains are first links AB and BD and second link EK. However link EK is one of the chains of link EF. Hence the second chain of loop ABDEKA is re-defined to be point E which is incident on the chain EK.

4.5.5 Determining the Masses a Counterweight Must Force-Balance

4.5.5.1 Formulation of the counterweight condition for link JA

Link JA is the first one of its chain and so the moment vector, $\underset{\sim}{M}_{v_1}$, can be determined using equation (4.12). It is:

$$\underset{\sim}{M}_{v_1} = m_1 . r_1 . e^{i\gamma_1} \tag{4.15}$$

From equation (4.8), the mass term, M'_{a_2}, assigned to link JA is:

$$M'_{a_2} = m_2 . \frac{r'_2}{\ell_2} . e^{i(\gamma'_2+\pi)} \tag{4.16}$$

This is the only mass term assigned to link JA and so the moment vector $\underset{\sim}{M}_{d_1}$ from equation (4.13) is:

$$\underset{\sim}{M}_{d_1} = M'_{a_2}.\ell_1 \qquad (4.17)$$

Note that the q's in equation (4.13) and (4.14) are unity for all cases for this linkage mechanism, since it possesses no prismatic joints. The term $\underset{\sim}{M}_{c_1}$ is zero, because link JA has only two joints.

All the moment vectors of equation (4.11) have now been determined for link JA. Thus the counterweight condition can now be written down, and, with reference to point A and the arc AJ, it is:

$$\mu_1.\lambda_1.e^{i\beta_1} + m_1.r_1.e^{i\gamma_1} + m_2.\frac{r'_2}{\ell_2}.e^{i(\gamma'_2+\pi)}.\ell_1 = 0 \qquad (4.18)$$

This completes the evaluation of the chain JA of link HJ.

4.5.5.2 Formulation of the counterweight condition for link FGH

The second chain associated with link HJ is based on link FGH. This chain has masses assigned to it from the point-chain F of loop GFEKG. Consequently the assigned masses must be found. Referred to F is a mass term, M_{a_7}, from the link EF which is to be left uncounterweighted. From equation (4.8) this term is:

$$M_{a_7} = m_7.\frac{r_7}{\ell_7}.e^{i\gamma_7} \qquad (4.19)$$

The mass m_7 is the only one which lies in link EF, and so the masses assigned from F to FGH are known. Link FGH is a ternary link (a ternary link has three joints), and the chain based on it uses the route arc HG. It is this arc to which the counterweight conditions will be referred. This link is the first one in this chain and so the moment vector $\underset{\sim}{M}_{v_3}$, with reference to G and the arc GH is:

$$\underset{\sim}{M}_{v_3} = m_3.r_3'.e^{i(\gamma_3'+\pi)} \tag{4.20}$$

A mass term is assigned from link HJ to point H, and from equation (4.9) is:

$$M_{a_2} = m_2.\frac{r_2}{\ell_2}.e^{i\gamma_2} \tag{4.21}$$

No other terms are assigned to joint H on the reference arc, and therefore the moment vector, $\underset{\sim}{M}_{d_3}$, may be determined. With reference to point G and the arc GH it is:

$$\underset{\sim}{M}_{d_3} = m_2.\frac{r_2}{\ell_2}.e^{i\gamma_2}.\ell_{3c} \tag{4.22}$$

The point chain F is incident on this chain, and in being so a mass M_{a_7}' is assigned to link FGH at F. Other than this no other chains are recorded as being incident on link FGH. Accordingly the moment vector, $\underset{\sim}{M}_{c_3}$, may be determined, and with reference to G and the arc GH is:

$$\underset{\sim}{M}_{c_3} = m_7.\frac{r_7}{\ell_7}.e^{i\gamma_7}.\ell_{3b}.e^{i(\varepsilon_3'+\pi)} \tag{4.23}$$

The three moment vectors associated with link FGH have been determined. Thus the counterweight condition for this link may be written down, and with reference to G and the arc GH, this is:

$$\mu_3.\lambda_3.e^{i\beta_3}+m_3.r_3'.e^{i(\gamma_3'+\pi)}+m_2.\frac{r_2}{\ell_2}.e^{i\gamma_2}.\ell_{3c}+m_7.\frac{r_7}{\ell_7}.e^{i\gamma_7}.\ell_{3b}.e^{i(\varepsilon_3'+\pi)} \tag{4.24}$$

4.5.5.3 Formulation of the counterweight condition for link EK

Link EK is the only link in the chain considered next. This link is a ternary link, but, since one joint is a double joint, it effectively has only one arc to which moment vectors are referred. Link EK is the

first link in the chain, and so the moment vector, $\underset{\sim}{M}_{v_8}$, with reference to point K and the arc KE is:

$$\underset{\sim}{M}_{v8} = m_8.r_8.e^{i\gamma_8} \tag{4.25}$$

A mass term M'_{a_7} is assigned to link EK at E and is given by:

$$M'_{a_7} = m_7.\frac{r'_7}{\ell_7}.e^{i(\gamma'_7+\pi)} \tag{4.26}$$

Another mass is also assigned to point E, because the point-chain E of link DE is incident here. The only mass lying in DE is m_6, and so the mass term, M_{a_6}, assigned to point E is:

$$M_{a_6} = m_6.\frac{r_6}{\ell_6}.e^{i\gamma_6} \tag{4.27}$$

These are the only mass terms assigned to point E, and therefore the moment vector $\underset{\sim}{M}_{d_8}$ can be written down. With reference to point K and the arc KE, this is:

$$\underset{\sim}{M}_{d_8} = (m_6.\frac{r_6}{\ell_6}.e^{i\gamma_6} + m_7.\frac{r'_7}{\ell_7}.e^{i(\gamma'_7+\pi)}).\ell_8 \tag{4.28}$$

Link EK is effectively a binary link and thus the moment vector $\underset{\sim}{M}_c$ is zero.

The counterweight condition for link EK may now be written down, since the three moment vectors associated with it are known. With reference to point K and the arc KE, this condition is:

$$\mu_8.\lambda_8.e^{i\beta_8} + m_8.r'_8.e^{i(\gamma'_8+\pi)} + (m_6.\frac{r_6}{\ell_6}.e^{i\gamma_6} + m_7.\frac{r'_7}{\ell_7}.e^{i(\gamma'_7+\pi)}).\ell_8 = 0 \tag{4.29}$$

4.5.5.4 Formulation of the counterweight condition for link BD

Link BD is the first link in the chain BD and AB. Consequently the moment vector, $\underset{\sim}{M}_{v_5}$, is:

$$\underset{\sim}{M}_{v_5} = m_5.r_5.e^{i\gamma_5} \tag{4.30}$$

Assigned to point D on link BD is a mass term, M'_{a_6}, which is a result of the mass m_6 which lies in DE. It is equal to:

$$M'_{a_6} = m_6.\frac{r'_6}{\ell_6}.e^{i(\gamma'_6+\pi)} \tag{4.31}$$

No other masses are assigned to point D, and so the moment vector $\underset{\sim}{M}_{d_5}$ can be determined, namely:

$$\underset{\sim}{M}_{d_5} = m_6.\frac{r'_6}{\ell_6}.e^{i(\gamma'_6+\pi)}.\ell_5 \tag{4.32}$$

Link BD is a binary link and therefore the moment vector $\underset{\sim}{M}_{c_s}$ is zero. The three moment vectors of the counterweight condition for link BC have been found. Thus this condition may now be written down and, with reference to point D and the arc BD, it is:

$$\mu_5.\lambda_5.e^{i\beta_5} + m_5.r_5.e^{i\gamma_5} + m_6.\frac{r'_6}{\ell_6}.e^{i(\gamma'_6+\pi)}.\ell_5 = 0 \tag{4.33}$$

4.5.5.5 Formulation of the counterweight condition for link AB

Link AB is the second link of the chain BD and AB. Accordingly the moment vector, $\underset{\sim}{M}_{v_4}$, with reference to point A and the arc AB, is:

$$\underset{\sim}{M}_{v_4} = m_4.r_4.e^{i\gamma_4} + (m_5+\mu_5).\ell_4 \tag{4.34}$$

The only mass term assigned to point B is M'_{a_6} and it had previously been assigned to link BD. Hence the moment vector $\underset{\sim}{M}_{d_4}$ with reference to point A and arc AB is:

$$\underset{\sim}{M}_{d_4} = m_6 . \frac{r'_6}{\ell_6} . e^{i(\gamma'_6+\pi)} . \ell_4 \qquad (4.35)$$

Link AB is a binary link and so the moment vector $\underset{\sim}{M}_{c_4}$ is zero.

All the moment vectors of the counterweight condition have been found and so this condition may now be written down. With respect to point A and arc AB, it is:

$$\mu_4 . \lambda_4 . e^{i\beta_4} + m_4 . r_4 . e^{i\gamma_4} + (m_5+\mu_5+m_6 . \frac{r'_6}{\ell_6} . e^{i(\gamma'_6+\pi)}) . \ell_4 = 0 \qquad (4.36)$$

This completes the formulation of the counterweight conditions for this linkage mechanism.

4.5.6 Calculation of the Parameters of the Counterweights

4.5.6.1 Selection of the Counterweights to use

In determining the masses and radial offsets of the counterweights, each of those counterweights which balance about a frame pivot will be cylindric in shape; as thick as possible; and placed in such a way that its circumference intersects with the balance point, see Figure 3.6. Such a counterweight gives the minimum moment of inertia condition. However, the use of this type of counterweight on non-frame pivoted links is not likely to give the minimum moment of inertia configuration for the force-balanced linkage. This is because much larger masses are required by such counterweights compared to those placed at a much further distance from the point of balance. Consequently the size of the counterweight needed to balance such counterweights is correspondingly large. This effect will be shown by using a minimum moment of inertia counterweight

on link BD. The parameters of a counterweight are identified as follows:

R = radius of the counterweight,
t = thickness of the counterweight,
ρ = density of the counterweight (for this case steel is used which has a density of 7833.0 kg/m^3).

4.5.6.2 Calculation of the parameters of the counterweight attached to link BD

The counterweight on link BD is force-balanced by that on AB. Hence it is necessary to calculate the one on BD first. The counterweight condition to be satisfied on link BD is given by equation (4.33) Therefore:

$$\mu_5.\lambda_5.\cos\beta_5 = 7.527 \times 10^{-2} \text{ kg.m} \qquad (4.37)$$

and:

$$\mu_5.\lambda_5.\sin\beta_5 = -1.373 \times 10^{-2} \text{ kg.m} \qquad (4.38)$$

Hence $\beta_5 = 349.66^{o}$ and $\mu_5.\ \lambda_5 = 7.65 \times 10^{-2}$ kg.m. The maximum permitted thickness for a counterweight added to link BD is 0.03m. Two different counterweights will be calculated. First the one which gives the minimum moment of inertia condition for this link. For this type of counterweight the radial offset of the mass centre, λ, equals the radius of the cylinder R, e.g. for this case $R_5 = \lambda_5$. Hence:

$$\mu_5.\lambda_5 = \rho_5.\pi.R_5^{\ 2}.t_5.R_5 \qquad (4.39)$$

Thus $\mu_5 = 1.248$ kg, $R_5 = \lambda_5 = 4.11 \times 10^{-2}$m and $I_5 = 1.054 \times 10^{-3}$ kg.m^2.

The magnitude of the mass of this counterweight is felt to be excessive, especially since it must be balanced by that one on link AB. Specifically the counterweight on link AB must counterbalance the term $\mu_5.\ell_4$.

Consequently another counterweight will be calculated whose radial offset will be defined to be 0.2m. This is the maximum offset permitted by the space available to this mechanism. The angular offset for this case is as for the previous one, but the parameters μ_5 and R_5 must be resolved. That is:

$$\mu_5 = \frac{7.651 \times 10^{-2}}{0.2} = 0.383 \text{ kg} \qquad (4.40)$$

Therefore R_5 is 2.276×10^{-2}m and $I_5 = 9.92 \times 10^{-5}$kg.m^2. If both of these counterweights should prove to be unsatisfactory another radial offset or counterweight radius can be selected and the new complementing parameter solved for.

4.5.6.3 Calculation of the parameters of the counterweight attached to link AB.

This condition the counterweight attached to link AB must satisfy is given by equation (4.36). Therefore:

$$\mu_4.\lambda_4.\cos\beta_4 = -0.2686 \text{ kg.m} \qquad (4.41)$$

and:

$$\mu_4.\lambda_4.\sin\beta_4 = 0.474 \times 10^{-2} \text{ kg.m} \qquad (4.42)$$

Hence $\beta_4 = 179.0^{\circ}$ and $\mu_4.\lambda_4 = 0.2687$ kg.m. The minimum moment of inertia counterweight will be used, since the balance is about a frame pivot. The maximum permissible counterweight thickness is 0.02m. Accordingly for the first case when $\mu_5 = 1.248$ kg $\mu_4 = 3.288$ kg, $R_4 = \lambda_4 = 0.0817$m and $I_4 = 1.098 \times 10^{-2}$ kg.m^2. For the second case when $\mu_5 = 0.383$ kg $\mu_4 = 2.618$ kg $\beta_4 = 178.5$, $R_4 = \lambda_4 = 0.0729$m and $I_4 = 6.97 \times 10^{-3}$ kg.m^2. As can be seen, a noticeable reduction in the mass and moment of inertia of the counterweight on AB is obtained when the lower mass counterweight is used on link BD.

The counterweights to be evaluated next are unaffected by the selection of different radial offsets for the counterweight on link BD.

4.5.6.4 Calculation of the parameters of the counterweight attached to link JA

The condition the counterweight on link JA must satisfy is given by equation (4.18). Therefore:

$$\mu_1.\lambda_1 \cos\beta_1 = -0.03105 \text{ kg.m} \qquad (4.43)$$

and:

$$\mu_1.\lambda_1.\sin\beta_1 = 0.0408 \text{ kg.m} \qquad (4.44)$$

Consequently $\beta_1 = 127.4^{o}$ and $\mu_1.\lambda_1 = 0.05135$ kg.m. Since the point of balance is a frame pivot a minimum moment of inertia counterweight will be used. Its maximum permissible thickness is 0.03m. Therefore $\mu_1 = 1.249$ kg, $R_1 = \lambda_1 = 0.0411$ m and $I_1 = 1.054 \times 10^{-3}$ kg.m^2.

4.5.6.5 Calculation of the parameters of the counterweight attached to link EK

The condition the counterweight attached to link EK must satisfy is defined by equation (4.29). Accordingly:

$$\mu_8.\lambda_8.\cos\beta_8 = -0.0167 \text{ kg.m} \qquad (4.45)$$

and:

$$\mu_8.\lambda_8.\sin\beta_8 = 0.0 \text{ kg.m.} \qquad (4.46)$$

Consequently $\beta_8 = 180^{o}$ and $\mu_8.\lambda_8 = 0.0167$ kg.m. A minimum moment of inertia counterweight will be used, since the point of balance is a frame pivot. Its maximum permissible thickness is 0.03m. Therefore $\mu_8 = 0.591$ kg, $R_8 = \lambda_8 = 0.0283$ m and $I_8 = 2.358 \times 10^{-4}$ kg.m^2.

4.5.6.6 Calculation of the parameters of the counterweight attached to link FGH

The condition the counterweight attached to link FGH has to satisfy is defined by equation (4.24). Accordingly:

$$\mu_3.\lambda_3.\cos\beta_3 = -0.01579 \text{ kg.m} \tag{4.47}$$

and:

$$\mu_3.\lambda_3.\sin\beta_3 = -0.01094 \text{ kg.m} \tag{4.48}$$

Consequently $\beta_3 = 281.31^{o}$ and $\mu_3.\lambda_3 = 0.01159$ kg.m. A minimum moment of inertia counterweight will be used, since the balance is about a frame pivot. Its maximum permissible thickness is 0.03m. Therefore $\mu_3 = 0.4628$ kg, $R_3 = \lambda_3 = 0.02504$m and $I_3 = 1.451 \times 10^{-4}$ kg.m^2. This completes the calculation of the parameters of the counterweights.

4.6 Comment

From section 4.5 it is seen that the full force-balance conditions of this complex linkage mechanism are obtained without solving the kinematic equations of motion. Furthermore the required force-balance is sought by this approach with an increased degree of understanding compared to the approach of Berkof and Lowen [7]. This is very important for industrial problems which, such as this one, had imposed practical constraints.

CHAPTER FIVE

EXPERIMENTAL RIG

5.1 Introduction

A survey revealed only one paper which measured the effect of balance on a linkage other than a slider crank. Kamenskii[22] compared a four-bar linkage in three situations (i) unbalanced, (ii) statically balanced and (iii) statico-dynamically balanced by measuring the deflections of the sprung frame link relative to ground for a mean speed of the crank of, apparently, 400 r.p.m.

The purpose of the experimental work of this thesis is different in some aspects to the above work. First the theoretical assumptions used in the analysis for predicting the inertia loads required testing. The assumptions are zero bearing clearance, no out of plane forces, no damping, inelastic elements (e.g. links and shafts) and constant crank speed. Second and in line with the work of Kamenskii the practical worth of balancing by two different methods needed to be established. One method is the force-balance procedure of Chapter Four and the other is the computer-based approach whose development is reported in Chapter Eight and Chapter Nine.

The first part of this chapter relates the development of a rig capable of making the necessary measurements for assessing the validity of the theoretical assumptions. Some problems which arose with it and the resultant actions taken are discussed. In addition to this, the selection, design and construction of the planar linkage used in the experimental work is reported. Part of this report deals with the measurements made to find the mass, mass centre position and moment of inertia of each moving link of this linkage, as well as the calculation of the maximum safe load at each of its joints.

5.2 Selection of the Measurements to be Made and the Associated Accuracies Required

To test the validity of the theoretical assumptions, whilst keeping the necessary instrumentation to a minimum, it was decided to measure only the frame bearing forces and the mean speed and fluctuations in speed of the drive shaft. The latter measurement provides a direct check on the assumption of constant crank speed, whilst the measurement of each frame bearing load gives both an indication of the combined accuracy of all the assumptions and a measure of the degree of force and moment balance. Additionally an indication of the level of torque balance can be obtained from measurements of the speed fluctuations.

About a $\pm$ 4% accuracy was specified for the force measurement system to provide a meaningful comparison between theory and practice. The higher level of accuracy of $\pm$2% was required for the measurement of mean speed, since the predicted inertia forces relate to the square of the drive shaft speed. On the other hand, the accuracy needed for measurements of fluctuations in mean speed was set at only $\pm$5%, because calculations made at the time suggested that they only formed at most $\pm$8% of the mean speed.

5.3 Development of the Force Measurement System

5.3.1 Selection of the Speed Range Examined

Industrial mechanisms had been observed to have nominally constant input speeds up to 10,000 r.p.m., though speeds between 2000 and 3000 r.p.m. seemed common. A low speed mechanism was selected to be studied first (i.e. 100 to 500 r.p.m.), because the time required to develop the more complex designs of higher speed linkages and associated balancing masses was considered to detract too much effort from the theoretical work of this thesis. This is not considered a severe limitation, as these measurements, to the author's knowledge, had not been made for any linkage. Also, such low speed linkages do occur in industry.

5.3.2 General Layout of the Bearing Force Measurement System

The bearing housings used to house the frame bearings were made in the form of a bolt to provide both the necessary attachment to the frame and the required pre-load on the load cell. This layout is the one recommended by the manufacturers of the load cell for this type of application. A photograph of a linkage and the two bearing housings used to attach it to the frame is shown in Figure 5.1.

A result of this layout is that a load applied by the linkage to one of its frame bearings is transmitted to the frame by parallel paths, namely the bearing housing and the associated load cell. Each of these load cells acts as a washer, and so loads applied at the bearings are transmitted as shear loads across the faces of the load cell. In contrast, each bearing housing acts as a cantilever, since the friction between the clamping nut and the frame and this nut and the housing tends to form an encastré support. Consequently a load applied at a frame bearing is supported, in part, as a moment about the encastré support of the bearing housing.

5.3.3 Selection and Design of a Means of Driving the Crank

There appeared to be two basic systems by which to drive the crank, one where the drive shaft passes through the load cell (Figure 5.2) and the other (Figure 5.3) where it does not. For three reasons, the former drive system (Figure 5.2) was selected. Firstly because industry does not normally use the double crank of the latter system. Secondly the former system appeared not to impose as severe a set of restrictions on the size and arrangement of the links and any attached counterweights as the second one does. Thirdly an existing drive unit was available which could be easily adapted to the design of the first system.

The flywheel from the existing drive system was retained to help approach the theoretical assumption made in this thesis that the crank of the experimental model rotates at constant speed. The 1.12 kilowatt thyristor

operated motor of the drive system was also kept, as it could provide the necessary level of power and the required adjustable speed drive. It was suggested in [23] that the pulses of torque produced by a thyristor based drive could appear as measured spikes of force. To help prevent this a rubber cushioned coupling was inserted between the motor and flywheel.

5.4 Linkage Model

5.4.1 Selection of a Suitable Linkage

A Watt's six-bar chain of the type shown in Figure 3.4 was selected as the test model, because it satisfies the seven main needs. One, it possesses only two frame pivots, and so it needs only two load cells. Two, it could be driven by the previously described drive system. Three, it could be used to examine the validity of the theoretical assumptions. Four, it can be designed to yield high levels of imbalance even at the low speed of 500 r.p.m. Five, it has five moving links, and so a reasonably wide choice exists as to which of its moving links to counterweight. Six, it can be used to examine the worth of linkages statically balanced and balanced by the method to be reported in Chapter Eight and Chapter Nine. Seven, the prediction of the inertia loads of this linkage is not difficult, since it is formed from only Assur groups of type one, namely dyads.

5.4.2 Design of the Linkage

As well as the linkage selected, another of the same type but with different link lengths could have been needed. Thus the design was required to cater for this with the minimum amount of re-machining. This was accomplished by constructing the links of the linkage from two types of components, basically bearing housings and a strut which inter-connects them. Consequently if a link size needed altering only a new strut needed to be machined. To avoid excessive out of plane forces, the linkage was designed such that except for the crank, all the mass centres of its links lie in one plane.

Flanged bearings possessing instrument class tolerances were chosen for all the joints not mounted directly on to the frame, to respectively enable a simple bearing housing design to be employed and to reduce the level of impacts associated with the presence of bearing clearance. Provision was made for attaching counterweights to the links by extending the bearing housings in a direction opposite to the strut. This direction was selected because force-balance theory suggested that counterweights would have to lie in this direction to obtain such a balance. Figure 5.1 is a photograph of the constructed linkage.

5.4.3 Measurement of the Mass, Mass Centre Position and Moment of Inertia of the Links

To predict the inertia forces, the mass, mass centre position and moment of inertia of each of the moving links of the linkage are needed. The mass was measured on a set of J.W. Towers model 7 scales which has a resolution of 5×10^{-4} kg.

The position of the mass centre of a link was found by using a knife edge to find three axes about which this link balanced, but such that each axis formed the side of a triangle. The mass centre of each link was taken to lie at the centroid of the triangle drawn on it by the above means. As the sides of each triangle were no greater than 0.001m, the maximum error in this measurement is believed to be about $\pm 2\%$.

A trifilar suspension was used to determine the moment of inertia of the links. Each measurement was repeated three times for different numbers of swings of the suspension system, specifically 30, 60 and 90. An error analysis suggests that the accuracy of the results is within $\pm 3\%$. Table 5.1 contains the results which can be related to the links to which they refer by the use of Figure 3.4.

5.4.4 Calculation of the Limit on Load for each Joint of the Linkage Model

The establishment of a limit above which the risk of failure of the linkage becomes unacceptable was needed to establish the permitted maximum speed. To provide the necessary degree of safety, a safety factor of 2:1 was to have been used to find the permitted maximum stress levels, and so the permitted maximum predicted loads. Now the presence of bearing clearance allows impactive re-contacts to occur whose magnitude can be at least twice the predicted loads. Equally bending moments about axes which lie in all three orthogonal planes can exist, since this linkage is not truly planar. The effect of these phenomena may be to induce joint loads considerably greater than the predicted ones. Accordingly a safety factor of 4:1 was used to calculate the permitted maximum predicted loads.

Each joint was considered as follows. First the most likely failure conditions associated with each joint were listed. The limit imposed on the joint load by each failure condition was then calculated, and, from these, the lowest selected for that joint. To calculate the failure load for a link, the peak magnitude of a bearing load was assumed to bear against the weakest section of the links against which it acts. A more sophisticated analysis was not used, becuase the time required to define the allowable polar load around each joint was deemed to be unacceptable, since obtaining a higher permissible level of speed will not yield any real gains to the purpose of this thesis. The calculations of the maximum permissible joint loads are contained in Appendix VII. These calculations suggest that the loads at joints A and D should not be allowed to exceed 6,900N and 1,090N respectively, whilst those at joints B, C, E, F, and G should not be greater than 1,250N.

5.5 Signal Conditioning and Recording

Each of the two signals from each of the two load cells were fed to a separate charge amplifier. If the total force on the frame was required, the four conditioned signals were then added by summing circuits.

The measurements of the above system or that of the speed detection system were recorded on a digital storage oscilloscope. This recorder digitizes incoming signals and stores them in a buffer store. The real time of these stored signals can be altered by this system and then processed, via an attached digital to analogue interface, to drive either an X-Y or an X-t and Y-t plotter. Permanent records obtained by this means are considered to be far superior to those produced by either a U.V. recorder or a photographed trace of an oscilloscope. A photograph of the instrumentation is shown in Figure 5.6.

5.6 Validation and Calibration of the Bearing Force Measurement System

The set of bi-directional load cells selected have a shear force measurement capability of $\pm$10kN at a resolution of 10mN and a linearity of 1% at full scale deflection. A series of tests based on applying static loads up to 500N confirms that this system has the precision to enable the required accuracy of $\pm$2% to be obtained.

Each bearing housing in acting as a clamp for a load cell carries part of the load. Assume each acts as a cantilever with the friction between the housing and clamping nut and this nut and frame tending to create an encastré support. Calculations suggest that in this situation the housings will carry 24% of the load and the load cells the rest. Accordingly this system was calibrated. Another load path via the drive shaft exists at the crank-frame-bearing, but calculations show that it carries a negligible part of the load, specifically 0.14%.

An important problem with the drive shaft was that it was found to be bent, and this caused a sinusoidally varying load of 5N peak to peak amplitude to appear as the shaft rotated. After work on straightening the shaft this was reduced to 0.3N which is considered a negligible proportion of the loads measured.

The sensitivity of each of the two orthogonal measurement axes of each of the two load cells needed to be both set equal to each other and scaled relative to computer plots of the theoretical predictions of the bearing loads. This latter requirement enabled the measurements to be plotted directly on top of the computer plots of the theoretical predictions. The scales were adjusted relative to a static load of 51 kgf. The linearity of the system was checked by applying static loads in 5.1 kgf steps from 0 to 51 kgf. A typical calibration curve is shown in Figure 5.4. It was envisaged that the measurement system would be used above this validated range. Specifically, for the test on the linkage of Figure 5.1, it was expected that loads up to 2000N could be detected. The entire required range was not validated, as it was found to be difficult in practice to apply static loads above 51 kgf. However for the following three reasons, it is considered acceptable to extrapolate the calibration curve up to the required range. First because the loads cells were new at this time and the stringent tests applied by the manufacturers showed them to be linear within $\pm$1% of the full scale deflection load of 10kN. Second, for the small deflections involved (approximately 1μm for 2000N) the cantilever support of the bearing housing is considered to be a linear system. Third, the calibration curves obtained show no detectable deviations from a straight line.

To test the validity of the extrapolation of the calibration curves, an eccentric mass was attached to the drive shaft and run over a range of speeds which loaded the crank-frame-bearing with a range of peak to peak

loads from 500N to 2000N. The results were found to agree closely with the extrapolated curves, namely within ±4%. Accordingly the extrapolation of the calibration curve is considered valid.

5.7 Speed Measurement System

5.7.1 Selection of a Suitable System

A shaft encoder[3] was considered the most suitable system by which to measure drive shaft speed, but it was found to be unsuitable in practice. This is because the largest disc apparently available at the time was 0.05m in diameter, whilst the drive shaft is of 0.017m diameter. Thus it was concluded that the system could not be mounted onto the drive shaft and still permit its associated optical pickup to be fitted. Accordingly another system was needed. The use of a tacho-generator was rejected, because none could be found which possesed a sufficient number of segments on its commutator, to either provide the required resolution or enable the frequency of the necessary pulse filters to be set high enough. However it was suspected that a pulse-based system having an analogue output could yield the necessary resolution and accuracy.

The system eventually designed was basically a shaft encoder except that a purpose built metal disc with an appropriate number of equi-spaced holes drilled in it was used. An optical switch was mounted such that it could detect the passage of these equi-spaced holes in the disc as the shaft rotated. This layout causes the photo-cell of the optical switch to produce a regular waveform whose frequency depended directly on the shaft speed. The waveform could then be used to produce an analogue signal whose voltage relates directly to shaft speed.

3. A shaft encoder is an optically flat disc with equi-spaced markings photographically etched into it. An optical switch is then used to detect the passage of these markings as the shaft, to which the disc is attached, rotates. The photo-cell of the optical switch is thus caused to produce a waveform whose frequency is a direct function of shaft speed.

5.7.2 Production of a Squarewave of at Least 720 times the Frequency of the Shaft Speed

To achieve the level of resolution required it was decided that at least two pulses per degree of crank rotation were needed. In part this was accomplished by manufacturing a disc with 360 equi-spaced holes each on that pitch circle diameter which gives the spacing between the holes equal to the diameter of a hole. Such a spacing gives a regular waveform whose frequency depends only on the angular velocity of the disc. The diameter selected for the disc is the largest one permitted by the available space on the rig, whilst the disc possessed the practical maximum number of holes.

A means of increasing the effective number of holes was then tried in order to obtain the required resolution. Specifically this was done by using not one but four optical switches. Each of the four switches was set to detect at the pitch circle of the 360 holes and a whole number of degrees plus a phase shift from one such hole; the phase shifts being 0^{o}, $0^{o}7\frac{1}{2}'$, $0^{o}15'$ and $0^{o}22\frac{1}{2}'$, since this allows the waveforms generated by each switch to form a waveform of four times the frequency of the constituent ones. The waveforms were added by feeding the signal from each optical switch to a squaring amplifier and then all four signals to logic circuits to produce a squarewave of four times the frequency of the pulses generated at each optical switch.

Initially a brass disc with 0.0008m diameter holes was used in conjunction with a brass block containing the four optical switches. It was found to be unsatisfactory for two main reaons. First an unsymmetrical waveform was generated, because the detected area is a circle detected by a surface which is a circle of the same size. Second the recorded waveform contained spurious phase shifts and peak changes which appear to be a function of three phenomena . One, inaccuracies in the positions of the supposedly equally spaced holes of the disc, as a result of skidding by the small diameter drill

(0.0008m) necessarily used. Two, particles present in the everyday atmosphere entering the holes and blocking a significant part of them, e.g. approximately 20% of the area of some holes had been found to be blocked. Three, optical interference as a result of reflection from the brass surfaces and formed fringes.

A second system apparently overcomes these problems. In this system the disc was made from Tufnol[4], which, on machining, gives a matt surface. Tests showed that this reduced the intensity of the reflections below the threshold of the photo-electric cell. Also slots were selected to be machined into the disc instead of holes. First to eliminate inaccuracies in machining due to drill skid and second to permit easier cleaning of the disc. Only a 180 slots were cut in order to reduce the effects of both machining errors and dirt particles by increasing the pulse width. Also this increased the ratio area detected/detecting area, which helped to regularize the produced waveform. New phase angles of 0^{o}, $0^{o}15'$, $0^{o}30'$ and $0^{o}45'$ were required, since only 180 slots were cut in the disc. The phase angles of the optical switches of this design, unlike the previous one, required setting by manually adjusting the position of each switch so that the waveform produced lay at the required phase angle to that waveform selected as the reference. The resultant system produced a regular waveform from each switch and an acceptable times four squarewave, see Figure 5.5

5.7.3 Production of an Analogue Signal of Shaft Speed

The circuit constructed to convert the times four squarewave into an analogue signal of speed needed testing. To test for linearity, a simulation of the times four squarewave was produced by a function generator

4 Tufnol is a trade name of a commercially available plastic.

and fed into the analogue circuit. The analogue voltage was then plotted against the squarewave frequency recorded on a timer counter for speeds from 0 to 600 r.p.m. No signs of non-linearity could be detected, see Figure 5.7a.

This circuit uses resistors and capacitors which cause it to act as a low pass filter. Hence it was necessary to establish the frequency at which unacceptable levels of phase shift and signal decrement occur. To do this, a frequency modulated squarewave was produced by modulating the sinewave signal at the required times four frequency (0 - 7,200 Hz) with another sinewave at the required frequency of oscillation of the drive shaft (0 - 50 Hz). The result was then output via saturation amplifiers to produce a frequency modulated squarewave. This simulates the results obtained from the pulse generator, when the drive shaft has a sinusoidally varying oscillation superimposed on its mean speed. The frequency modulated squarewave was then fed to the analogue circuit, and the result recorded on the digital oscilloscope along with the modulating sinewave signals. As expected, changing the simulated mean shaft speed did not alter the simulated shaft oscillations, and so these tests were conducted at one effective shaft speed of 300 r.p.m.

The above two signals were used to produce Lissajous' figures, where the amplitude of each was kept equal so that the phase shift between them could be obtained from these figures. These measured phase shifts were plotted against frequency, see Figure 5.7b. Next, at the low frequency of 1Hz, the amplitudes of these two signals were set equal. The frequency was then raised and the amplitude of the analogue signal recorded and plotted (Figure 5.7c) against the modulating frequency in the non-dimensional form amplitude of analogue signal/amplitude of modulating signal. These latter two graphs show that harmonics up to a frequency equivalent to 540 r.p.m.

can be measured, whilst meeting the desired accuracy of ±5%. However, for the work undertaken, a range up to 1800 r.p.m. was needed to enable the required first three harmonics of speed to be recorded at this accuracy: the first three harmonics of speed are considered to hold the main part of the information on speed fluctuations. Therefore further development of this apparatus is needed, specifically its 3dB break frequency should be raised to at least 30Hz.

It should be mentioned that this unit is the result of considerable development work, and it is expected that a natural frequency of at least 200 Hz can be obtained. Unfortunately time did not permit this development to be completed. The present circuit is given in Figure 5.8.

5.8 Safety System

The present linkage is limited to a speed of 600 r.p.m. and if this is exceeded by an excessive amount, e.g. 50% overspeed, the linkage will probably fail catastrophically. If feedback to the motor controller is lost the motor rapidly accelerates up to its maximum speed of 3000 r.p.m. Consequently a safety cutout was fitted. It comprises of a tacho-generator driven by the motor, where the voltage the tacho-generator produces is monitored. If this voltage reaches a specific level a relay is tripped which causes the motor to be shut down. To ensure the tacho-generator is working its signal is monitored by the voltmeter displayed in Figure 5.6.

5.9 Tests on the Experimental Rig

An initial series of tests were carried out to check the performance of the rig. Some problems were found and these are discussed along with the modifications made.

5.9.1 Vibration

Discrepancies between the measured and predicted frame bearing force loci were found to exist, and particularly at speeds in excess of 150 r.p.m. The main discrepancy is an apparent vibration superimposed on the bearing forces. A typical result showing this is given in Figure 5.9, and is a

measure of the rocker frame bearing load as two orthogonal components for a crank speed of 170 r.p.m. Clearly the apparent vibration appears to be present between a crank angle of 350^{o} and 50^{o} over which measurements from these plots suggest that the frequency varies from 67 Hz to 100 Hz. The mean frequency for this period was calculated to be 88.9 Hz. There are believed to be two explanations which are considered below.

First resonance in a cantilever mode of the linkage with its supporting input and output shafts was thought to be the cause of the above vibration. The resonant frequency of the output shaft was considered to be the lower of the two, as it has a much smaller diameter whilst carrying a similar mass. Hence it was examined in detail. (The output shaft is 0.01m in diameter and the distance between the point of attachment of the linkage and the assumed encastre support provided by the frame bearings is 0.025m.) The natural frequency of this system was predicted to be 890 Hz, see Appendix V. To confirm this, the output shaft was struck at the attachment point of the linkage and the resultant vibration recorded. It was found to have a frequency of 890 Hz, which is within 2% of the predicted one. Clearly this mode of vibration is not the one given in Figure 5.9.

A second possibility considered was torsional vibration of the drive shaft. This shaft is 0.017m in diameter and has a free length between the flywheel and the crank of 0.219 m. In Appendix VI, the natural frequency of the linkage and input shaft was calculated to be 95 Hz at a crank angle of 34^{o}. This lies within the measured frequency range of this vibration. A frequency variation is expected, as it is noted in Appendix VI that the effective inertia at the input shaft varies. Also these changes in inertia are significant, since an analysis shows that the link velocities undergo marked changes in this region: the effective moment of inertia at the input shaft is a function of the squares of the link velocities. At 34^{o} the measured

frequency was calculated to be 89.4Hz, which is within 6% of the predicted one. The results of this examination provided a strong indication that excessive torsional flexure of the input shaft was the problem. To help confirm this, the crank was struck both at the coupler-crank joint and whilst the crank lay at an angle of 34^{o}. The resultant vibration was found to have a frequency of 88.2Hz. Accordingly the vibrational phenomenon under examination is accepted as that due to resonance of the linkage with the drive shaft.

To replace the drive system with a more rigid one would take an amount of time not available if the planned experimental work was to be completed. However it was realised that this phenomenon could be turned to advantage. Now a computer-based program was being written which simultaneously seeks both dynamic balance and a reduction in the drive torque fluctuations of linkages: constraints on bearing force levels could also be applied. Consequently, this phenomenon could help highlight any reductions obtained in the levels of the drive torque fluctuations. Therefore this flexibility was retained as an acceptable feature of this rig even though it was realised that the upper usable range of speed is limited by this occurrence. In fact, it is thought that the maximum permissible speed should be reduced from 600 to 400 r.p.m.

5.9.2 Motor Controller

A drift in speed was found to occur, and over a period of ten minutes changes in speed of up to 7% were detected. This lack of precise control was considered to be too great and so the existing controller was replaced with a higher precision one. The first controller uses armature current feedback, whilst a more preferable system should use feedback which is a direct function of shaft speed. In fact, the shaft speed measurement system was selected as being a particularly suitable means of providing feedback. To both enable this feedback to be used and

to obtain a more precise control of speed, an Emotrol MS5 single phase controller produced by GEC Ltd. was purchased.

The precision of this controller is quoted at ± 1% for a temperature range of ±10°C. However this can be improved by providing a more stable temperature environment, i.e. ±2°C, in which case the degree of precision has been suggested to be better by at least one order of magnitude [25].

On running the drive system unloaded, measurements indicated that the speed varied by only ±0.1%. These measurements were taken by the speed measurement system of section 5.7 and by counting pulses over periods of 0.1, 1 and 10 seconds.

A photograph of the final version of the rig is given in Figure 5.10.

5.10 Discussion

It is considered essential that the rigidity of the drive shaft is substantially increased before using this rig to examine a wide range of balance problems. An increase in natural frequency to 400Hz with the present linkage and load cell is believed to be achievable, whilst still avoiding the use of a double crank. This is accomplished by externally clamping the load cell, as this enables the shaft diameter to be increased to 0.025m; and by using a new layout of the drive system to reduce the required length of this small diameter shaft to 0.05m.

5.11 Conclusion

The tests and calibrations reported in this chapter show that the rig is capable of making the required measurements at the desired levels of accuracy.

Though the observed torsional vibration of the drive shaft is considered an asset for part of the research programme, it will restrict the previously desired speed range. In the case of the unbalanced linkage the permitted top speed is reduced from 600 to 400 r.p.m. as a result of this vibration.

CHAPTER SIX

DETERMINATION OF AN APPROPRIATE COUNTERWEIGHT SET FOR THE EXPERIMENTAL LINKAGE

6.1 Introduction

This chapter reports the design of a set of counterweights to fully force-balance the Watt's six-bar linkage described in Chapter Five and a photograph of which is given in Figure 5.1. A schematic layout of this linkage is given in Figure 3.4 along with illustrations of its parameters which are of interest. The values of these parameters are contained in Table 5.1.

It has been pointed out that there are six valid sets of links to which counterweights can be added to obtain a force-balance of this Watt's six-bar linkage, as illustrated in Figure 3.5. Accordingly criteria are needed by which the advantages of each set can be compared in order to determine the most advantageous one. The criteria to be discussed are the magnitudes of the bearing loads, driving torque and out of balance moment.

By using the selection procedure of section 4.4.2 of Chapter Four, two of the six sets of links are eliminated from consideration. The conditions the counterweights must satisfy for the four remaining sets are then found. Two sets of counterweights are calculated for each set of conditions, based respectively on the "minimum moment of inertia" and "minimum practical mass" approaches described in Chapter Three. Results are presented from the analysis of these eight counterweight sets by a computer program to determine the percentage change in the loads with respect to the unbalanced linkage. As a result, the counterweight sets are placed in an order of preference. The design and construction of that set of the eight considered is reported. Also the possibility of estimating the likelihood of loss of contact in the bearings is discussed. Finally conclusions are drawn.

6.2 Selection of the Criteria for Comparing the Different Counterweight Sets

At least one of the six sets of counterweight conditions was expected to be used to determine a set of counterweights for use in an experimental examination of the worth of full force-balance. To aid the selection of which to use, it seemed appropriate to place the different sets in a descending order of preference, based on the severity of the problems that the addition of each counterweight set either creates or heightens. In this case, the problems in question were the bearing loads, out of balance moment and driving torque fluctuations.

For a bearing load, the peak load at a bearing was referred to the safe load limit calculated for the bearing in Appendix VII. In the case of the driving torque, the interest is in both the torsional vibration of the drive shaft and the lower frequency variations in crank speed. Accordingly it was suspected that all the harmonics of the torque needed to be monitored, as each may provide noticeable speed variations and significant torsional flexing of the drive shaft. A similar monitoring need was seen to be necessary for the out of balance moment, as each harmonic may give rise to both an excessive rocking or flexing of the frame and unacceptable levels of vibration in the surrounding structures and mechanisms. Now by the use of the "completeness relationship" of Bessel's inequality [26] it can be shown that:

$$2\,y_{rms}^2 = \frac{a_o^2}{2} + \sum_{n=1}^{\infty} a_n^2 + b_n^2 \qquad (6.1)$$

where y_{rms} = the root mean square of the waveform,
$\{a_o \ldots a_n\}$ = Fourier coefficients of the harmonics.
$\{b_1 \ldots b_n\}$

Therefore the rms levels of the driving torque and out of balance moment were monitored instead of the summated squares of the coefficients of the harmonics.

6.3 Eliminating Two of the Counterweight Sets from Further Consideration

The procedure of section 4.4.2 of Chapter Four suggested that, of the six sets given in Figure 3.5, sets c, d, e and f were not likely to yield lower levels of increases in the loads of interest when compared to sets a and b. Consequently they were provisionally eliminated from consideration. However the counterweight of each of sets e and f which both balances another counterweight and is balanced itself (i.e. that on link BCE of Figure 3.4) was seen to lie close to the crank and to be balanced by the crank based counterweight alone. Problems caused by inertia added to the crank were suspected to be not as great as those associated with adding inertia to other links, since this inertia addition only affects the load on the crank frame pivot. Accordingly it was felt that these two sets were still worthy of examination. The counterweight conditions for the four sets of links to be used are given in Appendix VIII.

6.4 Selection of Two Counterweight Sets for Each Counterweight Condition

Each set of full force-balance conditions was used to define two sets of counterweights. The first set is a result of using only the minimum moment of inertia counterweights defined by Epstein and Steinvolf [20]. The second set is similar except for those counterweights attached to links not pivoted about the frame. As discussed in section 3.5 of Chapter Three, it is felt that for these counterweights a mass much less than the minimum moment of inertia value usually yields significantly lower increases in loads. Consequently the counterweights for the second case were designed to have the lowest practical mass, which implies the highest practical offset. There are no theoretical constraints to the offset, but an appropriate practical limit used was the length of the link to which it is attached.

To distinguish between the four different sets of full force-balance conditions, the terms balance A,B,C and D are used. Balance A is for set b of Figure 3.5, balance B for set a, balance C for set f and balance D for set e. To identify the two different counterweight sets of each set of

counterweight conditions, the terms case 1 and case 2 are used. Case 1 refers to the use of all minimum moment of inertia counterweights, and case 2 to the appropriate replacement of some of these with practical minimum mass ones. The evaluated parameters of these eight sets of counterweights are given in Table 6.1.

6.5 Analysis of the Loads of Interest Before and After Force-Balance

The analysis section of a computer program was used to predict the loads of interest. This program has been written as part of the research of this thesis and is reported in Chapter Nine. A number of assumptions are made in the theory used in the program. These assumptions are constant crank speed; rigid links; no out of plane forces; no damping (e.g. frictionless bearings) and zero bearing clearance. The program calculates the peak and r.m.s. loads of a linkage before and after inertia is added to it. Further, it gives the percentage rises in the loads of each case analysed with reference to one of the cases selected as the reference case by the program user. For this investigation the unbalanced linkage was selected. Table 6.2 contains the results of this analysis which is for this planar linkage lying in a vertical plane.

6.6 Determination of the Relative Importance of the Criteria used to find the Order of Preference

Before the different counterweight sets could be placed in an order of preference, the relative importance of the different criteria by which this was to be done needed to be established. It was first assumed that the maintenance of the maximum crank speed of 600 r.p.m. was a major requirement, since the ability to achieve or maintain high running speeds seems to be both a general and an important industrial need. Accordingly the analysis of the loads in the previous section was made for a crank speed of 600 r.p.m.

The peak magnitude of the bearing loads was classed the most important criterion when a bearing load exceeds the safety limit, as there is then an unacceptable risk of failure and a consequent restriction on the maximum running speed. Of these loads, the most important was defined to be that which exceeds its safety limit by the greatest percentage of this limit. If the bearing loads were all found to be less than their respective safety limits, this criterion was classed the least important, since these levels of bearing loads are not considered to restrict the function of the linkage. The level of r.m.s. driving torque was classed the next most important criterion for it tends to define the incurred variation in crank speed and the level of the drive shaft vibration identified in section 5.7.2. of Chapter Five. Accordingly the importance of the r.m.s. level of out of balance moment was considered to be between the driving torque and those bearing loads which do not exceed the associated safety limit.

6.7 Establishment of the Order of Preference of the Counterweight Sets

The evaluation of this order started with the determination of the worst set and continued on to end with the identification of the best set. Table 6.2 contains both the load after force-balancing and its percentage change with respect to the unbalance case. Also this table contains for each joint the percentage of the associated safety limit (as defined in Appendix VII) reached by the load at this joint.

Table 6.2 shows that the level of the bearing load at joint B for each counterweight set was such that the order of preference was established purely with reference to this load. The sets are numbered 1 to 8, in descending order of preference.

A closer examination of balance A case 2 with reference to the other sets also reveals that this one gives the lowest rise in all the criteria defined to be of interest. Thus this set is clearly the best in relation to any of these criteria.

6.8 Design of an Appropriate Counterweight Set

An exact practical realisation of the counterweights of balance A case 2 is not possible, because in the positions specified there is either no or no adequate means of supporting a disc-shaped counterweight. Accordingly an arm must be provided in each case, but, in doing so, the required disc size is altered by the very presence of the arm.

For the disc attached to link FG, an arm was designed such that it could support the required disc part of the counterweight over the given speed ranges within the required factor of safety of 4:1. Additionally a check was made to see that the natural frequency of the disc and arm system was of the order of at least 200Hz. It is thought that vibrations of this order of frequency even at the highest running speeds of the linkage will not be significant. This is considered to be particularly so as a result of the torsional vibration present. The final design resulted in the combined disc and arm system having a measured mass of 0.432kg, a calculated moment of inertia of 1.36×10^{-4} kg.m^2 and a calculated natural frequency of 178 Hz. In the latter case the arm was considered to act as a cantilever support for the disc.

The counterweight attached to link CDG had to be re-calculated as the mass of the counterweight it balances, i.e. that on link FG, had changed. As a result, the parameters of this counterweight are now a measured mass of 3.45 kg and a calculated moment of inertia of 1.34×10^{-2}kg.m^2. The natural frequency of this counterweight system was not calculated, since inspection alone suggests its natural frequency is far in excess of the one attached to link FG.

It was necessary to completely re-design the counterweight attached to the crank AB, because spatial limitations will not permit the use of the disc type. Epstein and Steinvolf [20] showed that when limited space is available a semi-cylindrical counterweight should be used, whose position is such that the centre of its arc lies at the balance point. The equation

defining the first moment of mass, MR, of a segmental counterweight was formulated, and is:

$$MR = \rho.R^3.t\left(\frac{\sin\Theta_o}{2} - \frac{\sin 3\Theta_o}{6}\right) \qquad (6.2)$$

where: ρ = density,
t = thickness,
R = radius of the arc,
Θ_o = segmental angle (see Figure 8.1d).

Lead was selected for this counterweight, because of the limited space and since only low running speeds were to be used in the experimental work and consequently only low load levels experienced. Unfortunately, it is not possible to place the centre of arc of the counterweight at the point of balance and so it was offset. The counterweight could also interfere with the bearing housing of the frame bearings of the crank. To avoid this the counterweight thickness was limited to 0.012m. The maximum allowable radial dimension measured relative to the drive shaft is 0.07m. However this counterweight has to be supported at an angle such that the arc drawn between its mass centre and the drive shaft axis lies at 151.2^o in an anti-clockwise direction from the arc AB on the crank. This support limits the chord length (C in Figure 8.1d) of the counterweight to 0.132m, which sets Θ_o to 141^o. From equation (6.2), the first moment of mass of this counterweight was calculated to be 0.0264kg.m. However 0.04263 kg.m. is needed. Now the counterweight support has a mass of 0.127kg and the polar co-ordinates of its mass centre are 154^o and 0.009m relative to point A and the arc AB on the crank. It was felt that with respect to the accuracy needed the 2.8^o offset of the mass centre of the support from the position needed could be neglected. Accordingly an additional first moment of mass of 0.01509kg.m. was needed. Another segmental section was designed which has a 0.07m radius and a chord length of 0.132m. However, taken out of this

part of the counterweight is a segmental section to allow the counterweight to fit around the bearing housing of the frame pivot of the crank. The required thickness of this part of the counterweight was solved for using equation (6.2), and was found to be 0.00796m. This completed the design of the three necessary counterweights. Figure 6.1 is a photograph of the linkage force-balance by these counterweights.

Before these counterweights were used they were checked to assess the difference between them and the theoretical set on which they are based, i.e. balance A case 2. This was done by calculating the percentage changes in the frame bearing loads and the torque fluctuations relative to balance A case 2. Only the frame bearing loads and driving torque were calculated as they are the ones of interest in the experimental work. Table 6.3 contains the percentage differences between the theoretical and practical counterweight set.

It was also considered essential to examine the sensitivity of each of the counterweight parameters to enable the required machining and positioning tolerances to be identified. A reasonable machining and positional accuracy for the above parameters is thought to be $\pm$ 2%. Such a level of accuracy was studied by giving each parameter a 2% change except for the angular offset which was altered by 2^{o}. The percentage changes of the frame bearing loads and torque fluctuations relative to balance A case 2 are given in Table 6.4a, 6.4b and 6.4c for changes imposed on the counterweight on links AB, CDG and FG respectively. As can be seen from these tables the changes are generally less than 1% but no greater than 3% and so a $\pm$ 2% level of accuracy was considered acceptable.

6.9 Discussion

In carrying out the experimental tests on the rig, it was suspected that the effects of impact loads at the bearings might be recorded. The experimental examinations which were planned as part of the research of this thesis included the unbalanced six-bar linkage of Figure 5.1 and the same linkage when force-balanced by the counterweight set balance A case 2.

Fawcett and Burdess [27] suspected that high rates of change of the direction of the bearing force vector in regions where its magnitude is low can give rise to contact loss in a bearing with clearance. This event allows impactive re-contact to occur.

Earle's and Wu [28] did some work in predicting such contact loss quantitatively. They developed empirically a dimensional term whose magnitude is used to predict the point at which contact is lost. However Haines [29] has pointed out that despite the obvious potential of such an approach it is not clear at present, in view of the dimensional nature of this criterion, how to apply it to linkages having dimensions considerably different to those of these authors.

Accordingly it is thought that at present the reliable prediction of impacts is not possible and so, though it is considered important to this thesis, no such predictions are made.

In Chapter Three it was suggested that for a force-balance which is about a non-frame-pivot a more suitable counterweight is one with a much smaller mass and correspondingly larger offset than the minimum moment of inertia one of Epstein and Steinvolf [20]. Comparing case 1 (all minimum moment of inertia counterweights) with case 2 (practical minimum mass counterweights on non-frame-pivoted links), for each set of counterweight conditions, reveals that much lower load levels are obtained for the latter case in each set. Consequently, when designing a set of counterweights, it is considered essential to examine the use of practical minimum mass counter-weights on appropriate links.

6.10 Conclusion

The use of practical minimum mass counterweight can lead to realistic reductions in the rises in loads on a linkage due to adding counterweights to it.

The set of counterweights designed have machining and positional accuracies which in the worst case yields about a 6% difference between the predicted and measured loads.

From this design work it can be seen that at least one of the loads rose by about 100%, which is in line with the experiences of Lowen, Tepper and Berkof [19].

The development of methods for predicting both contact loss and the severity of the resultant impact on re-contact is an important area.

CHAPTER SEVEN

AN EXPERIMENTAL INVESTIGATION OF AN UNBALANCED AND A FORCE-BALANCED LINKAGE

7.1 Introduction

There are six parts to this chapter and the first is a specification of the precautions taken to ensure the validity of the measurements. Second the validity of the assumptions of constant speed and rigid drive is considered in detail. Third the experimental and predicted frame bearing forces are compared. Fourth the worth of the force-balance is considered. Fifth a set of two counterweights is tested where each counterweight is considered to possess a minimum in moment of inertia relative to its link for a given force-balance. Sixth some implications of the work of this chapter are discussed.

7.2 Precautions

A number of precautions were taken to help ensure the validity of this work. At the beginning of a days work the equipment was allowed to 'warm up' for at least one hour. After this the oscilloscope and X-Y plotter system was checked by inputting a squarewave signal of 3 volts peak to peak at 100Hz to the oscilloscope whilst its time base was set at 5ms/cm and its amplifier at 0.5 volts/cm. The recorded result was a squarewave of 6cm peak to peak and 3cm cycle width, and this was plotted by the X-Y plotter. This plot was checked to ensure the consistency of both the form and scale of this squarewave. No discernible differences were found for any of the checks performed and so the calibration of this system was considered valid for all this work. The scale used between these two recording systems was one centimeter of the oscilloscope screen to one inch on the X-Y plotter.

The load cells were checked each day to ensure the calibration was still valid, since on a number of occasions a loss of accuracy had been found to occur. It was felt that this was due to changes in room temperature: the manufacturers of the load cell claim a temperature error of -2.0 N/^{o}C.

Additionally, prior to taking a measurement of a frame force, a static load equal to the load range of the computer plot was placed on the rocker frame bearing and the displacement of the X-Y plotter noted. This was done to ensure both that the correct sensitivities of the instrumentation had been selected and that the calibrations were still valid. The latter point was considered important as loss of calibration had been experienced over a days use.

The mean drive speed was measured by counting the x4 squarewave pulses produced by the speed measurement system over a set time interval, i.e. a timer counter was used. This timer counter was checked by comparing it with two others, and since no differences were found its accuracy was accepted. The temperature stability of the speed measurement system was checked by calibrating it for two temperatures separated by $6^{o}C$. Negligible differences were found and so a daily calibration was not performed.

7.3 An Assessment of the Validity of the Theoretical Assumptions

7.3.1 Assumption of Constant Crank Speed

The assumption of constant crank speed is a critical one, since the bearing forces are a function of both the acceleration and the square of the speed of the crank. Speed fluctuations were measured for three mean crank speeds of 100, 200 and 300 r.p.m., and the results are given respectively in Figures 7.1a, 7.1b and 7.1c. The abscissa of time is replaced by one of crank angle, since it is considered more meaningful. Such a replacement is deemed valid because the maximum speed fluctuation of $\pm 4\%$ is within the required $\pm 5\%$ accuracy required for this measurement. It is seen that the peak to peak variation is similar for the range covered, namely 7.6 r.p.m. $\pm$ 0.5 r.p.m. Assuming the mid-point of the peak to peak variation equals the mean speed, the maximum percentage speed variation for 100 r.p.m. is $\pm$ 4%, for 200 r.p.m. is $\pm$ 1.8% and for 300 r.p.m. is $\pm$ 1.2%.

Accordingly the desired accuracy of restricting the speed fluctuations to within ± 2% is achieved for speeds above 200 r.p.m.

The measured speed fluctuations of the crank and estimates of its acceleration were to have been used to improve the accuracy of the predicted forces by using them rather than the assumptions of constant crank speed. However it is not now considered worthwhile for speeds above 200 r.p.m. in view of the smallness of the measured fluctuations and the relatively large effects of torsional vibration; though it may be used for speeds below 200 r.p.m. if time permits.

It is felt from the above measurements that the assumption of constant crank speed is reasonable above speeds of 200 r.p.m. However it is suspected that the percentage fluctuation quoted may well be greater in practice because of the poor frequency response of the speed measurement system. The form of the measured speed fluctuations suggests that harmonics higher than the 3rd play an important part in forming them. Accordingly the limit on only measuring speeds up to 540 r.p.m. may well have been exceeded by significant harmonics with a consequent loss in accuracy. It is felt that at the higher speed of 300 r.p.m. the measured fluctuation may be higher by as much as ± 0.5%.

7.3.2 Assumption of a Rigid Drive

7.3.2.1 Locating the measured load locus on the plot of the predicted one

A procedure devised for aligning the theoretical and experimental load plots was found to be unworkable because the centroids of the plotted load loci varied by as much as ± 20% relative to the predicted peak load for a given load and speed. An investigation of the above phenomenon revealed that it is due to two effects. First the X-Y plotter was found to have a repositioning error of about 5 mm and this accounts for up to 12% of the above positional error. Second the plots on the oscilloscope were also seen to have positional changes. Leakage of the load

cell charge through the charge amplifiers was discounted, since it has been found to be negligible over the period of time involved. The eccentricity of the drive shaft was also eliminated as this phenomenon also occurs at the rocker frame bearing. However it was noted that each of the bearing housings form an overconstrained system with the load cell and plate. Accordingly if slip occurs between two of the clamped surfaces, i.e. load cell and bearing housing, load cell and plate or bearing housing and plate, the pre-load will alter. An improvement was obtained by increasing the clamping load, but this still did not permit the above procedure to be used because of the re-positioning error of the X-Y plotter. Therefore the measured loads are positioned 'by eye' to lie as close to the predicted ones as possible. Obviously this eliminates the possibility of examining the differences in the theoretical and measured static loads, but it is difficult to conceive of what differences there could be.

7.3.2.2 Examination of the torsional vibrations

Figures 7.2a and 7.3a show that the level of torsional vibration at a mean speed of 100 r.p.m. is negligible throughout the cycle. On raising the mean speed to 200 r.p.m. the torsional vibration causes major differences between the measured and predicted frame bearing loads between the crank angles 340^{o} and 90^{o}, see Figures 7.2b and 7.3b. Figures 7.2b shows that the measured force at the crank is 1.6 times greater than the predicted one. A further increase in mean speed to 300 r.p.m. causes this factor at this bearing to rise to 1.9, see Figure 7.2c. At this point the measured force over this part of the cycle is considered to be so far in excess of the predicted one that investigations of further speeds are deemed unnecessary, since clearly the assumption of a rigid drive system is invalid for these higher speeds. The preliminary investigation of this vibration in Chapter

Five indicated that observable levels of vibration are present beyond speeds of 150 r.p.m. Consequently the assumption of a rigid drive is limited to below this speed.

7.3.3 Comment

The above investigation of constant crank speed and rigid drive invalidates the predicted loads, because the assumption of constant speed is only considered to be adequate above 200 r.p.m. whilst that of a rigid drive is considered inadequate above 150 r.p.m.

7.4 Comparison of the Predicted and Measured Loads for the Region which Excludes the Torsional Vibration

In the region between crank angles of 90^{o} and 340^{o} the measured and predicted forces are observed to be close for speeds of 200 (Figure 7.2b and 7.3b) and 300 r.p.m. (Figure 7.2c and 7.3c). The lack of accuracy for the lower speed of 100 r.p.m. (Figure 7.2a and 7.2c) is expected from the foregoing work on speed measurement. It is felt that the relationship between theory and practice is so close for these higher speeds that the theoretical assumptions can be considered valid for this region between the speed range 200 and 300 r.p.m.

7.5 Impact

For a mean speed of 100 r.p.m. and between the crank angles 180^{o} and 250^{o} some disturbances were noted, see Figure 7.2a. Recording this load against time showed that its frequency is far higher than that of the torsional vibration. Based on the work discussed in section 6.9 of Chapter Six, it appears that contact loss between a bearing and its journal and thereby impactive re-contact is likely to occur if the bearing load crosses rapidly from one quadrant of the bearing to the diagonally opposite one by passing through or close to the origin. An examination of the

predicted bearing loads reveals that the closest approach to the origin relative to the peak load between the crank angles of 240^{o} and 300^{o} is 49%. Consequently it is thought that impacts at the bearings are unlikely, even though the predicted loads are not considered an accurate model of the actual ones for this speed.

Another possibility arises because of a rather poor fit found at the drive pin between the crank and input shaft. The predicted torque is found to pass rapidly from a driving to a retarding one at a crank angle of about 270^{o}. Consequently these disturbances are thought to be due to the impactive take-up of this play as the torque reverses. Additionally, it is believed that these disturbances disappear at the higher speeds because the degree of torque reversals, if any, are less owing to the presence of the higher D.C. levels needed to overcome the increased losses due to friction and air resistance etc.

7.6 The Worth of the Force-Balance

Figures 7.5a, 7.5b and 7.5c show that on force-balancing the linkage noticeable levels of vibration occur at all three speeds, and, in particular, for speeds of 200 and 300 r.p.m. high levels of shaking force relative to the predicted values for the original linkage are noted. The presence of this imbalance cannot be due directly to the torsional vibration, since the force-balance is independent of the rotational motion of the crank about its frame pivot. In fact, it is thought to be due to the imperfections of the force-balance; the counterweight attached to link FG (Figure 3.4) vibrating on its arm and the linkage vibrating on the ends of the input and output shafts both translationally in the plane of its motion and rotationally about that axis which passes through the two ends of these shafts. It is likely that the resultant imbalance due to these phenomena is aggravated by the torsional vibration of the drive shaft. Accordingly four effects are considered to be present in the three measured shaking forces of Figure

7.5 These effects are more clearly seen by plotting the two components of the shaking force, i.e. X and Y, against crank angle. For example, the shaking force for 200 r.p.m. is given in Figure 7.6: these forces are measured against time, but, since the speed fluctuations for this mean speed are considered small, the time abscissa is replaced by one of crank angle.

Four ranges of disturbances are believed to be identifiable in this plot. First are those due to the imperfections of the force-balance occurring at shaft speeds and harmonics of shaft speed, say within a frequency range of 3-15Hz. Second are those caused by the torsional vibration of the drive shaft aggravating the imbalance, and calculations and measurements suggest their range is about 30-60Hz. Third are those related to the vibration of the linkage and its counterweights about the input and output shafts, and measurements suggest this range to be approximately 120-313Hz. Fourth is the vibration of the counterweight of link FG on the end of its arm: calculations suggest its natural frequency is 178Hz.

The presence of these four phenomena to some extent negates the effect of the counterweights selected in Chapter Six for the linkage of Figure 5.1 (In addition the added inertia has reduced the natural frequency of the drive, e.g. at a crank angle of 34^{o} the measured frequency is 38.6Hz). The results of the force-balance given in Figures 7.5a, 7.5b and 7.5c confirm this view since they show that relative to the predicted shaking force of the original linkage significant levels of force imbalance remain. Nevertheless on comparing these measured force imbalances with the measured shaking force of the original linkage substantial improvements are seen to have been obtained. Specifically the peak to peak force has been reduced by 70%, 63% and 56% for the respective speeds of 100, 200 and 300 r.p.m. Therefore in practice a considerable reduction of the shaking force has been obtained for these speeds.

It had been planned to examine speeds up to 600 r.p.m., but it is now felt that the speeds should be restricted to 300 r.p.m. for the force-balanced linkage owing to the high level of bearing loads attributed to the four previously discussed effects. However the present results indicate that the level of force-balance obtained decreases with increased speeds and that for speeds slightly in excess of 300 r.p.m. the reductions are less than 50%. Reductions below 50% are believed to be usually not worth initiating in an industrial environment. Accordingly it is felt that the level of force-balance beyond 300 r.p.m. will probably not be worthwhile.

In Chapter Six, the maintenance of the running speeds up to 600 r.p.m. had been defined to be a prime requirement. Therefore, clearly, in relation to this criterion a decrease in the performance of the linkage has been obtained. In conclusion, it is felt that this example of force-balance has proved counter-productive, except that it may find limited applications for speeds up to 300 r.p.m.

7.7 The Minimum Moment of Inertia Counterweight

In section 3.5 of Chapter Three it was concluded that a further reduction in the moment of inertia of a counterweight over the one proposed by Epstein and Steinvolf [20] could be obtained by attaching it to its link via a bearing. Relative to the link, the bearing effectively eliminates the moment of inertia of the counterweight about its centre of gravity; though this assumes bearing friction is negligible.

Two of these counterweights were constructed for the experimental model. This type of counterweight is not used on the crank of the model because there is insufficient radial clearance to permit its use. Additionally, eliminating the moment of inertia about the centre of gravity has no effect on the predicted loads, since the crank is assumed to rotate at constant speed.

No observable rotation of the two counterweights mounted on free central pivots could be detected over the range of speeds examined, namely from 50 to 300 r.p.m. A typical test is shown in Figure 7.7 and is for a speed of 200 r.p.m. Accordingly it is thought that the assumption of zero moment of inertia about the centre of gravity for these counterweights is a valid one.

7.8 Discussion

In Chapter Five it was concluded that the present drive system could be stiffened, and an estimate suggests that its natural frequency could be raised to about 400 Hz. In the light of the foregoing work it is thought that even this frequency may not be high enough when it is remembered that this linkage is designed for speeds up to 600 r.p.m. At 150 r.p.m. at which the torsional vibration is noticeable the ratio, frequency of torsional vibration : cyclic frequency, is 36:1 whilst at 170 r.p.m. at which this vibration is considered unacceptable it is 32:1. At 600 r.p.m. this ratio with the proposed stiffened shaft is also about 36:1, but to yield the ratio 32:1 its speed would have to be about 750 r.p.m. Accordingly it is felt that the torsional vibration should not prove a problem for the present linkage if the drive shaft is replaced with the stiffened one.

An important point this investigation is considered to highlight is that torsional vibration may well be one of the major problems for higher speed linkages. This is because the present experimental model exhibits these problems even though in relation to industrial linkages of this size it is fairly light, has no external loads and runs at low speeds. Consequently, it is thought that when an industrial linkage is found to exhibit vibrational problems torsional vibration should be treated as a prime suspect.

This work is also believed to indicate that a shaking force reduction should be obtainable in the case of a linkage with a flexible drive or drives merely by stiffening the latter.

PART II

COMPUTER-BASED SYNTHESIS OF DEVICES

CHAPTER EIGHT

A PRELIMINARY INVESTIGATION INTO SYNTHESIZING COUNTERWEIGHTS

8.1 Introduction

The brief survey conducted in Chapter One found that there are techniques available for obtaining specific results with particular devices. However the survey revealed no technique taken to the point of general application. The computer-based approaches of Porter and Sanger [13] and Sadler and Mayne [14b] are felt to hold promise for, as indicated by these authors, there is no reason in principle why such techniques cannot be used to attempt to meet any criterion with any conceivable device provided that both can be mathematically modelled. Accordingly such techniques will be studied.

In this approach, the dynamic characteristics of a linkage to be modified by attaching a device or devices to it are represented by a mathematical model commonly termed an 'error function'. The magnitude of this function is such that an increase in its magnitude represents a worsening in performance of the linkage, and conversely. Also the mathematical model is usually formulated such that the magnitude is zero when the desired performance has been met. The term 'error' refers to the difference between the actual and desired performance. The optimum values of the parameters of the device or devices used to improve the performance of a linkage are found by making an ordered search of the hyper-space formed from these parameters for that set which yields the lowest magnitude of the error function.

8.2 Limitations of Previous Work

It is felt that Porter and Sanger [13] provide an important step towards developing such methods, but that they omitted three important aspects. First they limited themselves to two counterweights, one placed

on the crank and the other on the rocker of their four-bar linkage. Second the available results for the bearing loads and shaking moment are constrained, since both the crank-based counterweight and the angular position of the rocker-based one are pre-defined according to force-balance considerations. Third no reasons are given as to why the r.m.s. values of the forces, moment and input torque are used.

Sadler and Mayne [14b] are seen as having provided a useful guide towards the establishment of a general optimization technique. However there are believed to be a number of limitations to this work. First only the case of counterweights attached to the crank and rocker are examined. Second the counterweights are assumed to be point masses in order to avoid considering the shapes required by each counterweight. Third, the mass of each of the two counterweights are either defined to be half the mass of the linkage or required to add up to the total mass of the linkage. In fact the work on force-balance in this thesis indicates that mass is an important design parameter. Fourth, it is difficult to estimate the improvements and the severity of any incurred problems, because the levels of the forces and moments prior to any mass addition are not given.

8.3 Problem Definition

It is observed in Chapter One that the majority of designers appear to be interested in only the gross motion of linkages, the dynamic characteristics being considered only when they affect either the gross motion characteristics or surrounding structures and mechanisms. Naturally there are some areas where the dynamics are part of the design rather than the constraint role, e.g. switch gear. However this thesis is concerned with the area where dynamics is a secondary consideration.

To achieve either fully or partly the desired changes in the dynamic characteristics, either devices can be attached to the linkage or the linkage can be lightened by appropriate drilling etc. It is assumed in this thesis that the linkage has already been lightened, but to a level which still provides the necessary strength to accommodate the increases in load due to mass being added. In the case of devices there seem to be eight practical types and they are (i) a mass fixed to a suitable link, (ii) two connected links (a dyad) whose ends are attached to different and appropriate links of a linkage, (iii) a linkage, (iv) an eccentrically rotating mass, (v) a Lanchester balancer, (vi) a cam or gear operated mass, (vii) springs and (viii) dampers.

It was considered inadvisable to examine all of the above devices given the time available, and so only mass devices (i.e. counterweights) were studied, as they appeared to be the most practical. Accordingly the aim of the work reported in this chapter was restricted to seeing whether counterweights could be realistically synthesized by computer-based numerical minimization techniques to meet specific dynamic requirements.

In regard to the dynamic criteria listed in Chapter One, only two were used in this initial study, and, since dynamic balance was classed an important industrial need, they were the frame shaking force and frame shaking moment. In general, it is thought that the shaking moment most suitable as an optimization parameter, for crank driven linkages, is that measured about the crank pivot, since it is suspected that the motor, drive shaft and associated structure tend to define the drive axis as the one on which the mass centre of the machine lies and about which the frame link will oscillate.

To enable this investigation to be completed quickly, a four-bar linkage was selected as the model with which to investigate device

synthesis. To achieve the aim of the work of this chapter the following three objectives were set. First, to find a suitable shape of counterweight to use. Second, to formulate an equation whose magnitude defines the performance of the linkage, and which, in this case, refers to the levels of imbalance of the frame shaking forces and moment. Third, to select a suitable numerical minimization routine. Finally the continued use of the counterweight shape used in this study is discussed.

8.4 Selection of an Appropriate Counterweight Shape

A counterweight may need to meet one of three requirements in force-balance situations. One, a minimum moment of inertia for a given force-balance to minimize the incurred additional out of balance couple; two, a practical minimum mass for a given force-balance to minimise the size of those counterweights which balance this one; and three, a minimum radial dimension for a given force-balance to enable it to fit into restricted spaces. The counterweight shapes which satisfy these conditions are shown by Epstein and Steinvolf [20] to be respectively a cylinder with a point on its periphery placedat the point of rotation and its length as long as possible (Figure 8.1a); a semi-cylinder with the mid-point of its peripheral chord placed at the point of rotation and its length made as long as possible (Figure 8.1b); and a segment which is placed as far from the point of balance as possible and whose arc radius is such that its arc centre lies at the point of balance (Figure 8.1c). For a given counterweight this is usually the axis of one of the joints of the link to which it is attached.

Moment balance is also simultaneously sought. Now increases in the moment of inertia from the minimum one can be achieved, along with reductions in the radial dimension, by seeking a segmental shape which lies between that of a cylinder and semi-cylinder, but such that the mid-point of the peripheral chord lies at the axis of rotation (type A

counterweight). If increases in moment of inertia are required, along with reductions in weight, a shape can be sought which lies between a semi-cylinder and a point mass, where the centre of the arc of the segment lies at the axis of rotation (type B counterweight). This scheme of changing the counterweight shape enables a wide range of possible requirements to be met.

Equations defining the mass, m, first moment of mass, m.r , and the moment of inertia, I, of these shapes were derived. For a type A counterweight they are:

$$m = \rho.R^2.t.\left[\pi-\theta_o+\frac{\sin 2\theta_o}{2}\right] \qquad (8.1)$$

$$m.r = \rho.R^3.t.\left[(\pi-\theta_o)\cos\theta_o+\frac{3\sin\theta_o}{4}+\frac{\sin 3\theta_o}{12}\right] \qquad (8.2)$$

$$I = \rho.R^4.t.\left[(\pi-\theta_o).\frac{(1+\cos 2\theta_o}{2}+\frac{3.\sin 2\theta_o}{4}\right] \qquad (8.3)$$

where ρ = density,
R = arc radius,
t = thickness,
θ_o = segmental angle.

These terms are illustrated in Figure 8.1d. The first moment of mass, equation (8.2), and the moment of inertia, equation (8.3), are referred to the axis of rotation.

For a type B counterweight, unlike type A, the axis of rotation lies outside the boundary of the counterweight, and therefore an arm may well be needed to connect it to its link. To cater for this, an arm of uniform width (z.C) and thickness (u.t) will be assumed to lie along the length of the line which emanates from the axis of rotation and ends at right angles to the peripheral chord of the segmental counterweight. (C and t are the dimensions shown in Figure 8.1d). Accordingly, for a type B

counterweight with connecting arm, the equations defining its mass, m, first moment of mass, m.r, and moment of inertia I are:

$$m = \rho.R^2.t.\left[\pi-\theta_o+(1-2.z.u).\frac{\sin 2\theta_o}{2}\right] \qquad (8.4)$$

$$m.r = \rho.R^3.t.\left[(2+z.u).\frac{\sin\theta_o}{4} + (3.z.u.-2).\frac{\sin 3\theta_o}{12}\right] \qquad (8.5)$$

$$I = \rho.R^4.t.\left[\frac{\pi-\theta_o}{2} +(1-z^3.u-z.u).\frac{\sin 2\theta_o}{6}+(1-2.z.u+2z^3.u)\frac{\sin 4\theta_o}{24}\right] \qquad (8.6)$$

The first moment of mass and the moment of inertia are referred to the axis of rotation. If an arm is not required either u or z can be set to zero.

8.5 Provision of a Mathematical Description of the Performance of the Linkage

To describe the performance of a linkage quantitatively, an expression is needed whose magnitude defines the performance of a linkage. Dynamic balance is the aspect of the performance selected, and specifically the r.m.s. values of the forces and moment. The r.m.s. values are chosen for the reasons previously given in section 6.2. Accordingly the performance of this linkage is defined by the magnitude, P, where P is given by:

$$P = a.\sqrt{\phi X^2} + b.\sqrt{\phi Y^2} + c.\sqrt{\phi M^2} \qquad (8.7)$$

where X = magnitude of the force applied by the linkage to the frame in a given direction,
Y = magnitude of the force applied by the linkage to the frame in a direction orthogonal to X,
M = moment applied by the linkage to the frame about the axis of the crank,
a,b,c, = adjustable weighting factors (which may be regarded as suitably dimensional).

The magnitudes of this equation or the relative magnitudes of its parts are not scaled.

In the computer program, a points approximation of the above equation is used, where n is the number of equi-spaced points. That is equation (8.7) is replaced by:

$$P = a.\sqrt{\sum_{i=1}^{n} X_i^2} + b.\sqrt{\sum_{i=1}^{n} Y_i^2} + c.\sqrt{\sum_{i=1}^{n} M_i^2} \qquad (8.8)$$

Porter and Sanger [13] found for their linkage that 36 points gave sufficient accuracy. Similarly, for this linkage, increasing the number of points beyond 18 yielded changes of less than 1.0% in the r.m.s. forces and moments, and so only 18 points are used.

A certain number of assumptions were made to keep the complexity of the calculations to a minimum in order to help obtain the lowest possible computing time. These assumptions are constant crank speed, rigid elements, zero damping, zero bearing clearance and no out of plane forces. They are considered reasonable assumptions, since only gross improvements were sought, e.g. frame forces reduced by at least 50% . Accordingly an accurate mathematical model is not considered essential; specifically, force and moment predictions within $\pm$5% are believed to be adequate.

8.6 Selection of a Numerical Minimization Technique

The numerical minimization technique is the means by which an ordered search is achieved. Basically it alters the counterweight parameters with reference to the result achieved by the previous alteration and, for some techniques, previous alterations. There are many types of these numerical minimization techniques each tending to employ different search patterns: the pattern defines the form of parameter alterations imposed. In [30] it is shown that each technique

tends to perform with varying degrees of success on different functions. These techniques can be generally classified into three categories: they are (i) a direct search method which uses only the magnitude of the error function; (ii) a first-order approximation which requires both the magnitude and the first-order derivatives with respect to the varied parameters and (iii) a second-order method which requires both the magnitude and the first and second order derivatives with respect to the varied parameters.

Experience has shown that there is no single method which works consistently well on the wide spectrum of problems encountered in practice. Consequently some means of identifying the most suitable one for the types of error function used in device synthesis is needed. Several attempts to identify general guidelines for the selection of methods have been reported, [30, 31, 32, 33]. Coulville's [31] conclusion is that second order methods, i.e. type (iii), perform better on average than those of categories (i) and (ii). Kelley and Myers [32] concludes 'a variable metric method exhibits substantially faster convergence than any of the other conjugate gradient methods'. Fletcher devised a type (ii) method, called a 'Rank One' method [34], developed from a type (iii) variable metric method [35]. Although, at the time, computational experience was limited, the Rank One approach possesses certain advantages, and so a computer-based numerical minimisation routine was written using this algorithm.

On using the Rank One minimization computer program its performance was found to be unsatisfactory for the task in hand as the search, in the main, tended to converge on to local minima far removed from the global one. This was not seen as a failure of the method but attributed to the apparently large number of minima present in the error function.

As a result, it was decided that a non-gradient-guided broad search pattern was needed instead of this point-search gradient-guided technique.

One method which had been implemented in a program developed by colleagues [36], appeared to be suitable and so was tried. It is called a Simplex Method and it is a type (i) approach. It derives its name from the use of a regular simplex to explore the parameter space, a regular simplex in n dimensions being n+1 mutually equi-distant points. Basically it replaces the worst vertex of the simplex, i.e. that having the highest magnitude of the error function, with the reflection in the centroid of the others. In addition to this, variable scaling of the simplex is provided by allowing it to contract and expand. Also unlimited expansion is permitted as long as it is successful. At the end of it a translation of the complete simplex to the new area is catered for. To form the initial simplex, random numbers are generated using the power residue method [37]. The sequence of numbers generated is dependent on the integer supplied by the user, and so a different simplex can be obtained by selecting a different integer to start. Youssef [38] recommended that the results of previous runs should be used for some or all of the vertices. For further information on this method, reference [39] should be consulted.

A listing of the final version of the complete computer program, program A, is given in the accompanying Ph.D. Thesis Supplement.

8.7 Results

The four-bar linkage used in this investigation is illustrated in Figure 8.2, and its inertial and kinematic parameters are given in Table 8.1. Compromises between force and moment balance were sought, where the relative importance of these two criteria was varied in a number of discrete steps. Four series of searches were undertaken, namely for counterweights attached to (i) the crank and coupler, (ii) the crank and rocker, (iii) the coupler and rocker and (iv) the crank, coupler and rocker.

A graph of the results obtained in each series of searches is given in Figure 8.3. These graphs were obtained by plotting the percentage reductions obtained in the forces and moment against the ratio, a/b, of the previously defined weighting factors: a logarithmic scale is used for the ratio of the weighting factors to provide a suitable abscissa. These results were then connected by straight lines to form a continuous curve. Since the results obtained indicate an apparently smooth curve, it is expected that the results obtained for other values of a/b would be within about $\pm$5% of the straight line approximation.

Significant difficulties were encountered in obtaining a force-balance condition for the coupler and rocker and the crank and coupler sets of counterweights. Specifically twice as many iterations were needed as those required for the crank and rocker set. In both these counterweight sets, the coupler based counterweight has to be balanced by the other counterweight. Therefore, to improve the force-balance of the linkage, the counterweights of each of these two sets must be increased in a corresponding fashion, and this may explain the additional iterations needed. However doubt must be cast on this explanation by the results of the set with three counterweights, since such difficulties were not found to occur here.

It is known from the force-balance work that each set of counterweights can give a full force-balance, and thus the important criteria to observe is the moment balance. From Figure 8.3a, it can be seen in comparison to the results of Figure 8.3b, 8.3c and 8.3d that the worst set of improvements in moment balance are yielded by the coupler and crank based counterweights. Figure 8.3b shows that significant improvements in the moment balance are achieved by using a coupler and rocker based set, but this is at the expense of large rises in the Y_{rms} force. An apparent maximum reduction of 56% in the shaking moment can be obtained with a 13% reduction in the X_{rms} force,

but this incurs a 100% rise in the Y_{rms} force. Figure 8.3c shows that similar levels of improvements in the shaking moment can be obtained by using a crank and rocker based counterweight set, whilst reducing the Y_{rms} force level to half that of the previous set. The maximum reduction in the moment for the crank and rocker set is 55% with a 9% reduction in the X_{rms} force and a 42% rise in the Y_{rms} force. Figure 8.3d indicates that further substantial reductions may be obtained in the moment by using three counterweights, i.e. it can be reduced by 70% whilst also reducing the X_{rms} force by 10% and only raising the Y_{rms} force by 56%. One result believed to emphasize the power of this approach is that giving reductions of 80%, 74% and 25% in the X_{rms} and Y_{rms} force and r.m.s. moment respectively. This is coupled with a 15% reduction in the r.m.s. driving torque fluctuations and a 20% reduction in the peak crank/frame bearing load, whilst increases of only 50%, 25% and 10% in the peak crank/coupler, coupler/rocker and rocker/frame bearing loads are incurred respectively. For comparison, consider a full force-balance using counterweights on the crank and rocker. This incurs increases in the peak bearing loads at the crank/frame, crank/coupler-coupler/rocker and rocker/frame joints of 25%, 40%, 50% and 105% respectively. This is along with increases of 40% in the r.m.s. driving torque fluctuations and 75% in the r.m.s. shaking moment.

Both the ability to obtain the results found and the quality of these results are believed to confirm the worth of this technique.

8.8 Discussion

On reflection it is thought that the apparent large number of minima found in the error function by the Rank One numerical minimization routine is far greater than expected. One possibility may be the use of the segmental shape for the counterweights. The important properties of a counterweight are its mass, first moment of mass and moment of inertia. In obtaining a force-balance, it is only the mass and first moment of mass which

are relevant. Accordingly mass was plotted against first moment of mass for six values of the angle θ_o: the angle θ_o is given in Figure 8.1d. It was observed that for a given first moment of mass increasing this angle from 0^o leads to increases in mass up to 90^o, but thereafter decreases. Thus it is realised that this property would act as a barrier to a search seeking low values of mass from a starting position having an angle $\theta_o < 90^o$. This is deemed a severe fault so much so that the use of this shape for counterweights is now considered unsuitable for use in numerical minimization based synthesis methods.

Another important outcome of the work reported in this chapter is the identification of four important research areas. First is that which deals with those constraints which prevent devices from either having unreal properties, e.g. negative mass, or exceeding permitted limits on size. Unless the form of a constraint is chosen carefully it has been found that it can prevent the device synthesis program from finding optimum solutions or cause the search to become unstable. Hence further research in this area is believed to be essential.

The second, related area is concerned with the further consideration of the appropriate class of shape to adopt for a counterweight for a numerical minimization based method.

The third area is concerned with the mathematical form of criterion that should be adopted for a given aspect of performance; e.g. peak or r.m.s. values of force. Since this computer-based technique permits the improvements of any form of criterion that can be mathematically modelled, it is important to establish the most relevant form for a given situation.

The fourth area is concerned with the magnitude of the error function. It was realised that this magnitude has no meaning other than for improvements over previous values. It is thought that if some means of scaling this magnitude could be found it would provide continuous feedback to the program

user on the progress of the search. This is more important for general techniques which are concerned with different types of linkages and performance characteristics.

CHAPTER NINE

DEVELOPMENT OF A COMPUTER-PROGRAM TO SYNTHESIZE COUNTERWEIGHTS FOR A PARTICULAR WATT'S SIXBAR CHAIN

9.1 Introduction

A number of relevant papers were published during the period between completing the computer program of Chapter Eight and starting the work associated with this chapter. Starr [40] published a discourse entitled 'Dynamic Synthesis of Linkages: An Emerging Field'. It separated the design process into three separate stages, namely kinematic synthesis, dynamic analysis and 'adjustments'; and then considered each stage in broad brief terms. The work of this thesis is concerned with attaching suitable devices to linkages to adjust their dynamic characteristics, and so it clearly lies within the adjustments stage. To distinguish the particular area of work of this thesis from the more general one considered by Starr, it is given the title 'Device Synthesis'. Such a title is considered to cover any method which yields the parameters of a device or set of devices which are attached to a linkage to obtain a required set of changes in its performance.

Conte, George, Mayne and Sadler [41] sought improvements in the dynamic parameters of a four-bar linkage by re-designing its kinematic parameters, but subject to the constraint that it maintained the required kinematic properties. They considered the links to be of rectangular cross-section and stiffened by requiring that the width of each link is one tenth the link length, whilst thickness is kept constant. The additional masses due to bearings are neglected. Considerable theoretical improvements are obtained, but the method is based on the assumptions that some degree of change is allowed in the kinematic behaviour. This approach, also, is seen to lie within the adjustments stage, and one which, if used, should precede the Device Synthesis stage.

Sadler [42] wrote about further work on six-bar linkages, but again the counterweights are both assumed to be point masseswith a restriction such that their total mass does not exceed half the mass of the linkage.

This chapter reports the development of a computer program which synthesizes sets of counterweights which will theoretically improve some or all of the dynamic characteristics of the linkage to which they are to be attached. This program was specifically designed around the experimental linkage of Figure 5.6. Thus the class of linkage catered for is restricted to a particular Watt's six-bar chain (and implicitly a four-bar linkage). The dynamic characteristics included in the program are the frame shaking force, the frame shaking moment, the driving torque and the bearing loads. Again the shaking moment is measured about the drive shaft. Maintenance of bearing contact is not catered for, because it was concluded in section 6.9 that appropriate theory does not exist to accurately predict contact loss in either the experimental linkage or a wide range of industrial linkages. Another criterion eliminated from consideration is the combined effective inertia of the linkage and its attached counterweights at the drive shaft, since relative to the flywheel this moment of inertia is negligible for the experimental linkage.

Each phase of work involved in producing this program is reported. The first phase is concerned with the development of constraints to prevent a counterweight from either having unreal properties such as negative mass or exceeding permitted limits on density, size or position. Second is the selection of another counterweight shape to succeed the present segmental one. Third is the investigation into ways of guiding the search for optimum counterweights. Ways in which to guide the search in a Device Synthesis approach are extremely important, since large numbers of parameters (>10) are simultaneously optimized in a typical case. The five possible counterweights for the linkage of Figure 5.6 collectively have twenty five optimizable parameters.

Tests on some features required for a more general program, which both caters for a wide variety of linkages, and is intended for use by industrial designers, are detailed. Typical is the means to scale both the magnitude of the error function and the weighting ratios such that they are meaningful to a designer unfamiliar with such techniques.

9.2 Selection of a Counterweight Shape

A disc shape having a variable position was selected for the counterweights for a number of main reasons. Its parameters do not form barriers to a search, as do those of a segmental counterweight. It can yield the minimum moment of inertia condition. Moreover, by a suitable choice of parameters it is equally possible to bring about a large increase in the moment of inertia of a link with only a small increase in mass, or a large increase in the moment of inertia with little or no increase in the first moment of mass about a given reference point. More generally, when a counterweight has insufficient radial clearance it can be re-designed to yield the 'best' compromise in mass, first moment of mass and moment of inertia; as in the case of the counterweight designed in section 6.8 for the crank of the experimental linkage.

In the computer program of Chapter Eight an arm had been included in the overall counterweight shape, when the counterweight is offset radially from the link. It is now thought that an arm should not be included for three reasons. One, the introduction of an arm to the counterweight shape will again complicate its characteristics, and this directly opposes the reason for selecting a new shape. Two, the addition of arms to the theoretical counterweights of the force-balance of Chapter Six led to only small changes in the peak frame bearing loads and driving torque. Specifically these changes are generally less than 7% but at most 15%. Three, even though a disc is radially offset from the reference point on a link, an arm may not be needed as the associated angular offset can cause the disc to still lie on its link.

Tests on some features required for a more general program, which both caters for a wide variety of linkages, and is intended for use by industrial designers, are detailed. Typical is the means to scale both the magnitude of the error function and the weighting ratios such that they are meaningful to a designer unfamiliar with such techniques.

9.2 Selection of a Counterweight Shape

A disc shape having a variable position was selected for the counterweights for a number of main reasons. Its parameters do not form barriers to a search, as do those of a segmental counterweight. It can yield the minimum moment of inertia condition. Moreover, by a suitable choice of parameters it is equally possible to bring about a large increase in the moment of inertia of a link with only a small increase in mass, or a large increase in the moment of inertia with little or no increase in the first moment of mass about a given reference point. More generally, when a counterweight has insufficient radial clearance it can be re-designed to yield the 'best' compromise in mass, first moment of mass and moment of inertia; as in the case of the counterweight designed in section 6.8 for the crank of the experimental linkage.

In the computer program of Chapter Eight an arm had been included in the overall counterweight shape, when the counterweight is offset radially from the link. It is now thought that an arm should not be included for three reasons. One, the introduction of an arm to the counterweight shape will again complicate its characteristics, and this directly opposes the reason for selecting a new shape. Two, the addition of arms to the theoretical counterweights of the force-balance of Chapter Six led to only small changes in the peak frame bearing loads and driving torque. Specifically these changes are generally less than 7% but at most 15%. Three, even though a disc is radially offset from the reference point on a link, an arm may not be needed as the associated angular offset can cause the disc to still lie on its link.

9.3 Constraints

There are thought to be two main types of constraint applied to the parameters of a counterweight, namely those that prevent it from having unreal properties such as negative mass (type one constraints) and those that restrain it from exceeding user-defined limits on density, size and position (type two constraints). Both of these types of constraint are applied to the five parameters which define the disc-shaped counterweight, where these parameters are density of disc material, disc radius, disc thickness and the radial and angular offset of the mass centre of the disc from the reference axes on the associated link.

9.3.1 Constraints which Prevent Counterweights from having Unreal Properties.

Since the user-specified lower limit on density, e.g. that of aluminium, will prevent it from having negative values, a type one constraint is not necessary.

Optimizing the disc radius can lead to negative values being found, but since radius is used as a squared term there is no need to prevent this occurrence. In fact applying a constraint to restrict it to positive values will probably hinder the search, as this action introduces a discontinuity. Accordingly negative values are allowed, but at the end of a search the modulus of the radius is taken to provide the output value.

Negative values of thickness define negative values of mass, first moment of mass and moment of inertia. Although negative values could be permitted to a limited extent to identify areas to be lightened, at present it is being assumed that linkages are already lightened to the required level. In the computer program reported in Chapter Eight the occurrence of these negative values is prevented by a barrier whose effect is to guide the search away from regions of negative thickness. However, it is now realised that the effect of this is to suggest it is faulty for a counterweight to tend to zero mass etc. Instead the occurrence of negative values can be interpreted

as a counterweight not being needed on the link in question. Therefore if thickness is found to be negative it is re-set to zero.

A barrier is also used in the computer program of Chapter Eight to prevent the radial offset from having negative values. However negative values of the radial offset are realistic and can be equally represented by a similar but positive value whilst also adding 180^{o} to the angular offset. Therefore, in the program of this chapter, if negative values of radial offset are detected a check is initiated. To begin with, the angular offset is examined to see if it is a variable paramerer. If it is, a 180^{o} is added and the new angle checked to see if it lies within the permitted range of values. Provided it does, the radial offset is re-set to a similar but positive value, whilst the new angular offset is retained. A failure in this check causes the radial offset to be set to zero, i.e. its lowest non-negative value, and the angular offset to be re-set to its original value.

There are no unreal values of the angular offset, but a check is made to ensure it lies within the range 0^{o} to 360^{o}. If it does not 360^{o} is appropriately added or subtracted.

9.3.2 Constraints to Prevent Counterweights Parameters breaking user-defined Limits

Typically user-defined limits are applied to prevent a counterweight set from being synthesized which would clash with other parts. These constraints are obtained from the limits placed by a designer on the value of each parameter of each counterweight. The constraints are then represented by a mathematical function, which so weights the value of the error function that it forms a barrier to restrict the search to permitted regions.

To enable the barriers to be applied before a constraint is broken, a second (inner) set of limits is formed from the initial (outer) set. The inner set is used to initiate the application of the weighting functions.

They are obtained by appropriately adding or subtracting a fraction, s, of the range defined by the outer limits, that is:

$$LL_1 = L_1 + s.(L_2 - L_1) \qquad (9.1)$$

$$LL_2 = L_2 - s.(L_2 - L_1) \qquad (9.2)$$

where L_1, LL_1 = outer, inner lower limit,
L_2, LL_2 = outer, inner upper limit.

The author's experience with constraints is limited, and, so far, no literature has been located on the preferred form of a barrier in a case similar to the present one. Accordingly, the ability to define barriers which range from sharply to gradually imposed ones is considered necessary in this research program. An exponential function, e^v, is thought to be a suitable mathematical function on which to base such a barrier, and to alter its severity (e^v-1) can be formed into a product with an adjustable severity factor, t.

The barrier function is required to reflect the degree by which a constraint has been broken. To accomplish this, the magnitude by which a parameter exceeds the inner limit is divided by the (outer) range to give the power, v, of the exponential function. That is, if the lower limit is broken, it is given by:

$$v = \frac{LL_1 - p}{L_2 - L_1} \qquad (9.3)$$

and when the upper limit is broken, by:

$$v = \frac{p - LL_2}{L_2 - L_1} \qquad (9.4)$$

where p = value of the counterweight parameter in question.

It is thought that the highest barrier function magnitude and the error function should be multiplied rather than added together, because the constraints are not commensurate with the dynamic criteria being normalized on a different basis. Therefore, it is obvious that if no constraints are broken the magnitude, B, of this scaling factor must be unity. Accordingly B is given by:

$$B = 1 + t.(e^{H(v).v} - 1) \qquad (9.5)$$

where H( ) = Heavyside unit operator.

Initially it was thought that some scaling of the magnitude of v might be needed, but experience showed it was not necessary for the linkage considered.

9.3.3 Constraints on Bearing Loads.

In addition to the constraints applicable to each counterweight, is a type of constraint applied to increases in the levels of the bearing forces due to the combined effect of the counterweights. The bearing load criterion is expressed as a constraint, since, in the main, it appears that bearing loads are not considered unless they approach a failure condition. Though expressed as a constraint the function representing it is added into the error function, as it is envisaged that some designers may wish to attempt to reduce some bearing loads by attaching counterweights to the linkage: adding this term into the error function rather than taking the product enables its importance relative to the other dynamic criteria to be specified.

A bearing load criterion of the type required has already been used in Chapter Six to help select from amongst eight counterweights the 'best' set. To do this, the peak load was assumed to be applied to the weakest section of this link through the bearing. The reasons for this simplification are felt to apply here also. Therefore the magnitude to be added to the error function, C, can be expressed by:

$$C = \sum_{j=1}^{m} w_j . H(F_j - L_j) . F_j \qquad (9.6)$$

where m = number of bearings to be considered,
w = weighting factor applied to the j^{th} bearing load,
F = peak load at the j^{th} bearing,
L = the level a designer does not wish the load at the j^{th} bearing to exceed.

9.4 Error Function

9.4.1 Scaling the Dynamic Criteria.

The error function of the program of Chapter Eight only caters for two criteria, and is only used to produce sets of curves. Consequently it was not essential to scale the criteria,because the series of results used to produce the curves could be found by adjusting one weighting factor relative to the other on the basis of the previous results. However in the new program up to five dynamic criteria can be specified. Accordingly the weighting factors need to be meaningful, e.g. if a weighting factor of two is applied to the shaking force and unity to the shaking moment it should define that the shaking force is twice as important as the shaking moment. Also these factors are required to maintain this relationship no matter what form of criterion is used for a given aspect of performance. Though at present only the r.m.s. form of criterion is used, the results of a study on the forms of criteria to adopt in given situations may be implemented later. This study is reported in Chapter Ten.

Sadler and Mayne [14b]non-dimensionalized their error function by dividing the forces by the total mass of the linkage, the frame link length and the square of the assumed constant crank speed. The moment is similarly treated except that the square of the frame link length is used. However this does not scale the magnitudes of the different forms of dynamic criteria relative to each other nor does it maintain a consistency in scale if the form of criterion is changed.

The method used in this computer program to achieve the desired scaling is to divide the function representing each aspect of performance by its magnitude for the original condition of the linkage. This has the effect of setting the magnitudes of the scaled criteria to unity for the original linkage, and thus enables meaningful weighting factors to be applied. A designer tends to select his weighting factors against the levels of the dynamic characteristics of the original linkage. Since the same form of criterion is used in the denominator, the consistency in scale is maintained when the form of criterion is changed.

One exception to the above choice of denominator is for the bearing load criterion. It is thought that each of these loads should be scaled relative to the limit a designer does not wish the load to exceed. This is because the load only affects the error function if it exceeds the limit and, besides, it is against this limit that a designer tends to select the weighting factor.

9.4.2 Scaling the Error Function

The concept of using the original linkage condition for scaling can also be applied to the error function. The magnitude of the error function in the computer program of Chapter Eight has no real meaning unless it is zero. However an error function index with a continuously meaningful value can be obtained by dividing the current magnitudes of the error function by its magnitude in the original linkage condition. Further, this result is multiplied by one hundred to provide a convenient 'depth of field'. This form of error function has been successfully used in the new computer program.

9.5 Formulating the Error Function

Previously only planar linkages which lie in horizontal planes were considered. Now one which lies in the vertical plane is examined, namely the experimental model of Figure 5.6. This means that the total force and

moment applied to the frame by the linkage has inertial and gravitational components. The gravitational components of the force is constant in time, but that of the moment is not, and so a moment balance is specific to one speed. It is not the total load on the frame which is required to be reduced, but its degree of variation in time. Accordingly the time differentials of the forces and moments are used.

The gravitational and inertial forces both cause variations in the torque required to maintain constant crank speed. In this case the torque can be used rather than the torque variations, since the summated torque is zero, i.e. the net energy input to the system is zero. A torque balance is also specific to one speed, as it also contains time-dependent terms.

The error function evolved from the arguments of section 9.4 is:.

$$E=B.\left[a.\sqrt{\frac{\sum_{i=1}^{n}\dot{X}_i^2}{\dot{X}_{rms}}}+b.\sqrt{\frac{\sum_{i=1}^{n}\dot{Y}_i^2}{\dot{Y}_{rms}}}+c.\sqrt{\frac{\sum_{i=1}^{n}\dot{M}_i^2}{\dot{M}_{rms}}}+d.\sqrt{\frac{\sum_{i=1}^{n}T_i^2}{T_{rms}}}+\sum_{j=1}^{m}\{w_j.H(F_j-L_j\}.F_j\right] \qquad (9.8)$$

where B = constraintscaling factor given by equation (9.6),
a,b,c and d = weighting factors,
n = number of evaluation points of the force, moment and torque,
m = number of bearing loads to be considered,
$\dot{X},\dot{Y}$ = a point evaluation of the two components of the time differential of the shaking force,
$\dot{X}_{rms},\dot{Y}_{rms}$ = r.m.s. value of the two components of the time differential of the shaking force of the original linkage,
$\dot{M}$ = point evaluation of time differential of shaking moment,
$\dot{M}_{rms}$ = r.m.s. value of the time differential of the shaking moment of the original linkage,
T = a point evaluation of the driving torque,
T_{rms} = r.m.s. value of the driving torque of the original linkage,
F = peak load at the j bearing,
L = the level it is undesirable that the j^{th} bearing load should exceed.

9.6 Search Strategies

A number of techniques have been evolved to try to improve the ability of the new computer program to find the 'global' minimum. An obvious area investigated is the provision of meaningful initial guesses and, particularly, ones close to the global minimum. This proved to be successful for force-balance, namely the procedure presented in Chapter Four. Attempts were

made to evolve similar techniques for moment and torque balances, but without success.

Another area is concerned with methods of guiding the search. One successful method is the incorporation of a check to see if counter-weight thickness or radius is such that the effect of the counterweight is negligible. In such an event the counterweight is eliminated.

Not as successful is a procedure to fix those variables which do not cause meaningful changes (0.1%) in the error function. Improvements in convergence are obtained, but this procedure was found to prevent known optima from being found. Consequently it was removed from the final version of the program.

9.7 MEDIC

The program was called Multiple Enhancement of Dynamics by Inertial Changes, as it possesses diagnostic (analysis) and prescriptive (synthesis) features. This section is concerned with briefly describing this program. Only the major segments of the program are considered. Although the numerical minimization is a major segment, it is not described, because it is not the author's work and it is adequately reported in [39]. An accompanying listing of the final version of the program is contained, under the title Program B, in the Ph.D. Thesis Supplement.

9.7.1 MAIN Segment

In all the program segments defaults are set, when meaningful, for all input variables. The primary controls of the program are situated in the MAIN segment. Information is read in to instruct the program on how many sets of masses, dampers and springs there are and what are the parameters of each. Also, both the number of dynamic criteria to be analysed and the number of searches to be carried out are input here. Figure 9.1 contains a flow diagram of this program segment.

One facility the program possesses but which is not used in the work of this thesis is the ability to model rotational dampers and rotational

springs, where these devices are attached between two connected links. A means of scaling them was introduced, as it was found to be difficult to gauge meaningful values for these devices. Specifically the 'unit spring' and 'unit damper' is introduced, where each such device possesses that spring stiffness or damping coefficient which respectively yield magnitudes of virtual work and work done which are equal to the virtual work of the original mechanism (the pre-load of the spring is user-defined).

9.7.2 Analysis and Output Segments: SUBROUTINE PERERR and SUBROUTINE PLTSRT respectively.

To provide the means to examine the effects of adding masses, dampers and springs to the linkage of Figure 5.6, an analysis segment was developed to calculate the r.m.s., peak and mean levels of the performance variables. The performance variables are the frame shaking force, the frame shaking moment, the driving torque for constant crank speed and the bearing loads and bearing torques, as well as the time derivatives of each of these variables. This segment is SUBROUTINE PERERR and its flow chart is given in Figure 9.2. Up to eight sets of masses, dampers and springs can be input to the program, where the percentage difference between the performance variables for each set is calculated with respect to that set defined by the user as the reference set. Alternatively, the user can select the original linkage as the reference set.

The output segment both lists the above analysis and, if requested produces either a table or graphical plot of the performance variables associated with each dynamic criterion. For each requested plot of a performance variable, the curves associated with each set of devices are plotted on top of one another. This output segment is called SUBROUTINE PLTSRT and its flow chart is given in Figure 9.2

SUBROUTINE PLTSRT calls SUBROUTINE KINSOL which solves the

kinematics of the linkage. It also calls SUBROUTINE DYNMIC, which solves the forces and torques at each of the bearings. If the total shaking force applies to the frame is needed SUBROUTINE ADD is called. SUBROUTINE XYPLOT is concerned with the production of the graphical plots. None of the latter four subroutines are described in this thesis.

9.7.3 Synthesis Segment: SUBROUTINE JSYNTH

This segment controls the synthesis of counterweights. To run it, n+1 sets of n initial conditions and one set of n upper and lower limits must be input. The integer n is the number of counterweight parameters to be optimized. There are three ways these initial conditions are obtained. First the program user can specify them. It is required that the user specifies at least one set, which contains the parameters of up to IK counterweights, where IK equals the number of moving links. The need to input an appropriate value for an initial condition can be avoided by specifying a value which lies outside the associated two limits. This causes the program to randomly generate a new value which lies within the limits. Second, sets of initial conditions may also be read from a disc file which contains values from previous runs. IRST is the integer specifying the number of these sets to be read in. This latter facility enables a search to be started with part of or the complete simplex from a previous search. Third, sets of initial conditions are randomly generated after the first two input stages in order to complete the required n+1 sets. The sets are generated within the defined limits.

A set of five integers, each relating to one link, identifies which link possesses a counterweight. To fix a counterweight parameter either limits are not specified or limits are set equal to one another. In the latter case the limits do not have to equal the initial conditions. A consequence of this input format is that two unequal limits must be specified for an initial condition which is to be optimized.

Each performance variable associated with each dynamic criterion and the error function are scaled within this program segment, and it is from here that both the numerical optimization segment, SUBROUTINE SIMPLX, is called and the optimized set of counterweights output. The flowchart of this program segment is given in Figure 9.4.

9.7.4 Error Function: FUNCTION DIFF

This program segment is called upon for two different purposes. Firstly, it is called upon to evaluate the performance of a set of counterweights. In this case it begins by examining type one constraints as described in section 9.3.1. In the flowchart, Figure 9.5, H indicates the parameter being examined; L_2,L_1 the upper and lower limits respectively, and c the range (L_2-L_1). Then type two constraints are examined as described in section 9.3.2, yielding the constraint factor B. Finally the aspect of performance associated with each dynamic criterion being sought and the bearing load constraints are evaluated, and from these the error function is calculated.

The other use of this program segment is to provide a scaling factor for the error function. In this case the constraints section is by-passed (since only the original linkage is considered), the program entering the error function section directly.

9.8 Practical Experience with MEDIC

In the main the program is found to work satisfactorily. In some cases, however, a paradoxical response can occur, in that increasing a weighting factor can lead to a deterioration in the level obtained for the associated variable, after a search from the same starting conditions as before. The probable explanation for this behaviour is that the search is being diverted in the early stages so that it converges upon a less favourable local minimum.

9.9 Discussion

The improved definition of the constraint, (i.e. type one constraints as described in section 9.3.1) is seen as a major advance in this approach to Device Synthesis, since significant improvements in the results found and a noticeable reduction in the number of iterations required to find a result were obtained on including these constraints in the computer program MEDIC.

A series of different results were sought with this program to test its capabilities. To provide a difficult test the search was started from a set of difficult initial positions. Specifically each counterweight, of the five used, was set such that its mass and mass centre position were respectively similar and near to the mass and mass centre position of the associated link, i.e. within $\pm$ 20%. Further the program was required to search for the optimum in a large number of counterweight parameters, specifically eighteen. Of the twenty five possible, it is the density of each counterweight and the disc radius and thickness of the crank-based one which are fixed to reduce this number to eighteen. The latter two variables are fixed, since the crank is assumed to rotate at constant speed and therefore the effect on performance of changes in disc radius or thickness is no different from the effect of changes in radial offset.

The results of the above series of tests showed that, of the twenty sets of dynamic criteria specified, nine led to a failure to improve the performance level beyond that of the unbalanced linkage, whilst six led to only slight improvements, namely less than 30%. The remaining five sets yielded significant levels of improvements, specifically at least a 50% improvement relative to the original linkage. Three of the sets of dynamic criteria were strongly biased towards a force-balance, and so such improvements were expected. The two other improvements obtained were when the dynamic criteria sought were strongly biased towards a moment and a torque balance respectively.

By comparison, a similar set of tests with the top dyad eliminated (leaving a four-bar linkage) led to no failures. This suggests that the more complex the linkage, the more important it is to provide initial guesses reasonably near a favourable local minimum, for the program to find a satisfactory solution at the first attempt. Failing this, experience showed that satisfactory solutions could still be obtained, but only by repeated searches with different initial guesses and/or weighting factors.

Some examples of the successful use of the program to meet specific dynamic criteria for the six-bar linkage are considered in the next chapter.

9.10. Conclusion

The program, MEDIC, is considered capable of forming the basis of a program for synthesizing counterweights for a wide range of linkages. First because it can search from arbitrary starting conditions. Second, because it can simultaneously optimize large numbers of counterweight parameters.

Some success with producing initial start positions and providing guides to the search is achieved. However, it is felt that further research into developing such techniques is needed, and particularly for a program which caters for many more device parameters (>25) and more complex linkages than the present one.

CHAPTER TEN

MEDIC : SOME BALANCE RESULTS AND AN EXPERIMENTAL INVESTIGATION OF ONE RESULT

10.1 Introduction

This chapter reports a series of different types of balance obtained by the computer program, MEDIC, as well as the experimental examination of one type of balance. In addition the mathematical form that should be adopted for a given aspect of dynamic performance in a given situation is briefly discussed and recommendations made.

10.2 A Series of Balances found by MEDIC

To show both the power and the versatility of MEDIC a number of different sets of balance types (i.e. solutions governed by different dynamic criteria) were sought. The results obtained are given in Table 10.1. One of these results, row A of this table, is the result of attempting to reduce the level of r.m.s. driving torque associated with the 'best' set of counterweights of Chapter Six, without significant sacrifice of force-balance. The percentage level of the drive torque fluctuations relative to those for the original linkage condition is specific to one speed for a planar linkage whose motion occurs in a vertical plane. Accordingly improvements were sought at the permitted maximum speed of 300 r.p.m. for the force-balanced linkage. The weighting factors were selected such that the relative importance of the dynamic criteria were as follows: 95% for the time differential of the shaking force; 5% for the r.m.s. torque level; but, if at some stage during the search a bearing load exceeded its safety limit, this bearing load was set at 95% whilst the combined importance of the first two criteria, whose relative importance remains fixed, was re-set from 100% to 5%. A reduction in the r.m.s. level of torque was obtained, specifically the level of torque relative to the original level was reduced from 59% to 47%. However a reduction in force-

balance was incurred, namely from 100% to 95%. It would appear from this investigation that the existing full force-balance was already near an optimum for torque fluctuation.

Row B of Table 10.1 is the result of a search for a driving torque-balance at 300 r.p.m. but with consideration to the level of the frame-shaking force. As can be seen from this row, no significant rises are incurred in the r.m.s. or peak levels of any of the loads.

Row C is a search for a compromise between a force and torque-balance. By accepting a lower level of torque-balance, it can be seen that substantial reductions in the frame shaking force can be obtained. It is felt that this result is near the optimum design for the experimental linkage.

Row D is a search for a force and moment balance at 100 r.p.m. However, in this case the plane of motion of the linkage is horizontal, and so a balance obtained at one crank speed is theoretically valid at any speed. This row shows that the r.m.s. shaking force-level may be reduced by about 50%, without incurring any rise in the shaking moment or substantial rises in the peak bearing loads.

Row E is a search for a force-balance with consideration to the level of r.m.s. driving torque, and whilst severe constraints on the permitted levels of the peak bearing forces were imposed. A substantial force-balance was obtained without either incurring rises in the r.m.s. torque level or any load exceeding its associated load limit.

Row F is the result of a search for a torque-balance at 600 r.p.m. The results given were obtained from an analysis of the linkage when balanced by the constructed, as opposed to theoretical, counterweights. This balance is considered in greater detail in the next section. This series of results confirms the practical versatility of the program.

10.3 Partial Balance of the Driving Torque Fluctuations

10.3.1 Search for a Counterweight Set.

An obvious practical application of the program is to attempt to reduce the level of torsional vibration of the drive shaft, in order that the maximum permitted speed, at present 400 r.p.m., can be raised. It was decided to pursue this by seeking a torque-balance at the original maximum speed limit of 600 r.p.m., particularly because a theoretical investigation showed that the effects of the gravitational force at speeds of 400 r.p.m. or more are small. Consequently a torque-balance at 600 r.p.m. is still worthwhile at 400 r.p.m.

The weighting factors were set such that the importance of the torque-balance was 100%; but, if at some stage during the search a bearing load exceeded its safety limit, the bearing load weighting was 80% and the torque-balance weighting 20%. A counterweight set consisting of two counterweights was suggested by MEDIC as being an optimum, specifically one attached to the crank (link AB in Figure 3.4) and the other to the coupler (link BCE). The set yields a 59% reduction in the r.m.s. level of torque at 600 r.p.m.

It was noted that the first moment of mass of the counterweight attached to the crank is similar to that of the one previously constructed as part of the 'best' counterweight set of Chapter Six. As it is difficult to attach counterweights to this link, because of space limitations, it was decided to see if the present one could be used for the torque-balance. To do this, another search was initiated for a coupler mounted counterweight, where the parameters of the crank-based one were adjusted and fixed to represent the constructed counterweight. Although the r.m.s. level of torque reduction obtained thereby is slightly lower, viz 54%, the use of this second set of counterweights for the experimental investigation was still considered worthwhile.

10.3.2 Design of the Coupler Mounted Counterweight

A photograph of the partial torque-balance counterweight set is given in Figure 10.1. Upon testing, it was found necessary to stiffen the arm supporting the disc by means of a web thus forming a T-section. The calculated natural frequencies for this new counterweight in the plane of motion of the linkage and in that vertical plane orthogonal to the first one are 233 Hz and 95 Hz respectively.

10.3.3 Experimental Investigation

The counterweight set was first tested at a speed of 100 r.p.m. and the measured peak to peak speed fluctuation (Figure 10.2a) was found to be higher than for the original linkage condition (Figure 7.1a). This was expected, since theory predicts that this set of counterweights raises the r.m.s. level of driving torque by 72% at this speed. At 200 r.p.m. the predicted r.m.s. torque is similar to that of the unbalanced case, specifically it is less by only 17%. This is reflected in the similarity in the peak to peak speed fluctuation levels for the counterweighted (Figure 10.2b) and unbalanced (Figure 7.1b) case. At 300 r.p.m. a noticeable reduction in the peak to peak speed fluctuation is obtained for the counterweighted case (Figure 10.2c) compared to the unbalanced case (Figure 7.1c); this is expected, since the counterweight set reduces the r.m.s. torque level by 44% at this speed. On raising the speed to about 360 r.p.m., the out of balance forces and moment reach a level which caused the rig to rock on its base to such an extent that the overall worth of this counterweight is put in question.

The measured loads at joint A (Figure 10.3a) and joint D (Figure 10.3b) show that the levels of vibration have been reduced significantly at 200 r.p.m. compared to the unbalanced case (respectively Figures 7.2b and 7.3b). On comparing the measured frame shaking force for the

torque-balanced case (Figure 10.3c) with the unbalanced case (Figure 7.4b) it was found that only a 5% rise in the peak to peak frame force amplitude had been incurred.

At 300 r.p.m. a noticeable vibration is apparent at joint A (Figure 10.4a) and joint D (Figure 10.4b) over that region of these load loci between the crank angles 320^{o} and 340^{o}, but it is substantially less than that for the unbalanced case, Figures 7.2c and 7.3c. Also the use of this counterweight set has reduced by 28% the measured peak to peak amplitude of the shaking force at 300 r.p.m.; compare Figure 10.4c with Figure 7.4c. It is further suspected that this torque-balance has reduced the extent by which the frame rocks at speeds beyond 300 r.p.m., because it was noted that the frame starts to rock at a higher speed for the torque-balanced case than for the unbalanced case. Therefore it is concluded that the use of this counterweight set is worthwhile.

Although the above counterweight set leads to improvements in dynamic performance, it is not considered an optimum set, as the frame is still caused to rock at speeds below the desired maximum speed. Therefore, it is felt that a compromise between the present level of torque-balance and a force and moment balance should be sought. One result considered to be far closer to the optimum set is row C of Table 10.1. Unfortunately, time did not permit a search for the optimum set to be conducted; but on the basis of existing results it is thought that it would enable the linkage to operate at 400 r.p.m. without either incurring severe torsional vibration of the drive shaft or causing the frame to rock on its base.

10.4 The Mathematical Form to Adopt for a Given Aspect of Performance

10.4.1 Introduction

Since the previous two sections of this chapter have confirmed the versatility and practicality of a numerical minimization based approach to Device Synthesis, it is now considered timely to examine more closely the specification of appropriate criteria of dynamic performance for the variety of situations a designer is likely to meet. This in turn requires an examination of the different reasons for wishing to balance linkages.

10.4.2 The Reasons for Balancing Linkages

The main dynamic characteristics a designer may require his linkage to possess were identified in Chapter Eight, but the reasons why these features are desirable were not considered. These reasons are of obvious importance, particularly with the advent of such approaches as MEDIC, where a desired performance needs to be specified accurately in order that the search for an optimum is neither misled nor over or underconstrained. It is thought that there are five main reasons why a designer may wish to balance a linkage and they are as follows:
(i) to stop the machine frame or drive shafts from flexing and causing such problems as loss of kinematic purpose (Figure 10.5a); (ii) to stop the displacement or 'walking' of a machine (Figure 10.5b); (iii) to avoid fatigue failures (Figure 10.5c); (iv) to reduce noise (Figure 10.5d); and (v) to eliminate or reduce disturbances to surrounding mechanisms or structures (Figure 10.5e).

Except for bearing loads, dynamic performance has been represented quantitatively in this thesis solely by its r.m.s. value. This is because the modes of vibration of the machine were not considered, and so it seemed sensible to give equal weighting to all the harmonics of

excitation. In the next section, from a clearer understanding of the reasons for balancing, suggestions are made as to the mathematical function which should be adopted to represent dynamic performance in a number of particular but likely situations for each balance reason.

10.4.3 Loss of Kinematic Purpose

10.4.3.1 Introduction

The kinematic purpose of a linkage may be vitiated, as a result of the out of balance forces, moments and torques causing a frame structure or drive shaft to flex excessively. To avoid this either the frame structure or drive shaft in question can be stiffened or the linkage appropriately balanced. An insight into the form of balance solution required may be gained by considering a single mode of vibration. In doing this, the relevant aspect of performance is different for different ranges of the ratio, forcing function frequency (e.g. running speed)/natural frequency of the mode concerned. There appear to be four cases and they are examined in the following four sub-sections.

10.4.3.2 All significant forcing frequencies well below natural frequency.

In a mass-elastic system with damping <0.05 critical damping, the deflection resulting from a forcing function, all of whose significant harmonics of excitation have frequencies well below the natural frequency of the mass-elastic system, can be calculated from the quasi-static case; i.e. the peak load, $\underset{\sim}{A}$, defines the maximum displacement. Accordingly, it is suggested that the peak load should be used to represent dynamic performance in this situation. However the peak load may occur at a non-critical time within the mechanism cycle. Consequently of more importance can be the need to reduce or eliminate the effects of loads at a specific interval or intervals within the machine cycle, e.g. when the needle of a sewing machine is passing through a loop of thread to form a stitch. Therefore these critical intervals may need to be given

prominence over the rest of the cycle.

10.4.3.3 All major forcing frequencies well below natural frequency but a minor harmonic is close to this resonant frequency.

Although the amplitude of the harmonic nearest to the resonant one, A_r, may be relatively small (<0.02 of the magnitude of $\underset{\sim}{A}$), the dynamic magnification factor, μ_r, associated with the resonant condition may lead to the minor harmonic having significant effects. Accordingly the mathematical form of dynamic performance to adopt in this situation is $[\underset{\sim}{A} + \mu_r.A_r]$.

It is difficult to establish an accurate value of the dynamic magnification factor, since it is difficult to estimate accurately the damping coefficient. The assumption made throughout this section that damping is <0.05 critical damping implies that $\mu<10$. Estimation of a suitable value will depend on the designers experience in the field of application in question.

10.4.3.4 A major component of the forcing function in the resonant range.

If at least one major component of the forcing function lies within the resonant region, the effect of the dynamic magnification factor needs to be accounted for on each significant harmonic. Accordingly, for n significant harmonics, the mathematical form of dynamic performance to adopt in this situation is $\sum_{i=1}^{n} \mu_i.A_i$.

In many cases an accurate definition of the mass-elastic system will not be available. However, for harmonics with frequencies in the resonant range, say $\omega_n/2$ to $2\omega_n$ (ω_n is the natural frequency), it may be conservatively assumed that $\mu_i=\mu_r$, where μ_r is chosen as described in 10.4.3.3. Higher harmonics may be neglected in comparison to this, and lower harmonics treated quasi-statically, i.e. by assuming $\mu_i=1$.

10.4.3.5 All the major forcing frequencies well above the natural frequency.

In a system where the frequencjesof excitations are well above that of the natural frequency of the vibration mode and damping <0.05 critical damping, the spring and damping forces, moments and torques can be neglected in comparison with the inertial forces. For this case, from Newton's second law of motion, it can be shown that a good approximation of displacement X at the point of application of the load is $\frac{1}{I} \iint \underset{\sim}{F} dt^2$, where $\underset{\sim}{F}$ is the forcing function; I is the effective inertia of the machine frame (appropriately its mass or moment of inertia) referred to the point of application of the load; and t is time. The displacement at any other point will be related to this by the mode shape. Since the effective inertia of the machine is constant (assuming the frame to be substantially heavier than the linkage), a suitable mathematical criterion of performance in this case is $\iint \underset{\sim}{F} dt^2$.

10.4.4 Displacement of the Machine

10.4.4.1 Translational displacement of the machine.

A machine being displaced by the time-varying forces generated by its mechanisms is probably the classic balance problem. Two general cases are considered. The first is where the machine, which is considered to be rigid, is elastically supported, e.g. a hand held pair of electric clippers or a machine mounted on vibration isolation mounts. The machine and support then forms a system with low natural frequency, so that, as in sub-section 10.4.3.3, the preferred mathematical criterion of performance is $\iint \underset{\sim}{F} dt^2$.

The second case to consider is where a rigid machine stands directly on a rigid floor. In this case, a downwards vertical force whose line of action passes through the base of the machine cannot cause the machine to be displaced, and so can be neglected. Similarly a force directly opposite to this one does not cause the machine to displace if it is less

than m.g; where m is the mass of the machine and g the gravitational acceleration. Accordingly, if F_v is the vertical force, a suggested mathematical criterion of performance in the vertical direction is $\iint[H(F_v-m.g).(F_v-m.g)]dt^2$, where H( ) is the Heavyside unit operator.

Horizontal displacement is resisted both by the inertia of the machine and the frictional force between the machine and ground. Now the magnitude of the frictional force F_f is given by $\mu_f.H(m.g-F_v).(m.g-F_v)$. If the magnitude of the horizontal force, F_h, does not exceed the friction force it can be neglected. Thus, the suggested mathematical criterion of performance in the horizontal directions is $\iint|H(F_h-F_f).(F_h-F_f)|dt^2$. The difference between static and dynamic friction has been neglected, although it could be accounted for if required.

10.4.4.2 Rocking of the machine.

The machine can also be caused to rock, as a result of the time-varying moments its mechanisms produce. A rigid machine whose flat base stands directly on a flat rigid floor can only pivot about those two horizontal edges of its base.which are orthogonal to the plane of motion of the mechanism causing the disturbance. The moment due to the out of balance inertia forces and couples, as well as the gravitational force, is calculated about each of these points; that is M_A about the left hand edge and M_B about the right hand edge: the moments are defined to be positive anti-clockwise. Accordingly the mathematical criterion of performance in this situation is suggested to be $\iint H(M_A).M_A.dt^2 - \iint H(-M_B).M_B.dt^2$.

10.4.5 Fatigue

Fatigue is the progressive cracking of a material, and is caused by the application of a cyclically varying stress. In this case, the stress is a result of the component in question being strained, cyclically, by applied time varying loads. Assuming a linear stress strain relationship, the need is to minimize displacement, as detailed in section 10.4.3.

10.4.6 Noise

The major noise exciter in mechanisms is impact, and probably the most common impact case is that which can occur between the two bearing surfaces of a joint. One way of eliminating impact at some joints is to use force-form closed bearings [43.] Another method is to redistribute and add inertia to the linkage. Unfortunately, as discussed in section 6.9, no quantitative criterion exists by which to predict, for a wide range of linkage types and with a reasonable degree of accuracy, when loss of contact between the bearing surfaces of a joint will occur. Richards [44] concluded from studies on noise in mechanical machinery that reductions in noise energy levels of about 90% need to be achieved to yield noticeable improvements.

10.4.7 Transmission of Vibrational Energy

Transmission of vibrational energy can cause problems of loss of kinematic integrity, bearing failure, fatigue and noise in surrounding structures and mechanisms. In the majority of cases, the need is to eliminate that harmonic of the forcing function which is transmitting the greatest energy to the surrounding part in question; i.e. the harmonic of vibration of this part whose value $\mu_i.A_i$ is the greatest, and continuing in a descending order of priority with harmonics of decreasing magnitudes $\mu_i.A_i$. So again, as in sub-section 10.4.3.4, the preferred mathematical form is $\sum_{i=1}^{n} \mu_i.A_i$; although, if required, the simplification suggested in this sub-section may also be used in this case if appropriate.

10.5 Discussion

Though the foregoing section on the mathematical criteria of performance to use is considered a step forward, it is still felt that a more detailed and rigorous investigation is needed in this area.

In the light of the work of section 10.4, the desired dynamic performance of the experimental rig was reconsidered. The base of the rig was observed not to translate. Also calculations showed that the highest upwards vertical force generated by the linkage, at that speed at which the frame is displaced, was not large enough to raise off the floor that end of the rig at which this force acted. Closer observations of the base of the rig revealed that it was rocking in the plane of motion of the linkage. Accordingly the mathematical criterion to use is that suggested in sub-section 10.4.4.2.

There is also a need to reduce the torsional vibrations of the drive shaft. Since the ratio forcing function frequency/natural frequency of the drive shaft and linkage in the critical region is about 0.07, the relevant aspect of performance is that given in sub-section 10.4.3.2, i.e. the peak torque. It is of significance that the present constructed set of counterweights for the torque-balance at 600 r.p.m. yields a theoretical reduction in peak torque of 63%: the r.m.s. reduction was 54%. Thus it is now suggested that a new set of counterweights is searched for using the above recommended mathematical criteria. It is further recommended, on the basis of experience with the present rig, that the peak torque be made three times as important as the out of balance moment.

10.6 Conclusion

The torque-balance sought for a speed of 600 r.p.m. has significantly improved the performance of the linkage, but further improvements are considered possible.

A numerical minimization approach to Device Synthesis has proved to be both versatile and practical.

PART III

CONCLUDING REMARKS

CHAPTER ELEVEN

DISCUSSION, SUGGESTIONS FOR FURTHER WORK AND CONCLUSIONS

11.1 Discussion

The procedure of Chapter Four is considered to be fully developed apart from a possible simplification to the means of identifying the masses a counterweight must force-balance (sub-section 4.5.5). It is felt that full force-balance will have limited application in industry, owing to the problems force-balance can introduce, e.g. significant increases in bearing loads and torque fluctuations. An important application of the procedure, however, is the provision of initial guesses for the numerical minimization approach to synthesizing counterweights which was presented in Part II of this thesis.

The practicality and versatility of a numerical minimization approach to synthesizing counterweights has been demonstrated both by the theoretical results and by the practicality of that one investigated experimentally. Additionally, the computer program, MEDIC, has proved to be capable of searching for and finding a worthwhile result in a space of eighteen dimensions, whilst starting from an apparently difficult initial position. However, it is thought that the simplex algorithm used at present will prove to be inadequate, if the complexity of both the linkages examined and the dynamic performance sought is significantly increased.

The suggestion of particular mathematical criteria of dynamic performance to use in a number of likely situations, section 10.4, is considered an advance in what is felt to be a neglected area of research. Unfortunately, it is suspected that even these mathematical criteria, which relate to a single mode of vibration, do not possess the required level of sophistication to enable an overall dynamic requirement, e.g. the elimination of frame vibration, to be represented quantitatively.

However it may prove to be so difficult to establish general mathematical criteria that criteria will have to be derived for each machine.

It had been intended to investigate the synthesis of dyads as well as counterweights, but time permitted only a preliminary investigation of the former device. One major use of a dyad is believed to be as a replacement for a flywheel, since its energy storage capabilities can be designed to alter radically during the cycle of the mechanism to which it is attached. Additionally, it is thought that dyads may prove to be useful for force-balancing reciprocating mechanisms such as the nine-bar linkage of Figure 4.3. It had also been intended to augment the energy storage capabilities of dyads by adding springs to them, e.g. by replacing their joints with torsion bars.

A paper by Matthew and Tesar [45] on the design of springs for energy storage purposes proposes a method based on an algebraic form of kinematic synthesis, which can be applied to complex multi-link systems whose kinematics are defined.

11.2 Suggestions for Further Work

One important area requiring further work is the selection and development of numerical minimization algorithms for use in Device Synthesis. Two possible algorithms which may prove useful are presented. Price [46] developed a new random search procedure, which he describes as 'efficient in searching for global minima of multimodal function with or without constraints'. Ragsdell [47] examined the abilities of a number of different algorithms, one of which was his own, to solve a kinematic synthesis problem previously considered by Tomas [48]. The study suggested that his approach was at least an order of magnitude improvement on the DAVIDON-FLETCHER-POWELL [49] gradient based search, and the Griffith-Stewart OPTI-SEP program [50]. The algorithm developed by Ragsdell is based on a reduced gradient approach: a Fortran implementation

of this program is available under licence. The abilities of both these numerical minimization algorithms could be investigated with a suitable adaption of the computer program MEDIC.

In this thesis, the assessment of improvements in the dynamic performance of a linkage has been based on the alterations achieved in the frame and drive shaft loads. However, unless the mathematical criteria of performance are extremely sophisticated or the machine is very simple, the results so obtained may be far from the best possible in terms of the ultimate purpose of the balancing exercise. An alternative method which avoids the need to model the frame is based on modelling the mechanism and the associated devices being synthesized. To accomplish this, the mechanism and its attendant devices are replaced by sets of shakers: the forces generated at a frame pivot by the mechanism and its devices are now produced by two (for planar mechanisms) or three (for spatial mechanisms) orthogonally mounted shakers. It is proposed that each shaker is controlled by a mini-computer such that it approximates that force in its line of action which would be generated by the mechanism and its devices.

There appear to be a number of ways in which the above system can be used. First an engineer can alter, in discrete steps, the parameters of the mathematical models of the devices stored in the mini-computer until his observations of the behaviour of the machine structure suggest a suitable parameter set has been located. Second, the first approach could be extended in a manner such that instead of the designer altering the parameters of the devices a Device Synthesis program does so on the basis of a subjective index of performance input by the designer after each change. The constraints could be applied either by the designer or the mini-computer.

Third, those parts of the machine structure, along with any surrounding structures or mechanisms, which are exhibiting problems due to the dynamic loads generated by the mechanism being examined could be appropriately instrumentated. The resulting signals could then be processed electronically to form an analogue signal of performance. This signal could then be fed back to the computer, via an analogue to digital interface, to provide the error function. If one such approach proves to be viable then, truly, a mechanism could be matched optimally to its environment.

Further work is also needed to identify the range of possible uses for each of the devices listed in section 8.3.

11.3 Conclusion

Theory has been developed by which the force-balance conditions of multi-link, multi-degree-of-freedom planar linkages can be established. This theory has been incorporated into a procedure for determining the counterweights required to fully force-balance these linkages. The procedure possesses some simplifications to and overcomes certain problems with a previous procedure [21].

A major use for the above procedure is to provide initial guesses, when appropriate, for numerical minimization approaches to counterweight synthesis.

The present counterweight synthesis program, MEDIC, has proved to be a robust and effective program, and has produced a promising series of results in an exercise aimed at improving the dynamic performance of a particular Watt's six-bar linkage. One result has been tested experimentally and proved to yield a significant improvement to the dynamic performance of the linkage.

A counterweight has been designed and constructed whose effective moment of inertia with respect to the link to which it is attached is

zero at this point of attachment.

Further work is required before attempting to produce a Device Synthesis program which is capable of synthesizing many types of devices for a wide range of linkages each of which possesses many different dynamic problems. The main areas in which research is required are the development of a numerical minimization routine or routines specifically suitable for the problem of Device Synthesis; a more detailed and rigorous analysis of the reasons for balancing in order to obtain more accurate specifications of the required dynamic performance; generalization to a wider range of devices and linkages including linkages with shaft flexibility and/or speed variations; and the identification of the particular uses of each type of device, along with the means, if any, of providing initial values of their parameters.

An alternative to the two approaches to Device Synthesis of this thesis is worth investigating. In this approach the mechanism and its associated devices are physically simulated by a system of numerically controlled electro-mechanical shakers: the system is then matched optimally to the actual machine frame and, if required, the surrounding structures and mechanisms.

REFERENCES

[1] Chace, M.A. and Smith, D.A., 'DAMN - digital computer program for the dynamic analysis of generalized mechanical system'. Trans.SAE80, 969-983 (1971).

[2] Uicker, J.J. Jr., 'User's guide for IMP (Integrated Mechanisms Program): a problem oriented language for the computer-aided design and analysis of mechanisms' NSF Rep. Res.Grant GK-4552, University of Wisconsin Madison, Wisc. (1973).

[3] Lowen, G.G. and Berkof, R.S., 'Survey of Investigations into the Balancing of Linkages', J. Mechanisms, 3, 221-231 (1968).

[4] Kamenskii, V.A., 'On the problem of the number of counterweights in the balancing of plane linkages', J. Mechanisms 3(4), 323-333 (1968).

[5] Grant, S.J. and Fawcett, J.N.,'Control of clearance effects in mechanisms', ASME 77-WA/DE-2 (May 1977).

[6] Davies, T.H., 'On the balancing of mechanisms and machines with particular reference to high speed linkages', Machine Design Eng. 6(3), 40-51 (1968).

[7] Berkof, R.S. and Lowen, G.G., 'A New Method for Completely Force Balancing Simple Linkages', Trans. ASME, J.Engng.Ind. 21-26(1969).

[8] Tepper, F.R. and Lowen, G.G., 'General Theorems Concerning Full Force Balancing of Planar Linkages by Internal Mass Redistribution', Trans. ASME, J. Engng. Ind. 789-795 (1972).

[9] Shchepetil'nikov, V.A., 'The Determination of the Mass Centres of Mechanisms in Connection with the Problems of Mechanism Balancing', J. Mechanisms, 3, 367-389 (1968).

[10] Berkof, R.S. and Lowen, G.G., 'Theory of Shaking Moment Optimization of Force-Balance Four-Bar Linkages', ASME paper No. 70-Mech.-12.

[11] Berkof, R.S.,'Complete Force and Moment Balancing of Inlin Four-Bar Linkages', Mech. and Mc. Theory, 8, 397-410 (1973).

[12] Tomas, J., 'Optimum Seeking Methods Applied to a Problem of Dynamic Synthesis in a Loom', J. Mechanisms, 5, 495-504 (1970).

[13] Porter, B and Sanger, D.J.,'Synthesis of Dynamically Optimal Four-Bar Linkages', Proc. Inst. Mech. Eng. Conf., C69/72 (1972).

[14a] Smith, M.R. and Maunder, L., 'Inertia Forces in a Four-Bar Linkage', J.M.E.S. 9, No. 3, 218-225 (1967).

[14b] Sadler, J.P. and Mayne, R.W., 'Balancing of Mechanisms by Non-Linear Programming', Proc. 3rd App. Mech. Conf., Oklahoma State Univ. 29.1-29.17 (Nov. 1973).

[15] Mehmke, R., 'Uber die Geshwindigkeiten beliebiger Ordnung eines in seiner Ebene bewegten ahnlich veranderlichen eben Systems', Civil Ing. 487/(1833).

[16] Paul, B., 'Unified Criterion for the Degree of Constraint of Plane Kinematic Chains', Trans. ASME, J.App. Mechanics, 196-200 (March 1960).

[17] Deo, N.,'Graph Theory with Applications to Engineering and Computer Science', Prentice-Hall, Englewood Cliffs (1974).

[18] Grubler, M., 'Getriebelehre', Springer, Berlin (1917).

[19] Lowen, G.G., Tepper, F.R. and Berkof, R.S., 'Quantitative Influence of Complete Force Balancing on the Forces and Moments of Certain Families of Four-Bar Linkages', Mech. Mach. Theory, 9, 3/4, 299-323 (Autumn 1974).

[20] Epstein, Yu.V. and Steinvolf, L.I., 'On the Optimum Shape of Rotating Counterweights', Trudy Seminara po TMM 15 (57), 47-60 (1955).

[21] Oldham, K. and Walker, M.J., 'A Procedure for Force-Balancing Planar Linkages using Counterweights', J.M.E.S., 20,4, 177-182 (1978).

[22] Kamenskii, V.A., 'On the Question of Balancing of Plane Linkages', J. Mechanisms, 3,303-322 (1968).

[23] Reece-Jones, J. (Verbal Communication), Principal Lecturer, Mech. Eng. Dept., Liverpool Polytechnic, Byrom Street, Liverpool.

[24] Engineering Sciences Data Unit, 'Stress Concentration Data', Engineering Sciences Data Unit, 4 Hamilton Place, London, W1 65004 (1965).

[25] Wilson, A. (Verbal communication), Technical Adviser, GEC-Elliot Industrial Controls, Kidsgrove, Stoke-on-Trent, Staffs.

[26] Courant, R. and Hilbert, D.,'Methods of Mathematical Physics', Interscience New York, Vol. 1 (1953).

[27] Fawcett, J.N. and Burdess, J.S., 'Control of Clearance in Four-Bar Linkages', IFToMM, C, 111-126 (1971).

[28] Earles, S.W.E. and Wu, C.L.S.,'Predicting the Occurrenceof Contact Loss and Impact at a Bearing from a Zero Clearance Analysis', IFToMM, 4, 1013-1018 (1975).

[29] Haines, R.S., 'Two-Dimensional Vibro-Impact at Revolute Joints: State of the Art', Internal Report Ta.50, University of Newcastle upon Tyne, (1978).

[30] Eason, E.A. and Fenton, R.G., 'A Comparison of Numerical Optimization Methods for Engineering Design', Trans. ASME, J.Engng. Ind. 196-200 (February, 1974).

[31] Colville, A.R., 'A Comparative Study on Non-linear Programming Codes', IBM New York Scientific Centre, Report No. 320-2949 (June 1968).

[32] Kelley, H.J. and Myers, G.E., 'Conjugate Direction Methods for Parameter Optimization', Proc. 18th Congress of the International Astronautical Federation, Belgrade, Yugoslavia (September 1967).

[33] Box, M.J., 'A New Method of Constrained Optimization and a Comparison with other Methods', Compt. J., 8, 42-52 (1965).

[34] Fletcher, R., 'Variance Algorithm for Minimization', Comp. Journal, Vol. 13, No. 3, 317-322 (Aug. 1970).

[35] Davidon, W.C., 'Variable Metric Method for Minimization' Argonne Natl. Lab. Report 5990 (Rev.)

[36] Youssef, A.H., Oldham. K., and Maunder, L.M.,'Optimal Kinematic Synthesis of Planar Linkage Mechanisms', IFToMM, 2, 393-398 (Sept. 1975).

[37] I.B.M. 'Random Number Generation and Testing', Manual C20-8011-9(1959).

[38] Youssef, A.H., 'Dynamics and Control of Linkage Mechanisms having Two Degrees of Freedom', Ph.D. Thesis, University of Newcastle upon Tyne, (1974).

[39] Oldham, K., 'The Kinematics and Vibration of Planar Linkage Mechanisms', Ph.D. Thesis, Department of Mech. Eng., University of Newcastle upon Tyne (November 1977).

[40] Starr, P.J., 'Dynamic Synthesis of Linkages: An Emerging Field', Design Engineering Technical Conference, ASME paper No. 74-DET-64 (October 1974).

[41] Conte, F.L., George, G.R., Mayne, R.W. and Sadler, J.P., 'Optimum Mechanism Design Combining Kinematic and Dynamic-Force Considerations', Design Engineering Technical Conference, ASME paper No. 74-DET-55 (October 1974).

[42] Sadler, J.P.,'Balancing Six-Bar Linkages by Non-linear Programming', IFToMM, 1, 139-144 (Sept. 1975).

[43] Fawcett, J.N., 'Maintaining contact brings rewards', Engineering, 741-743 (September 1975).

[44] Richards, E.J., 'Noise and Mechnical Machinery', Stephenson Lecture, Mechanical Engineering Department, University of Newcastle upon Tyne, (30th November, 1978).

[45] Matthew, G.K. and Tesar, D., 'Synthesis of Spring Parameters to Satisfy Specific Energy Levels in Planar Mechanisms', Trans. ASME, J. Engng. Ind. 341-352 (May 1977).

[46] Price, W.L., 'A Controlled Random Search Procedure for Global Optimization', Towards Global Optimization, Ed. Szego and Dixon, North Holland Press (1977).

[47] Ragsdell, K.M., 'On the Application of the Generalized Reduced Gradient Method to Mechanism Synthesis', IFToMM, 2, 405-410 (Sept. 1975).

[48] Tomas, J., 'The Synthesis of Mechanisms as a Nonlinear Programming Problem', Journal of Mechanisms, Vol. 3, 119-130 (1968).

[49] Fletcher, R. and Powell, M.J.D., 'A Rapidly Convergent Descent Method for Minimization', Computer Journal, 6(2), 163-168(1963).

[50] Griffith, F.E. and Stewart, R.A., 'A Non-linear Programming Technique for Optimization of Continuous Processing Systems', Management Science, Vol. 7, 379-392 (1961).

APPENDIX I

FORCE BALANCE CONDITIONS OF A CHAIN OF LINKS

Consider a revolute jointed chain of s links which consists of one heavy link, link N, connected by light links to the frame pivot O (see Figure 2.1). Let the moment vector of the chain about the frame pivot O and with reference to the arc OS be $\underset{\sim}{\sigma}$. Then:

$$\underset{\sim}{\sigma} = m_n.(r_n.e^{i(\gamma_n+\theta_n)} + H(s-n).\sum_{j=n+1}^{s} \ell_j.e^{i\theta_j}) \qquad (A1)$$

where m_n = mass of link N,

r_n, γ_n = respectively, the radial and angular polar co-ordinates of the mass centre of link N with reference to the arc ℓ_n and the axis of the joint connecting N to the link directly below it,

θ = angle of a link with respect to a ground datum,

ℓ_j = length of the j^{th} link.

The links are numbered sequentially starting from that link furthest from the frame pivot O, i.e. 1^{st} link, to finish at that link pivoted about O, namely the s^{th} link. A Heavyside unit operator (i.e. H(i)=0 if i≤0 and 1 if i<0) is used in equation (A1) so that when link N is also the last link, i.e. n=s, the term $\sum_{j=n+1}^{s} \ell_j.e^{i\theta_j}$, which has no meaning for this condition, disappears.

Now consider all the links of the chain to have mass. The moment vector of this chain becomes:

$$\underset{\sim}{\sigma} = \sum_{n=1}^{s} m_n.(r_n.e^{i(\gamma_n+\theta_n)} + H(s-n) \sum_{j=n+1}^{s} \ell_j.e^{i\theta_j}) \qquad (A2)$$

To balance this chain of links mass is added to make equation (A2) time-invariant. The only time-dependent variables of this equation are the θ's, and so it is only these terms that have to be eliminated. Consider a simple counterweight added to the k^{th} link of the chain of links n=1,s in

Figure 2.2 Let its moment vector about O ~~and~~ with reference to the arc OS be $\underset{\sim}{\sigma}_c$, then:

$$\underset{\sim}{\sigma}_c = \mu_k.(\lambda_k.e^{i(\beta_k+\theta_k)} + H(s-k).\sum_{j=k+1}^{s} \ell_j.e^{i\theta_j}) \qquad (A3)$$

where μ_k = mass of the counterweight attached to the k^{th} link,

λ_k, β_k = respectively, the radial and angular co-ordinates of the mass centre of the k^{th} counterweight referred to point K and the arc ℓ_k.

By adding equation (A3) to equation (A2), noting that there are k-1 links more remote from the frame pivot than the k^{th} link in this chain, the coefficient of the term $e^{i\theta_k}$ can be shown to be:

$$\mu_k.\lambda_k.e^{i\beta_k} + m_k.r_k.e^{i\gamma_k} + H(k-1).\ell_k.\sum_{n=1}^{k-1} m_n \qquad (A4)$$

With a suitable choice of counterweight parameters, i.e. $(\mu_k.\lambda_k)$ and β_k, this coefficient, which is independent of time, can be set to zero permanently: the time-dependent term $e^{i\theta_k}$ is thus eliminated. In doing so, the mass of the counterweight is now part of the coefficients of the remaining θ terms and, from equation (A3), is seen to be $\mu_k.H(s-k)\sum_{j=k+1}^{s} \ell_j.e^{i\theta_j}$. This means that each successive counterweight has also to balance all the counterweights used above it. Consequently, a chain of links must be force-balanced in order starting from the top link and finishing at the frame pivoted links. Thus, in balancing a chain of links, the general force-balance condition to be satisfied on the k^{th} link, at which there will have been k-1 previous balance stages, is:

$$\mu_k.\lambda_k.e^{i\beta_k} + m_k.r_k.e^{i\gamma_k} + H(k-1).\ell_k.\sum_{n=1}^{k-1} (m_n+\mu_n) = 0(k=1,2,\ldots s) \qquad (A5)$$

This is with reference to the axis of its lower joint, point K, and the ℓ_k^{th} arc, i.e. KJ. The actual points about which the balance defined by each of these s conditions occur are the axes of the s joints connecting the links. That is the positions of the counterbalanced mass centres are sequentially transferred, from joint axes to joint axes, down the chain.

APPENDIX II

TO EVALUATE THE DEPENDENCE WITHIN A LOOP

The position with respect to Q and the arc QT of a general fixed point A in link P is:

$$\rho_p.e^{i\phi_p} = \ell_a.e^{i(\theta_p + \varepsilon_a)} + H(p-1) \sum_{j=1}^{p-1} \ell_j.e^{i\theta_j} \qquad (A6)$$

see Figure 2.3. Now from the closure condition of the loop it can be stated that:

$$\sum_{j=1}^{p-1} \ell_j.e^{i\theta_j} + \ell_p.e^{i\theta_p} + \sum_{j=p+1}^{s} \ell_j.e^{i\theta_j} = 0 \qquad (A7)$$

Hence, using the relationship:

$$\ell_p + \ell'_a.e^{i\varepsilon'_a} = \ell_a.e^{i\varepsilon_a} \qquad (A8)$$

and substituting equation (A7) into (A6) gives:

$$\rho_p.e^{i\phi_p} = \frac{\ell'_a}{\ell_p}.e^{i(\varepsilon'_a+\pi)}.H(p-1).\sum_{j=1}^{p-1} \ell_j.e^{i\theta_j} + \frac{\ell_a}{\ell_p}.e^{i(\varepsilon_a+\pi)}.H(s).\sum_{j=p+1}^{s} \ell_j.e^{i\theta_j} \qquad (A9)$$

Thus the position of the general fixed point A in P can be presented by the summation of two vectors $\underset{\sim}{B}$ and $\underset{\sim}{C}$, where $\underset{\sim}{B}$ and $\underset{\sim}{C}$ come from equation (A9) such that:

$$\rho_p.e^{i\phi_p} = \underset{\sim}{B} + \underset{\sim}{C} \qquad (A10)$$

where:

$$\underset{\sim}{B} = \frac{\ell'_a}{\ell_p}.e^{i(\varepsilon'_a+\pi)}.H(p-1).\sum_{j=1}^{p-1} \ell_j.e^{i\theta_j} \qquad (A11)$$

and:

$$\underset{\sim}{C} = \frac{\ell_a}{\ell_p} .e^{i(\varepsilon_a+\pi)} .H(s). \sum_{j=p+1}^{s} \ell_j.e^{i\theta_j} \qquad \text{(A12)}$$

For convenience, the angles (i.e. $\sum_{j=p+1}^{s} \theta_j$) in the p+1 to s chain will be measured from the other joints (instead of referring the position of the mass centre to the joint between the k^{th} and $(k-1)^{th}$ link, the one connecting the $(k-1)^{th}$ link to the k^{th} link is used) see Figure 2.3, such that:

$$H(s). \sum_{j=p+1}^{s} \ell_j.e^{i\theta_j} = H(s). \sum_{j=p+1}^{s} \ell_j.e^{i(\theta'_j+\pi)} \qquad \text{(A13)}$$

Therefore equation (A12) becomes:

$$\underset{\sim}{C} = \frac{\ell_a}{\ell_p} .e^{i\varepsilon_a} .H(s) \sum_{j=p+1}^{s} \ell_j.e^{i(\theta'_j+\pi)} \qquad \text{(A14)}$$

By observation of equation (A11) it can be seen that $\underset{\sim}{B}$ is a factored length ℓ_a/ℓ_p of the RQ chain, and offset from this chain by an angle $\varepsilon'_a+\pi$. Equally, from equation (A12), it is seen that $\underset{\sim}{C}$ is a factored length ℓ_a/ℓ_p of the STQ chain and offset from this chain by an angle ε_a.. The vectors $\underset{\sim}{B}$ and $\underset{\sim}{C}$ are shown in Figure 2.3. Thus, within a loop of revolute jointed links, there is a dependence in that the locus of a fixed point in one of the links can be expressed as a function of the kinematics of the other links in the loop.

APPENDIX III

FORCE BALANCE CONDITIONS FOR A DEPENDENT LINK

Consider a mass M placed at point A in link P of Figure 2.3. The moment vector $M.\rho_p.e^{i\phi_p}$ of this mass with reference to point Q and the arc QT can be expressed as:

$$M.\ \rho_p.e^{i\phi_p} = M.\underset{\sim}{B} + M.\underset{\sim}{C} \qquad \text{(A15)}$$

To balance the mass M equation (A15) must be made time-invariant.

Equation (A15) can be expanded by using equations (A11) and (A14) to give:

$$M.\rho_p.e^{i\phi_p} = M.\frac{\ell'_a}{\ell_p}.e^{i(\varepsilon'_a+\pi)}.H(p-1)\sum_{j=1}^{p-1}\ell_j.e^{i\theta_j} + M.\frac{\ell_a}{\ell_p}.e^{i\varepsilon_a}.H(s).\sum_{j=p+1}^{s}\ell_j.e^{i\theta'_j} \qquad \text{(A16)}$$

From equation (A16) it can be seen that the term $M.\underset{\sim}{B}$ in equation (A15) can be eliminated by balancing the mass term M'_a over the links in the RQ chain, where:

$$M'_a = M.\frac{\ell'_a}{\ell_p}.e^{i(\varepsilon'_a+\pi)} \qquad \text{(A17)}$$

Similarly to eliminate $M.\underset{\sim}{C}$ the mass term M_a must be balanced over the links in the ST chain, where:

$$M_a = M.\frac{\ell_a}{\ell_p}.e^{i\varepsilon_a} \qquad \text{(A18)}$$

A force-balance across link TQ is unnecessary since it is a frame-link.

APPENDIX IV

CONDITIONS RELATED TO A PRISMATIC JOINT

Consider a mass M fixed in or referred to the link ST of the chain STOQ of otherwise light links, see Figure 2.4. Assume that the chain lies within the loop QRSTOQ in which there are s links. The moment vector, $\underset{\sim}{T}_a$, of the mass M with reference to point Q and the frame arc QO is:

$$\underset{\sim}{T}_a = M.(\ell'_a.\, e^{i(\theta_k+\varepsilon'_a)} + H(s-k)\,.\sum_{j=k+1}^{s} \ell_j.e^{i(\theta_j+\pi)} \qquad \text{(A19)}$$

where ℓ'_a = radial offset of the mass centre of M from joint T,

ε'_a = angular offset of the mass centre of M about joint T from the arc ℓ_k,

k = subscript which identifies the link and associated counterweight in the chain.

However link RS and ST are connected prismatically and so lie at fixed angle to each other. Therefore:

$$\theta_k = \theta_{k-1} + \eta - \pi \qquad \text{(A20)}$$

Hence using equation (A20) to eliminate θ_k from equation (A19) gives:

$$\underset{\sim}{T}_a = M.(\ell'_a\,.\, e^{i(\theta_{k-1}+\varepsilon'_a+\eta-\pi)} + H(s-k).\sum_{j=k+1}^{s} \ell_j.e^{i(\theta_j+\pi)} \qquad \text{(A21)}$$

Thus the time-variant terms of link ST can be eliminated by the addition of a counterweight to link RS, e.g. in this case such that:

$$\mu_{k-1}.\lambda_{k-1}.\, e^{i\beta_{k-1}} + M.\ell'_a.e^{i(\varepsilon'_a+\eta-\pi)} = 0 \qquad \text{(A22)}$$

where μ, λ and β are the counterweight parameters previously defined in Chapter Two. The effect of this addition is to redistribute the masses such that the mass of the counterweight, μ_{k-1}, appears at joint R and the mass, M, on link ST at joint T. Obviously link ST is a dependent link, since it relies on the two chains RQ and TO to achieve its balance.

Consider the alternative case where the mass M is fixed in or referred to link RS in the chain SRQ of otherwise light links. Link RS is defined to be the dependent link. The moment vector, $\underset{\sim}{T}_b$, of the mass M with reference to point Q and the arc QO is:

$$\underset{\sim}{T}_b = M.(\ell_a.e^{i(\theta_{k-1} + \varepsilon_a)} + H(k-1).\sum_{j=k-1}^{1} \ell_j.e^{i\theta_j} \qquad (A23)$$

Substituting for θ_{k-1} in equation (A23) from equation (A20) gives:

$$\underset{\sim}{T}_b = M.(\ell_a.e^{i(\theta_k + \varepsilon_a - \eta + \pi)} + H(k-1).\sum_{j=k-1}^{1} \ell_j.e^{i\theta_j} \qquad (A24)$$

Thus, to eliminate the time-variant terms of link RS, a single counter-weight can be added to link ST such that:

$$\mu_k.\lambda_k.e^{i\beta_k} + M.\ell_a.\ e^{i(\varepsilon_a - \eta)} \qquad (A25)$$

The constant π associated with $(\varepsilon_a - \eta)$ is eliminated since the position of the transposed arc ℓ_a is referred to the arc ℓ_k at joint T and not S.

Thus for two links connected by a prismatic joint there are two balance cases to consider, i.e. when each is defined as the dependent link. Consider the case when the dependent link is the first link met in going clockwise round a loop which contains both them and the frame link. For a mass M fixed in or referred to this link, a moment vector, $\underset{\sim}{M}_a$, is referred for elimination to that revolute joint and that arc on the other link that lies within this loop, where:

$$\underset{\sim}{M}_a = M.\ell_a.e^{i(\varepsilon_a - \eta)} \qquad (A26)$$

In addition, a mass M is referred to the axis of that revolute joint of this dependent link that lies within the loop.

Consider the alternative case when it is the second link of the loop which is dependent. Then, for a mass, M, fixed in or referred to this

link a moment vector, $\underset{\sim a}{M'}$, is referred for elimination to that revolute joint and that arc on the other link that lies within the loop, where:

$$\underset{\sim a}{M'} = M.\ \ell_a^{-}.\ e^{\,i(\varepsilon_a' + \eta - \pi)} \qquad \text{(A27)}$$

A mass M must also be referred to that revolute joint of this dependent link that lies within the loop.

APPENDIX V

THE RESONANT FREQUENCY OF THE OUTPUT SHAFT AND MASS OF THE LINKAGE IT SUPPORTS

The deflection, δ, of a cantilever of length L and second moment of area I under a load P is given by:

$$\delta = \frac{P.L^3}{3.E.I} \qquad \text{(A28)}$$

where E = Young's Modulus for the material of the cantilever.

The stiffness, K, of this cantilever can thus be shown to be:

$$K = \frac{P}{\delta} = \frac{3.E.I}{L^3} \qquad \text{(A29)}$$

At a crank angle of 34^{o}, theory predicts that the effective mass, M, of the linkage supported by the output shaft is 1.21 kg. Now the natural frequency of a simple spring mass system, w_n, is given by:

$$w_n = \frac{1}{2\pi}\sqrt{\frac{K}{M}} = \frac{1}{2\pi}\sqrt{\frac{3.E.I}{L^3.M}} \qquad \text{(A30)}$$

For this output shaft $I = 9.817 \times 10^{-10} m^4$, L = 0.025m and $E = 200 \times 10^9 N/m^2$, which gives a natural frequency of 890 Hertz.

APPENDIX VI

DETERMINATION OF THE TORSIONAL VIBRATION FREQUENCY OF THE DRIVE SHAFT LOADED BY THE LINKAGE MECHANISM

To determine the natural frequency in torsion of the drive shaft and linkage system the effective moment of inertia of the linkage mechanism referred to the drive shaft is needed. Classically this is given by:

$$J = \sum_{r=1}^{n} M_r \left(\frac{V_r}{\theta_i}\right)^2 + \sum_{r=1}^{n} J_r \left(\frac{\Theta_r}{\theta_i}\right)^2 \qquad \text{(A31)}$$

where
- n = number of parts,
- r = subscript identifying a single part,
- m = the mass of a part,
- J = the polar moment of inertia of a part,
- V = translational velocity of the mass centre of a part,
- θ = angular velocity of a part,
- θ_i = angular velocity of the part to which the moment of inertia is being referred.

The translational velocities, $V_1, V_2 \ldots V_n$ and the angular velocities $\theta_1, \theta_2 \ldots \theta_n$ are found from a computer program. The effective moment of inertia of the mechanism at the drive shaft is calculated to be 8.63×10^{-3} kg.m^2.

Before the natural frequency can be determined, the torsional stiffness, K, of the drive shaft is needed. This is given by:

$$K = \frac{G.J}{L} \qquad \text{(A32)}$$

where
- G = Bulk Modulus of Rigidity,
- J = polar moment of inertia,
- L = length of the shaft.

The shaft is made from steel and thus its Bulk Modulus of Rigidity is about 8.28×10^{10} N/m^2, and, since its diameter is 0.017m, its second moment of area is 8.20×10^{-9} m^4. The free length between the flywheel and crank is 0.219m. Accordingly its stiffness is calculated to be 3.1×10^3 N.m/rad.

A reasonable model of this vibrational system is two rotors (i.e. the linkage and the flywheel) connected by a torsional spring. However the

flywheel has a much larger moment of inertia than that of the linkage, namely 0.153kg.m^2 as opposed to 8.63×10^{-3}kg.m^2. Hence the flywheel can be considered to provide an encastré support about which the 'linkage rotor' resonates with the torsional spring. Consequently the natural frequency of this system, f, is given by:

$$f = \frac{1}{2\pi}\sqrt{\frac{K}{J}} \qquad \text{(A33)}$$

Accordingly f is calculated to be 95 Hertz.

APPENDIX VII

DETERMINATION OF THE PERMISSIBLE JOINT LOADS AND DRIVING TORQUE

A7.1 Calculation of the Load Limit for Joint A.

Figure 3.4 contains a schematic layout of the linkage being considered. There are felt to be two likely modes of failure at joint A, and these are considered under the following heads (i) Failure in Shear of the Drive Pin and (ii) Failure of a Link Joint A Connects.

A7.1.1 Failure in Shear of the Drive Pin.

A tapered pin is used to transmit the torque between the drive shaft and crank. Its smallest diameter is 0.004m and its permissible level of stress is $75 \times 10^6 N/m^2$. A permissible stress is defined to be the yield or proof stress divided by four, i.e. it accounts for the safety factor of 4:1. Assuming the pin will fail in double shear and noting that the drive shaft is 0.017m in diameter, the driving torque should not be allowed to exceed 128N.m.

A7.1.2 Failure of a Link Joint A Connects

Joint A connects the steel crank AB to the frame link AD. Of the two, the crank is considered the most likely to fail by the tear-out of the drive shaft from it. From reference [24], it is known that for a bar loaded by a pin the maximum permissible load, P, is given by:

$$P = \sigma . \frac{d.t}{K} \qquad \text{(A34)}$$

where σ = maximum permissible stress ($88 \times 10^6 N/m^2$),
d = diameter of the drive shaft (0.017m),
t = thickness of the crank (0.012m),
K = stress concentration factor (2.6).

Accordingly the maximum permissible load for joint A is found to be 6,900N.

A7.2 Determination of the Load Limit for Joint B

There are felt to be three likely modes of failure for joint B and these are considered under the following heads (i) Failure of the Bearing Pin in Shear, (ii) Bearing Failure and (iii) Failure of a Link Joint B Connects.

A7.2.1 Failure of the Bearing Pin in Shear

The pin is considered to be loaded in single shear, and a stress concentration factor of 2:1 is imposed, since the pin is stepped. This pin is of 0.008m diameter and its permissible stress is $75 \times 10^6 N/m^2$, and so the load should not be allowed to exceed 1,550N.

A7.2.2 Bearing Failure

Two bearings are used at this joint. For a life of 200 hours, the manufacturers recommend that the dynamic load should not exceed 775N. Accordingly the limit imposed to avoid premature bearing failure is 1,550N.

A7.2.3 Failure of a Link Joint B Connects

Joint B connects the steel crank AB to the aluminium link BCE. Link BCE is offset from the crank and so the forces lie in two planes. Link BCE has a heat-shrunk-fitted pin, which is located in the crank by the above two bearings. The likely failure condition is believed to be the tear-out of this pin from the aluminium link, because the crank is both stronger and is seen as being rigid relative to BCE.

Before this load limit can be calculated, an allowance for the pre-stress induced by the heat-shrunk-fitted pin must be made. From reference [24], the induced stress, σ_p, is given by:

$$\sigma_p = \frac{E.\varepsilon.(1+r^2)}{2+\{\frac{E(1-\gamma_1)}{E_1} - (1-\gamma)(1-r^2)\}} \qquad \text{(A35)}$$

where $r = \frac{\text{pin diameter (0.01m)}}{\text{link width (0.03m)}}$,
ε = interference fit (5×10^{-5}m),
E = Young's Modulus for the link (70×10^{9}N/m^2),
E_1 = Young's Modulus for the pin (200×10^{9}N/m^2),
γ = Poisson's ratio for the link (0.33),
γ_1 = Poisson's ratio for the pin (0.27).

Thus σ_p is calculated to be 5×10^{6}N/m^2, and so the permissible stress is 30×10^{6}N/m^2. From equation (A34), knowing d = 0.01m, t=0.01m and K=2.4, the permissible load is found to be 1,250N. This is the lowest limit, and therefore the predicted load at joint B must not be allowed to exceed 1,250N.

A7.3 Determination of the Load Limit for Joint C

Joint C connects the two links BCE and CDG. There are felt to be two likely modes of failure which are considered under the following heads (i) Failure of a Link Joint C Connects and (ii) Bearing Failure. The limit associated with bearing failure is identical to that calculated in section A7.2.2, since the bearing assembly is the same.

A7.3.1 Failure of a Link Joint C Connects

The two links joint C connects lie in the same plane, and thus the likely mode of failure is felt to be the tear-out of the pin fitted into link CDG. This link possesses a heat-shrunk-fitted pin similar to that of section A7.2.3, and so an allowance of a pre-stress of 5×10^{6}N/m^2 must be made. From equation (A34), since d=0.01m, t=0.01m and K=2.4, the permissible load is calculated to be 1,250N. This is the lowest limit, and so it is taken as the maximum permissible load for joint C.

A7.4 Determination of the Load Limit at Joint D

There are felt to be two modes of failure associated with the load at joint D, and they are considered under the following heads (i) Failure of a Link Joint D Connects and (ii) Failure of the Output Shaft in Shear.

A7.4.1 Failure of a Link Joint D Connects

The aluminium link is felt to be considerably more prone to failure than the steel frame. Failure at this link is assumed to be the tear-out

of the output shaft which is heat-shrunk-fitted into link CDG, as the deflection of this shaft is felt to be insignificant for this purpose. An allowance of a pre-stress associated with the heat-shrink fit of the shaft must be made. It is $3.5 \times 10^6 N/m^2$. Accordingly, since the permissible stress is $29.5 \times 10^6 N/m^2$, d=0.01m, t=0.01m and K=2.7, the permissible load is 1,090N.

A7.4.2 Failure of the Output Shaft in Shear

The output shaft is stepped down from its 0.015m diameter at link CDG to 0.01m in order to fit into the frame bearings. It is thought that this smaller diameter section might fail. A stress concentration factor of 2:1 is applied, because of the diametral step, and so the permissible stress is $3.8 \times 10^6 N/m^2$. Accordingly the permissible load to avoid this failure is 11,300N.

From the above analyses, the permissible load at joint D is found to be 1,090N. This limit defines the maximum permissible level of the shaking moment about the crank pivot, namely 273N.m.

A7.5 Determination of the Load Limits at Joints E, F and G

The similarities in the layouts of the bearings and links at joints C, E, F and G are such that the load limit previously calculated for joint C also applies to these other joints, i.e. 1,250N.

As a result of this analysis it was found that the maximum permissible speed can be increased to 600 r.p.m., whilst still leaving a wide margin to accommodate increases in load due to the addition of counterweights.

APPENDIX VIII

FORCE-BALANCE CONDITIONS FOR THE EXPERIMENTAL MODEL

Balance A

Link AB

$$\mu_1.\lambda_1.e^{i\beta_1}+m_1.r_1.e^{i\gamma_1}+\left[m_2.\frac{r_2'}{\ell_{2c}}.e^{i(\gamma_2'+\pi)}+m_5.\frac{r_5'}{\ell_5}.e^{i(\gamma_5'+\pi)}.\frac{\ell_{2b}}{\ell_{2c}}.e^{i(\varepsilon_2'+\pi)}\right].\ell_1=0 \quad (A36)$$

Link CDG

$$\mu_3.\lambda_3.e^{i\beta_3}+m_3.r_3'.e^{i(\gamma_3'+\pi)}+\left[m_5.\frac{r_5'}{\ell_5}.e^{i(\gamma_5'+\pi)}.\frac{\ell_{2a}}{\ell_{2c}}.e^{i\varepsilon_2}+m_2.\frac{r_2}{\ell_{2c}}.e^{i\gamma_2}\right].\ell_{3c}$$

$$+(m_6+\mu_6+m_5.\frac{r_5}{\ell_5}.e^{i\gamma_5}).\ell_{3b}.e^{i(\varepsilon_3'+\pi)}=0 \quad (A37)$$

Link FG

$$\mu_6.\lambda_6.e^{i\beta_6}+m_6.r_6'.e^{i(\gamma_6'+\pi)}+m_5.\frac{r_5}{\ell_5}.e^{i\gamma_5}.\ell_6=0 \quad (A38)$$

Balance B

Link AB

$$\mu_1.\lambda_1.e^{i\beta_1}+m_1.r_1.e^{i\gamma_1}+\left[m_2.\frac{r_2'}{\ell_{2c}}.e^{i(\gamma_2'+\pi)}+(m_5+\mu_5+m_6.\frac{r_6'}{\ell_6}.e^{i(\gamma_6'+\pi)}).\frac{\ell_{2b}}{\ell_{2c}}.e^{i(\varepsilon_2'+\pi)}\right].\ell_1=0 \quad (A39)$$

Link CDG

$$\mu_3.\lambda_3.e^{i\beta_3} + m_3.r_3'.e^{i(\gamma_3'+\pi)} + \left[m_2.\frac{r_2}{\ell_{2c}}.e^{i\gamma_2} + (m_5+\mu_5+m_6.\frac{r_6'}{\ell_6}.e^{i(\gamma_6'+\pi)}).\frac{\ell_{2a}}{\ell_{2c}}.e^{i\varepsilon_2} \right].\ell_{3c}$$

$$+ m_6.\frac{r_6}{\ell_6}.e^{i\gamma_6}.\ell_{3b}.e^{i(\varepsilon_3'+\pi)} = 0 \qquad \text{(A40)}$$

Link EF

$$\mu_5.\lambda_5.e^{i\beta_5} + m_5.r_5.e^{i\gamma_5} + m_6.\frac{r_6'}{\ell_6}.e^{i(\gamma_6'+\pi)}.\ell_5 = 0 \qquad \text{(A41)}$$

Balance C

Link AB

$$\mu_1.\lambda_1.e^{i\beta_1} + m_1.r_1.e^{i\gamma_1} + \left[m_2+\mu_2+m_3.\frac{r_3'}{\ell_{3c}}.e^{i(\gamma_3'+\pi)} + (m_6+\mu_6).\frac{\ell_{3b}}{\ell_{3c}}.e^{i(\varepsilon_3'+\pi)} \right.$$

$$\left. + m_5.\frac{r_5}{\ell_5}.e^{i\gamma_5}.\frac{\ell_{3b}}{\ell_{3c}}.e^{i(\varepsilon_3'+\pi)} + m_5.\frac{r_5'}{\ell_5}.e^{i(\gamma_5'+\pi)} \right].\ell_1 = 0 \qquad \text{(A42)}$$

Link BCE

$$\mu_2.\lambda_2.e^{i\beta_2} + m_2.r_2.e^{i\gamma_2} + \left[m_3.\frac{r_3'}{\ell_{3c}}.e^{i(\gamma_3'+\pi)} + (m_6+\mu_6+m_5.\frac{r_5}{\ell_5}.e^{i\gamma_5}).\frac{\ell_{3b}}{\ell_{3c}}.e^{i(\varepsilon_3'+\pi)} \right].\ell_{2c}$$

$$+ m_5.\frac{r_5'}{\ell_5}.e^{i(\gamma_5'+\pi)}.\ell_{2a}.e^{i\varepsilon_2} \qquad \text{(A43)}$$

Link FG

As equation (A38)

Balance D

Link AB

$$\mu_1.\lambda_1.e^{i\beta_1} + m_1.r_1.e^{i\gamma_1} + \left[m_2 + \mu_2 + m_6.\frac{r_6}{\ell_6}.e^{i\gamma_6}.\frac{\ell_{3b}}{\ell_{3c}}.e^{i(\varepsilon_3'+\pi)} + m_3.\frac{r_3'}{\ell_{3c}}.e^{i(\gamma_3'+\pi)} + m_5 + \mu_5 + m_6.\frac{r_6'}{\ell_6}.e^{i(\gamma_6'+\pi)} \right].\ell_1 = 0 \qquad \text{(A44)}$$

Link BCE

$$\mu_2.\lambda_2.e^{i\beta_2} + m_2.r_2.e^{i\beta_2} + \left[m_6.\frac{r_6}{\ell_6}.e^{i\gamma_6}.\frac{\ell_{3b}}{\ell_{3c}}.e^{i(\varepsilon_3'+\pi)} + m_3.\frac{r_3'}{\ell_{3c}}.e^{i(\gamma_3'+\pi)} \right].\ell_{2c}$$

$$+ \left[m_5 + \mu_5 + m_6.\frac{r_6'}{\ell_6}.e^{i(\gamma_6'+\pi)} \right].\ell_{2a}.e^{i\varepsilon_2} = 0 \qquad \text{(A45)}$$

Link EF

As equation (A41)

LINKS TO WHICH COUNTER-WEIGHTS ARE ADDED	% RISE IN LOADS RELATIVE TO THE ORIGINAL LINKAGE CONDITION					
	PEAK BEARING LOADS				RMS MOMENT ABOUT CRANK PIVOT	DRIVING TORQUE
	A	B	C	D		
CDG, BCE and FG	391	415	645	749	395	575
AB, CDG and FG	91	326	251	230	144	193

TABLE 3.1 PERCENTAGE RISE IN LOADS DUE TO TWO DIFFERENT FORCE-BALANCES

LINK	LINK SUFFIX	MASS	RADIAL OFFSET		ANGULAR OFFSET		LINK LENGTH
			r	r'	γ	γ'	
		kg	$x10^{-2}$m	$x10^{-2}$m	degrees	degrees	$x10^{-2}$m
JA	1	1.505	3.13	-	300.0	-	8.98
HJ	2	0.17	1.9	1.9	0.0	180.0	3.87
FGH	$3\,^{a}_{b}$	1.805	0.7	-	141.0	-	5.93 8.23
AB	4	2.475	0.25	-	310.0	-	8.98
BD	5	1.631	5.45	-	171.1	-	18.37
DE	6	0.137	1.9	1.9	0.0	180.0	3.81
EF	7	0.093	1.9	1.9	0.0	180.0	3.81
EK	8	1.985	0.4	-	180.0	-	7.62

TABLE 4.1 KINEMATIC AND INERTIA PARAMETERS OF THE INDUSTRIAL NINE-BAR LINKAGE

LINK	LINK SUFFIX	MASS	MOMENT OF INERTIA	RADIAL OFFSET		ANGULAR OFFSETS				LINK LENGTHS
				r	r′	γ	γ′	ε	ε′	
		kg	$x10^{-3} kg.m^2$	$x10^{-2} m$	$x10^{-2} m$	degrees	degrees	degrees	degrees	$x10^{-2} m$
AB	1	0.3775	-	3.15	2.85	0.0	180.0	-	-	6.00
BCE	a 2b c	0.740	0.373	12.60	8.20	12.77	160.14	48.19	131.81	15.00 15.00 20.00
CDG	a 3b c	0.540	0.243	11.60	6.70	7.87	166.29	45.82	142.64	11.00 13.00 18.00
AD	4				FRAME	LINK				25.00
EF	5	0.6445	0.405	8.00	9.80	11.67	170.49	-	-	17.50
FG	6	0.4275	1.443	11.40	4.00	7.65	157.72	-	-	15.00

FIGURE 5.1 KINEMATIC AND INERTIA PARAMETERS OF THE WATT'S SIX-BAR LINKAGE

RESULT		Parameters of the counterweights required to fully force-balance the Watt's six-bar linkage													
		LINK	mass	radial offset	ang. offset	LINK	mass	moment of inertia	radial offset	ang. offset	LINK	mass	moment of inertia	radial offset	ang. offset
			kg	$x10^{-2}$ m	deg.		kg	$x10^{-2}$ $kg.m^2$	$x10^{-2}$ m	deg.		kg	$x10^{-2}$ $kg.m^2$	$x10^{-2}$ m	deg.
Balance A	case 1	AB	0.963	4.424	152.15	CDG	4.061	1.676	26.836	354.50	FG	1.199	1.460	19.932	0.59
	case 2	AB	0.963	4.424	152.15	CDG	3.347	1.138	26.187	357.38	FG	0.382	0.148	30.493	1.21
Balance B	case 1	AB	1.905	6.221	139.35	CDG	4.258	1.842	26.500	9.92	EF	1.328	1.793	5.195	182.38
	case 2	AB	1.423	5.378	143.54	CDG	3.366	1.151	25.894	6.54	EF	0.383	0.149	2.791	182.38
Balance C	case 1	AB	4.453	9.512	172.58	BCE	4.385	1.953	9.439	163.72	FG	1.199	1.460	19.932	0.59
	case 2	AB	2.746	7.469	170.67	BCE	1.227	0.153	0.250	171.67	FG	0.382	0.148	30.493	1.21
Balance D	case 1	AB	4.834	9.911	178.51	BCE	4.567	2.119	9.633	209.38	EF	1.328	1.793	5.195	182.38
	case 2	AB	2.899	7.675	176.80	BCE	1.237	0.155	5.132	200.88	EF	0.383	0.148	19.932	0.59

TABLE 6.1 PARAMETERS OF THE EVALUATED COUNTERWEIGHT SETS

FORCE BALANCE	JOINT A	JOINT B	JOINT C	JOINT D	JOINT E	JOINT F	JOINT G	DRIVING TORQUE	SHAKING MOMENT	ORDER OF PREFERENCE
	F(N) %F %EXCESS	F(N) %F %EXCESS	F(N) %F %EXCESS	F(N) %F %EXCESS	F(N) %F %EXCESS	F(N) %F %EXCESS	F(N) %F %EXCESS	T(N.m) %EXC. %RMS	M(N.m) %EXC. %RMS	
A case 1	1503.0 97.2 21.8	1581.0 119.5 126.5	1172.2 222.1 93.8	1571.4 241.8 83.1	242.9 -6.7 19.4	50.5 38.0 4.0	418.8 234.0 33.5	52.4 40.9 112.6	321.2 11.5 242.9	3
A case 2	1122.5 47.3 16.3	1197.0 66.2 95.8	772.4 112.2 61.8	1183.3 157.4 62.6	284.0 9.1 22.7	91.4 149.8 7.3	202.1 61.2 16.2	39.9 31.2 59.2	250.4 8.9 167.2	1
B case 1	1877.0 146.2 27.2	2027.4 181.4 162.2	1190.0 227.0 95.2	1969.7 328.4 104.2	734.6 182.3 58.8	98.3 168.6 7.9	185.0 47.5 14.8	66.2 51.7 171.9	457.7 16.3 404.8	4
B case 2	1273.6 67.1 18.5	1383.0 92.0 110.6	797.4 119.1 63.8	1343.5 192.2 71.1	437.3 68.0 35.0	151.6 314.3 12.1	233.8 86.5 18.7	44.9 35.1 84.4	309.2 11.0 239.6	2
C case 1	1570.6 106.0 22.8	3155.5 338.0 252.4	1283.8 252.8 102.7	1468.7 219.4 77.7	242.9 -6.7 19.4	50.5 38.0 4.0	418.8 234.0 33.5	63.5 49.6 143.7	298.8 10.7 274.8	7
C case 2	1497.8 96.5 21.7	2234.7 210.2 178.8	1329.2 265.2 106.3	1441.0 213.4 76.2	284.0 9.1 22.7	91.4 149.7 7.3	202.1 61.2 16.2	57.0 44.5 125.4	295.5 10.6 253.0	5
D case 1	15662 105.4 22.7	33403 363.6 267.2	1308.8 259.6 104.7	1457.9 217.1 77.1	734.6 182.3 58.8	98.3 168.6 7.9	185.0 47.5 14.8	57.8 45.2 116.0	297.1 10.6 238.7	8
D case 2	15014 96.9 21.8	2291.3 218.0 183.3	1244.3 213.6 99.5	1441.8 213.6 76.3	437.3 68.0 35.0	151.6 314.3 12.1	233.8 86.5 18.7	55.1 43.0 113.0	295.9 10.6 238.3	6
safe load (N)	6.9×10^3	1.25×10^3	1.25×10^3	1.89×10^3	1.25×10^3	1.25×10^3	1.25×10^3	128.0	2.8×10^3	

F,T and M= peak bearing force, driving torque and shaking moment respectively. %EXC. or %EXCESS= %of the safe load limit.

%RMS =%rise in r.m.s. value relative to original linkage condition.
%F,%T and %M=%rise in peak value relative to the original linkage condition.

TABLE 6.2 COMPARISON OF THE WORTH OF THE DIFFERENT SETS OF COUNTERWEIGHTS.

%DIFFERENCE BETWEEN THE THEORETICAL AND PRACTICAL COUNTERWEIGHT SET							
LOAD ON JOINT A			LOAD ON JOINT D			DRIVING TORQUE	
X_{rms}	Y_{rms}	PEAK	X_{rms}	Y_{rms}	PEAK	R.S	PEAK
5.9	5.6	6.3	13.2	15.0	12.6	5.6	7.0

TABLE 6.3 COMPARISON BETWEEN THE THEORETICAL AND PRACTICAL COUNTERWEIGHT SET

IMPOSED CHANGE	%CHANGE IN FORCE-BALANCE			%CHANGE IN PEAK LOAD AT JOINT A
	X_{rms}	Y_{rms}	PEAK	
2% change in density or thickness	0.57	0.94	0.33	-0.35
2% change in radial offset	0.57	0.94	0.33	-0.21
2° shift in angular offset	1.00	1.65	0.57	-0.40

(a) CHANGES IMPOSED ON THE CRANK COUNTERWEIGHT

IMPOSED CHANGE	%CHANGE IN FORCE BALANCE			%CHANGE IN LOAD ON JOINT A	%CHANGE IN LOAD ON JOINT D	%CHANGE IN RMS DRIVING TORQUE
	X_{rms}	Y_{rms}	PEAK			
2% change in density or thickness	1.75	1.42	1.74	-0.45	0.46	-0.37
2% change in disc radius	3.44	2.80	3.4	0.85	1.95	0.82
2% change in radial offset	1.75	1.42	1.74	1.05	1.02	0.97
2° shift in angular offset	1.53	5.00	3.02	0.50	1.22	0.53

(b) CHANGES IMPOSED ON COUNTERWEIGHT ATTACHED TO CDG

IMPOSED CHANGE	%CHANGE IN FORCE-BALANCE			%CHANGE IN LOAD ON JOINT A	%CHANGE IN LOAD ON JOINT D	%CHANGE IN RMS DRIVING TORQUE
	X_{rms}	Y_{rms}	PEAK			
2% change in density or thickness	0.24	0.66	0.41	-0.75	-0.42	-0.85
2% change in disc radius	0.39	1.07	0.67	-0.65	-0.29	-0.75
2% change in radial offset	0.24	0.46	0.36	0.09	0.15	0.12
2° shift in angular offset	0.46	0.63	0.59	0.43	0.33	0.49

(c) CHANGES IMPOSED ON COUNTERWEIGHT ATTACHED TO FG

Note: all imposed changes are increases on original values

TABLE 6.4 CHECK ON SENSITIVITY OF FORCE-BALANCE TO MACHINING AND POSITIONING ERRORS

LINK (LINK SUFFIX)	MASS kg (lb)	MOMENT OF INERTIA kg.m^2 (lb.in^2)	RADIAL OFFSET m (in)	ANGULAR OFFSET degrees	LINK LENGTH m (in)
CRANK(1)	0.227 (0.5)	-	0.0762(3.0)	0.0	0.1524(6.0)
COUPLER(2)	0.454 (1.0)	0.00351 (12.0)	0.1524 (6.0)	0.0	0.3048(12.0)
ROCKER(3)	0.454 (1.0)	0.00351 (12.0)	0.1524 (6.0)	0.0	0.3048(12.0)
FRAME(4)	-	-	-	-	0.3048(12.0)

TABLE 8.1 KINEMATIC AND INERTIAL PARAMETERS OF THE FOUR-BAR LINKAGE OF CHAPTER EIGHT

BALANCE	PURPOSE	DRIVING TORQUE		TIME DIFF. OF SHAKING FORCE		SHAKING MOMENT	JOINT A	JOINT B	JOINT C	JOINT D	SPEED
		PEAK %RMS (N.m)	%PEAK %EXC.	PEAK $\%X_{rms}$ (N/s)	%PEAK $\%Y_{rms}$	PEAK %PEAK %EXCESS (N.m)	PEAK %PEAK %EXCESS (N)	PEAK %PEAK %EXCESS (N)	PEAK %PEAK %EXCESS (N)	PEAK %PEAK %EXCESS (N)	RPM
A	Attempt to improve full force-balance of Chapter six (vertical plane).	9.2 47.1	64.8 7.2	418.4 -95.4	-94.8 -95.7	-68.2 2.4 158.8	252.5 37.5 3.7	283.3 61.7 22.7	187.0 100.6 15.0	308.9 147.0 16.3	300
B	Torque-balance (vertical plane).	-3.0 -55.0	-46.3 2.3	6821.1 16.1	-14.9 31.9	27.7 1.0 31.3	205.8 12.1 3.0	191.3 9.3 15.3	125.6 34.8 10.0	133.4 11.5 8.6	300
C	Force and torque balance sought (vertical plane).	-17.9 -37.7	-25.4 14.9	27431.6 -61.8	-57.2 -70.6	100.8 3.6 25.3	446.1 -41.5 6.5	1251.4 73.7 100.1	451.8 24.2 36.0	513.6 11.7 27.2	600
D	Force and moment balance sought. (horizontal plane).	0.7 0.0	0.8 0.5	9.7 -48.2	-48.8 -49.3	-2.8 0.1 -1.1	16.0 -25.4 0.2	20.5 1.5 1.6	10.2 1.8 0.8	12.3 -0.8 1.0	100
E	Force and torque balance sought, with severe constraint on crank: frame force. (vertical plane).	-26.1 -4.1	8.4 20.4	22719.5 -68.2	-64.6 -74.9	142.0 5.1 72.5	662.6 -13.1 9.6	1254.2 74.1 100.3	655.2 80.0 52.4	719.9 56.6 57.6	600
F	Torque-balance given by constructed counterweights (vertical plane).	-9.0 -54.4	-62.7 7.0	518894 25.8	-19.1 58.9	125.4 4.5 32.6	978.7 28.4 14.2	1075.0 49.3 86.0	557.8 53.3 44.6	616.4 34.1 49.3	600

%RMS and %PEAK refer respectively to the rises in rms or peak value of the parameter relative to the original linkage.
%EXC. or %EXCESS equals the percentage a parameter is of the associated safety limit.
%X and %Y refer respectively to the percentage rise in the horizontal and vertical shaking forces.

TABLE 10.1 A RANGE OF BALANCES FOUND BY MEDIC

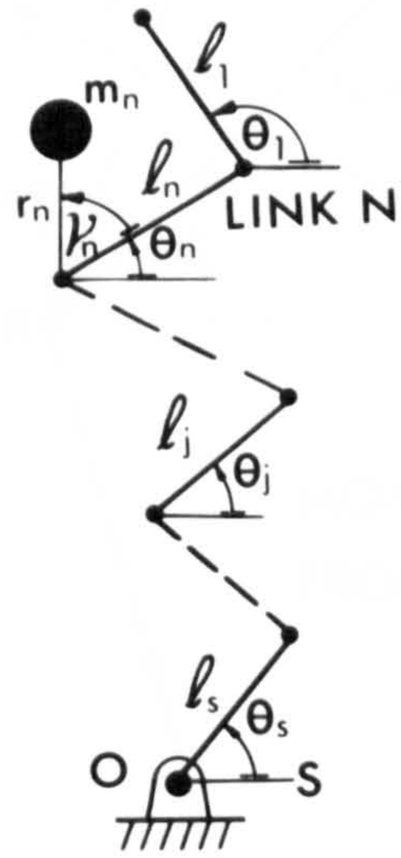

FIGURE 2.1 CHAIN OF S LINKS

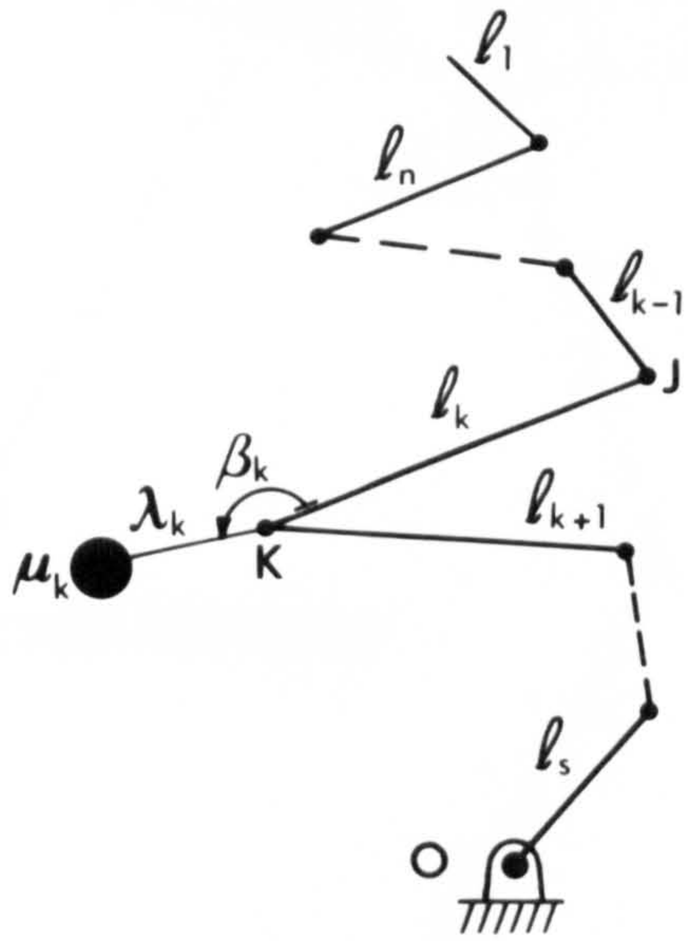

FIGURE 2.2 COUNTERWEIGHT TO LINK K.

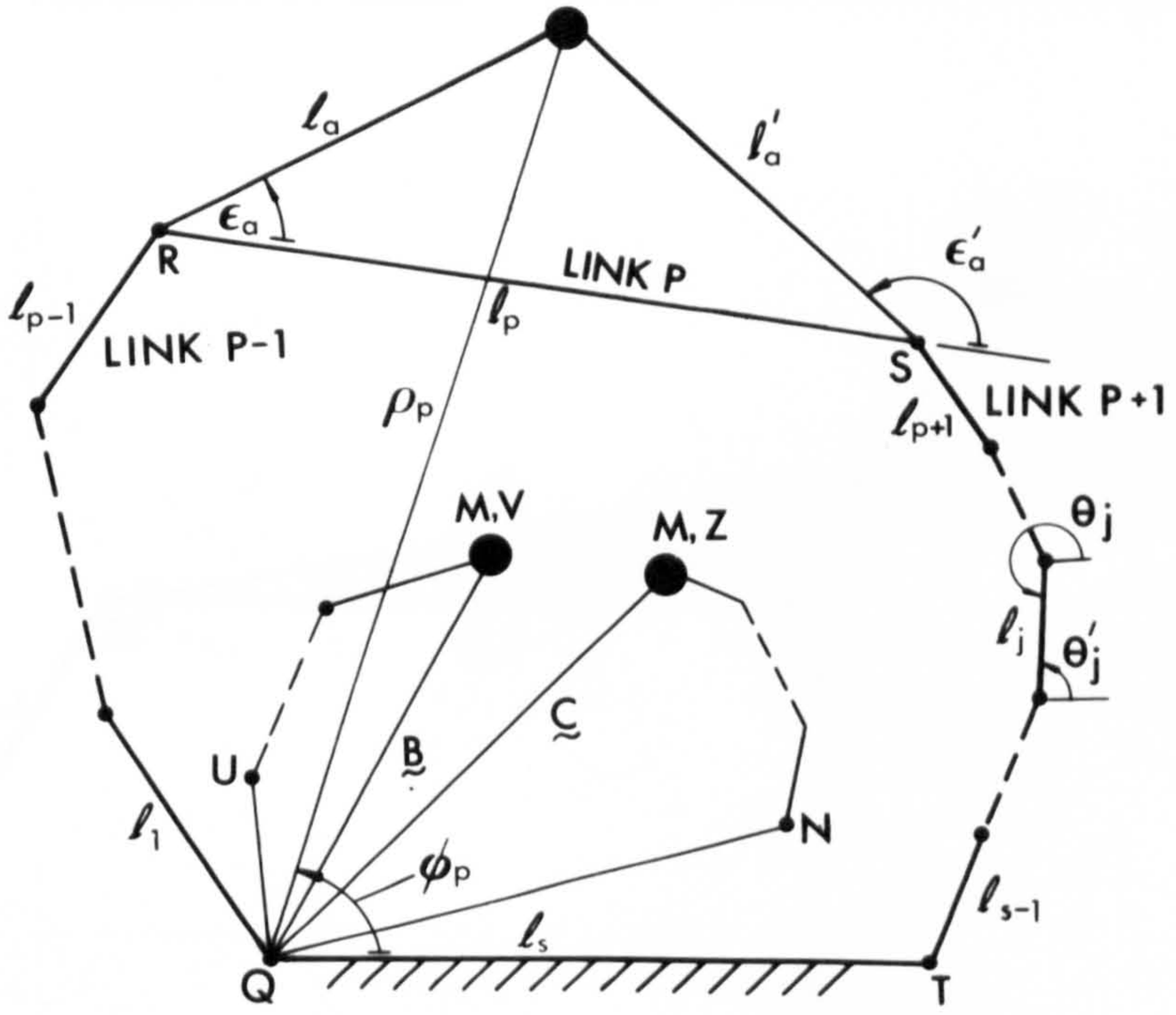

FIGURE 2.3 A DEPENDENT LINK WITHIN A LOOP

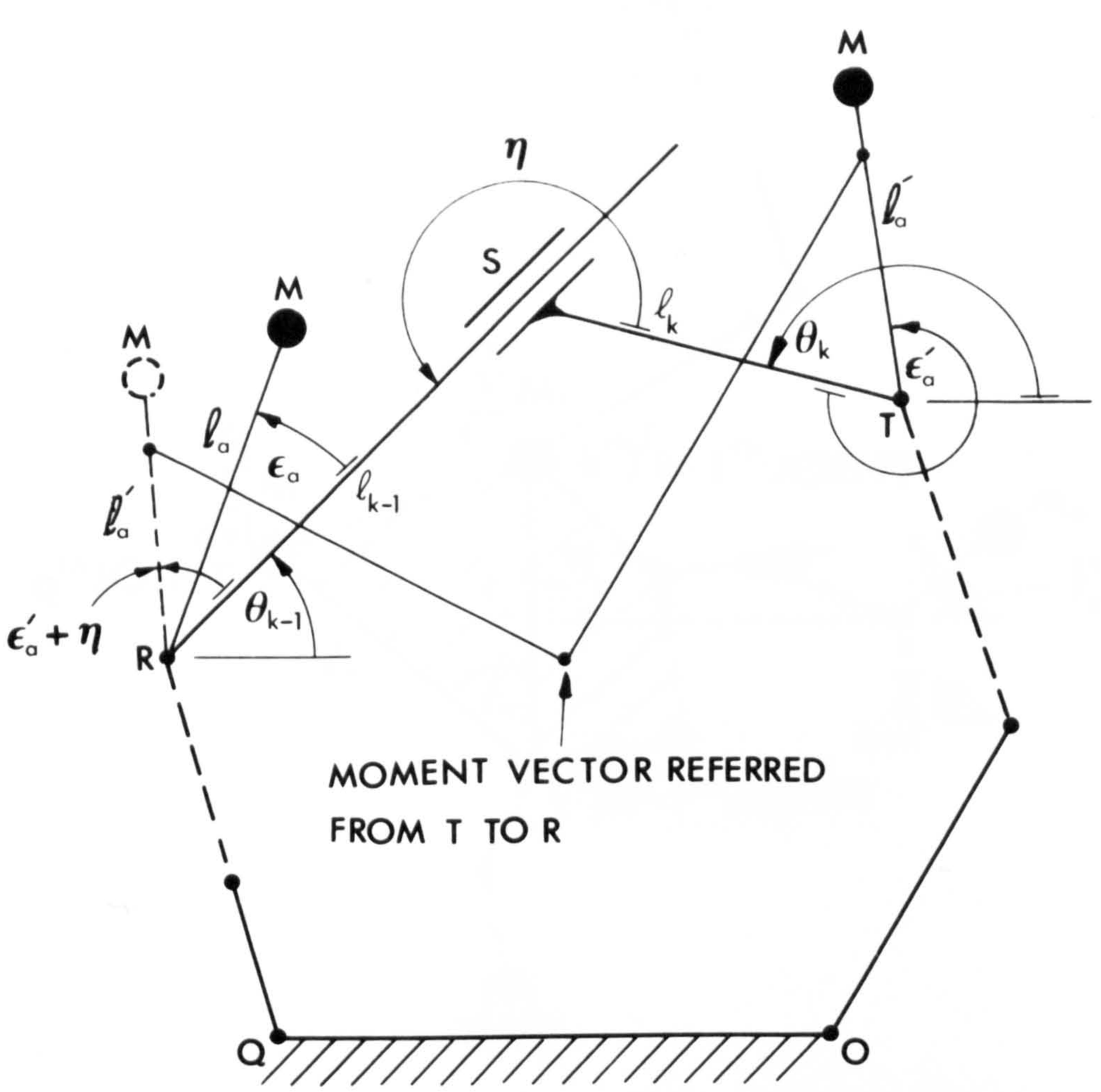

FIGURE 2.4 A LOOP WHICH CONTAINS A PRISMATIC JOINT

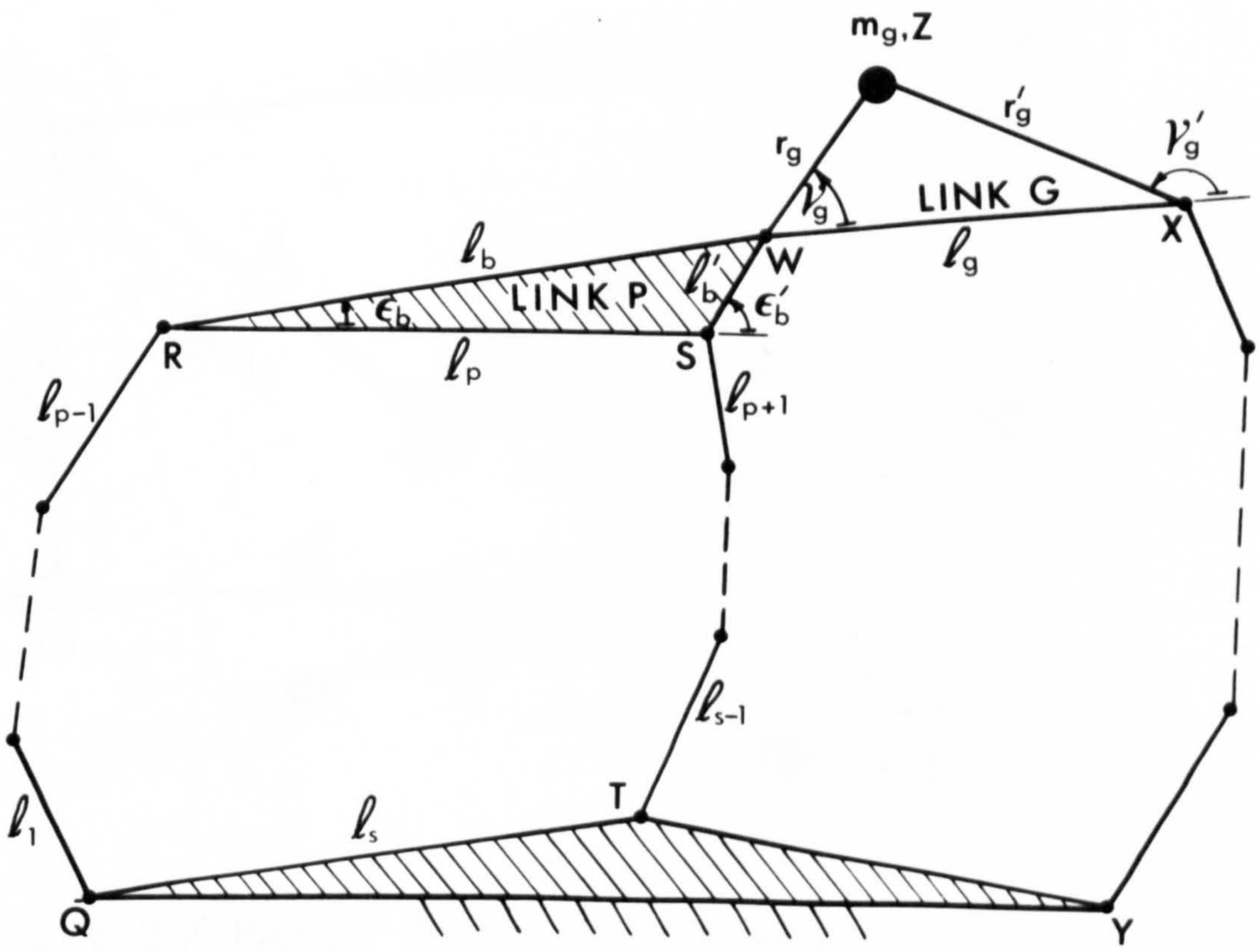

FIGURE 2.5 DEPENDENT LINK INCIDENT ON ANOTHER

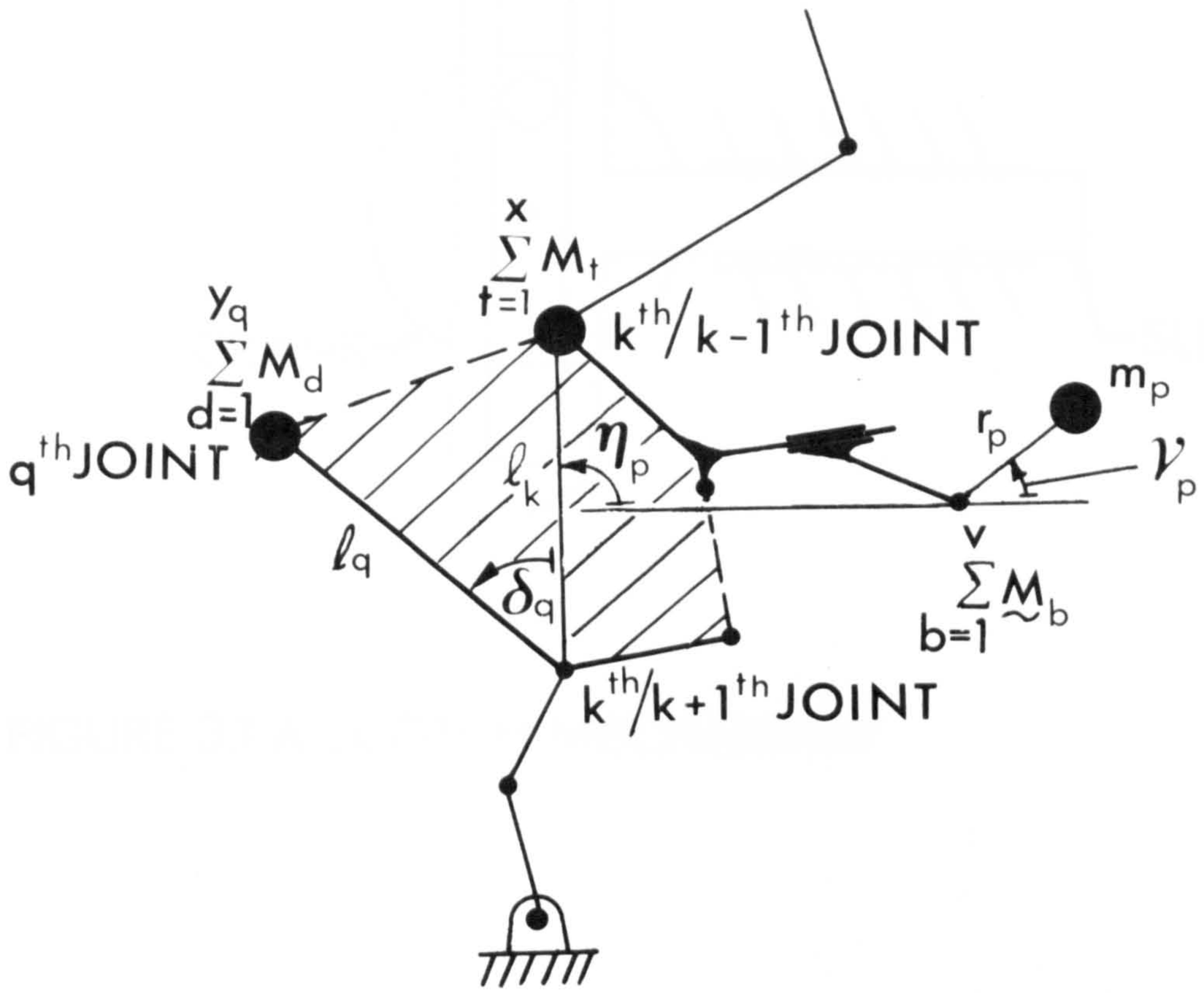

FIGURE 2.6 MASSES FIXED IN AND ASSIGNED TO A LINK IN A COUNTERWEIGHT CHAIN FROM OTHER SUCH CHAINS

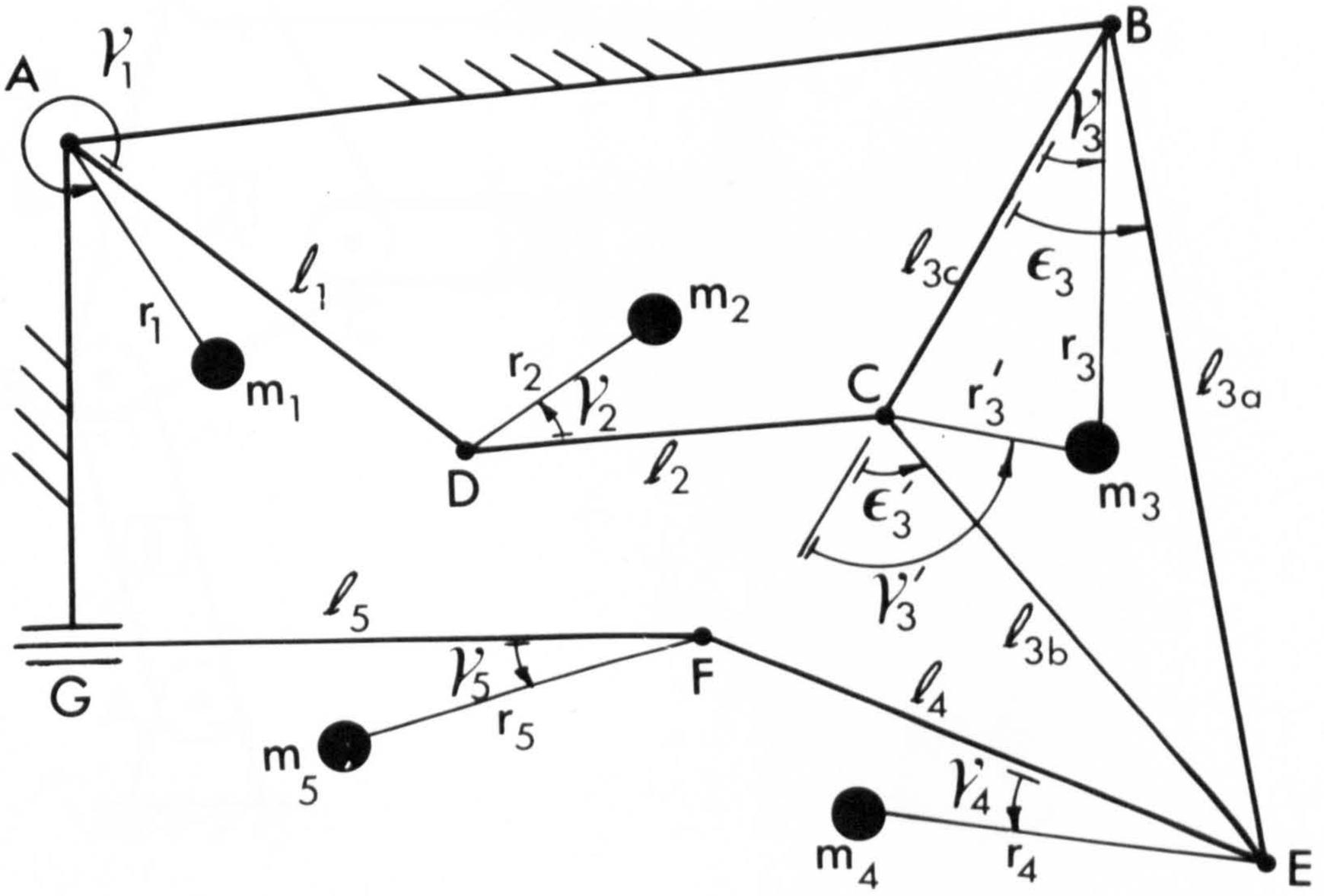

FIGURE 2.7 PAPER FEED MECHANISM

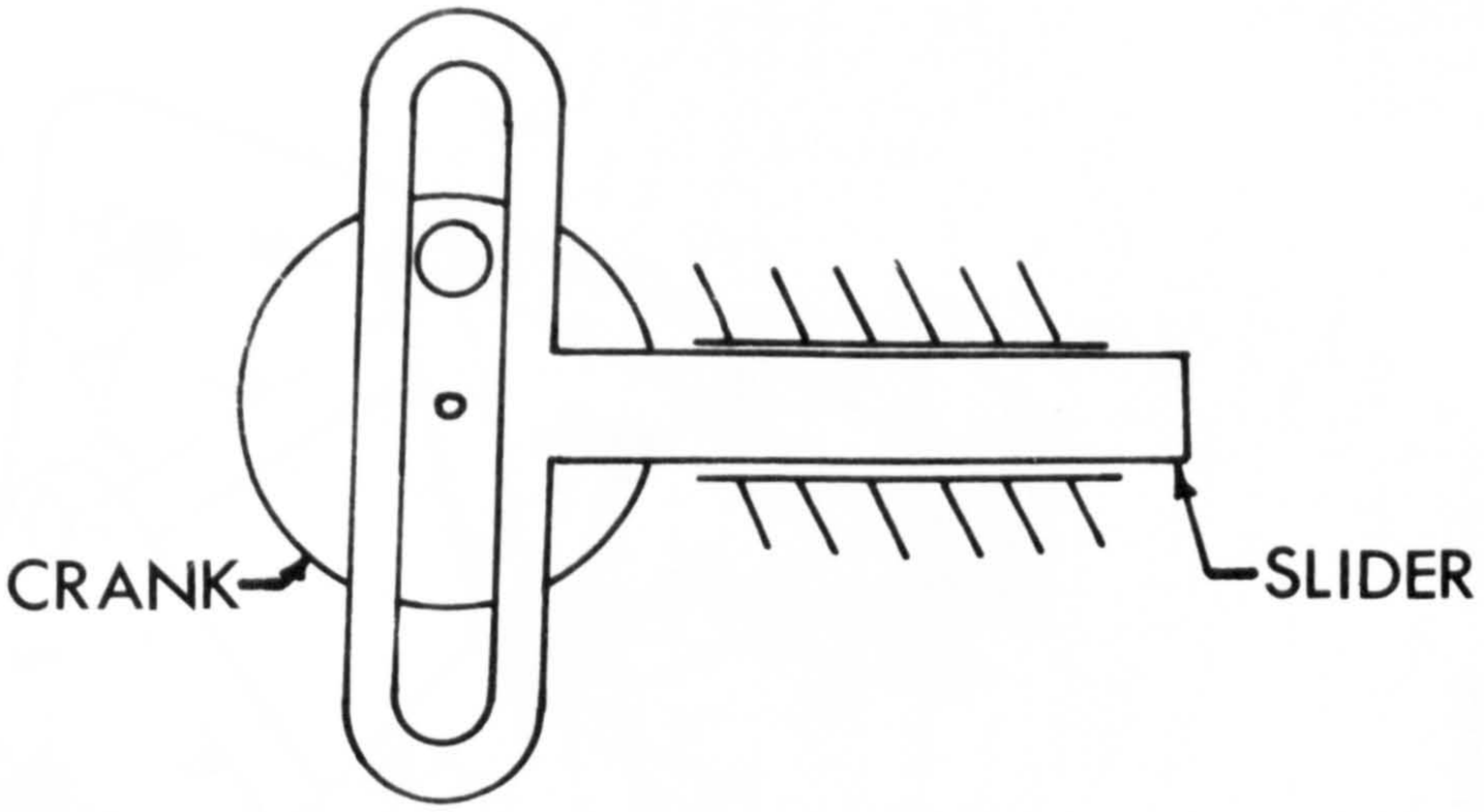

FIGURE 3.1 A SCOTCH MECHANISM

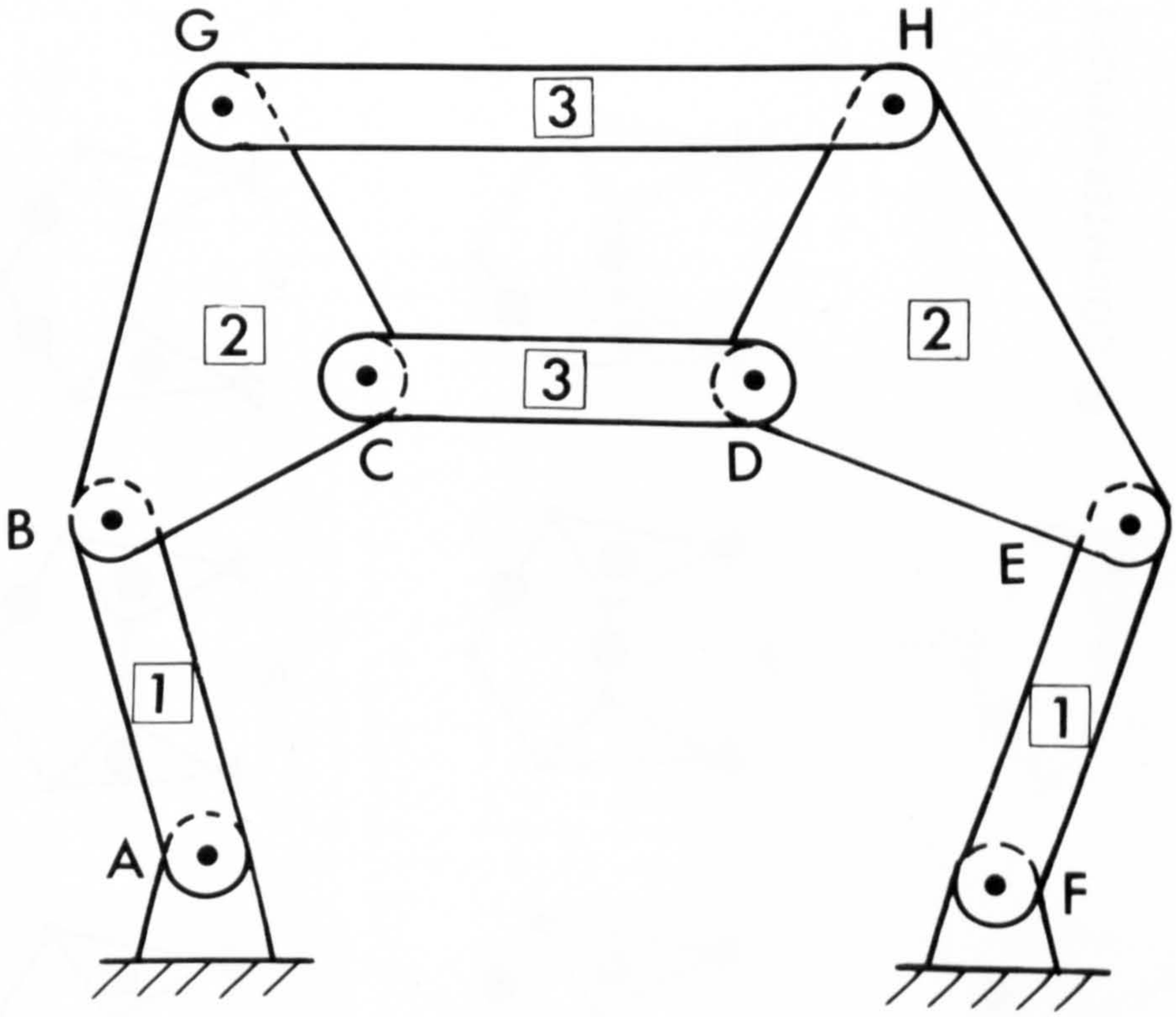

FIGURE 3.2 SEVEN-BAR LINKAGE

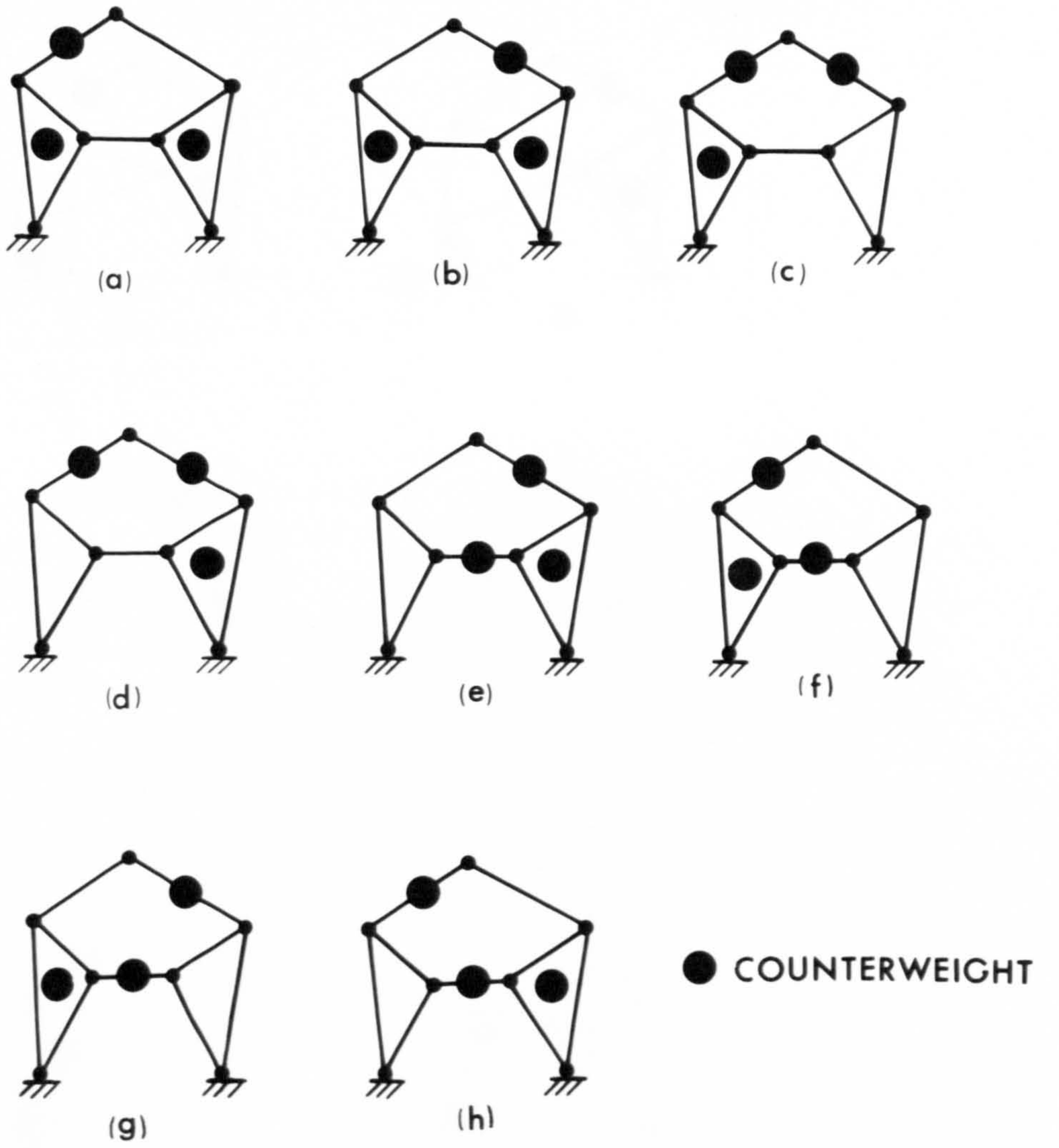

FIGURE 3.3 EIGHT DIFFERENT WAYS OF BALANCING ONE STEPHENSON CHAIN

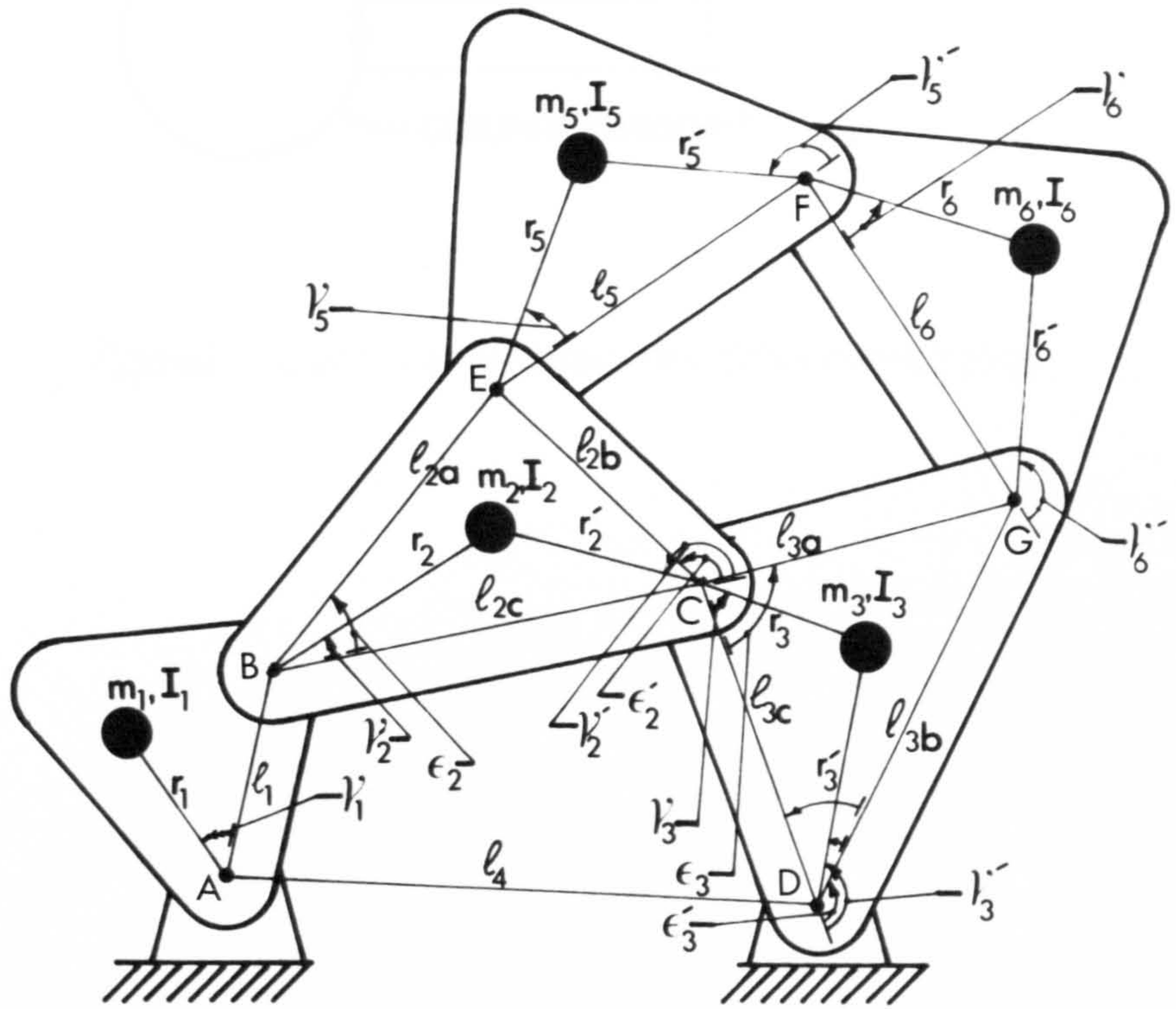

FIGURE 3.4 WATT'S SIXBAR LINKAGE

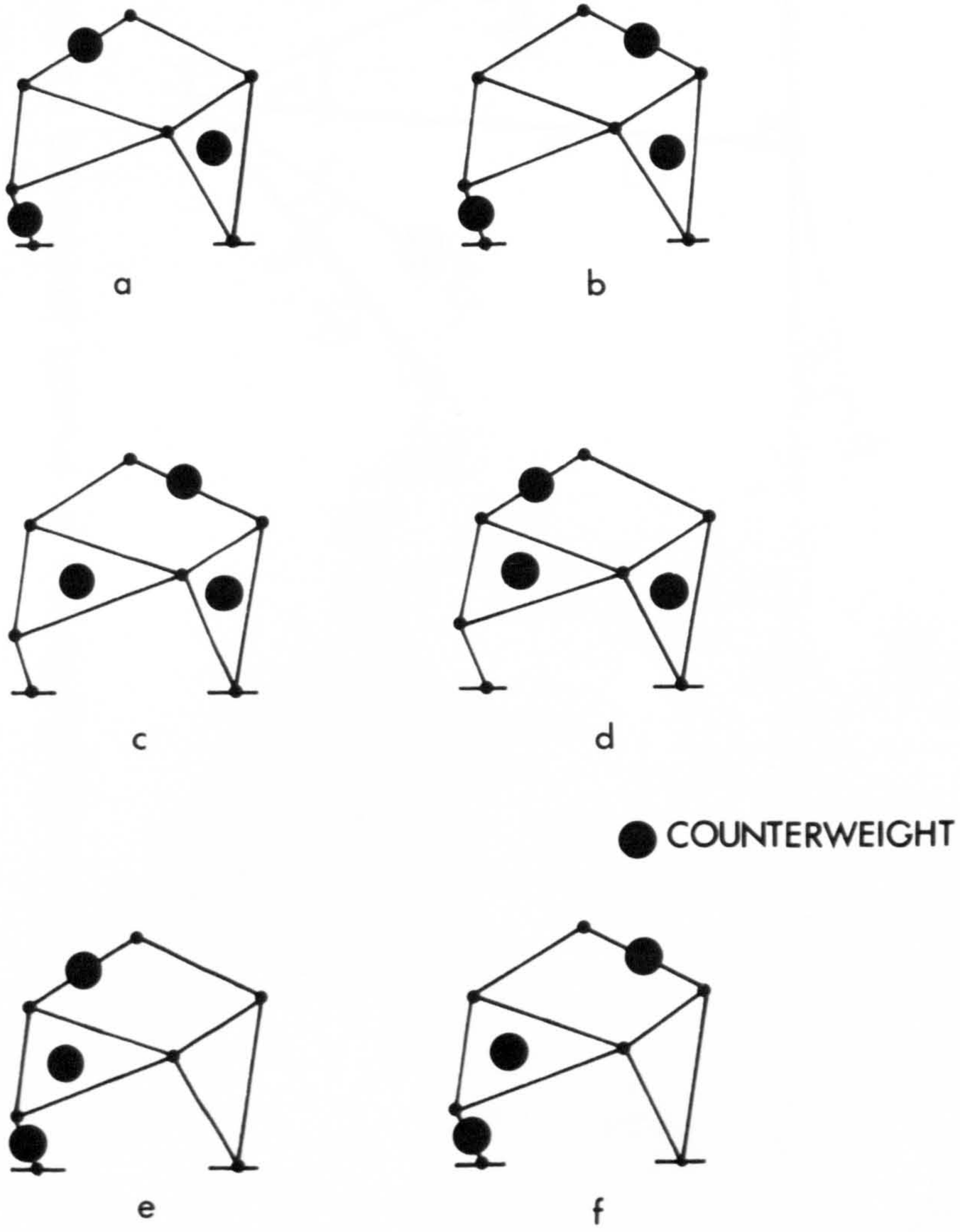

FIGURE 3.5 SIX BALANCES OF A WATT'S CHAIN

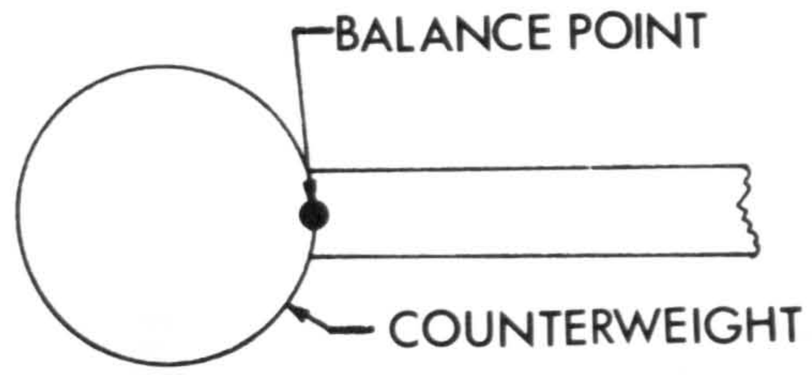

FIGURE 3.6 EPSTEIN & STEINVOLF COUNTERWEIGHT

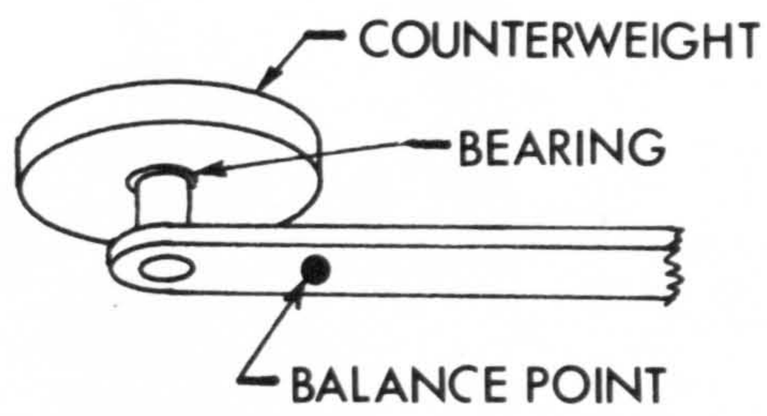

FIGURE 3.7 MINIMUM MOMENT OF INERTIA COUNTERWEIGHT

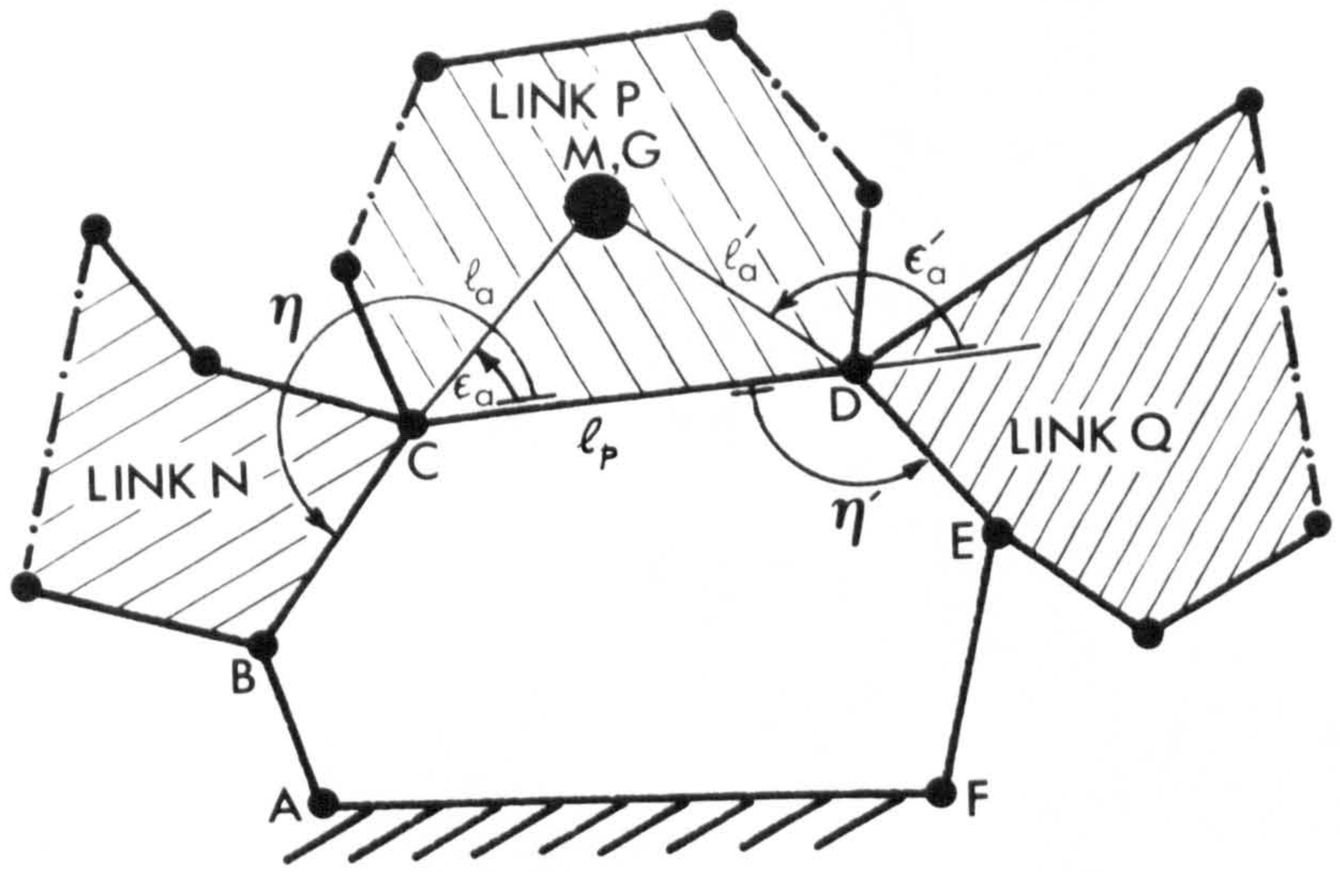

FIGURE 4.1 THREE GENERAL LINKS WITHIN A LOOP

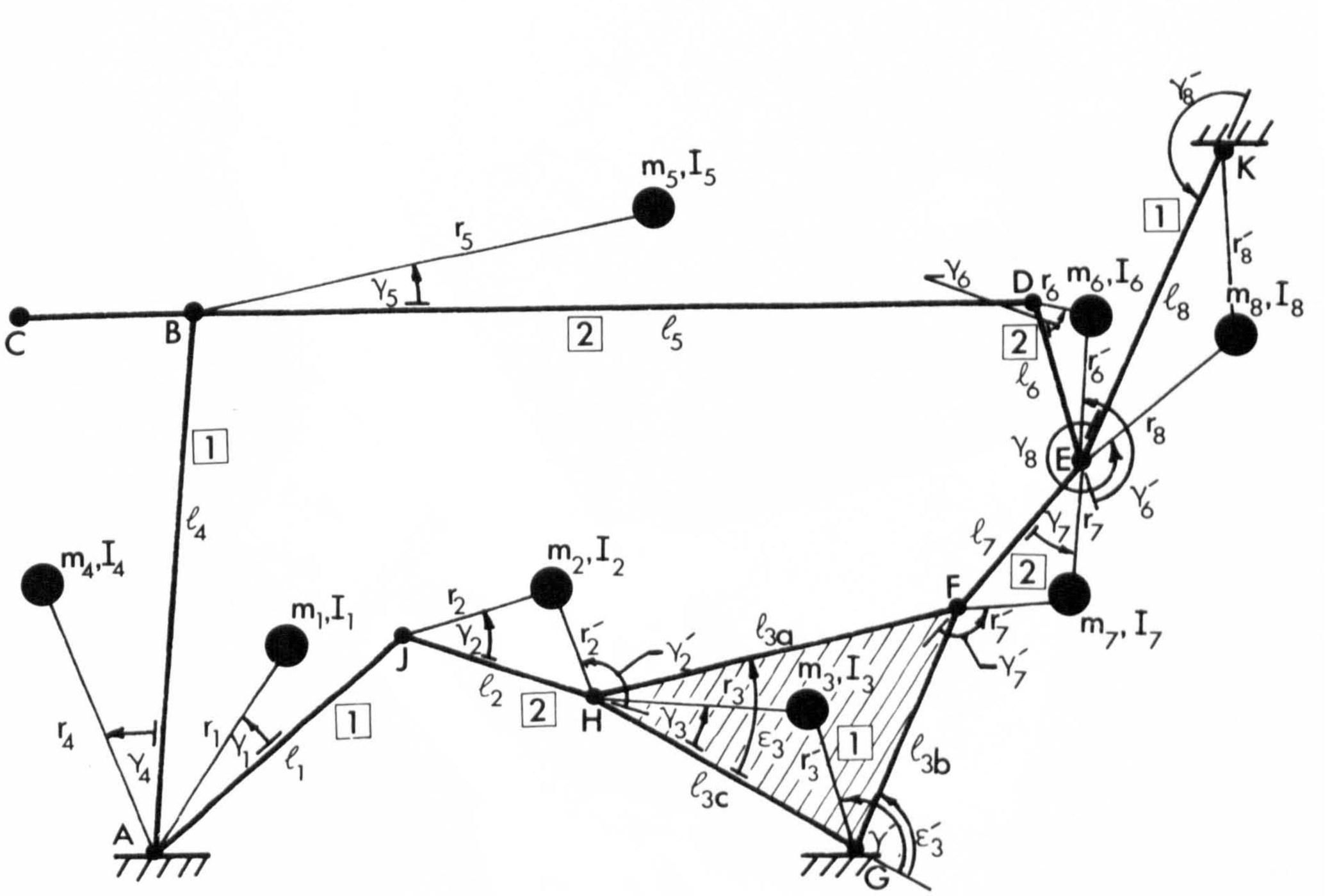

FIGURE 4.2 SCHEMATIC LAYOUT OF THE NINE-BAR LINKAGE

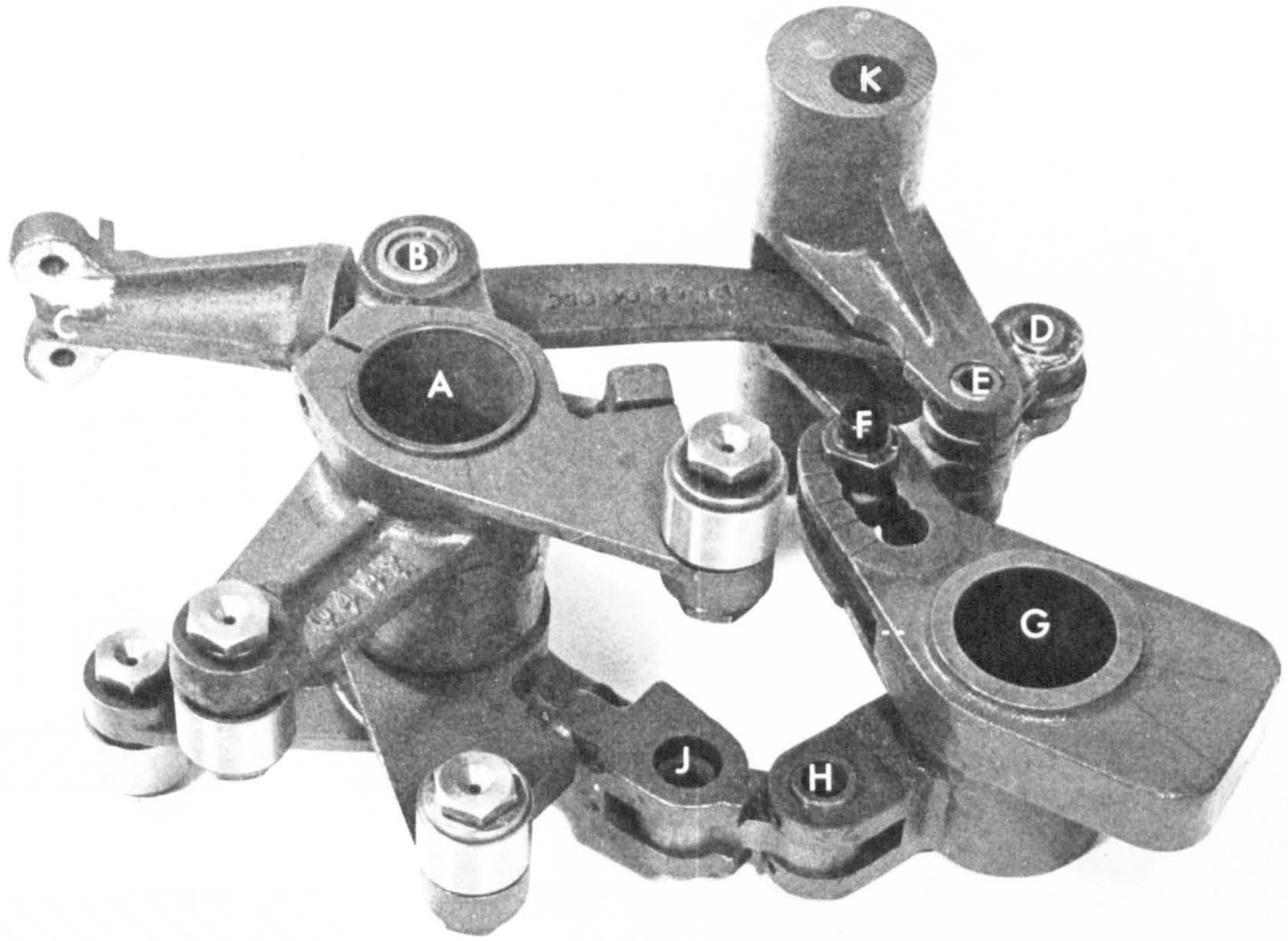

FIGURE 4.3 AN INDUSTRIAL NINE-BAR LINKAGE

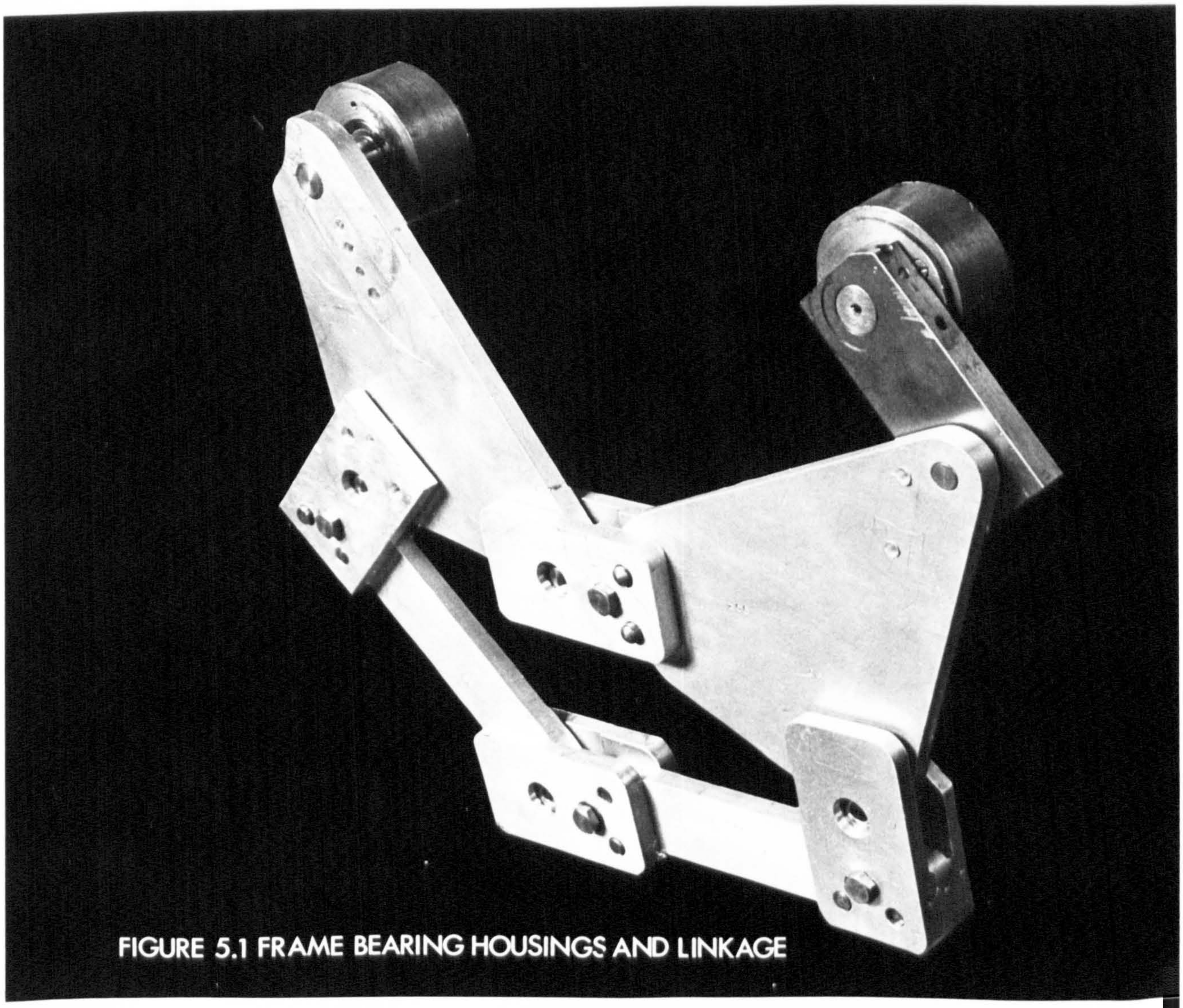

FIGURE 5.1 FRAME BEARING HOUSINGS AND LINKAGE

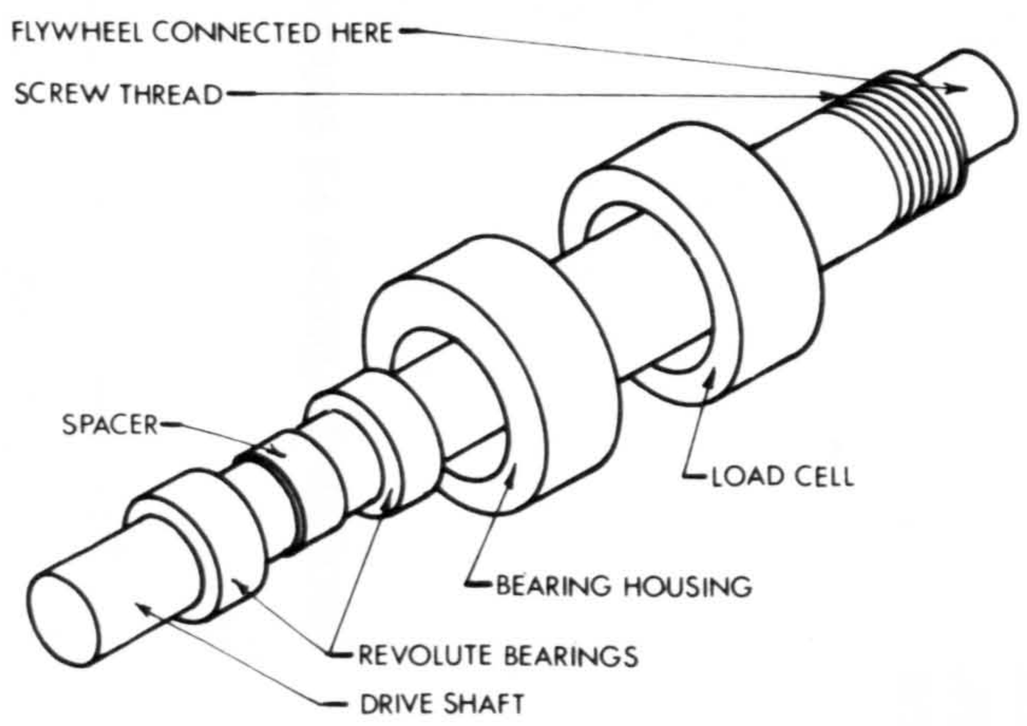

FIGURE 5.2 DRIVE SHAFT PASSED THROUGH LOAD CELL

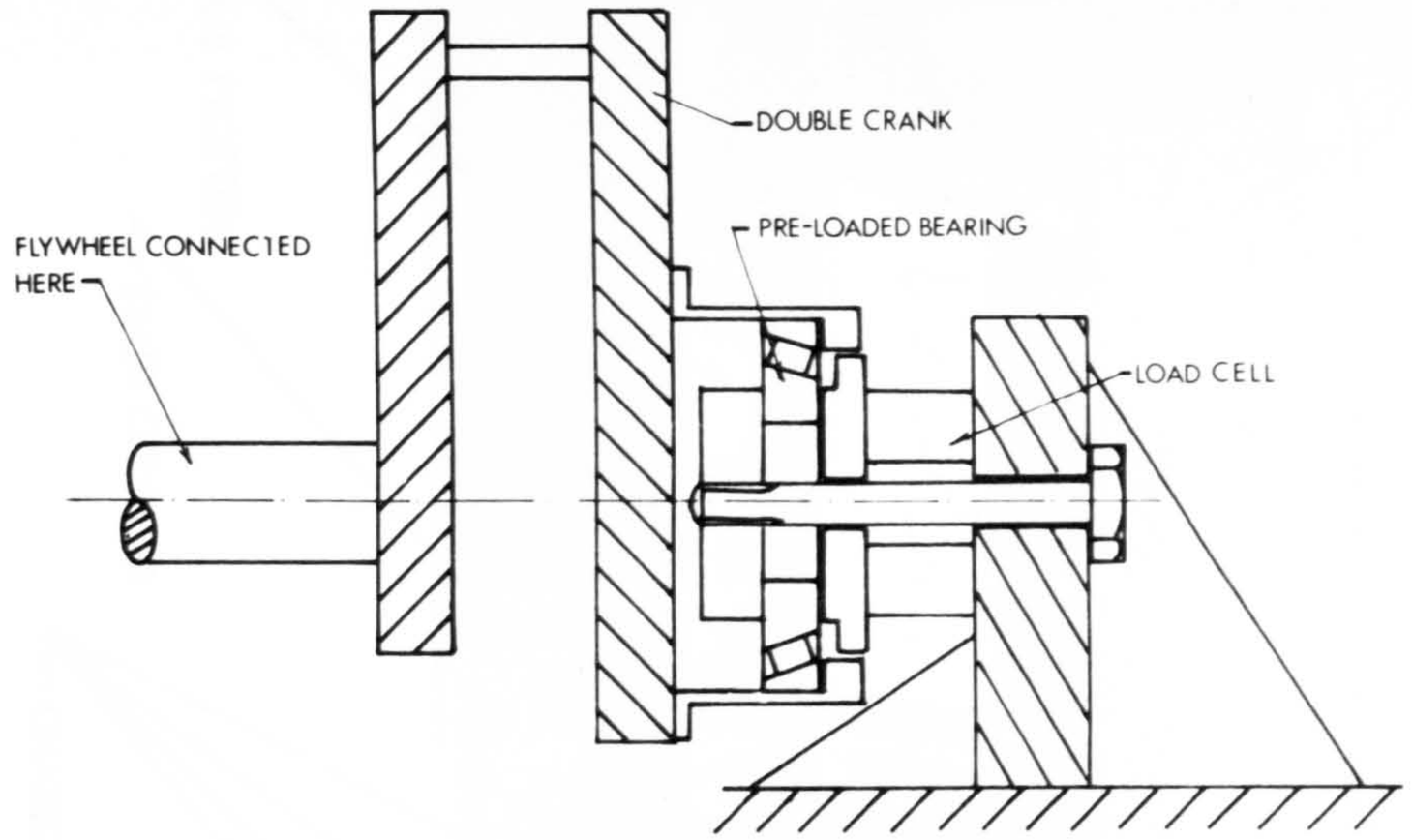

FIGURE 5.3 DRIVE SHAFT EXTERNAL TO THE LOAD CELL

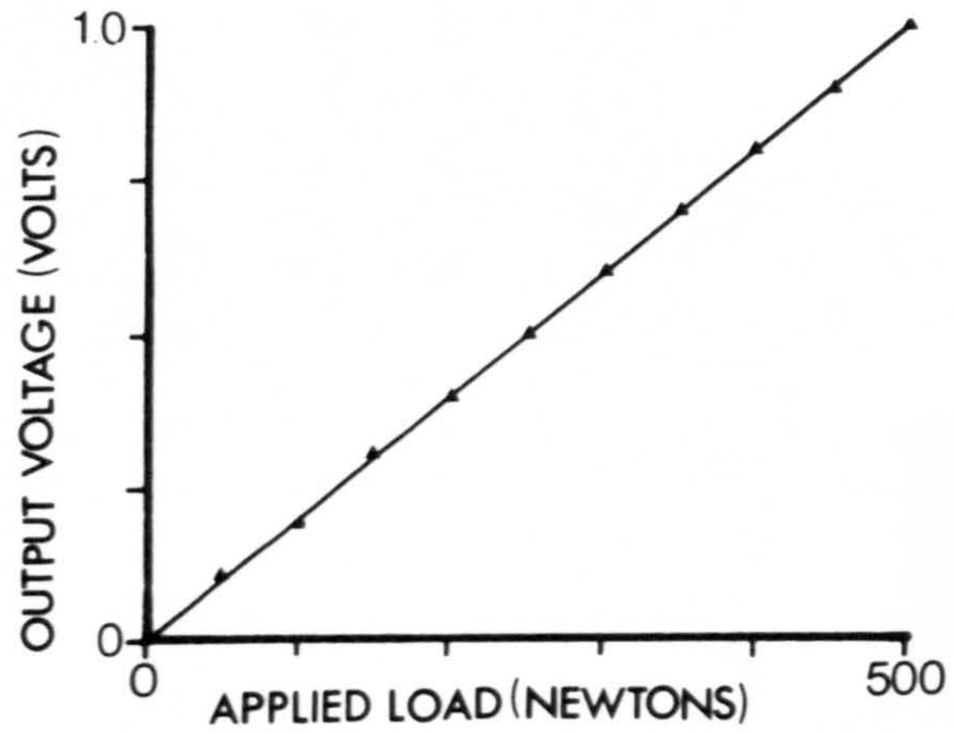

FIGURE 5.4 LOAD CELL CALIBRATION CURVE

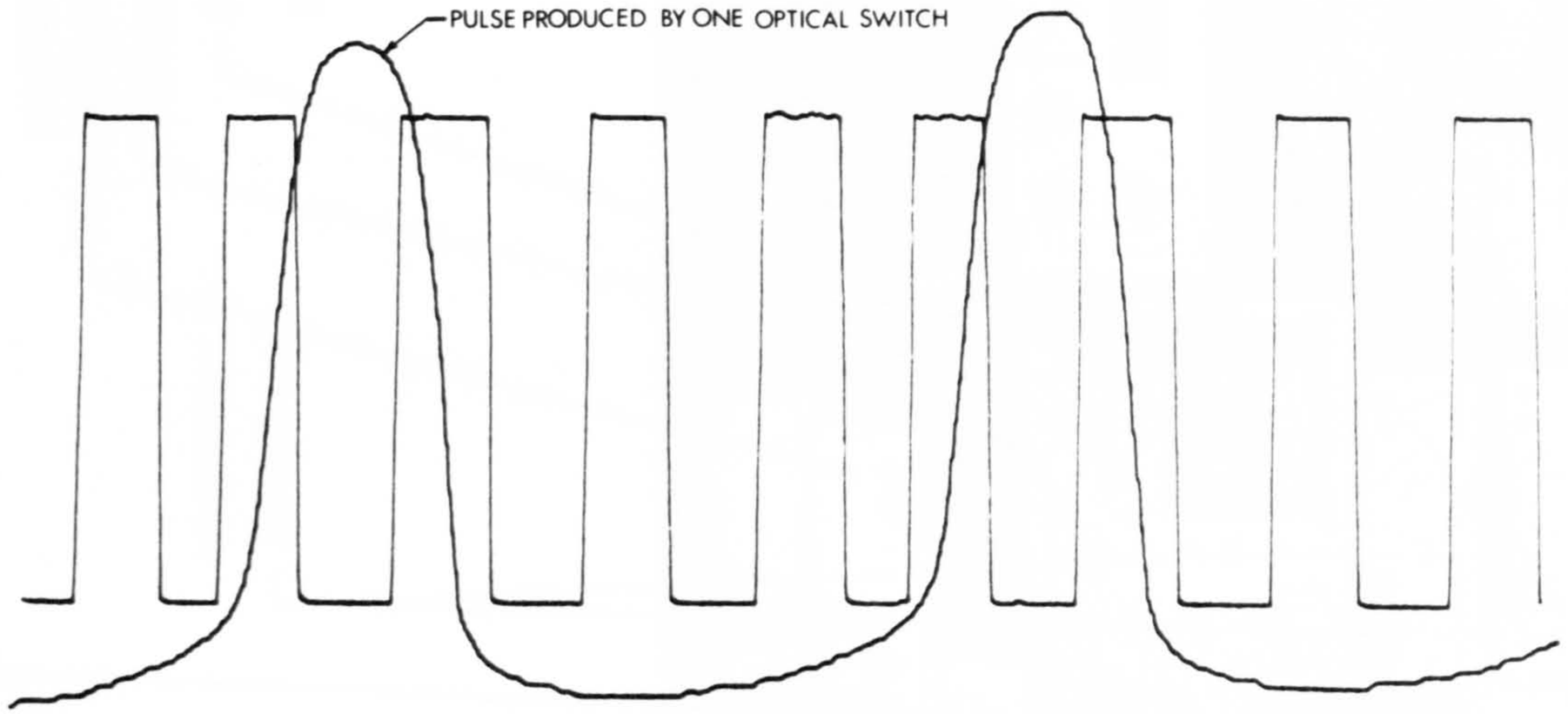

FIGURE 5.5 SQUAREWAVE OF TIMES FOUR FREQUENCY

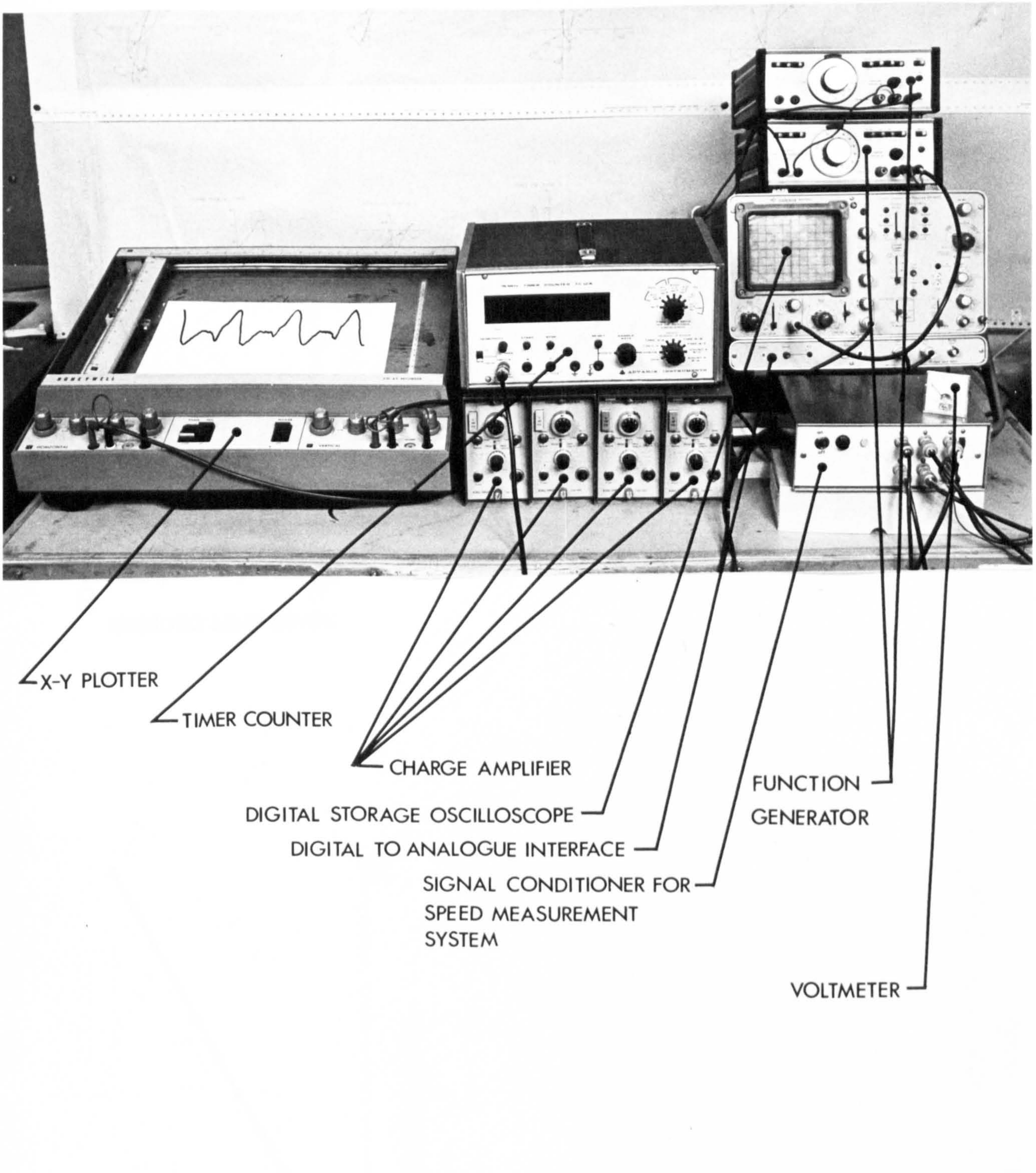

FIGURE 5.6 INSTRUMENTATION

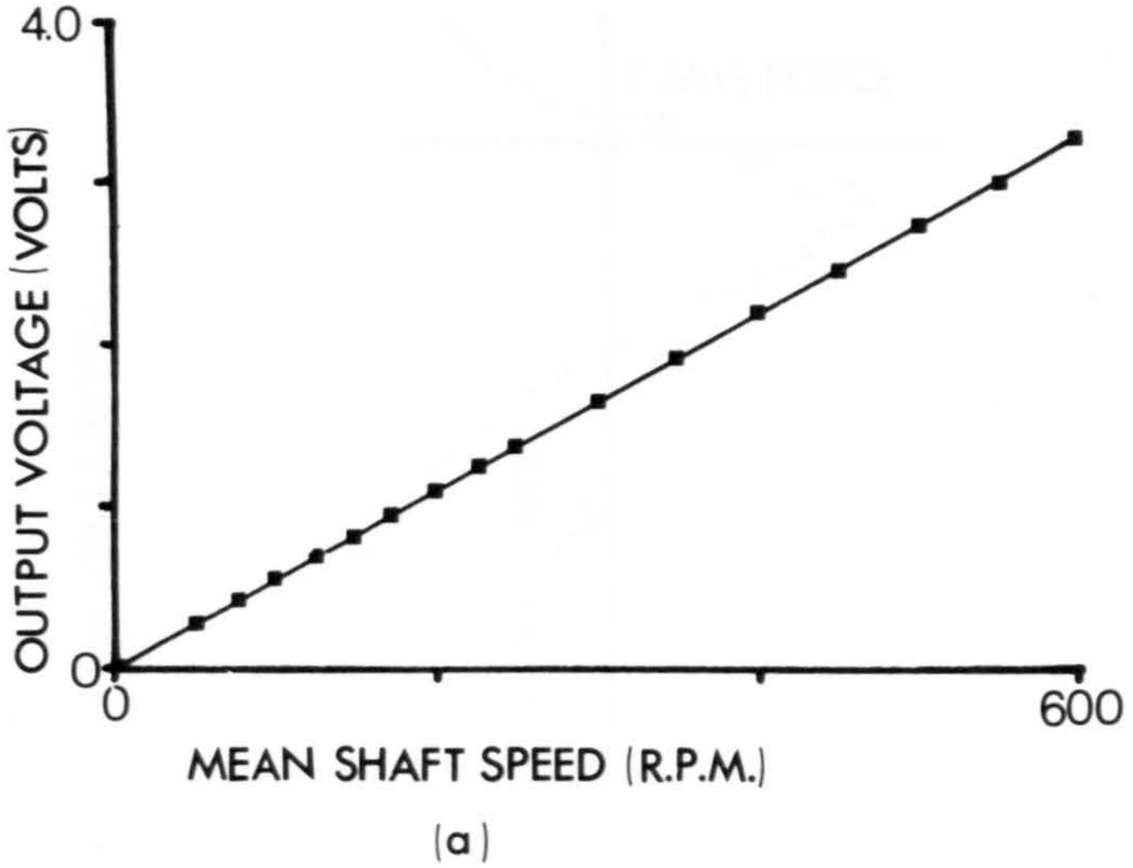

(a)

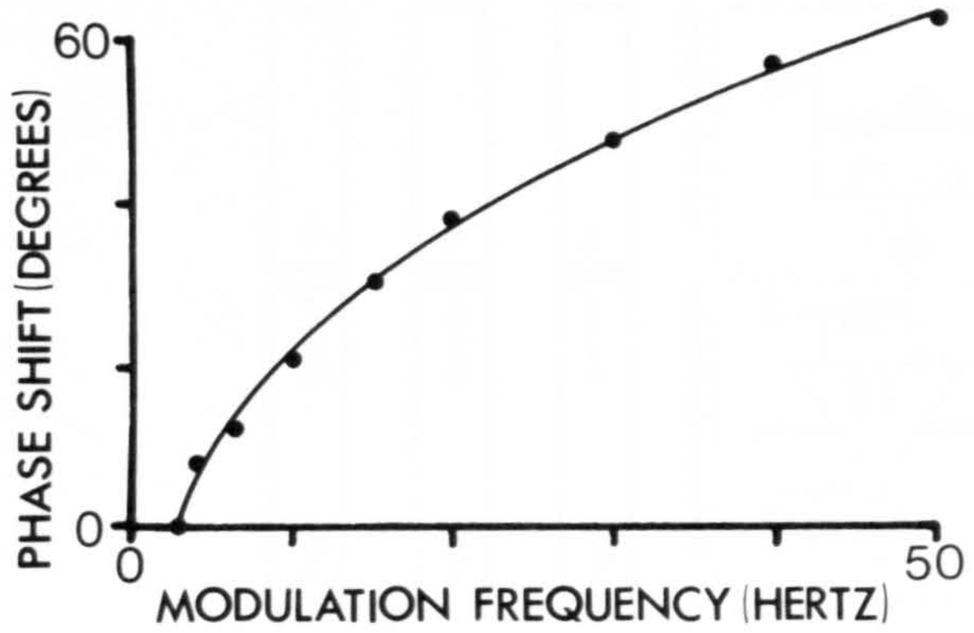

(b)

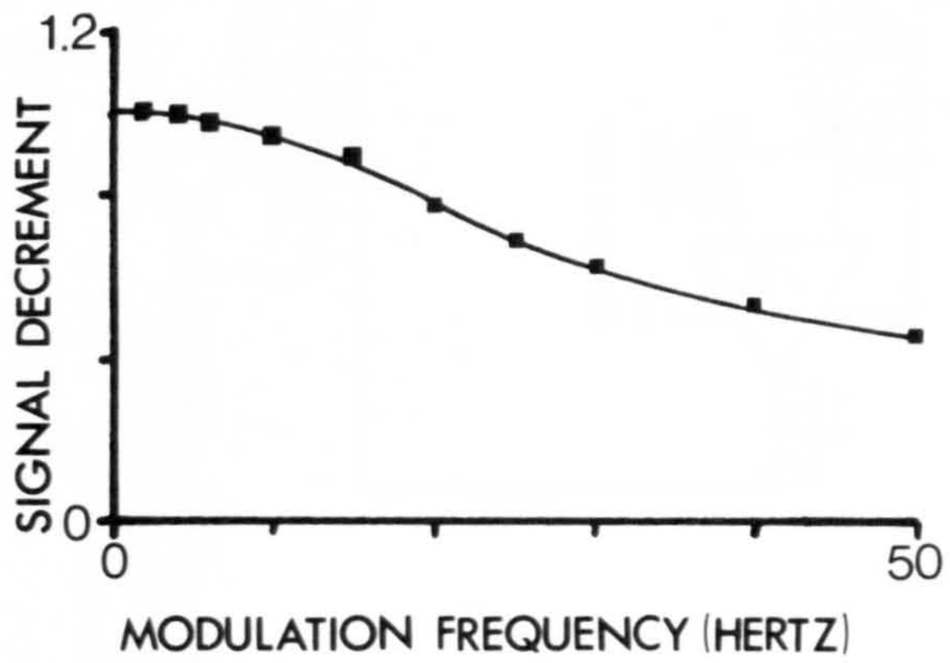

(c)

FIGURE 5.7 CALIBRATION CURVES OF DRIVE SHAFT SPEED MEASUREMENT SYSTEM

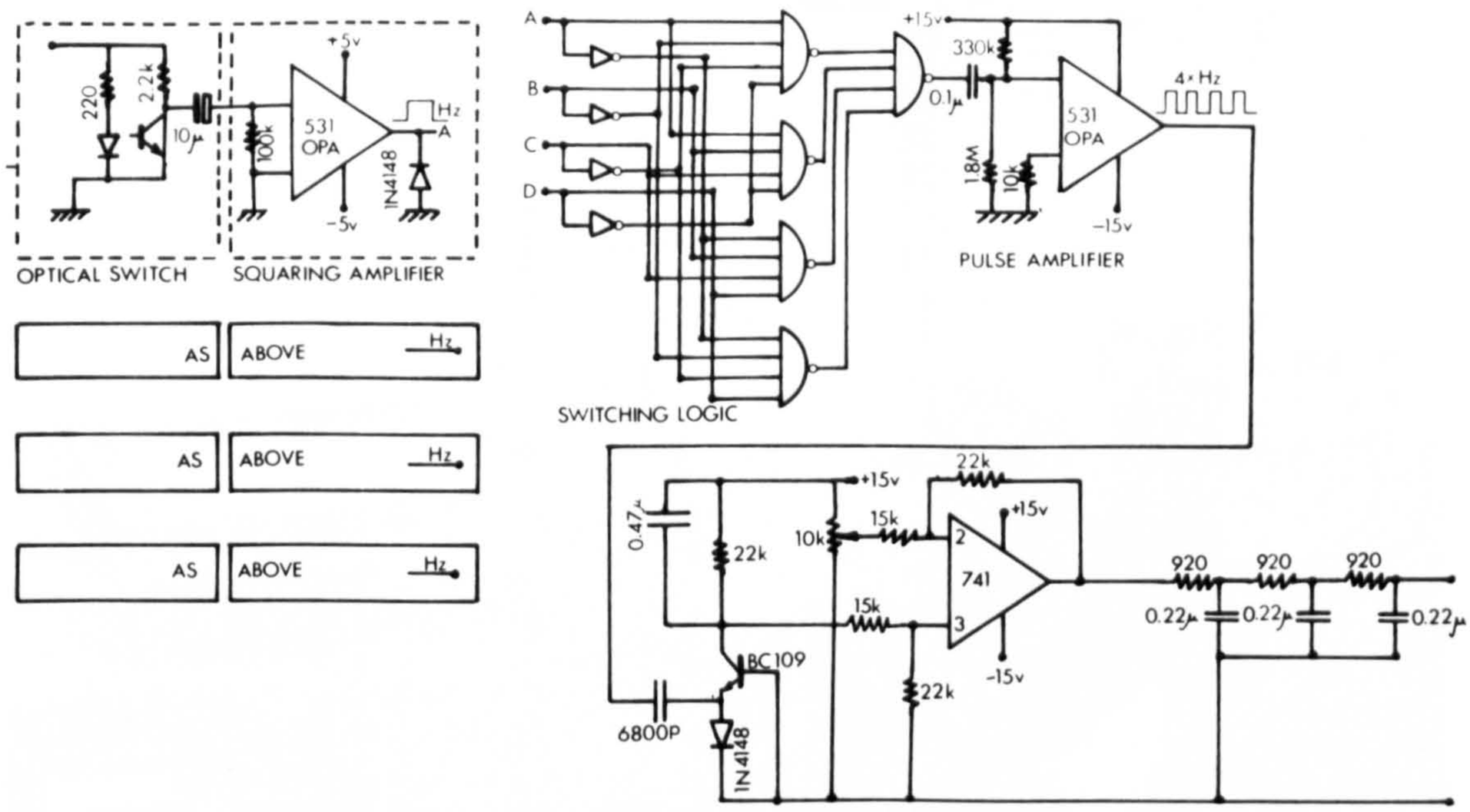

FIGURE 5.8 SIGNAL CONDITIONER FOR SPEED MEASUREMENT SYSTEM

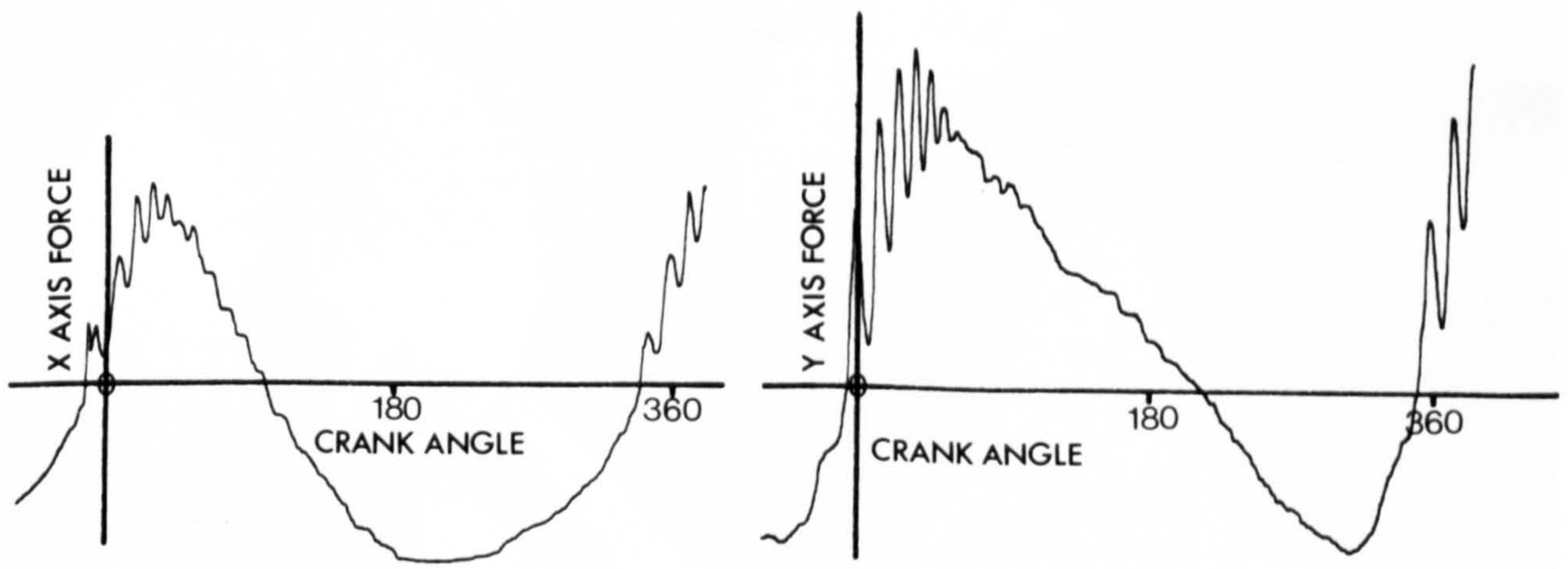

FIGURE 5.9 ROCKER FRAME FORCE FOR 170 R.P.M.

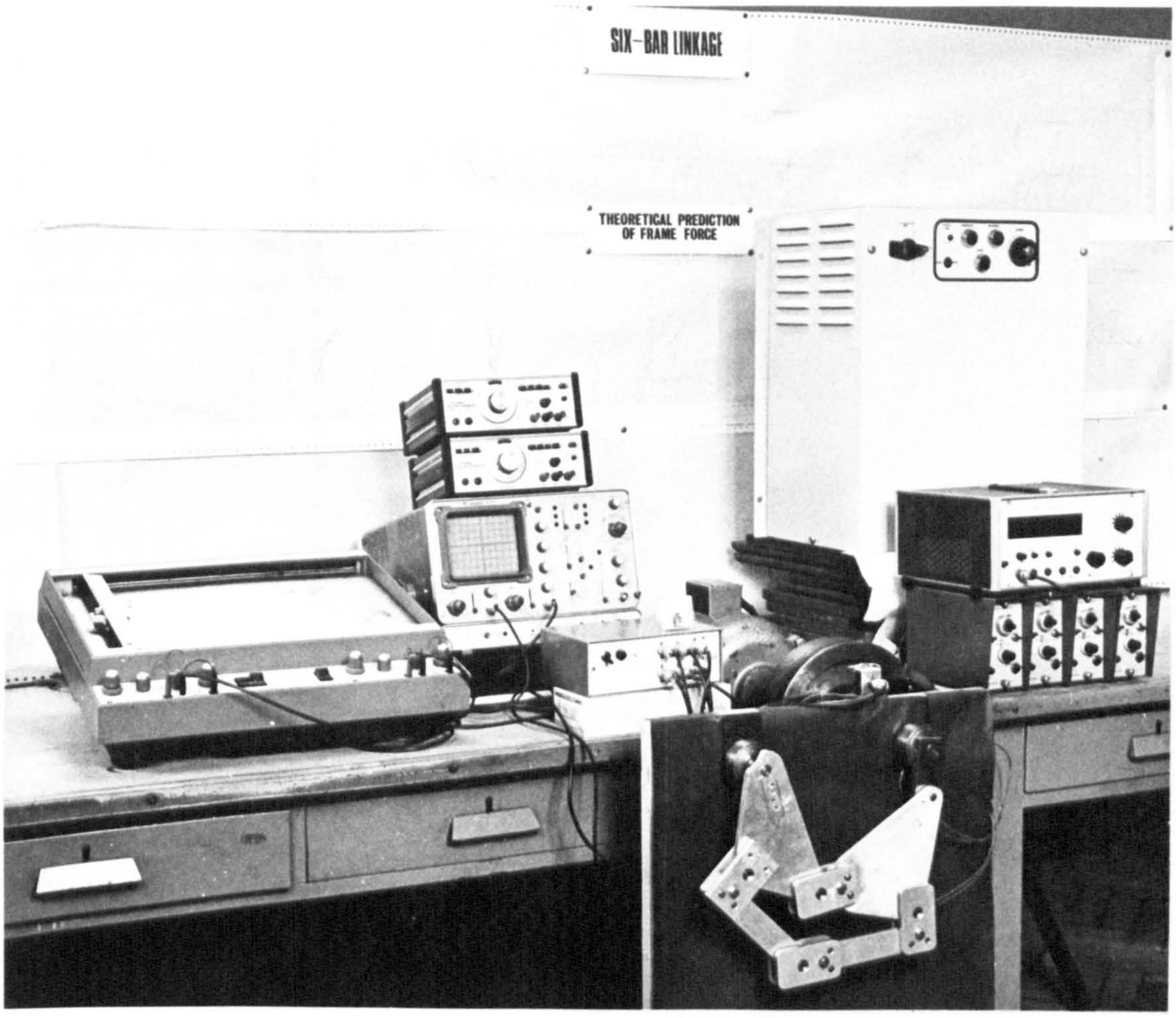

FIGURE 5.10 EXPERIMENTAL APPARATUS

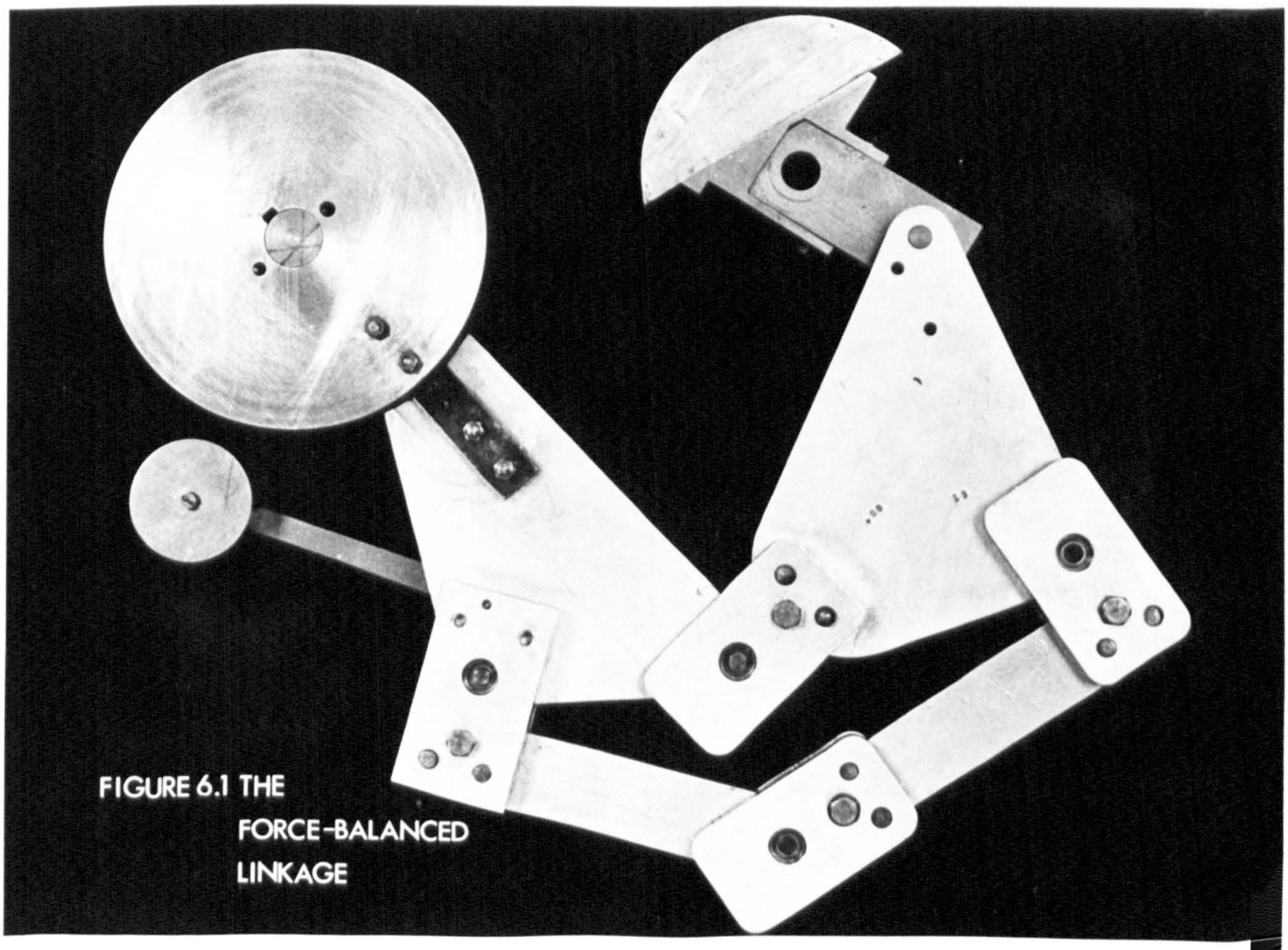

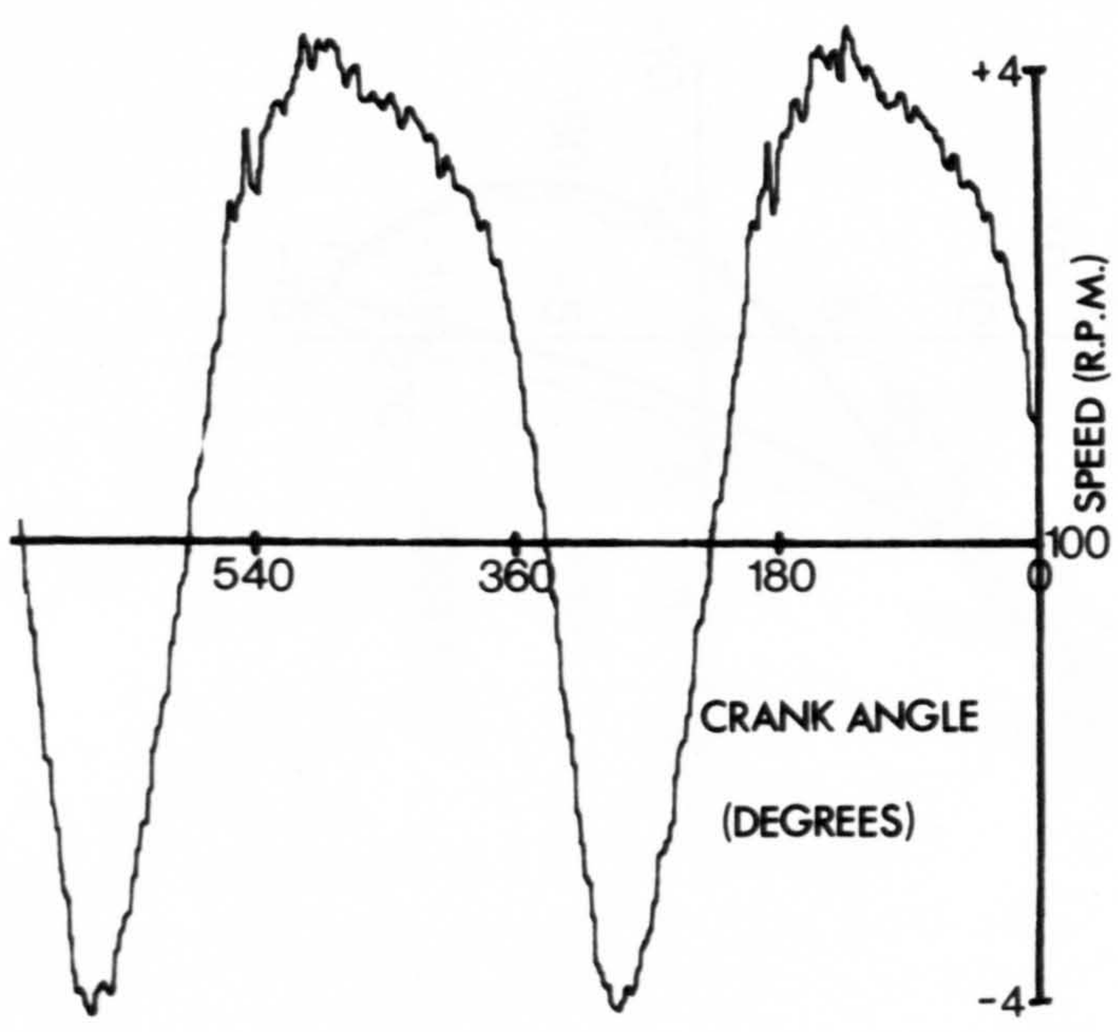

(a)

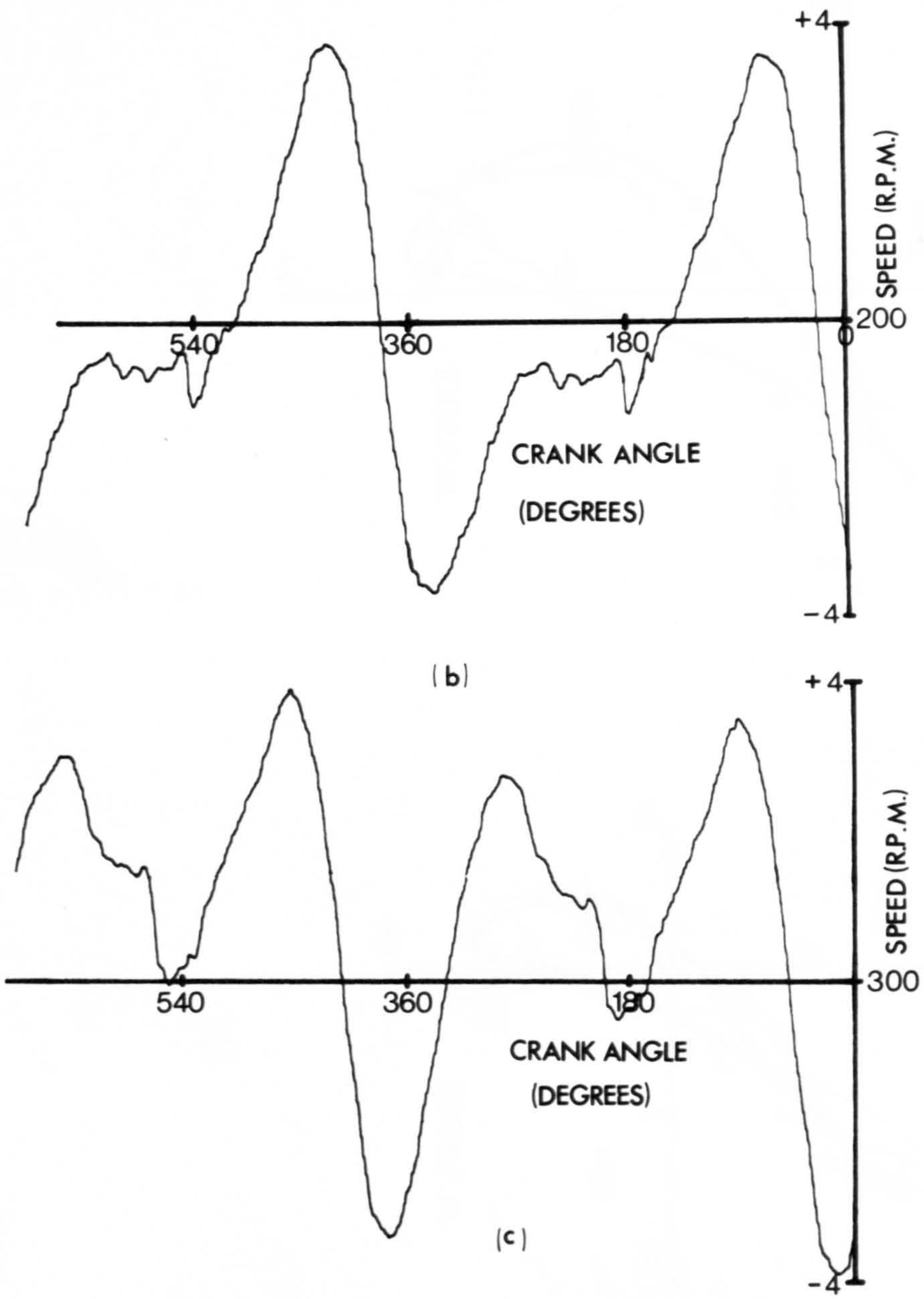

(b)

(c)

FIGURE 7.1 SPEED FLUCTUATIONS

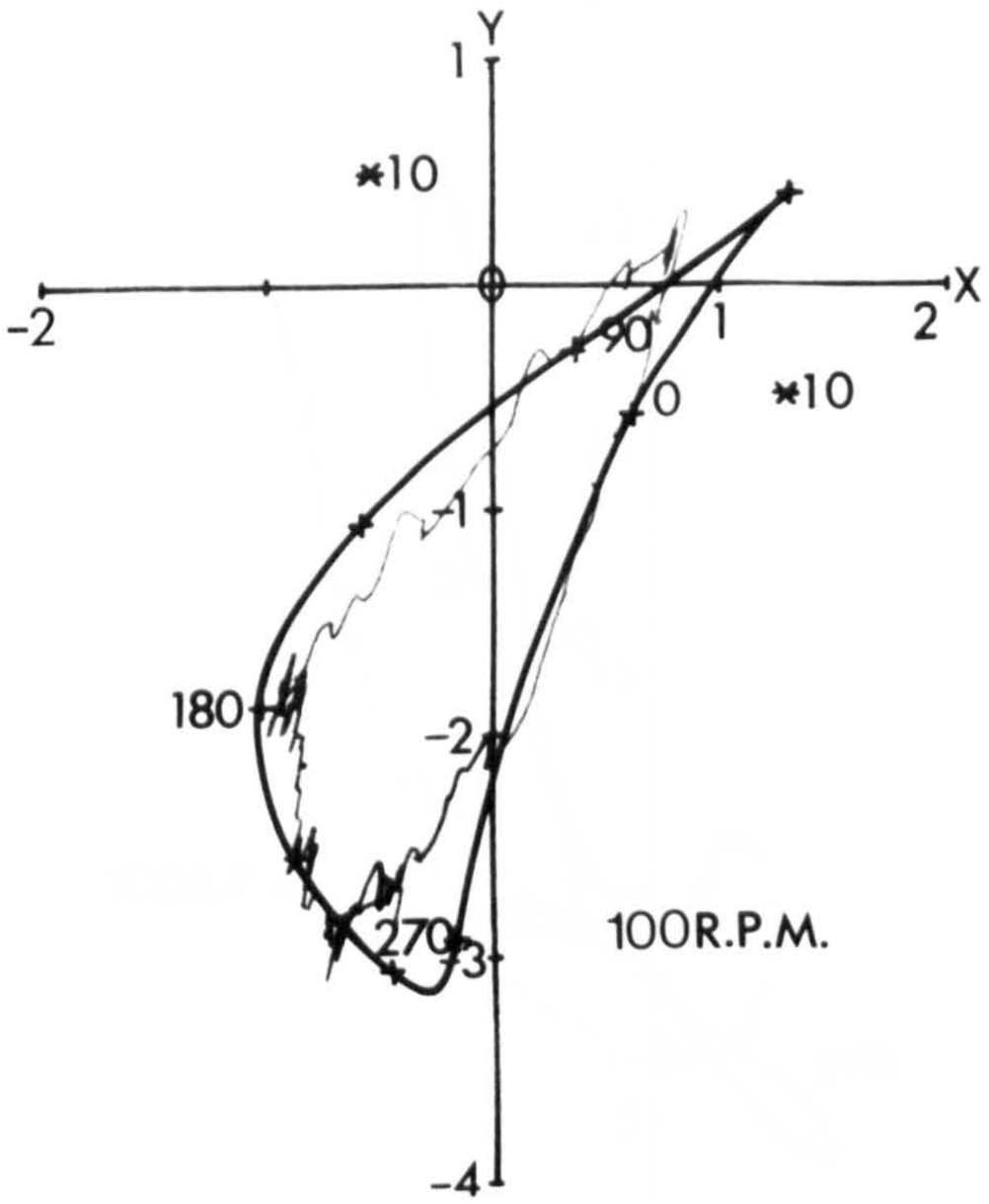

100R.P.M.

(a)

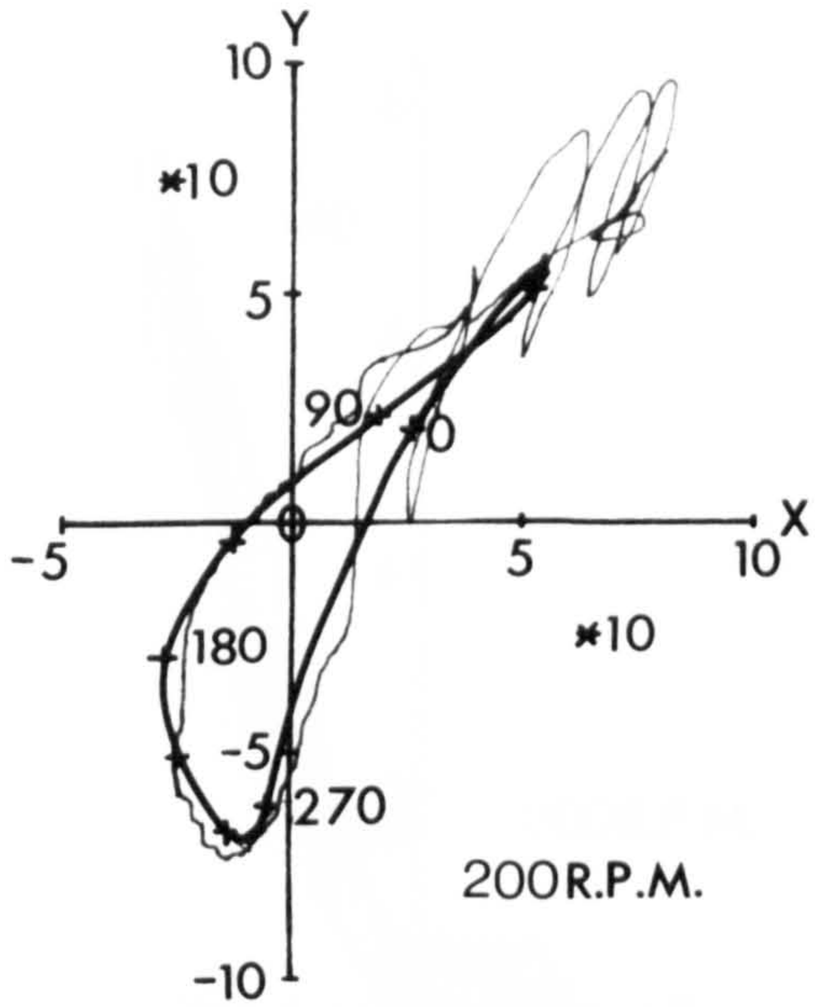

200R.P.M.

(b)

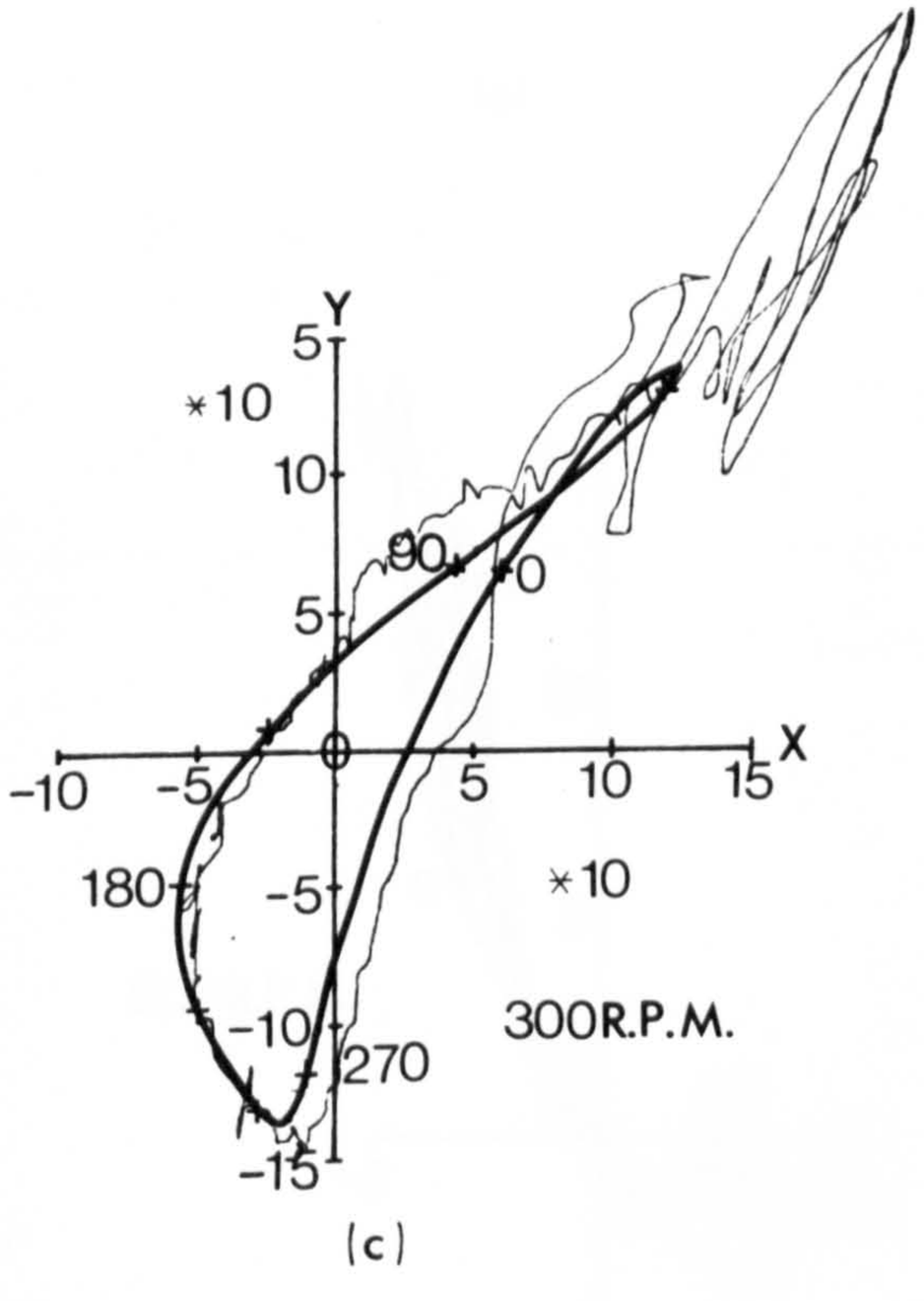

300R.P.M.

(c)

Y = VERTICAL FORCE

(NEWTONS)

X= HORIZONTAL FORCE

FIGURE 7.2 CRANK FRAME FORCE

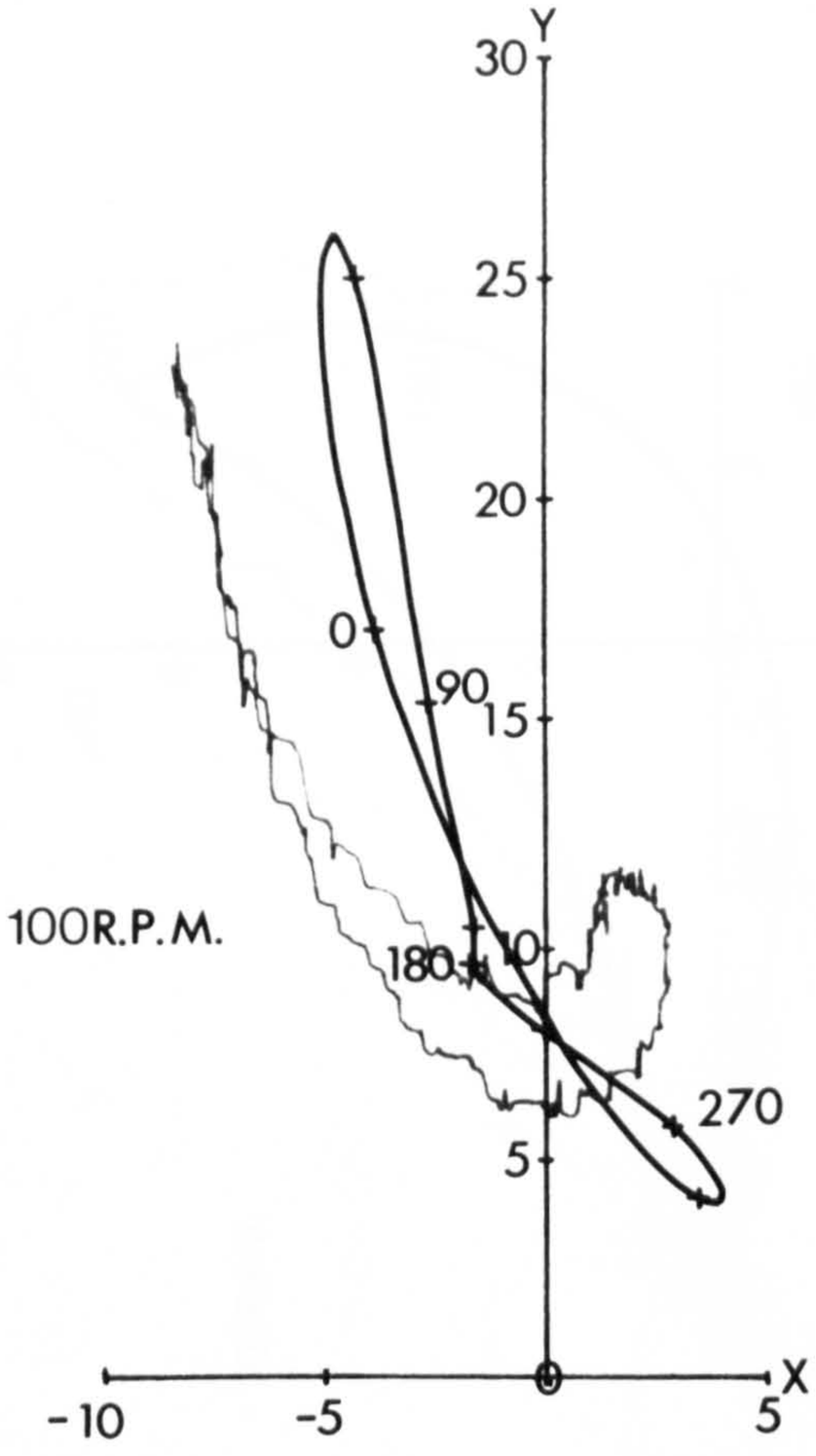

(a)

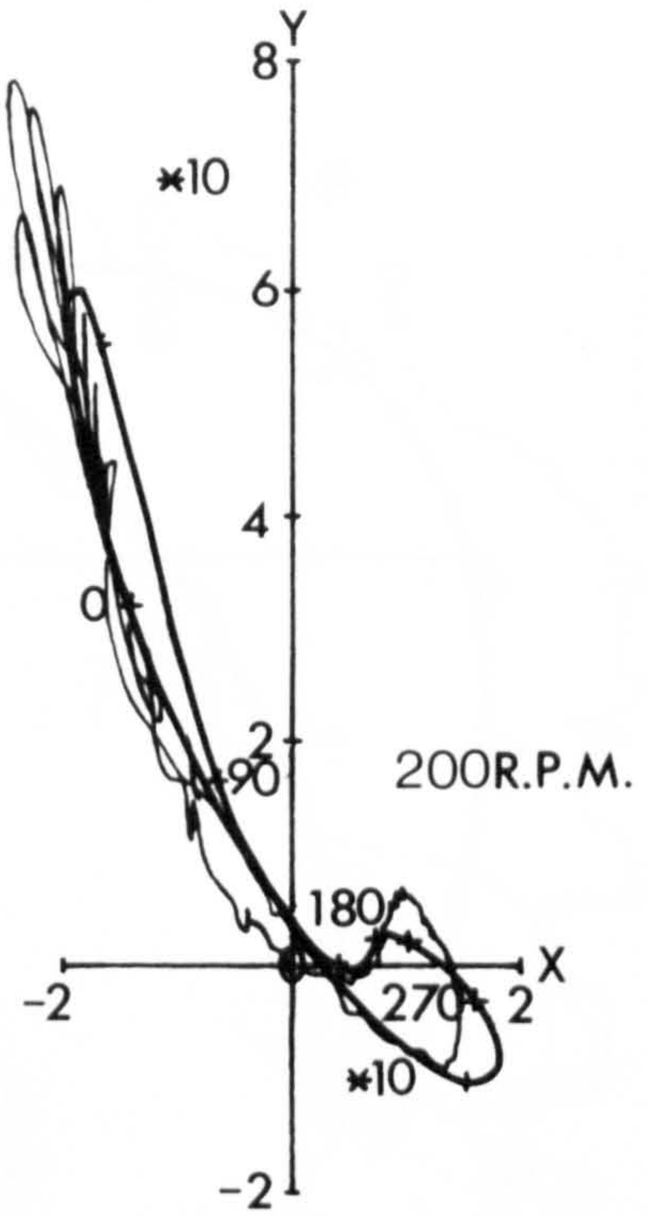

(b)

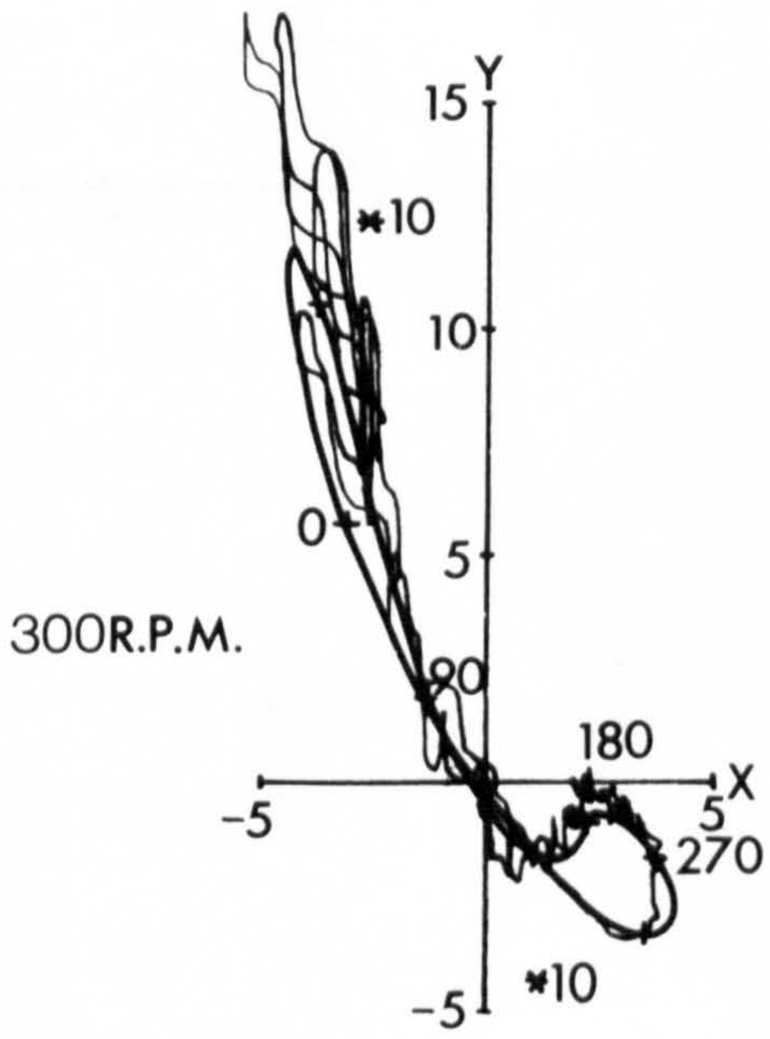

(c)

Y=VERTICAL FORCE

(NEWTONS)

X=HORIZONTAL FORCE

FIGURE 7.3 ROCKER FRAME FORCE

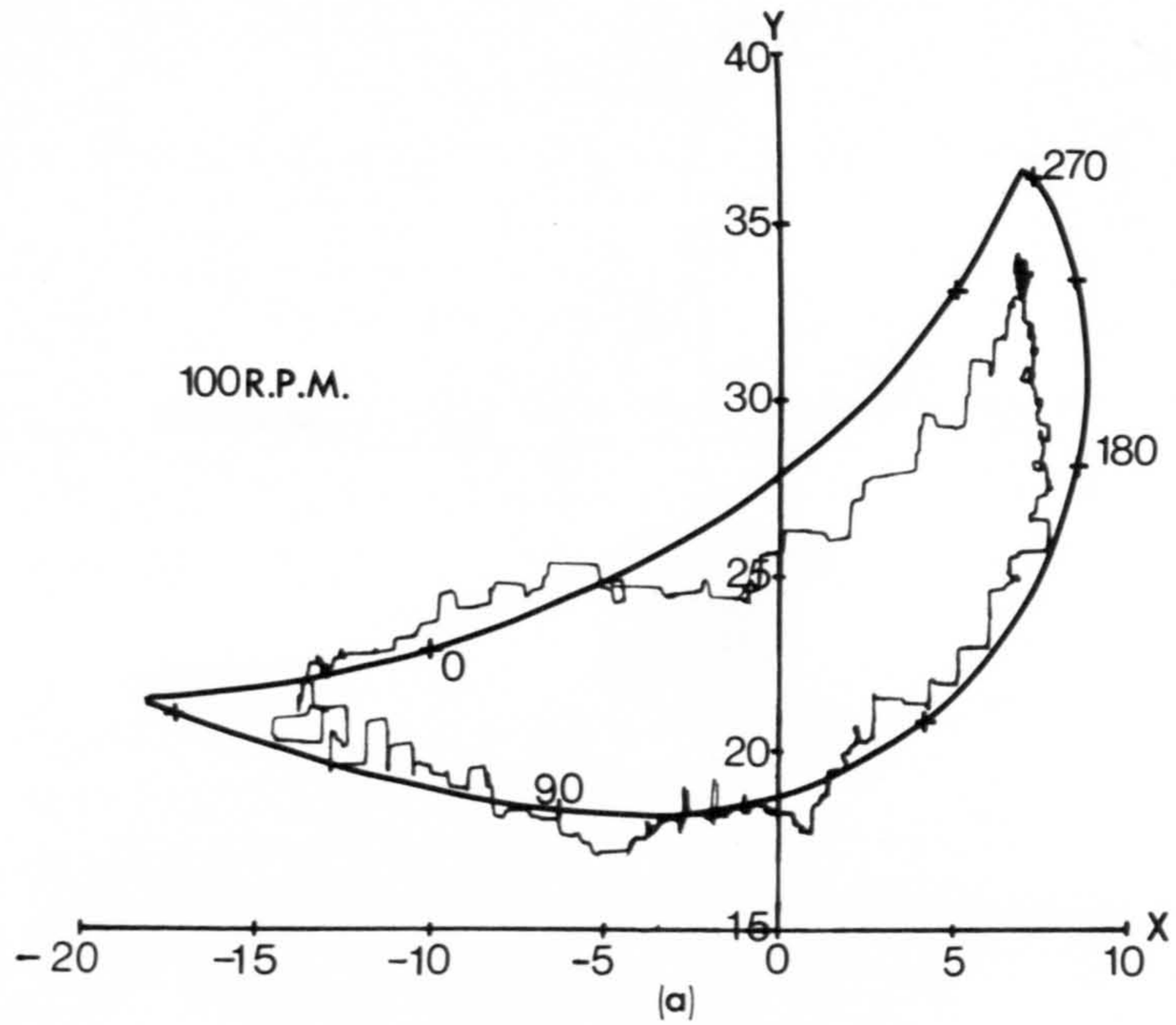

(a)

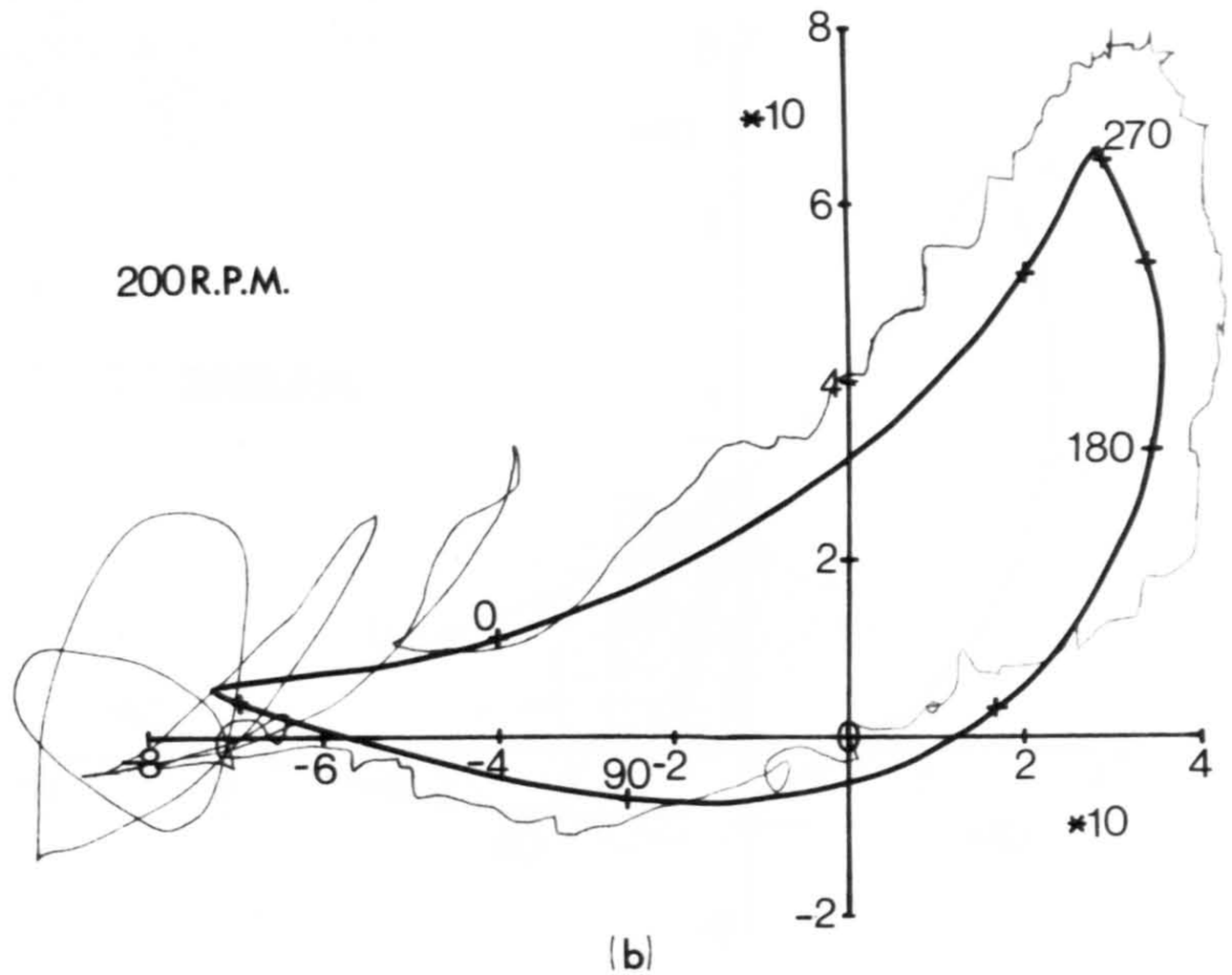

(b)

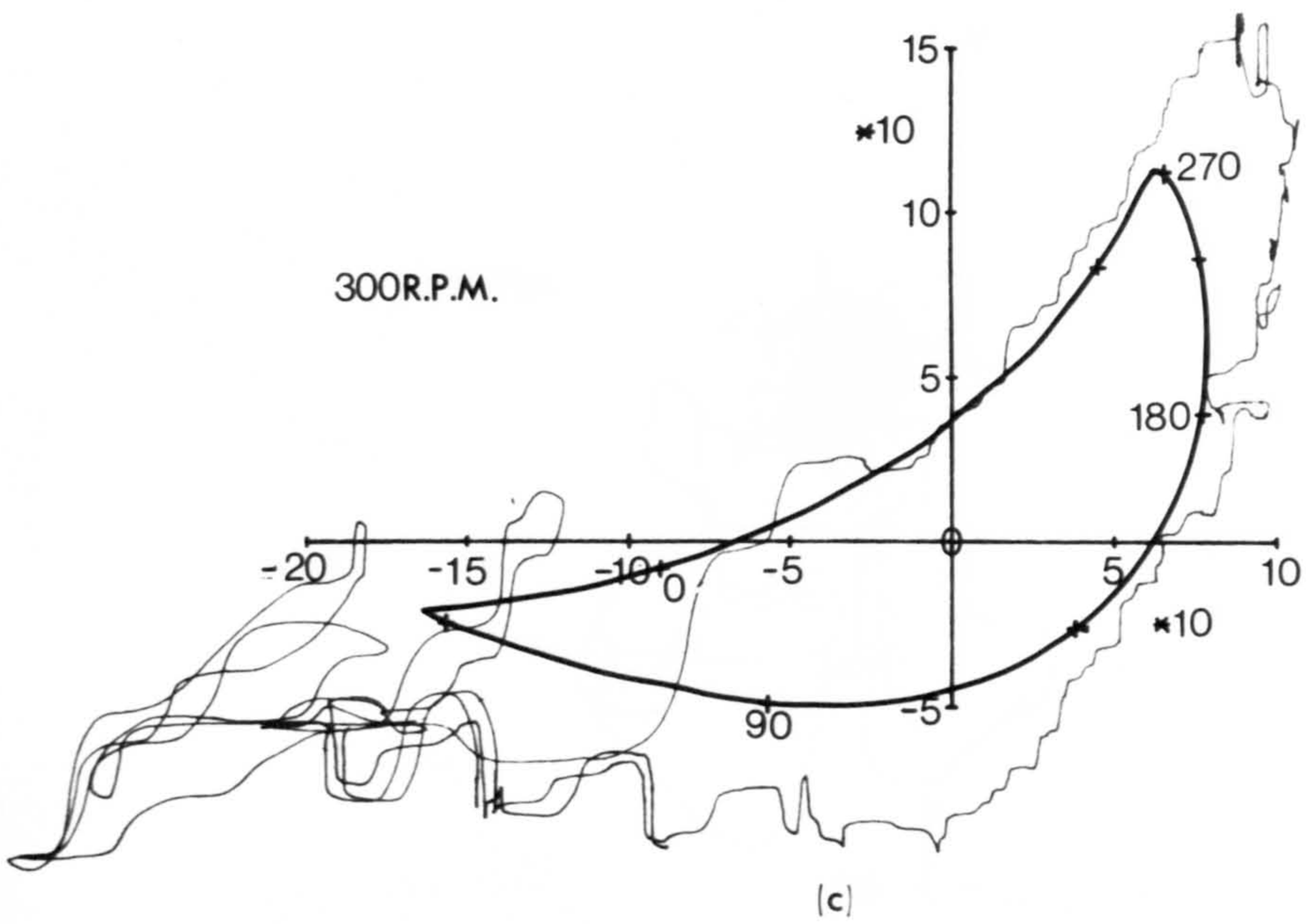

(c)

Y=VERTICAL FORCE

(NEWTONS)

X=HORIZONTAL FORCE

FIGURE 7.4 SHAKING FORCE: NO COUNTERWEIGHTS

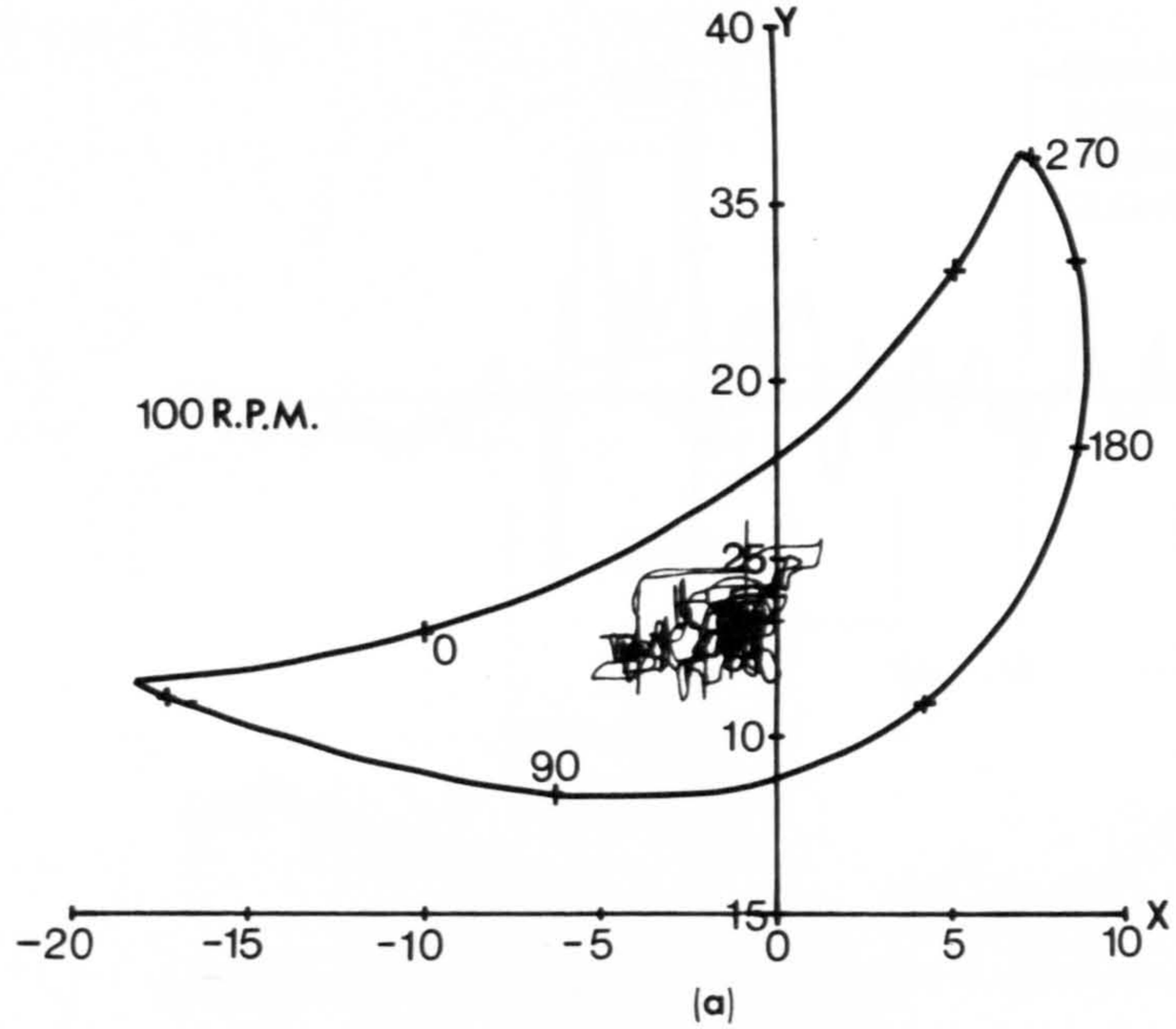

(a)

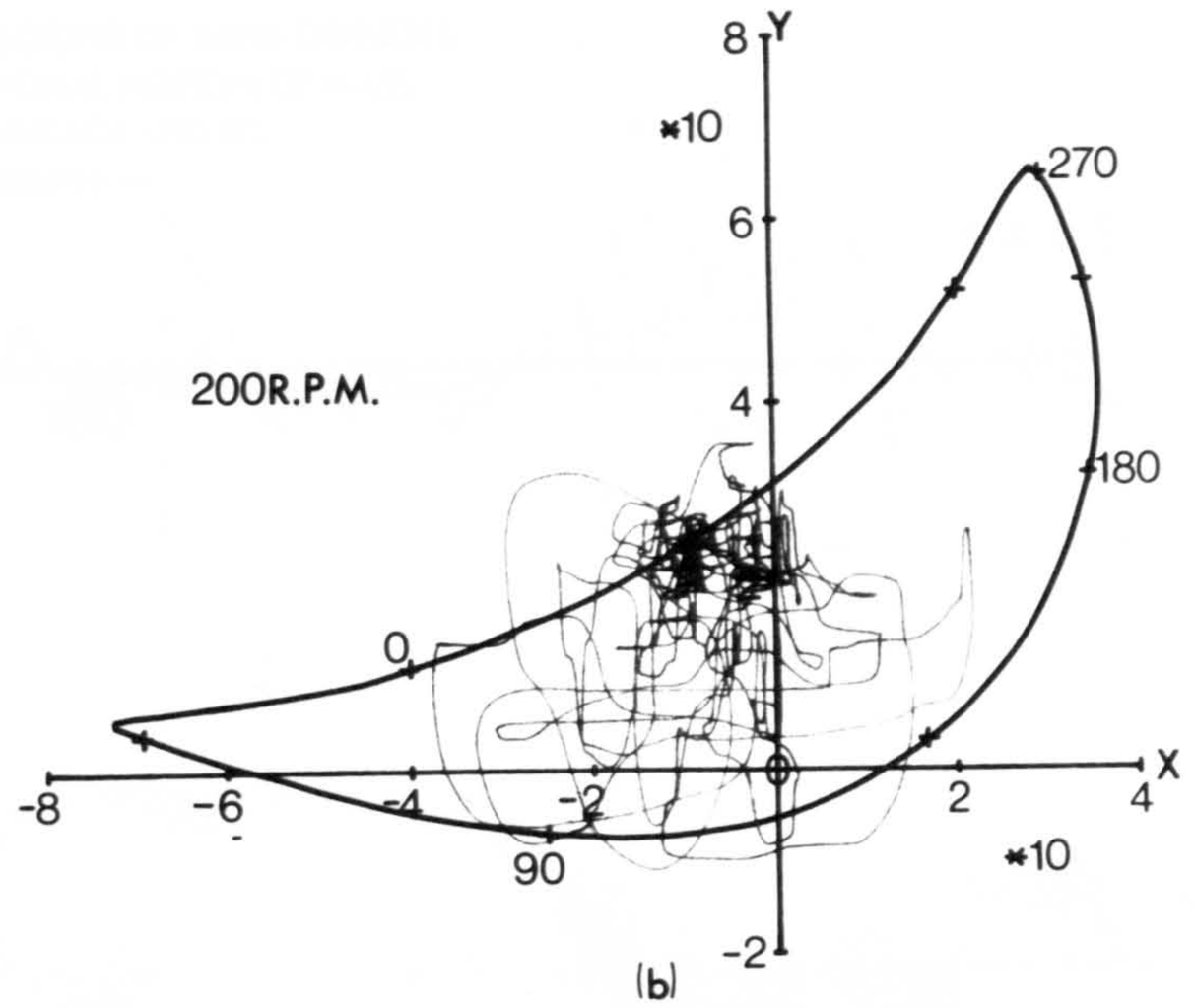

(b)

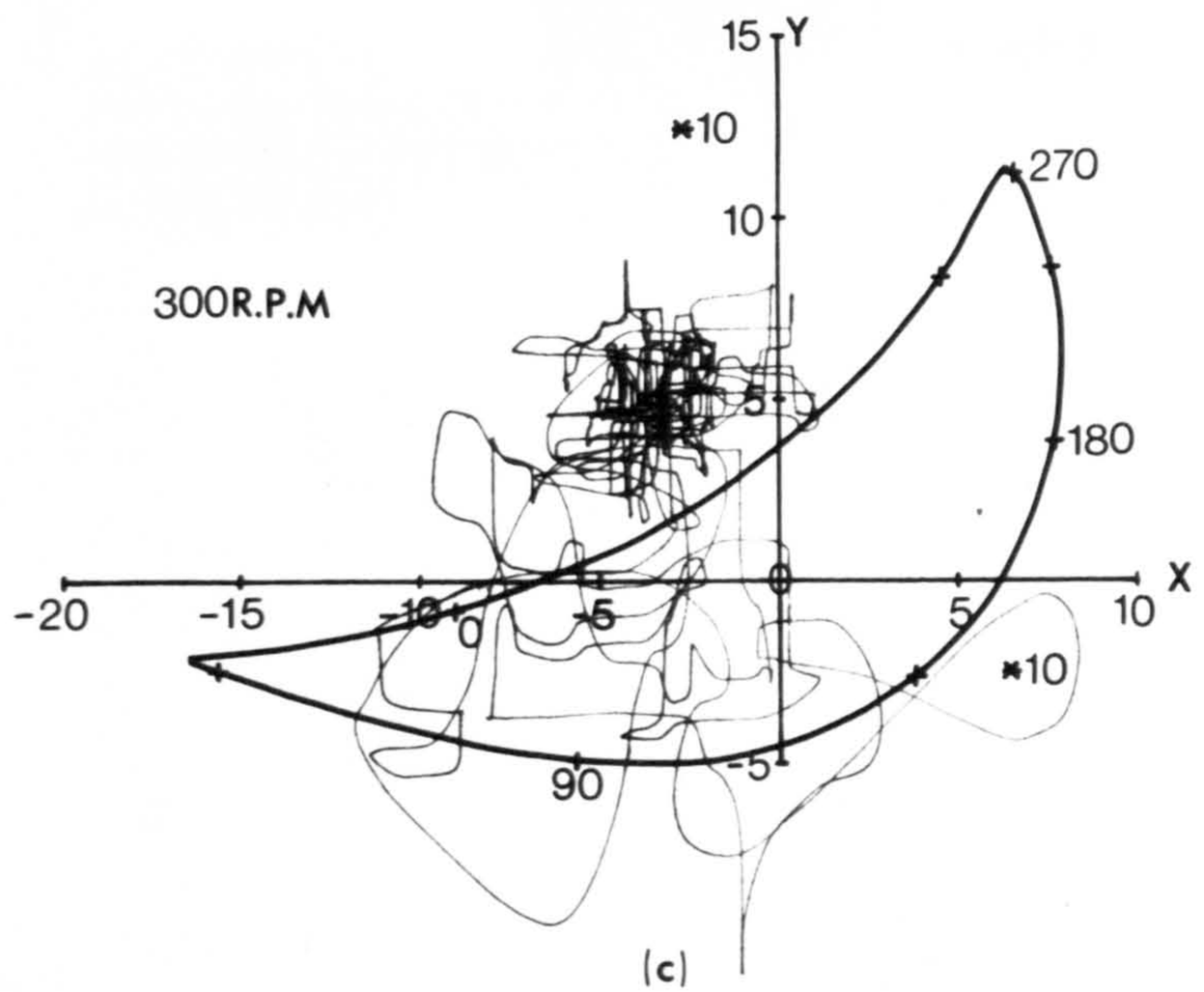

(c)

Y=VERTICAL FORCE

(NEWTONS)

X=HORIZONTAL FORCE

FIGURE 7.5 SHAKING FORCE: COUNTERWEIGHTS ADDED

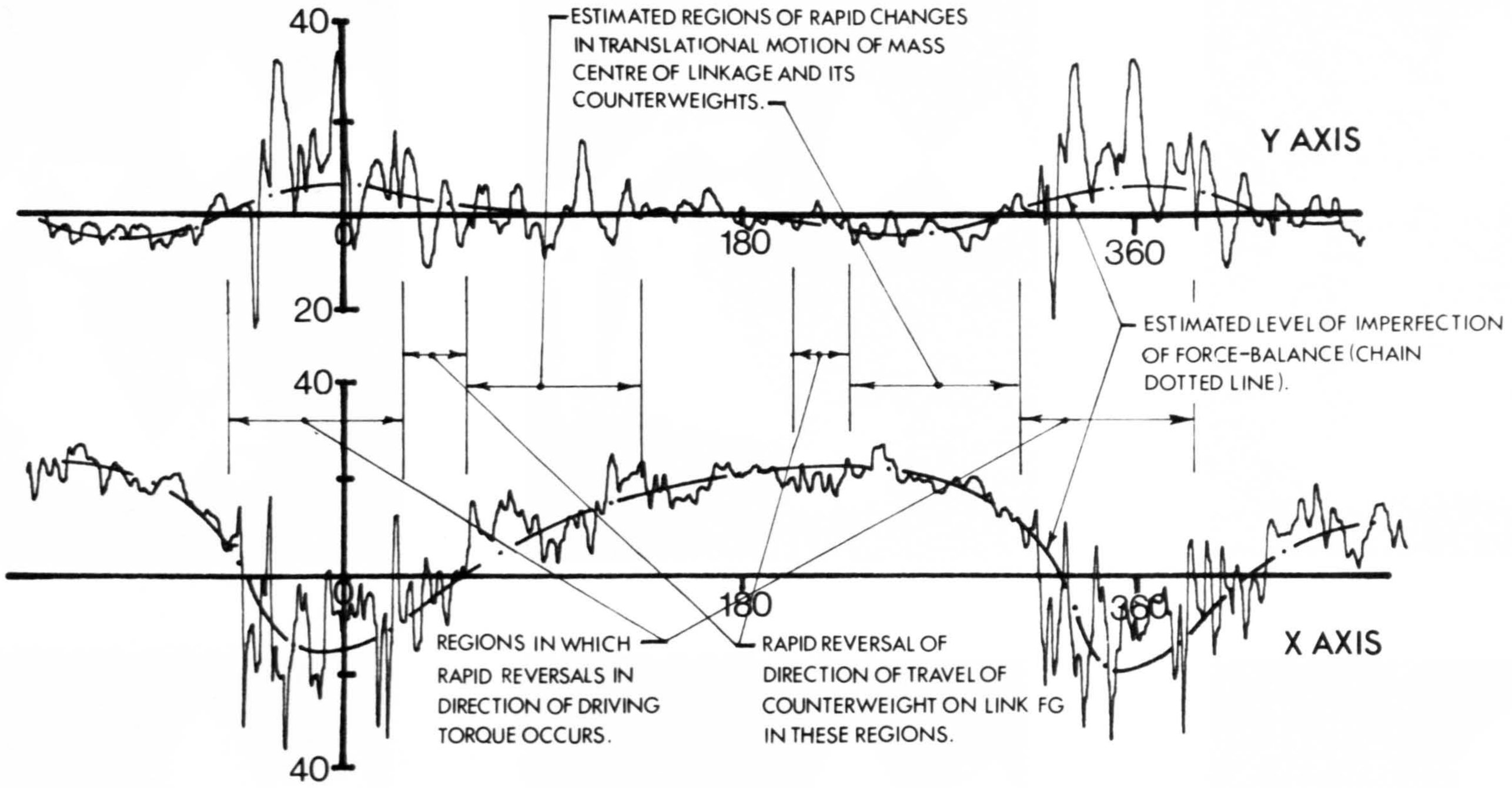

FIGURE 7.6 FRAME SHAKING FORCE AT 200 R.P.M.

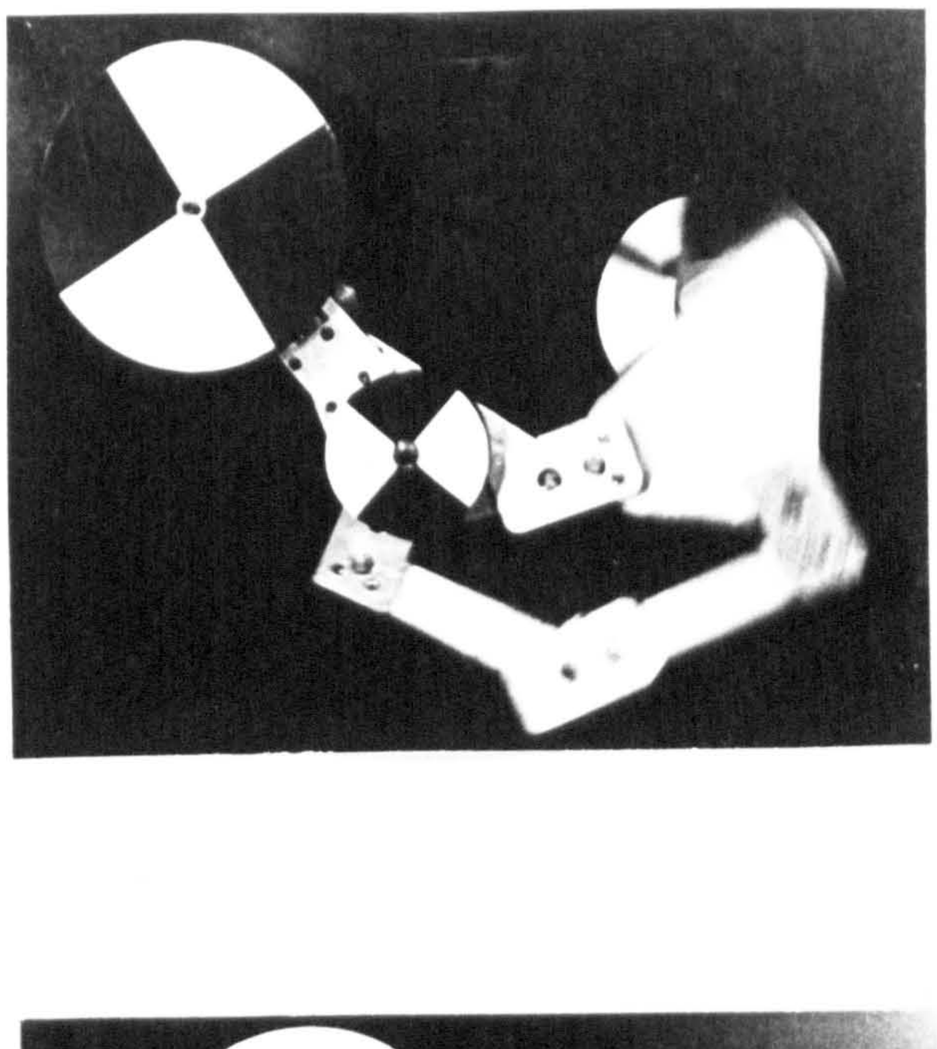

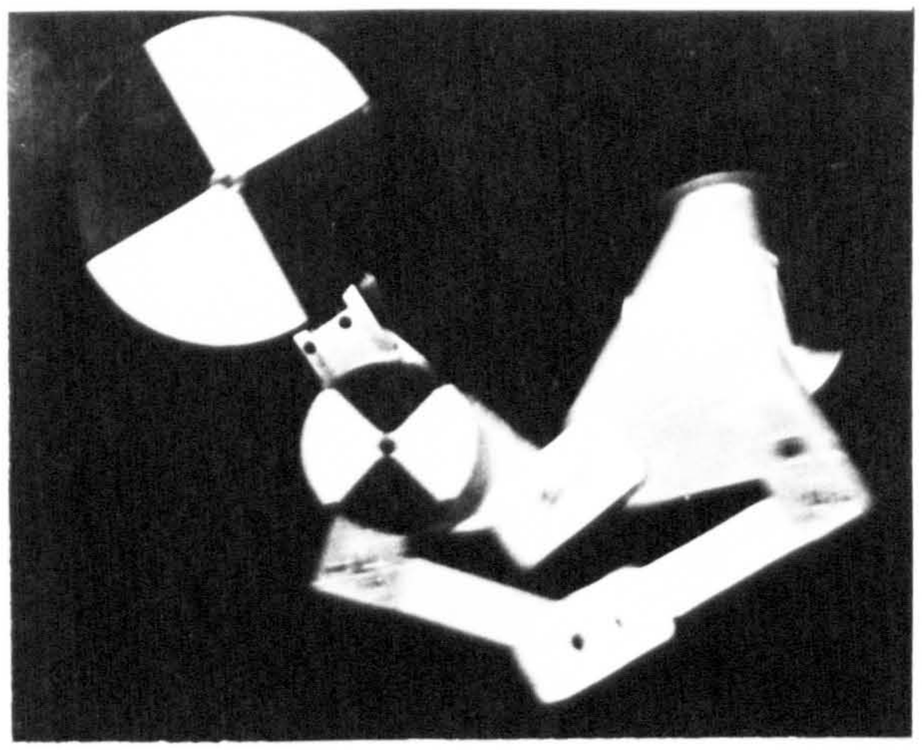

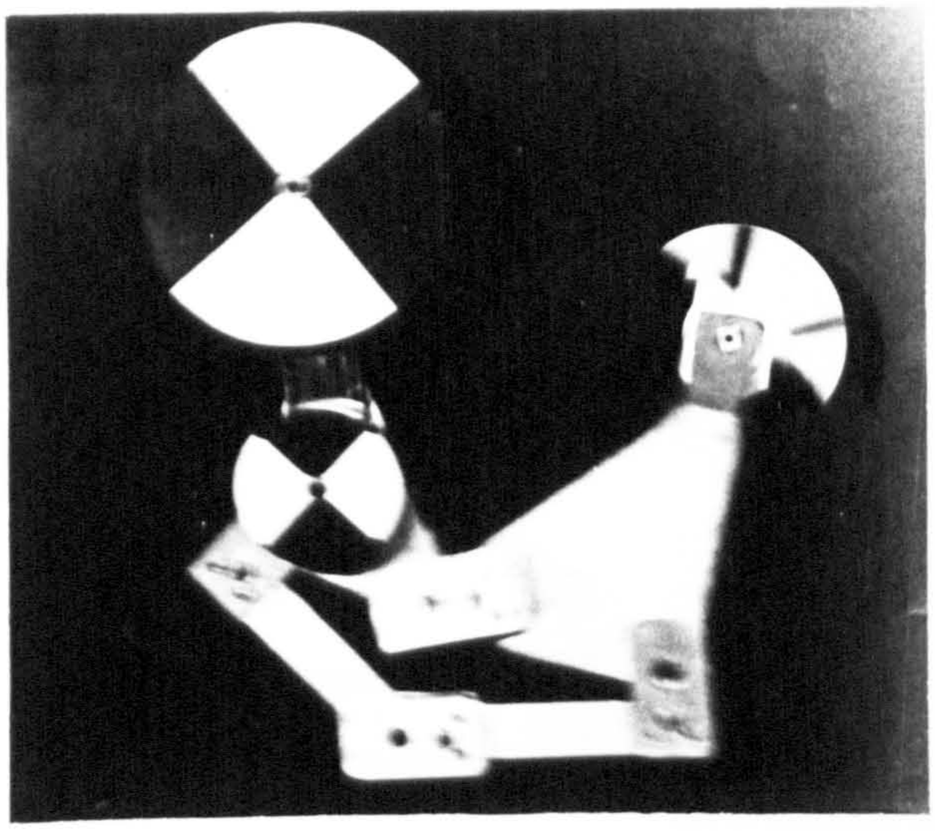

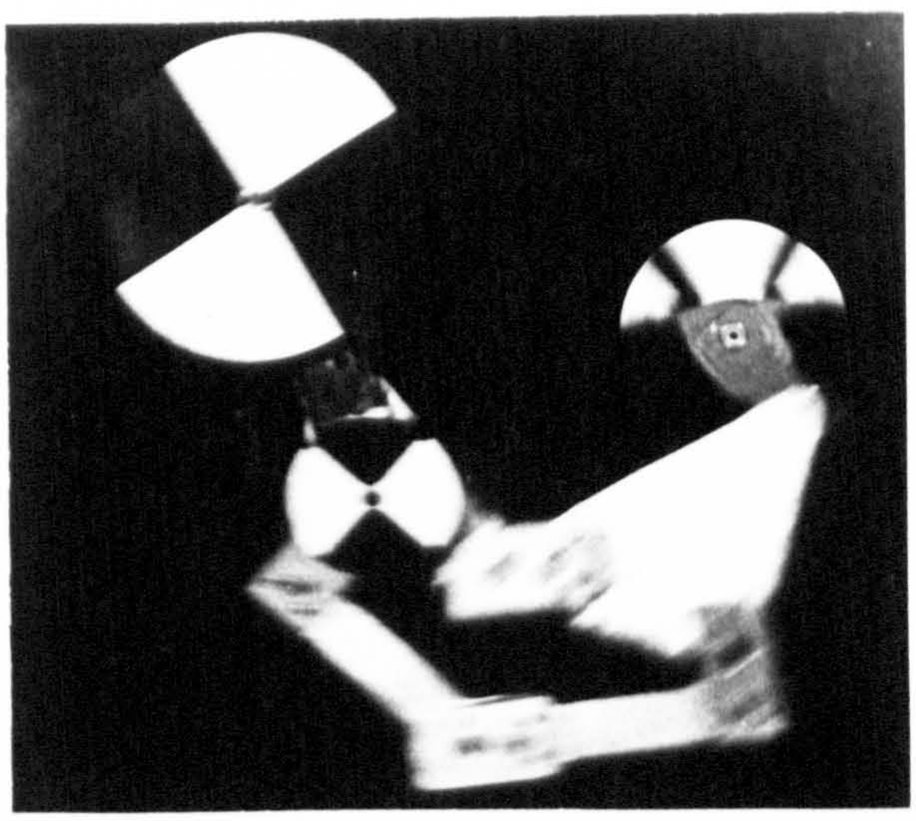

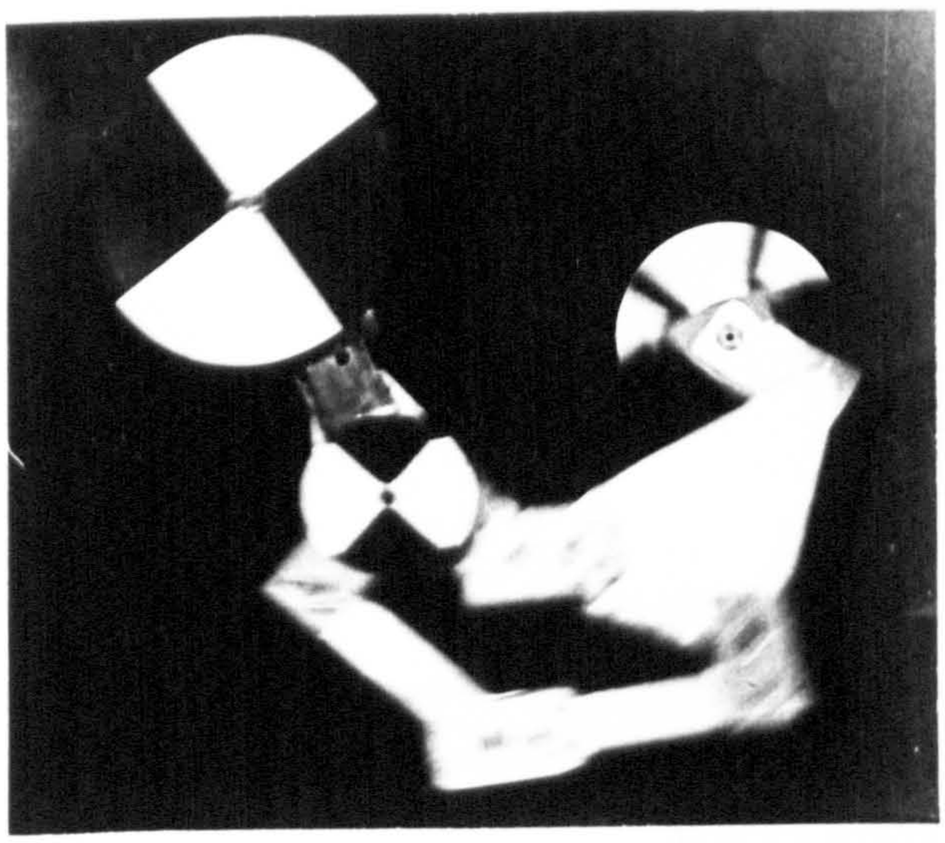

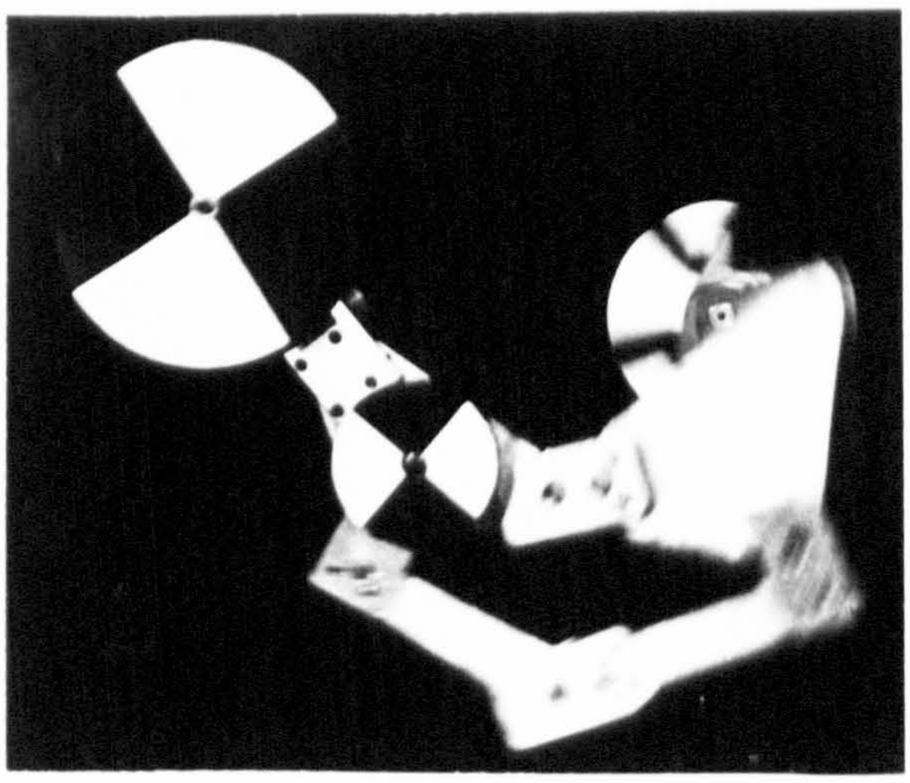

FIGURE 7.7 MINMUM MOMENT OF INERTIA COUNTERWEIGHTS

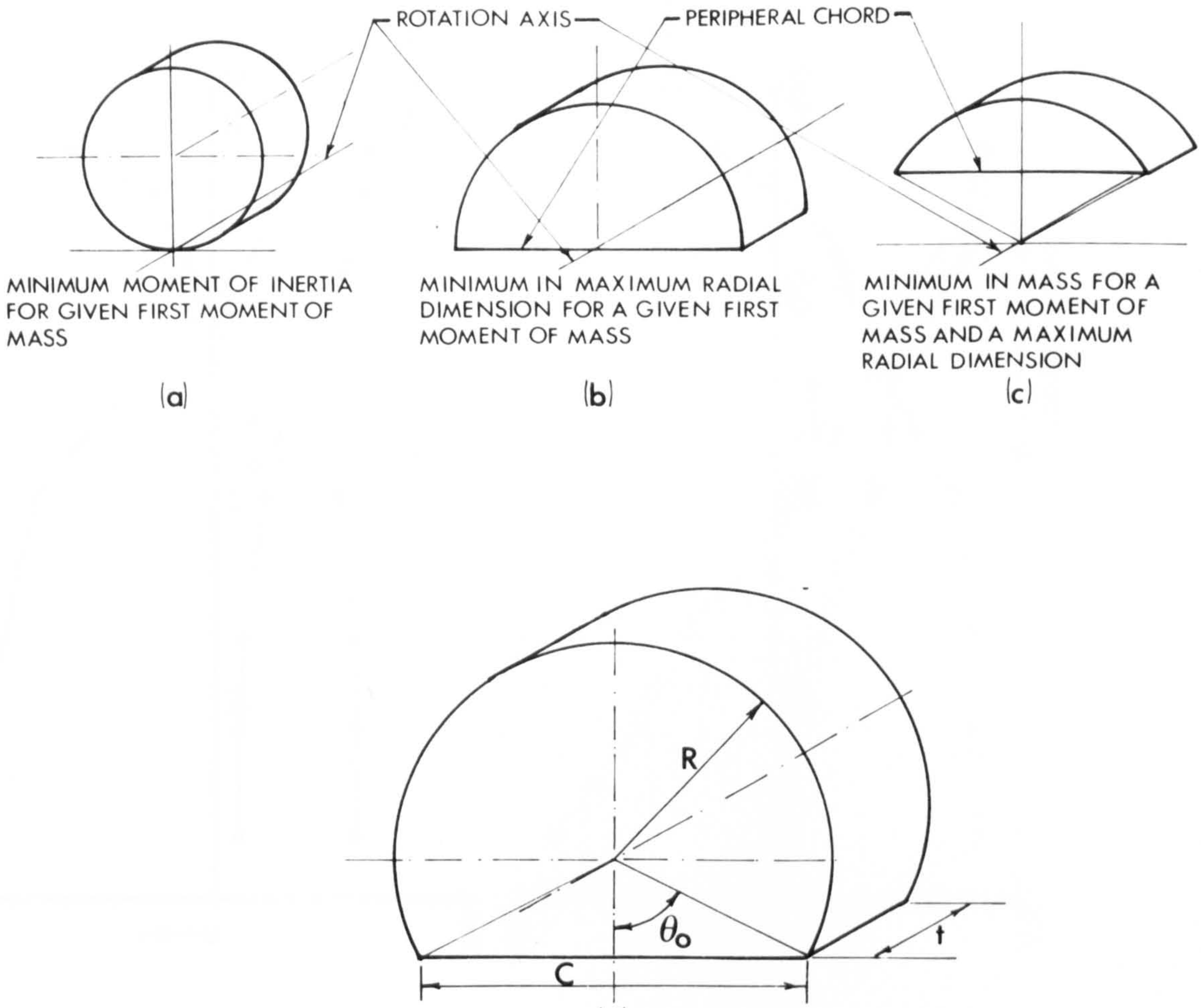

FIGURE 8.1 SEGMENTAL COUNTERWEIGHT

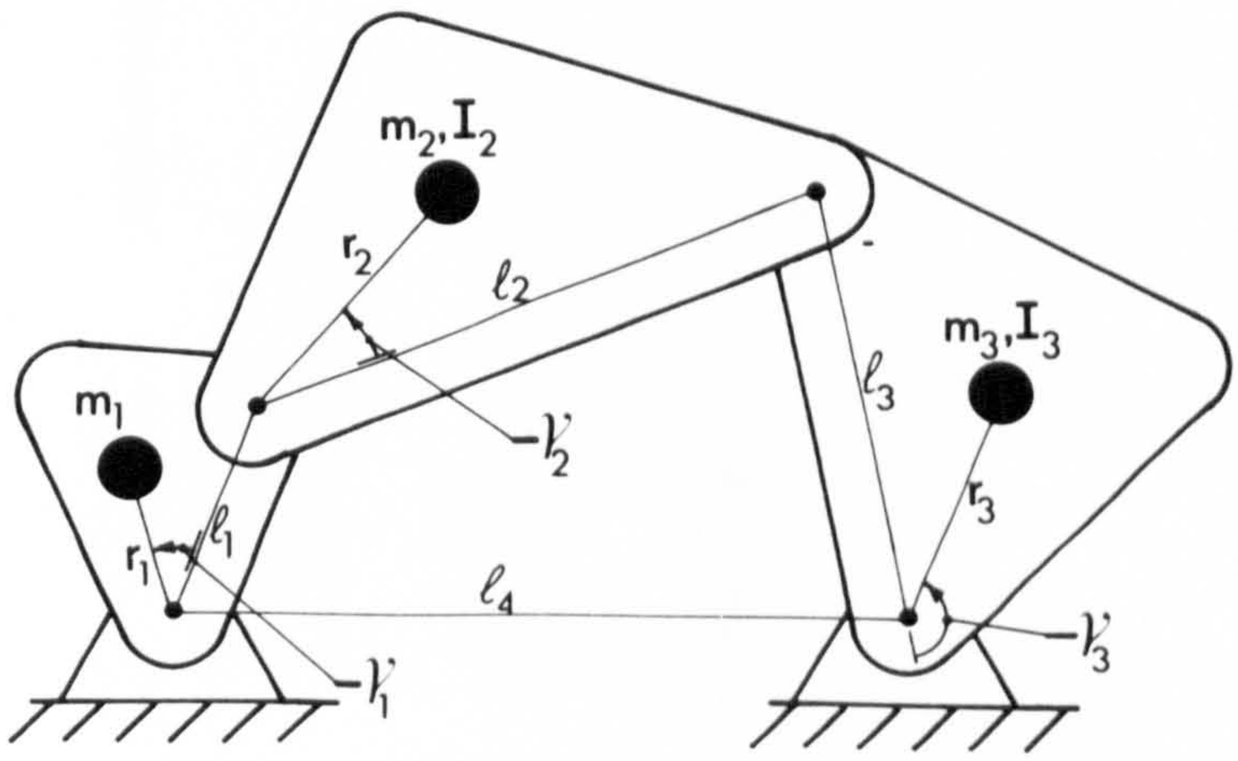

FIGURE 8.2 FOUR-BAR LINKAGE

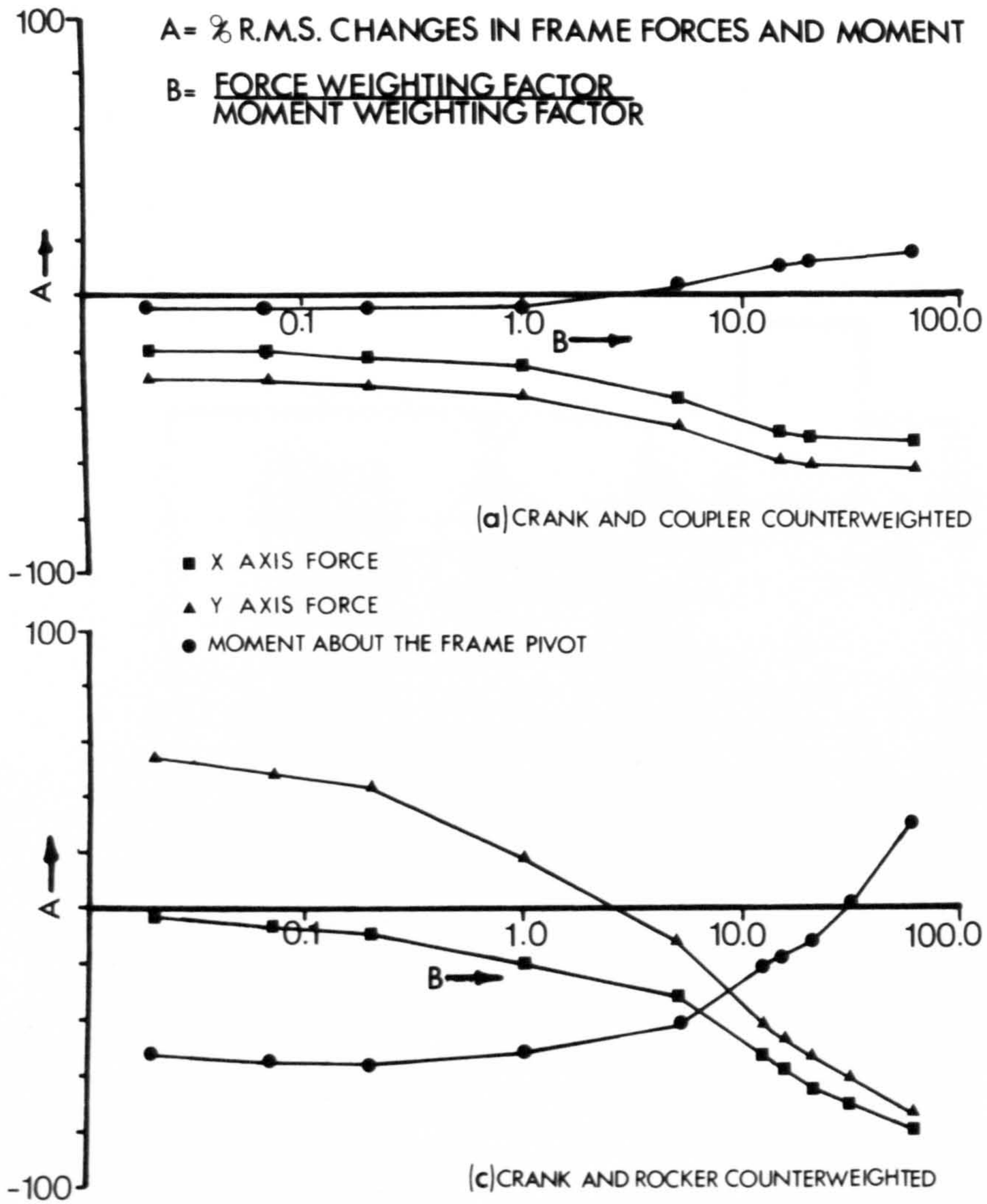

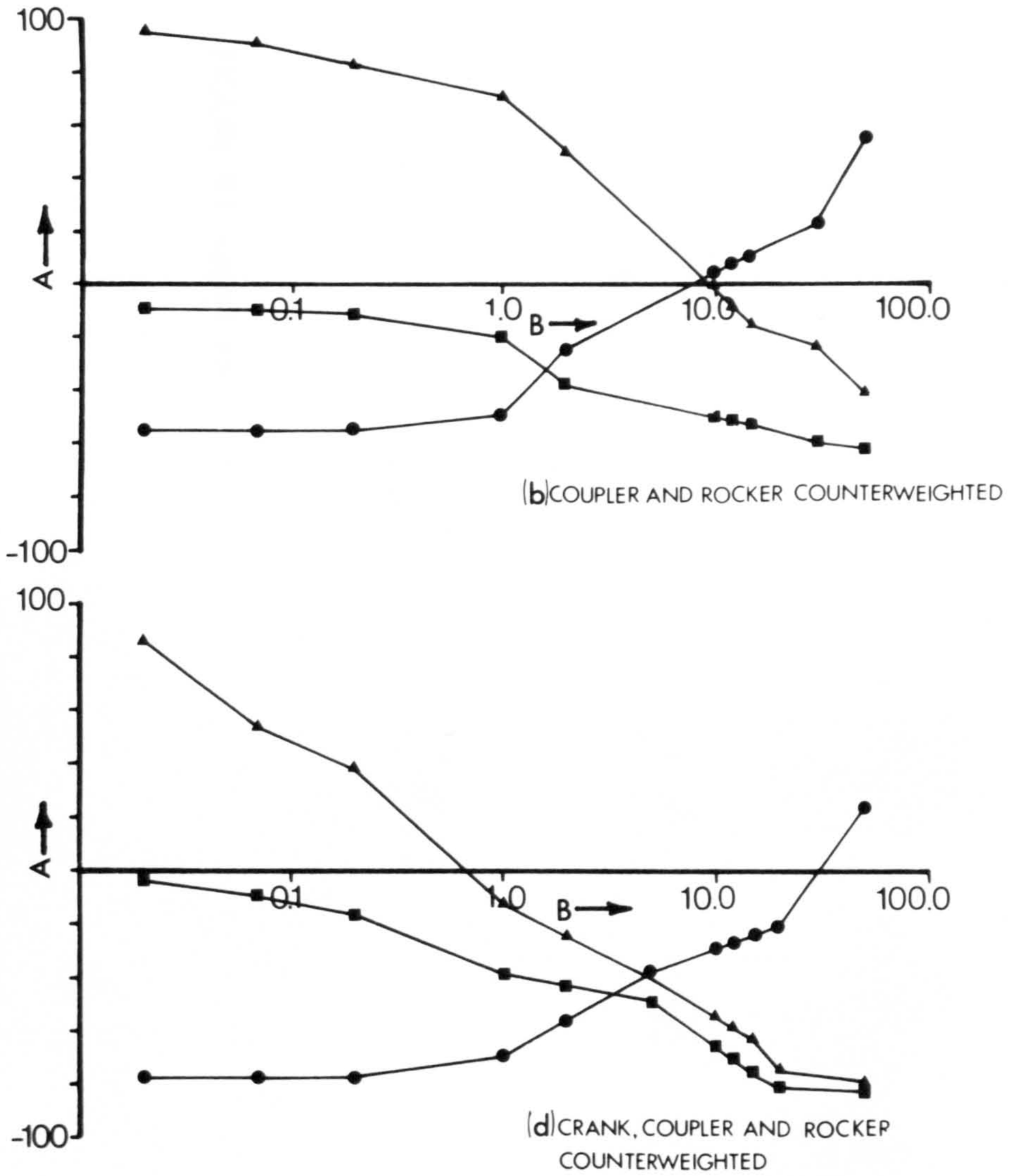

FIGURE 8.3 PARTIAL FORCE AND MOMENT BALANCES OF A FOUR-BAR LINKAGE

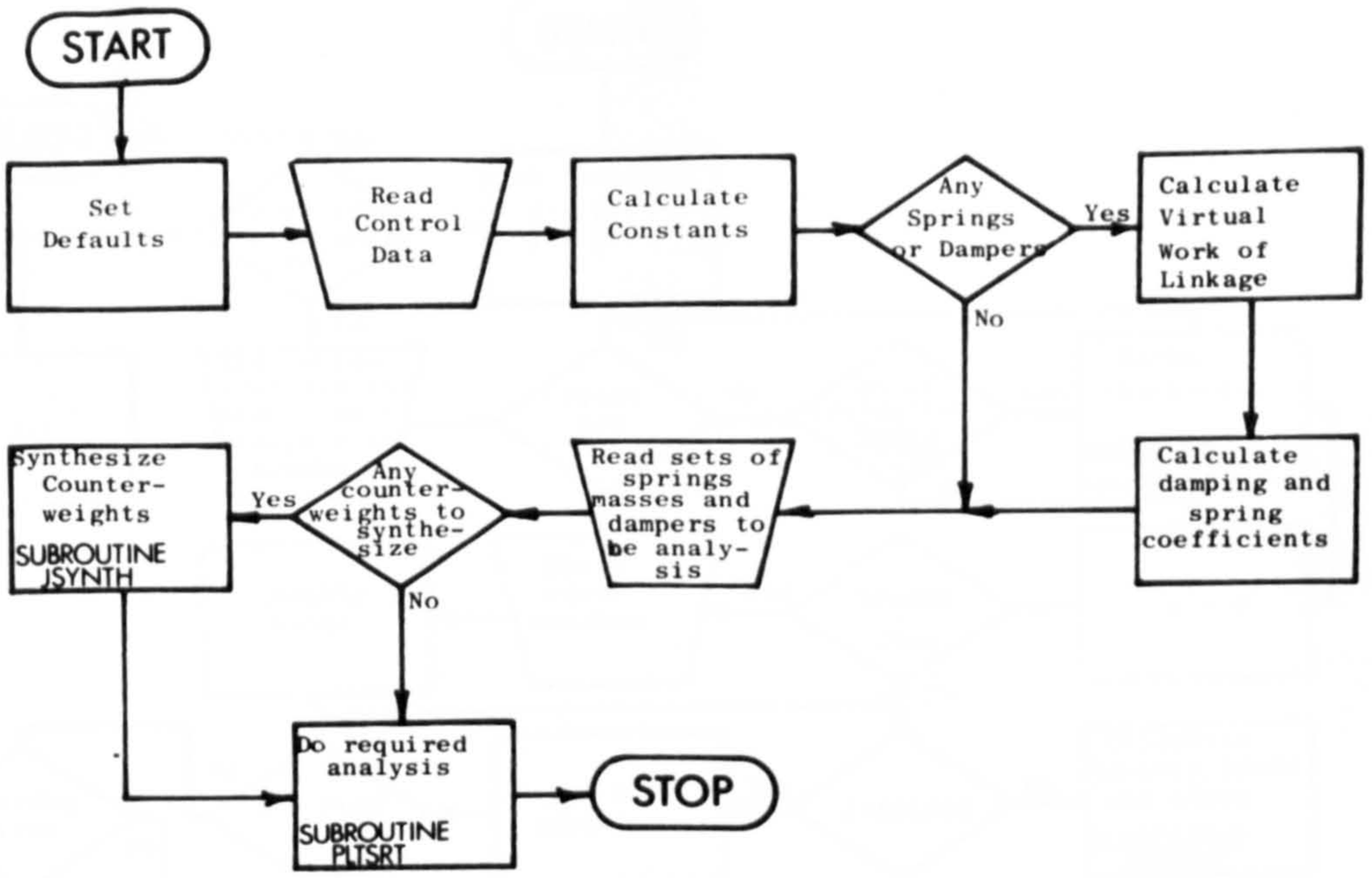

FIGURE 9.1 MAIN PROGRAM

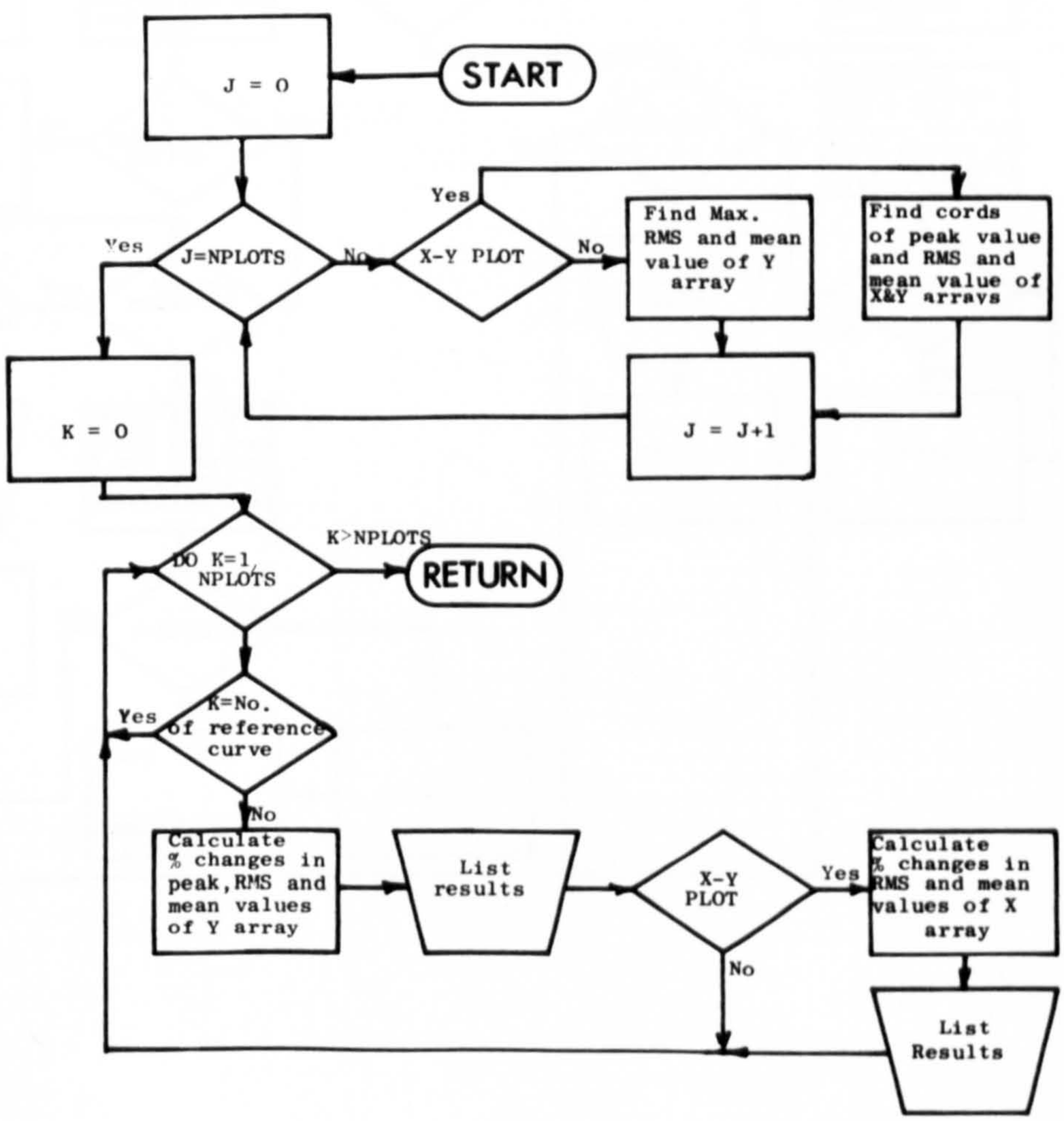

FIGURE 9.2 SUBROUTINE PERERR

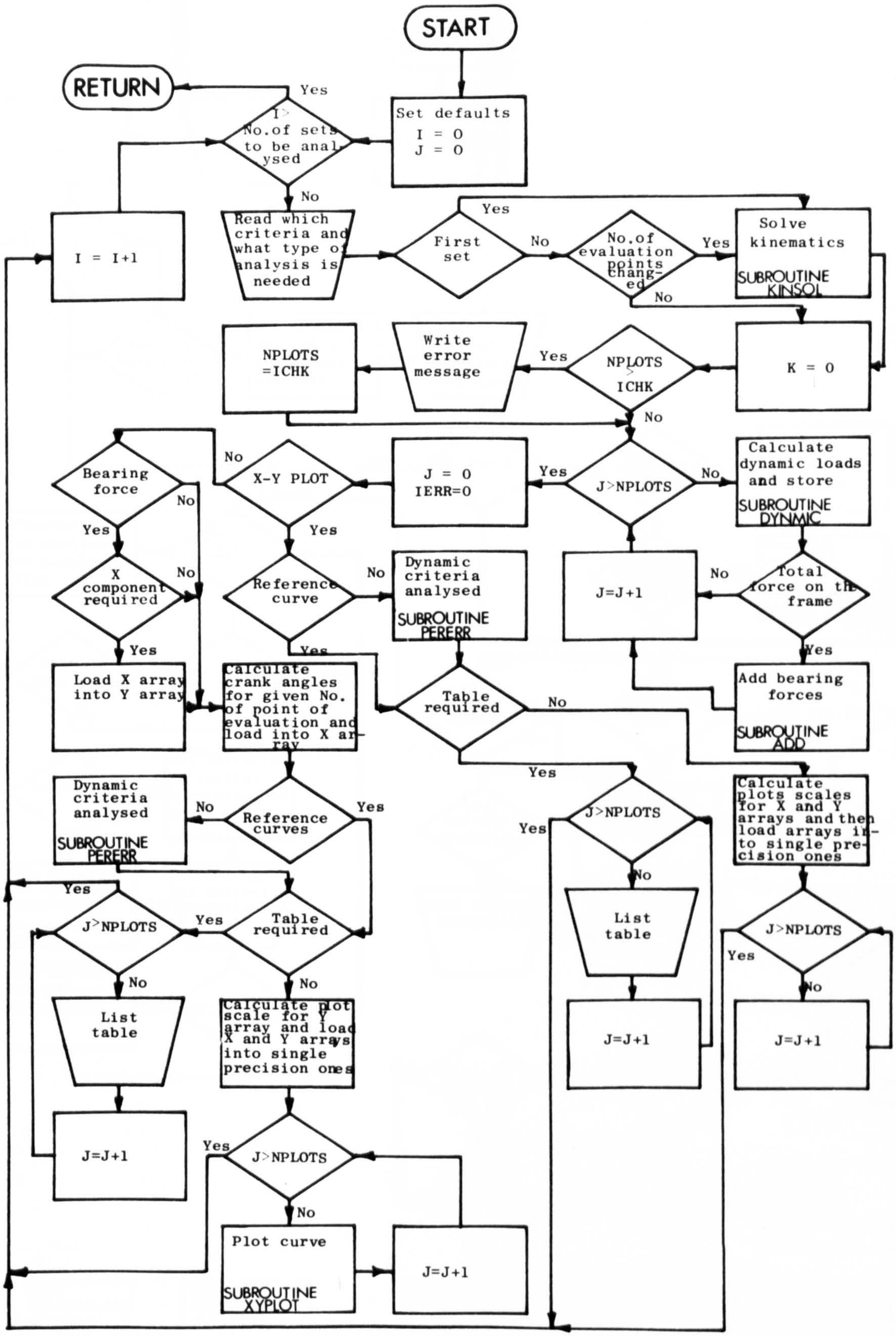

FIGURE 9.3 SUBROUTINE PLTSRT

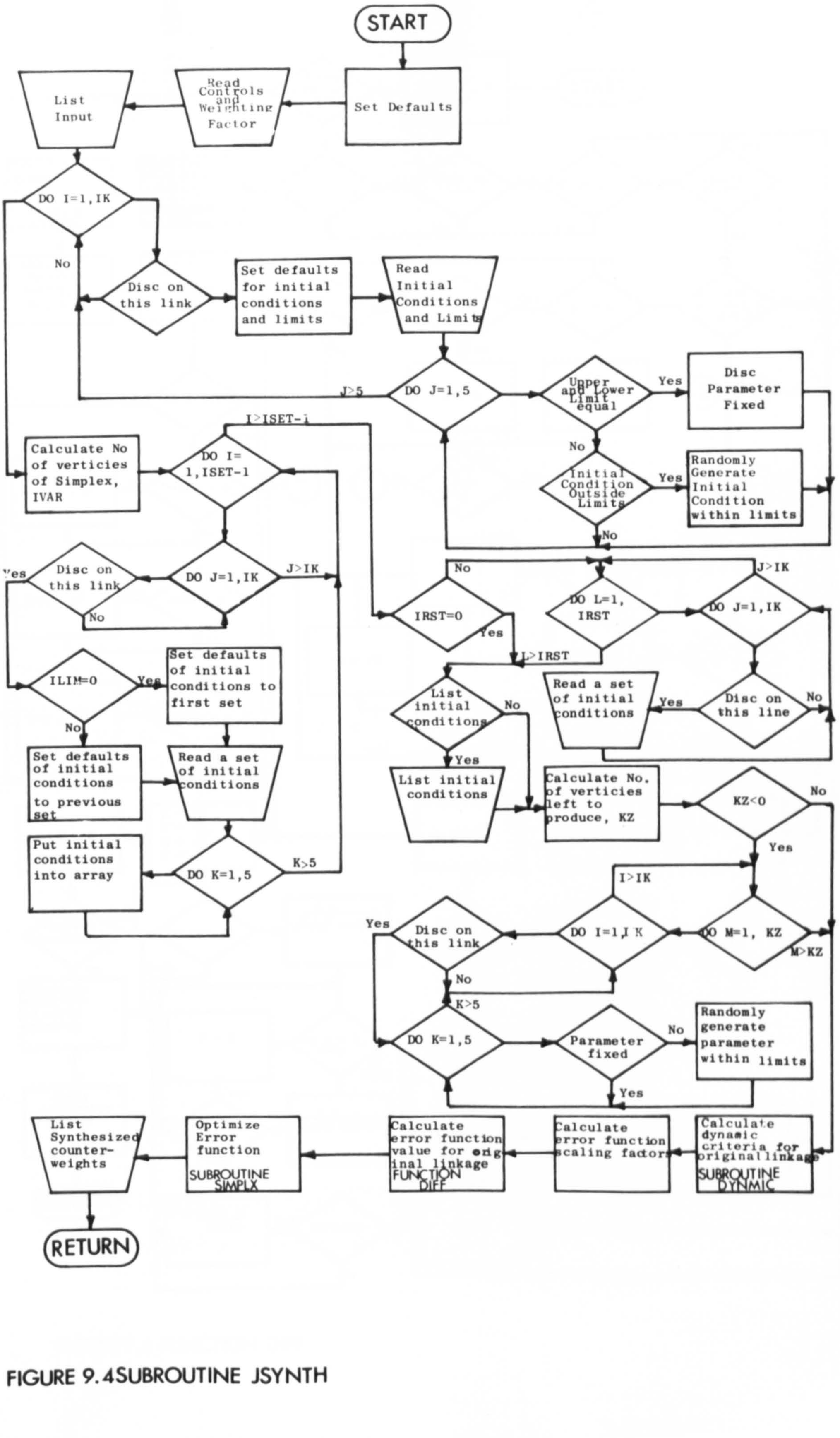

FIGURE 9.4SUBROUTINE JSYNTH

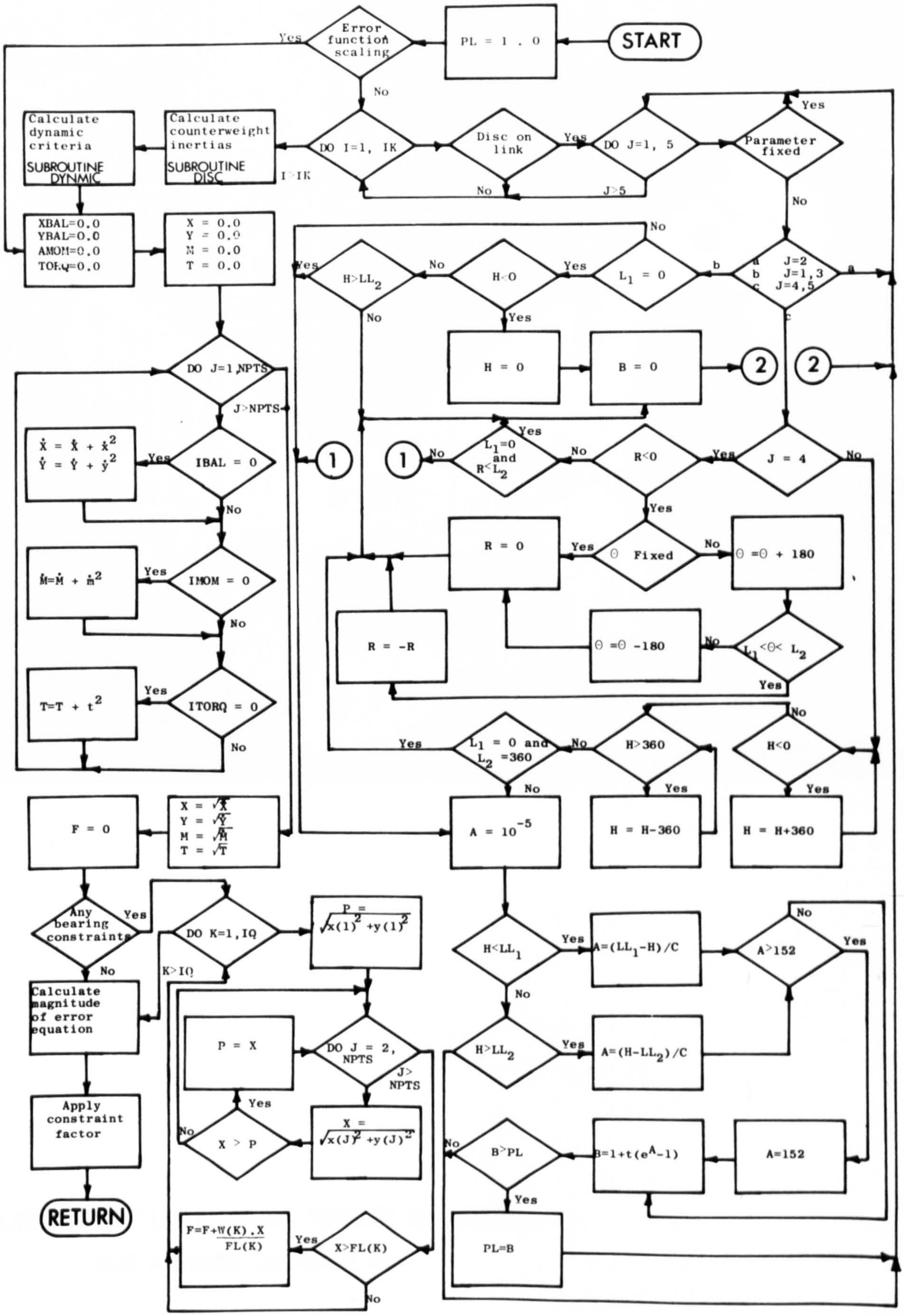

FIGURE 9.5 FUNCTION DIFF

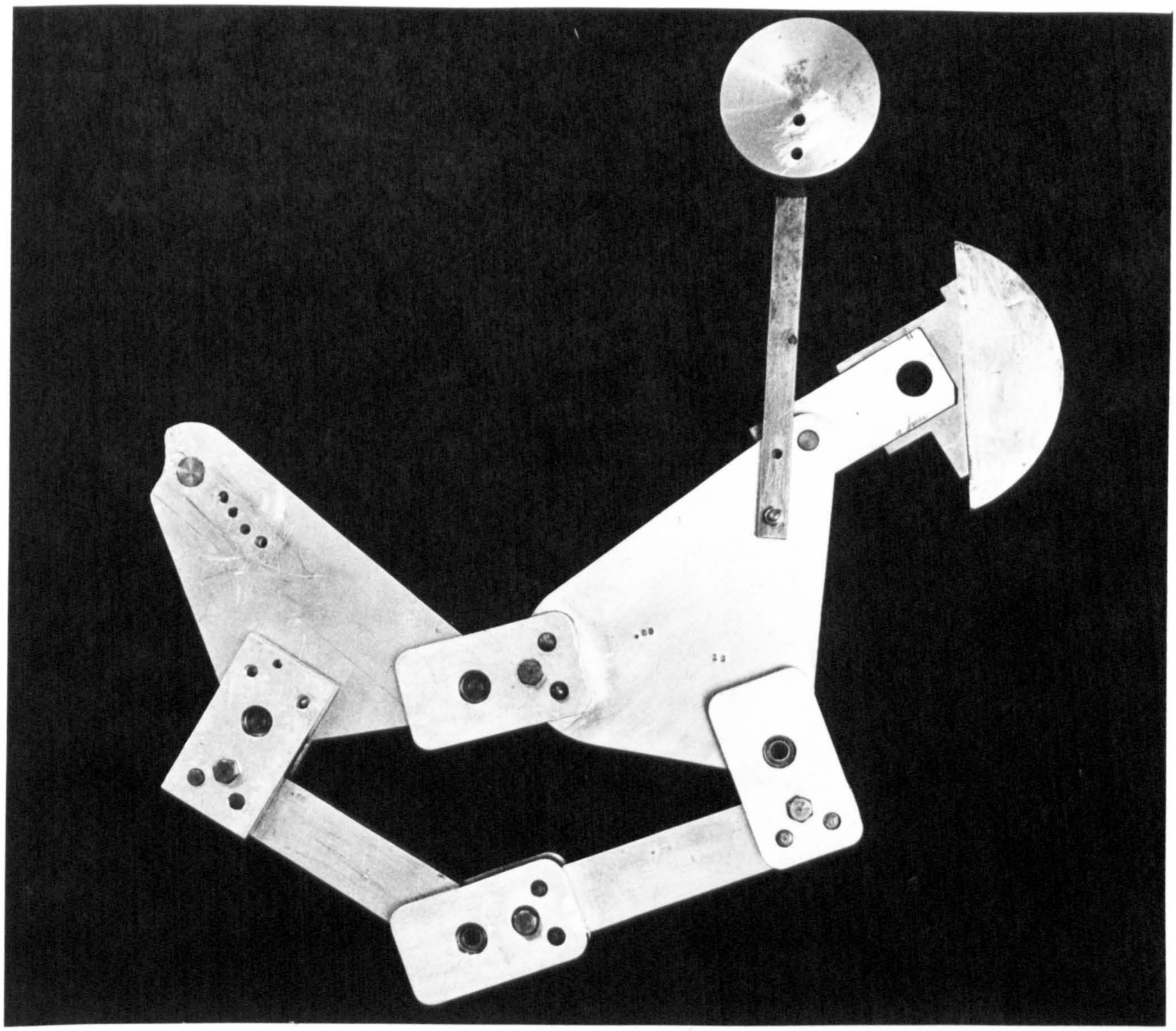

FIGURE 10.1 PARTIAL DRIVING TORQUE BALANCE
FOR A SPEED OF 600 R.P.M.

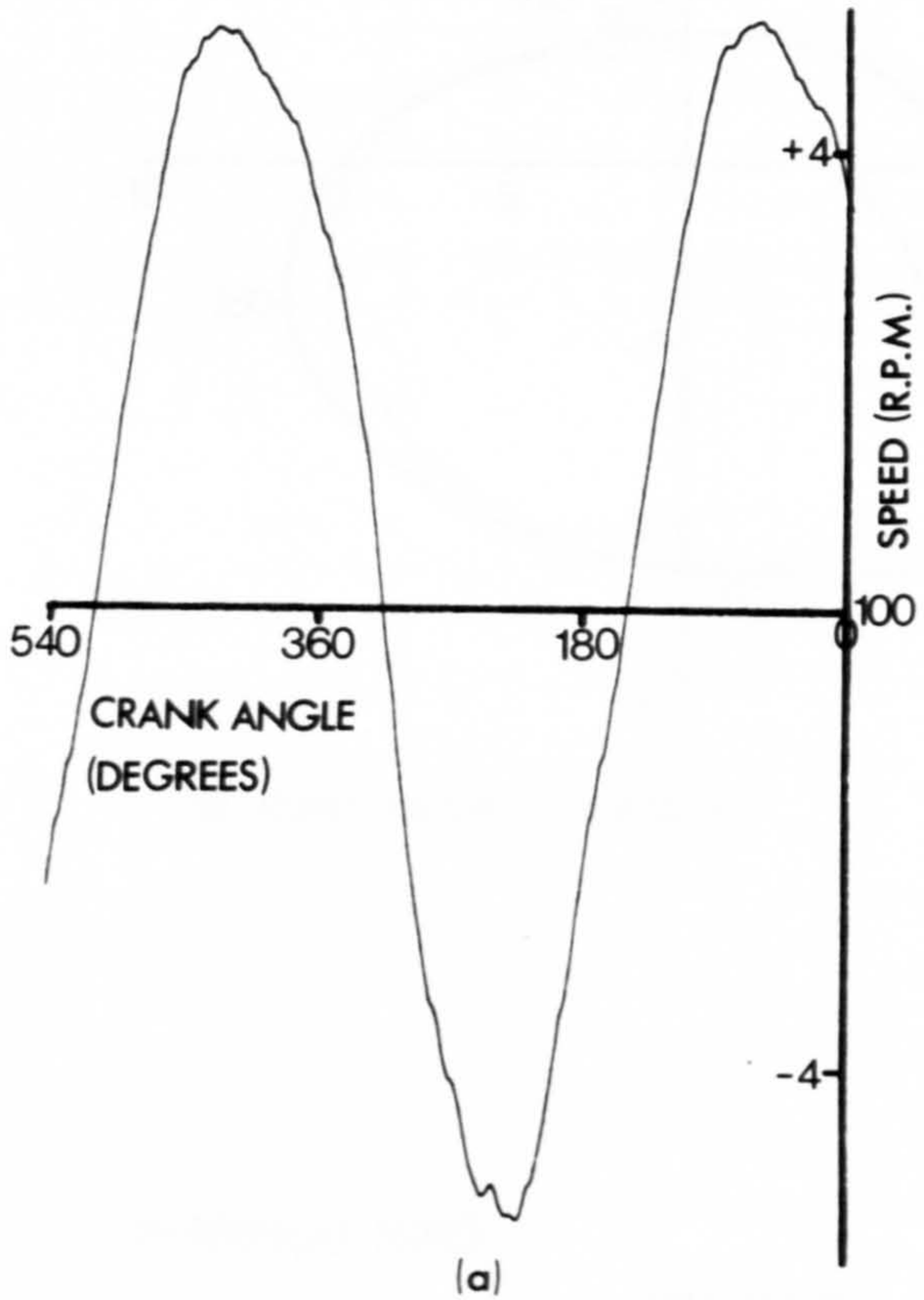

(a)

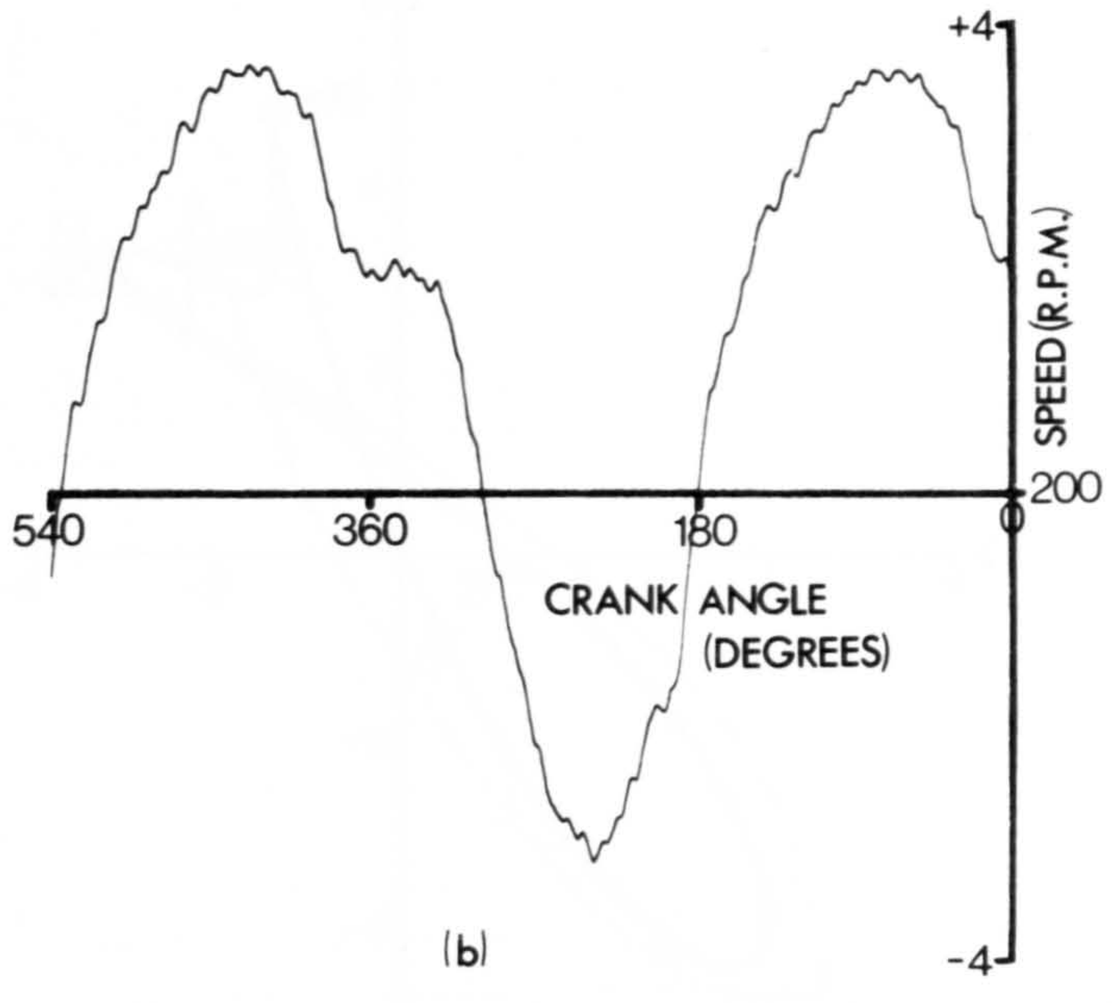

(b)

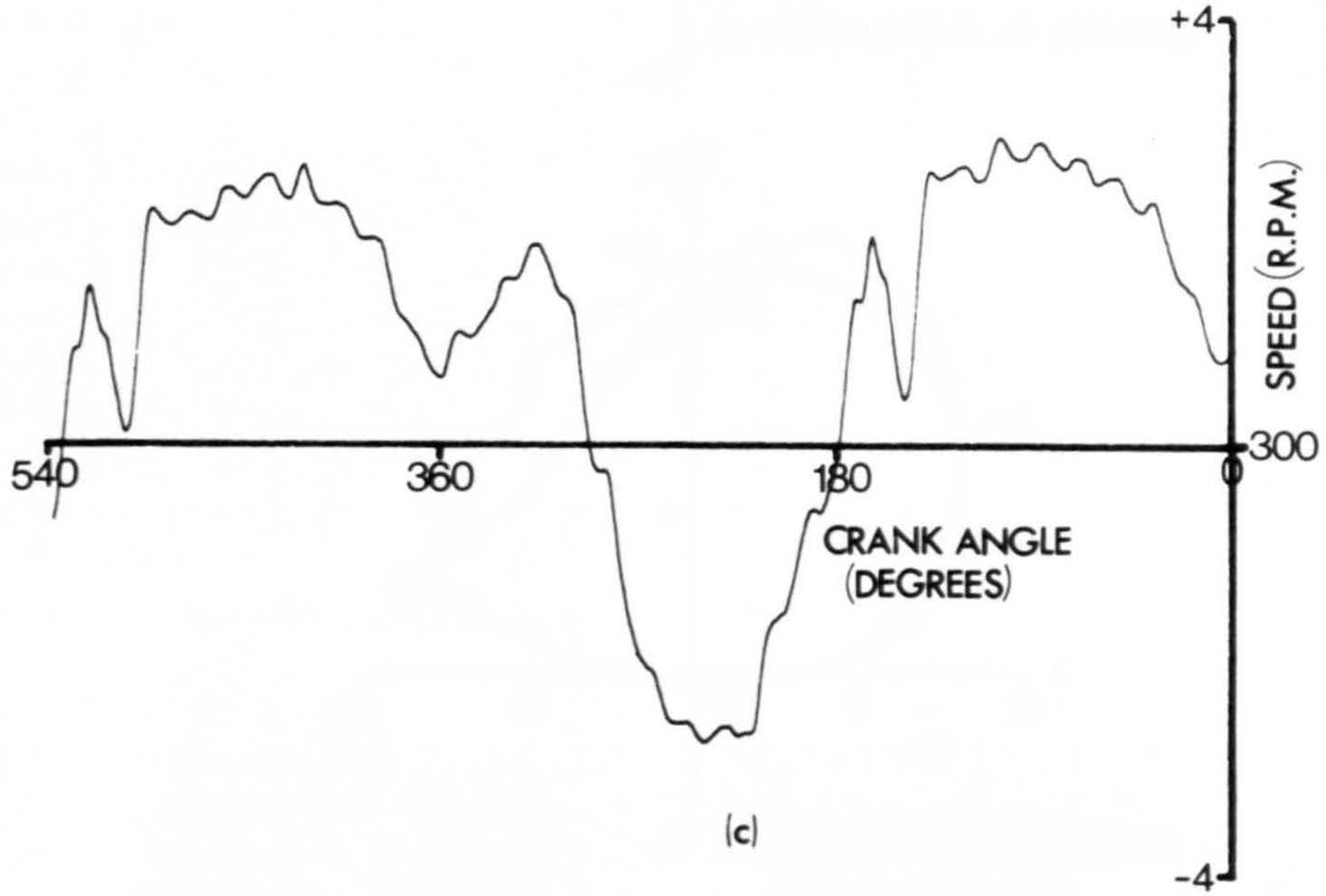

(c)

FIGURE 10.2 SPEED FLUCTUATIONS

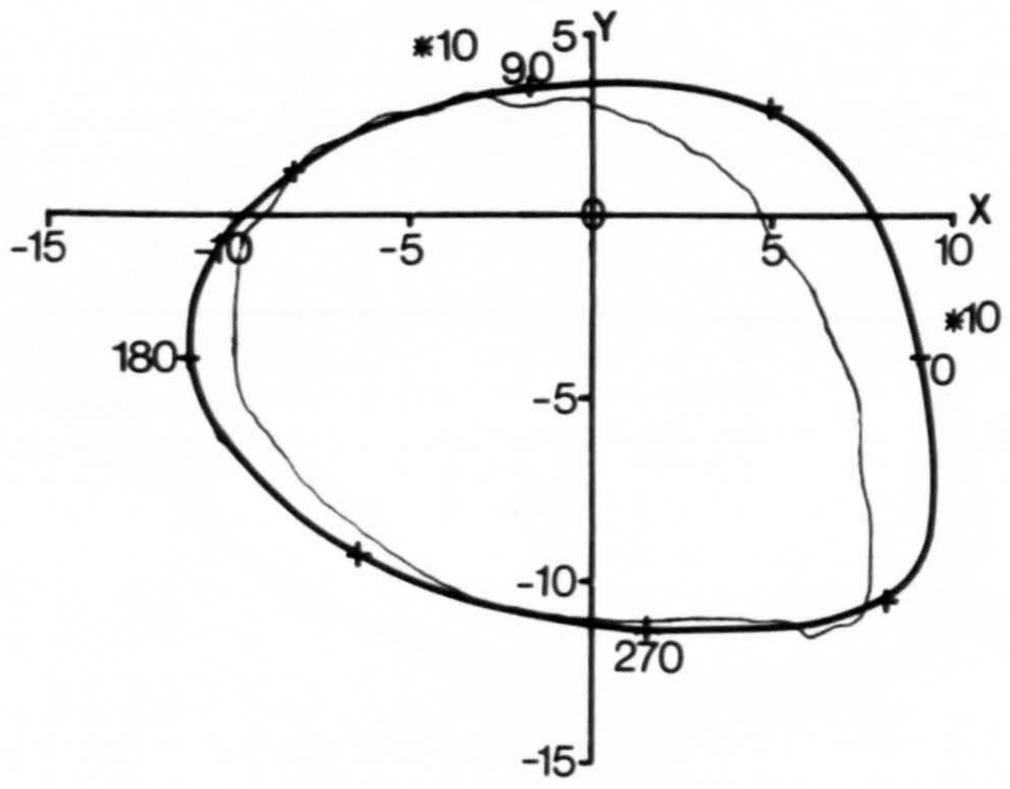

(a) LOAD LOCUS AT JOINT A

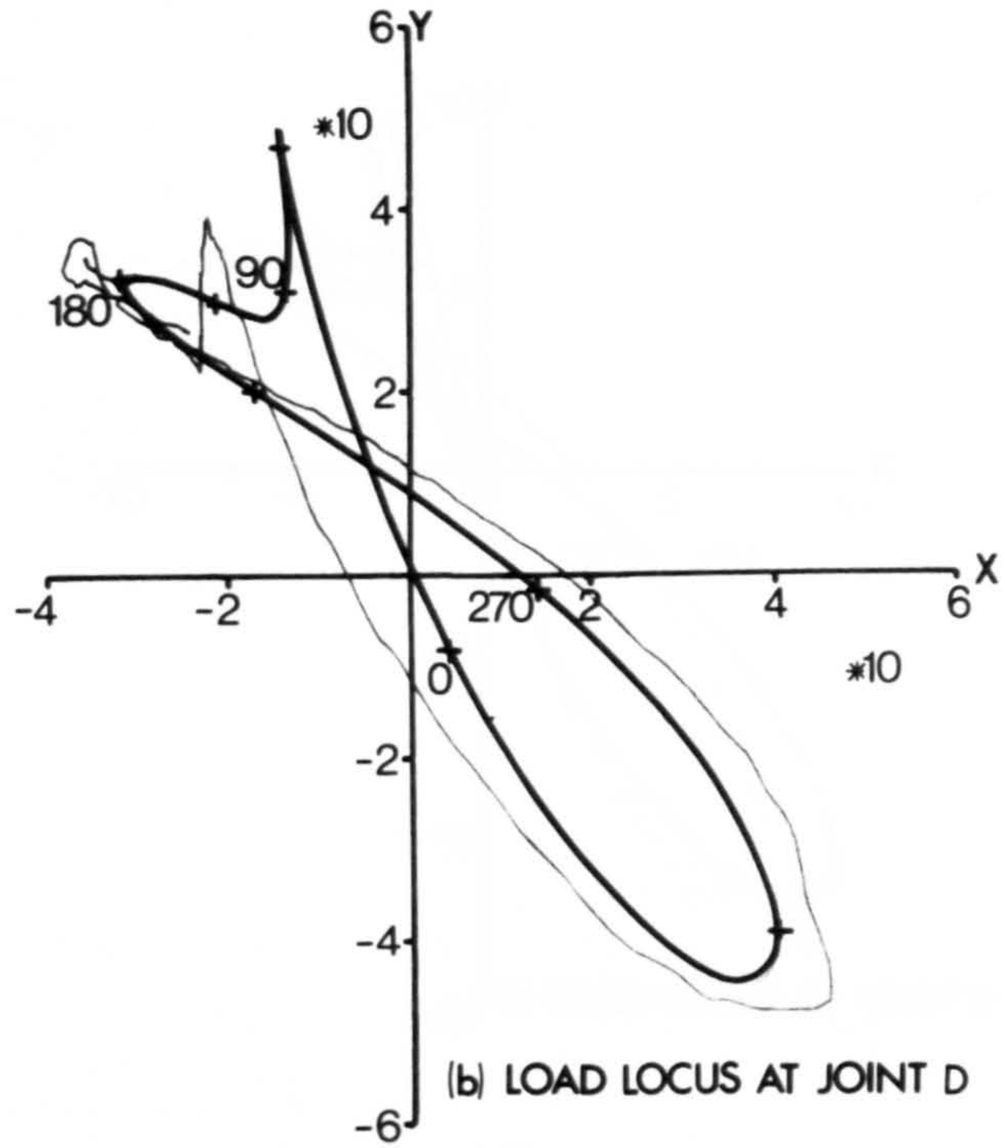

(b) LOAD LOCUS AT JOINT D

Y= VERTICAL FORCE

(NEWTONS)

X=HORIZONTAL FORCE

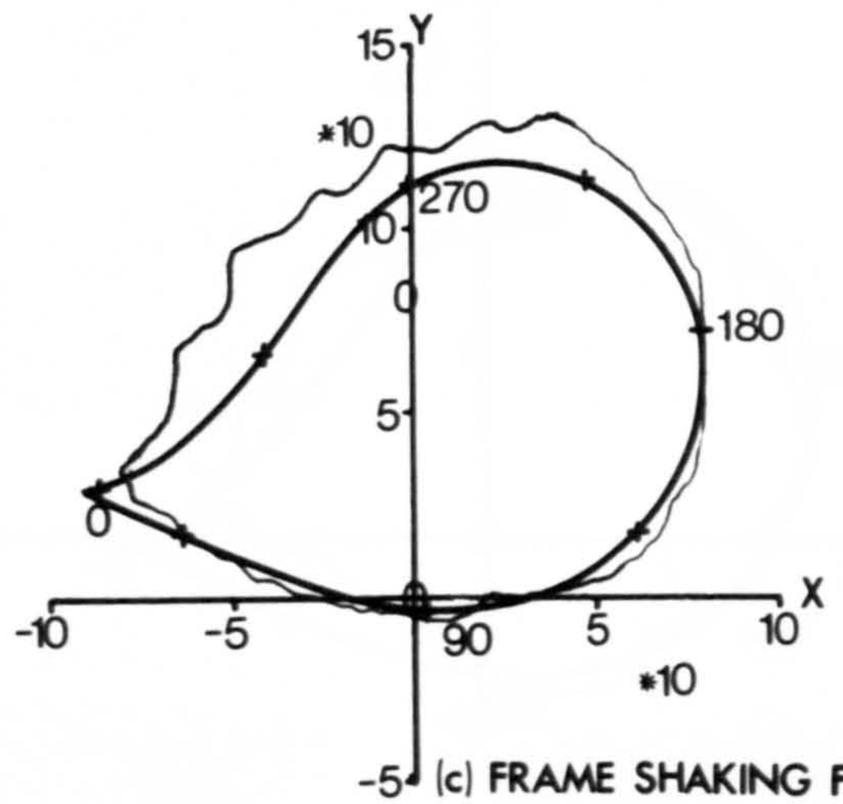

(c) FRAME SHAKING FORCE

FIGURE 10.3 MEASURED LOADS AT 200 R.P.M.

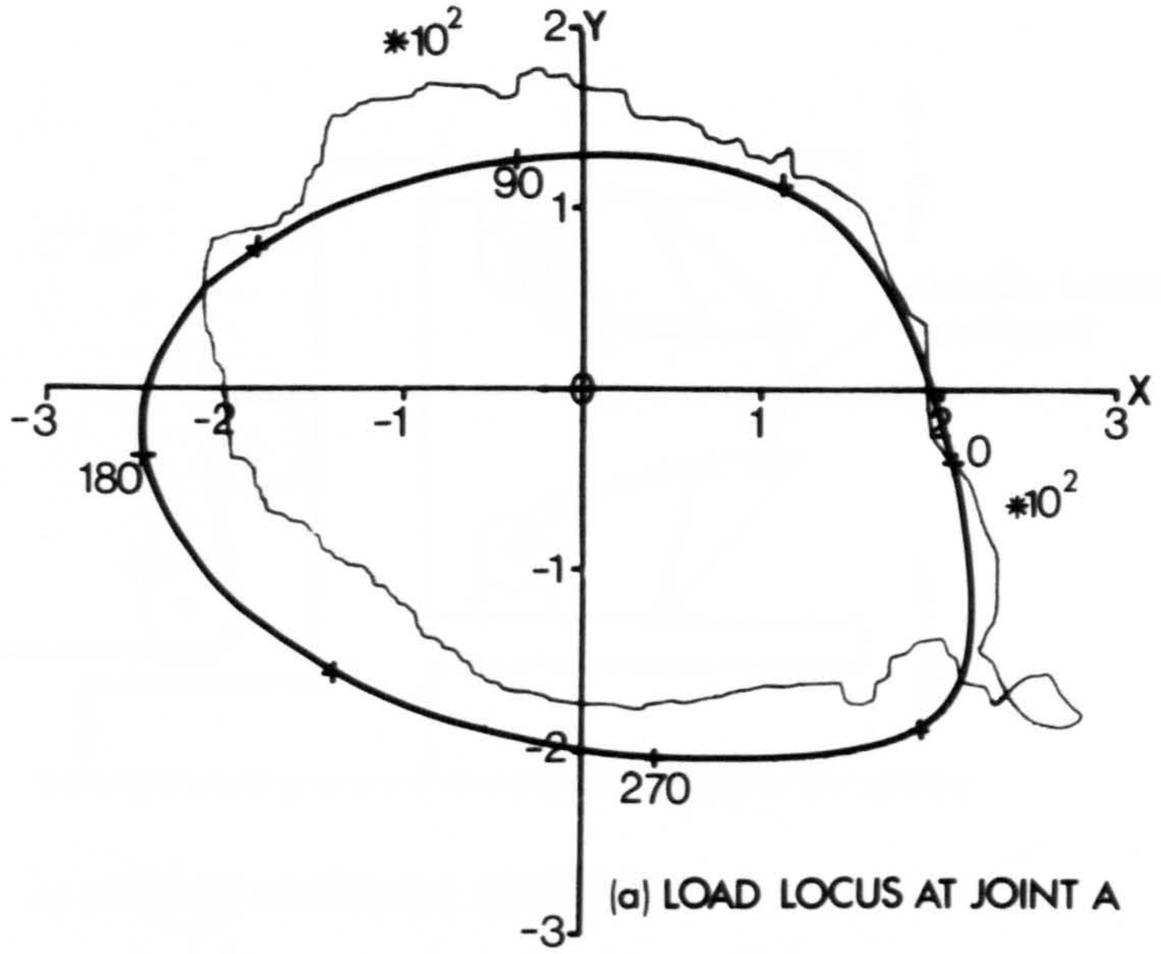

(a) LOAD LOCUS AT JOINT A

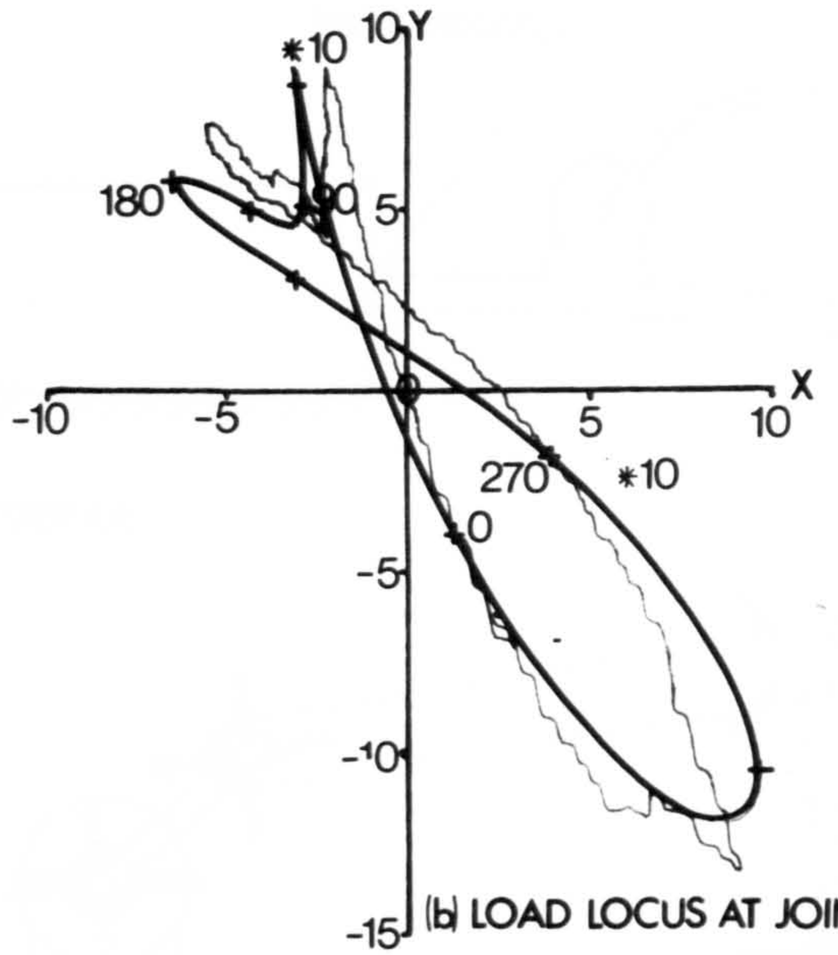

(b) LOAD LOCUS AT JOINT D

Y=VERTICAL FORCE

(NEWTONS)

X=HORIZONTAL FORCE

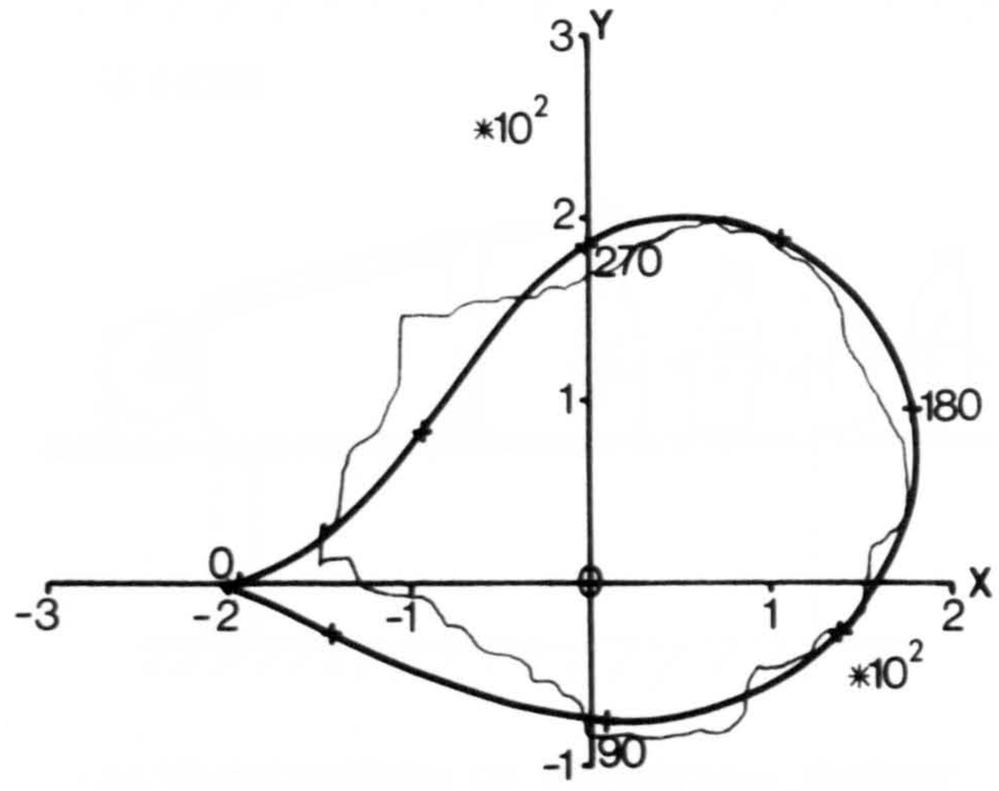

(c) FRAME SHAKING FORCE

FIGURE 10.4 MEASURED LOADS AT 300 R.P.M.

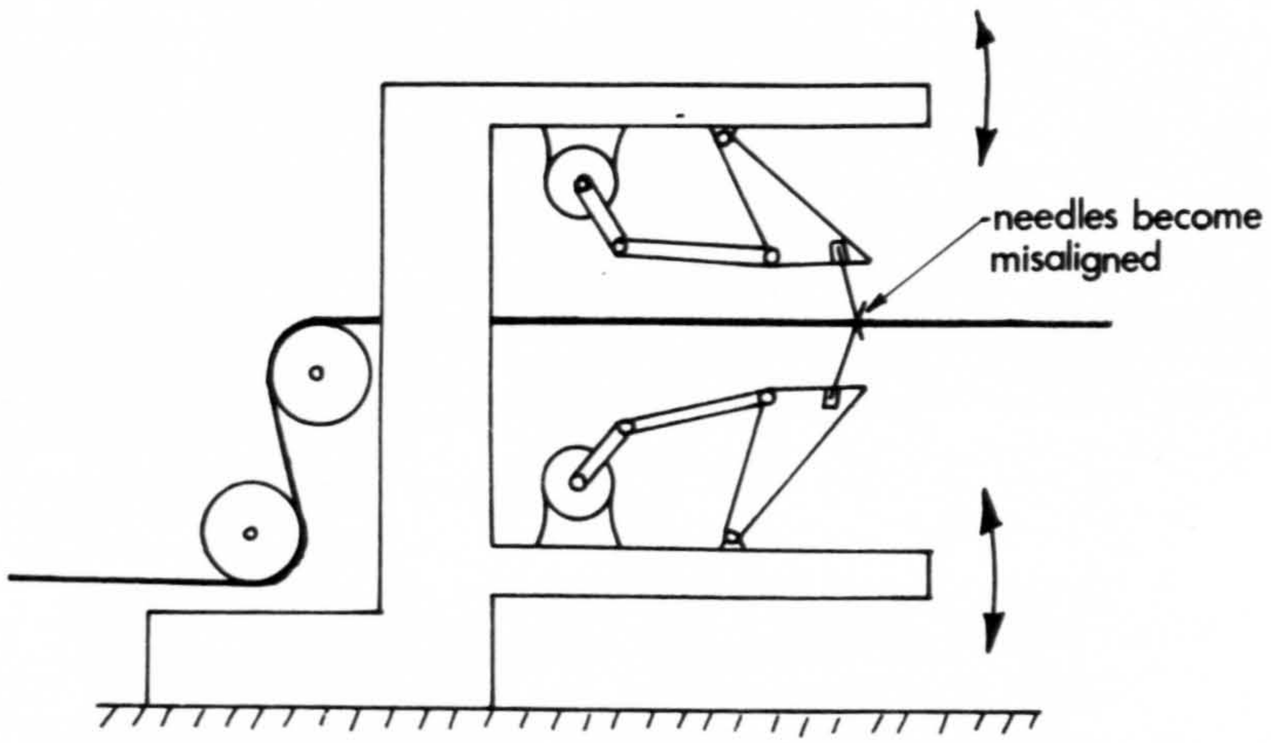

(a) LOSS OF KINEMATIC PURPOSE

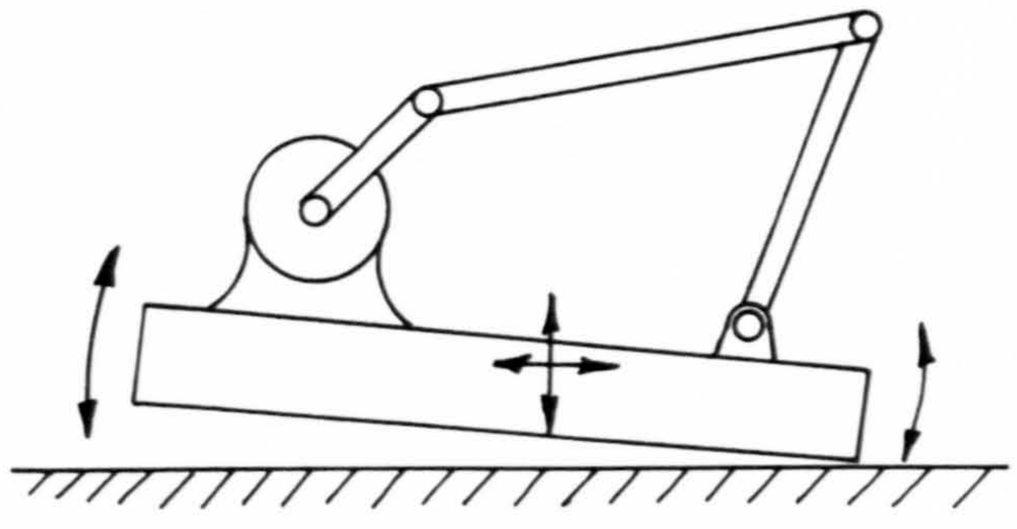

(b) DISPLACEMENT OF THE MACHINE

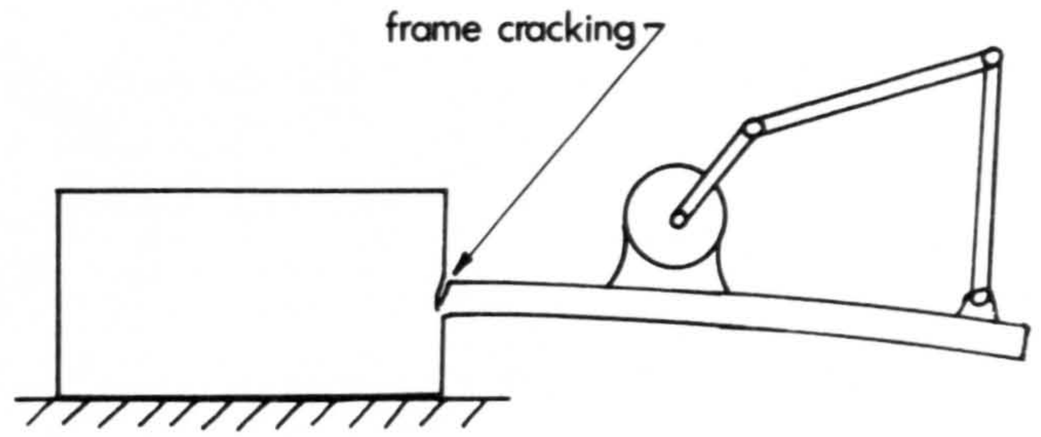

(c) FATIGUE

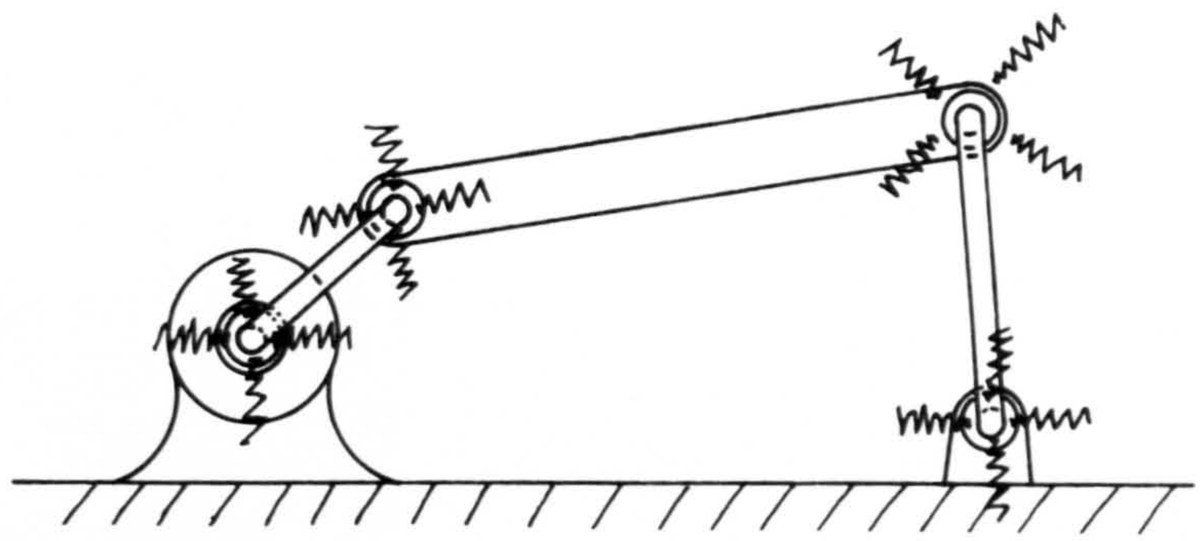

(d) NOISE

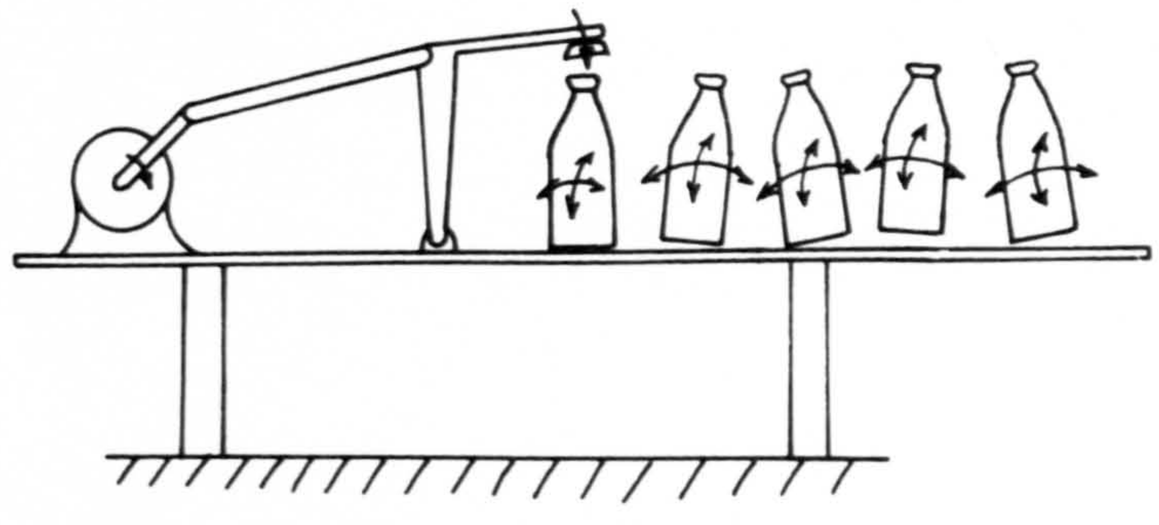

(e) TRANSMISSION OF VIBRATIONAL ENERGY

FIGURE 10.5 FIVE REASONS FOR BALANCING MECHANISMS

Large Charts or

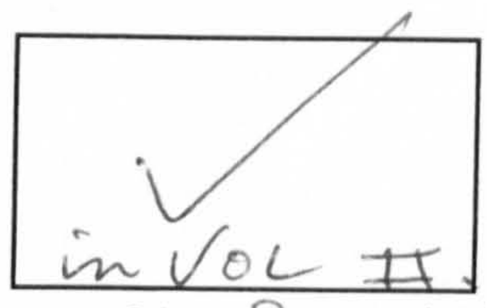

Pull-out pages

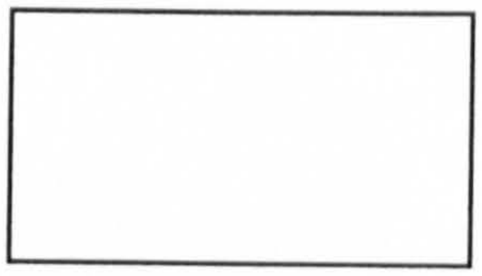

related to this thesis have not been filmed.

Please apply direct to the issuing university/awarding body.